THE UNIVERSITY OF MICHIGAN

INDUSTRY PROGRAM OF THE COLLEGE OF ENGINEERING

DIFFUSION IN BINARY LIQUID METAL SYSTEMS

John B. Edwards

A dissertation submitted in partial fulfillment
of the requirements for the degree of
Doctor of Philosophy in the
University of Michigan
Department of Chemical and Metallurgical Engineering
1966

December 1966

IP-761

ensm

UMR4734

Doctoral Committee:

Professor Edward E. Hucke, Co-Chairman
Professor Joseph J. Martin, Co-Chairman
Associate Professor Richard E. Balzhiser
Assistant Professor Harry B. Mark, Jr.
Associate Professor Robert D. Pehlke

ACKNOWLEDGEMENTS

This investigation was carried out at the Department of Chemical and Metallurgical Engineering, University of Michigan, under the direction of Professor Edward E. Hucke and Professor Joseph J. Martin. The author would like to express his sincere thanks to Professors Hucke and Martin for their encouragement, guidance, and interest throughout his graduate study. Thanks is also extended to the other members of the authors doctoral committee: Professors, Richard E. Balzhiser, Harry B. Mark, and Robert D. Pehlke, for their interest and contributions.

This investigation would not have been possible without the financial support of the United States Atomic Energy Commission under contract AT(11-1)-1352 .

The author would like to acknowledge the assistance of his fellow graduate students. Special thanks to Thomas McSweeney whose help in developing the numerical techniques used in this study was invaluable. Thanks also to Andrew Padilla and to William Ballamy for their helpful discussions and many suggestions during the course of this investigation.

The assistance of Carl Leonard, Cleatis Bolen, Douglas Connell, Elmer Darling, Robert Reed, Peter Severn and John Wurster in the development and fabrication of the experimental equipment is appreciated.

Thanks to the Industry Program staff for their aid in publishing

this dissertation. Thanks also to Jane Dillon for her aid and suggestions in the preparation of the manuscript.

Above all, thanks to my mother and to my brother for their encouragement. To Ken and Della Cowing and to Luke and Amelia White for their friendship and assistance. Thanks also for my many young friends who have made life more interesting and meaningful. Particularly to Kenneth Cowing, Rick Helmreich, Pete Kostishak, and Barry Wicks whose friendship has meant much to me.

TABLE OF CONTENTS

TABLE OF CONTENTS (CONT'D)

TABLE OF CONTENTS (CONT'D)

LIST OF TABLES

LIST OF FIGURES

LIST OF FIGURES (CONT'D)

LIST OF FIGURES (CONT'D)

LIST OF APPENDICIES

NOMENCLATURE

a	Radius of diffusion path, cm
a_o	Integral of initial concentration distribution
a_1	Activity of alkali metal A in anode
a_2	Activity of alkali metal A in cathode
A	Alkali metal A
A_s	Area of diffusion path, cm^2
A^+	Ion of alkali metal A
A'	Constant
A(B)	Alloy of alkali metal A with heavier metal B
b	Geometric parameter, ratio of atomic radius of particle to interactomic spacing
B	Heavy metal
c	Concentration, gr atoms/cm^3 alloy
C	Concentration, gr atoms/cm^3 alloy
C_i	Equilibrium concentration of alkali metal in fused salt
c_o	Initial concentration of cathode alloy
C_o	Initial concentration of cathode alloy
C_p	Particular solution for differential equation with dependent variable C
c_s	Surface concentration of cathode alloy
C_s	Surface concentration of cathode alloy
C*	Concentration after 1/2 time step in numerical solution

$\bar{C}$	Average concentration
$C_{I,J}$	Concentration at grid point I,J
d	Diameter of diffusion path, cm
d_a	Interatomic spacing
D	Diffusion coefficient, cm^2/sec
D_o	Pre-exponential term in Arrhenius expression
D'	Convective component of diffusion coefficient
D_A^*	Self diffusion coefficient of A
D_{AB}	Interdiffusion coefficient
D_{eff}	Effective diffusion coefficient
E	Activation energy for diffusion, cal/gr atom
E_c	Repulsive contribution to total lattice energy
E_i	Bond energy of pure i
E_s	Bond energy of pure s
ΔE_{is}	Partial molal energy of solute i in solvent s
f	Constant arising in solution of differential equation
f'	Drag force
f"	Force acting on particle
F	Faraday's number, 23,066 cal/volt
F_R	Distance from grid point to boundary in R direction for numerical solution
F_Z	Distance from grid point to boundary in Z direction for numerical solution
g	Acceleration due to gravity
G	Gibbs free energy, cal/gr atom

G^{o}	Standard free energy, cal/gr atom
$\overline{G}$	Partial molel free energy, cal/gr atom
$\overline{G}^{o}$	Partial molal standard free energy, cal/gr atom
Gr	Grashof number
h	Plank's constant
h_c	Height of finite cylinder
H	Enthaply, cal/gr atom
$\overline{H}$	Partial molal enthalpy, cal/gr atom
ΔH_c	Coulombic interaction contribution to activation energy
ΔH_i	Activation energy for impurity diffusion
ΔH_s	Activation energy for pure solvent diffusion
ΔH_v	Latent heat of vaporization
ΔH^*	Enthalpy of activation
i	Current, amp
i_m	Maximum cell current, amps
I	Summation index in R direction for numerical solution
I_c	Discharge current of cell, milliamps
j	Index of summation for infinite series
j^*	Critical fluctuation
$\vec{J}$	Summation index in Z direction for numerical solution
J	Flux, gr atoms cm^{-2} sec^{-1}
J(x,t)	Flux, gr atoms/sec
$J_{r=a}$	Flux at boundary of hemispherical surface

$J_{x=0}$	Flux at origin of 1-D system
k	Boltzman's constant
k_f	Force constant
k'	Waser-Pauling force constant
K	Constant in exponential term of time dependent boundary condition, sec^{-1}
K_v	Specific rate constant for viscous flow
L	Length of capillary
M	Quantity of solute per unit cross-sectional area of diffusion path
n	Index of summation for infinite series
n_e	Number of electrons transferred per atom in electrochemical reaction
N_{Na}	Atomic fraction sodium in cathode alloy
N_K	Atomic fraction potassium in cathode alloy
p	Osmotic pressure
P	Pressure, kg/cm^2
q	Screening constant
Q	Quantity of matter transferred from anode to cathode, gr/atoms
Q_i	Activation energy of diffusion of solute i in solvent s
Q_s	Activation energy for self diffusion of solvent s
r	Distance in radial direction, cm
R	Gas constant
R_c	Cell resistance, ohms
R_i	Initial cell resistance, ohms

R_f	Final cell resistance, ohms
R_o	Distance in radial direction, cm
s	Complex variable in Laplace Operational mathematics
S	Entropy, cal/gr atom °K
$\overline{S}$	Partial molal entropy, cal/gr atom °K
ΔS^*	Entropy of activation
t	Time, sec.
t_o	Time, sec
T	Absolute temperature, °K
T_m	Melting temperature °K
U	Dependent variable in differential equation
$\overline{U}$	Laplace transform of dependent variable
U_p	Particular solution for differential equation with dependent variable U
v	Independent variable
$\vec{v}$	Velocity
V_m	Molar volume, cm^3/gr atom
ΔV	Volume change per gr atom on melting
x	Distance, cm
z'	Relative valence of solute with respect to solvent
Z	Distance in axial direction for cylinderical coordinates, cm
Z_c	Coordination number
Z_o	Distance in axial direction for cylinderical coordinates, cm

Greek Symbols

α	Constant
β	Coefficient of sliding fraction
β'	Constant dependent on solute-solvent pair
γ	Configurational constant
γ_A	Activity coefficient of A
δ	Concentration coefficient of volumetric expansion
ϵ_{A_s}	Probable error in area of diffusion path
ϵ_{C_o}	Probable error in initial composition of cathode alloy
ϵ_{C_s}	Probable error in surface concentration of cathode alloy
ϵ_D	Probable error in diffusion coefficient
ϵ_J	Probable error in current
ϵ_o	Constant
ϵ_t	Probable error in time
ζ	Effective number of neighbors of diffusing atom lying in plane perpendicular to direction of motion
η	Absolute viscosity, cp
λ_1, λ_2	Interatomic distances perpendicular to direction of motion
λ_3	Interatomic distance in direction of motion
λ_v	Jump distance for viscous flow
ν	Vibrational frequency of atoms, sec^{-1}
ρ	Density
ρ_o	Density of infinitely dilute solution
σ	Number of nearest neighbors

τ	Time, sec
τ'	Number of nearest neighbors in a plane
$\varphi(x)$	Initial concentration distribution
φ	Potential, volts
φ_a	Anode potential, volts
φ_c	Cathode potential, volts
φ_o	Open-circuit cell potential, volts
φ_s	Potential at cathode-electrolyte interface, volts
φ_d	Cell discharge potential, volts

ABSTRACT

A new experimental technique was developed for measurement of diffusion coefficients in liquid metals. This technique involved the discharge of a liquid metal concentration cell in which diffusion in the cathode alloy was rate limiting. Diffusion coefficients were obtained from measurement of cell potential and discharge current.

Diffusion coefficients have been measured for potassium in mercury, sodium in lead, and sodium in tin for a range of temperature and alloy compositions. The coefficients obtained were reproducible, internally consistent, and have values reasonable for diffusion in liquid metals. The probable error in the measurements was $\pm$ 25% and this error was due primarily to uncertainties in the thermodynamic data available for evaluation of the cell potential. The reproducibility, however, was better than $\pm$ 5% in all cases.

Unlike other methods which have been used to study diffusion in liquid metals, this method makes accessible the flux of diffusate entering the diffusion path. An anomoly has been observed in this flux which has been attributed to a non-planar cathode-electrolyte interface in the concentration cell. This effect is probably not peculiar to this technique and may be present in other methods where two phases are contacted. Its presence has not been detected before since other methods do not permit measurement of the flux. Numerical

calculation shows that the actual quantity of diffusate due to this effect, will be a few percent greater than what is predicted by the usual mathematical solutions of Fick's law where a planar interface is assumed.

A survey of the literature pertaining to diffusion in binary liquid metal alloys is presented. This includes a critical review of existing experimental data and theoretical models for diffusion in liquid metals. The experimental techniques most commonly used to measure diffusion coefficients in liquid metals are discussed. Convective and surface effects are also considered.

I. INTRODUCTION

Diffusion in liquid metals has been the subject of numerous investigations. Unlike studies of aqueous and organic systems, it is not possible to use optical methods to study diffusion in liquid metals. The principle advantage of optical methods being, it is possible to determine the rate at which material enters the diffusion path. From this, anomalous phenomena such as initial disturbances can be detected and isolated.

The major objectives of this thesis are:

(1) To develop a technique suitable for studying diffusion in liquid metals, which in addition to determination of the diffusion coefficient permits observation or calculation of the rate at which material enters the diffusion path;

(2) To use this technique to measure diffusion coefficients for potassium in potassium amalgams and for sodium in sodium-lead and sodium-tin alloys.

Briefly, the method developed is as follows. One metal serves as the anode of a concentration cell. The second liquid metal, or an alloy of it with the first, forms the cathode. A fused salt electrolyte separates the anode and cathode metals. Upon discharge of this cell, metal is transferred from anode to cathode via movement of ions through the electrolyte. Cell design insures that diffusion of metal from the

cathode-electrolyte interface into the body of the cathode alloy is rate limiting. The rate at which metal enters the diffusion path is obtained from the discharge current.

A solution of Fick's second law can be obtained for a given cell geometry. Deviations of the flux from that predicted by this solution can be attributed to anomolous effects and calculation of the diffusion coefficient based only on that portion of the data for which the solution of Fick's law is a good approximation.

This method is useful for studying diffusion in binary liquid metals where:

(1) Sufficient thermodynamic data is available to determine the cell potential as a function of the cathode alloy composition.

(2) A suitable electrolyte, containing only cations of the anode metal, is available. This electrolyte must be molten throughout the temperature range investigated and must not react with the anode and cathode metals or with the material of which the cell is constructed.

(3) The metal couple must produce a cell potential of at least 0.10 volt over the composition range investigated.

The three alloy systems chosen for this investigation meet these criteria. In the cases,potassium in potassium amalgams and sodium in sodium-lead, diffusion coefficient data exists in the literature against which the results of proposed method can be checked.

II. LITERATURE REVIEW

A. DEFINITION AND SIGNIFICANCE OF DIFFUSION COEFFICIENTS

The diffusion coefficient is usually defined as the proportionality constant between the mass flux of a component in a system and the concentration gradient which gives rise to this flux.

$$\vec{J} = - D \text{ grad } C \qquad (1)$$

This equation states, the diffusive flux $\vec{J}$ is opposite in direction to the concentration gradient and proportional to its absolute value. If the diffusion coefficient is taken to be a constant, then the above equation states that a linear relationship exists between the flux of a component and its concentration gradient. In cartesian coordinates this equation becomes

$$J = - D \frac{\partial C}{\partial x} \qquad (2)$$

and is usually referred to as Fick's first law. Fick's second law is obtained from equation (2) and the continuity equation.

$$\frac{\partial C}{\partial t} = \frac{\partial}{\partial x} \left(D \frac{\partial C}{\partial x} \right) \qquad (3)$$

If the diffusion coefficient is independent of composition, equation (3) becomes,

$$\frac{\partial C}{\partial t} = D \frac{\partial^2 C}{\partial x^2} \qquad (4)$$

These equations describe the diffusion of a substance, the concentration of which, C, is defined to be the amount of this diffusing substance per unit volume of solution.

Description of diffusion with the conventional Fick's law equations is by no means the only approach. Sandler and Dahler (126) have shown that the telegraphers equation in some respects provides a more rigorous description of diffusion than does the familiar diffusion equation. Solutions of Fick's second law predict a concentration change throughout a system for all time however small. The approach of Sandler and Dahler assigns to diffusion, wave properties, and the concentration disturbance is confined to a "signal cone" rather than extending throughout the system. A finite amount of time is required for the disturbance to travel from its origin to a given point. This should serve to point out that description of diffusion phenomena with the diffusion equation is more a matter of convention than necessity. It seems to this writer that much is to be gained by examining the mathematical description of diffusion from a fresh viewpoint as Sandler and Dahler have done.

The development thus far takes no account of atomistic considerations. Consider a plane surface within the system. An individual

atom in this system can move with equal probability in any direction. If the atoms in the system are indistinguishable, the net flow of atoms across this plane, which is due entirely to random thermal motion, will be zero. This satisfies equation (1), no concentration gradient exists and the flux is zero. Now, consider the case where the system contains two distinguishable species, A and B. Let their concentrations on opposite sides of the plane differ. The motion of the atoms of each species is assumed to be random so a given atom has an equal probability of moving in any direction. The flux of atoms of species A crossing the plane in a particular direction will be the product of the probability an atom will move in this direction and the concentration of A atoms on the side of the plane from which the particular atom is coming. A atoms will cross the plane in both directions, but since the concentration of A atoms on one side is greater than on the other, there will be a net transfer of A from the side of higher concentration to that of lower concentration. If the system is to remain static there must be a compensating flow of B atoms in the opposite direction. If A and B are isotopes of the same element such that one is radioactively distinguishable, it is possible to measure the self diffusion coefficient of the element by observing movement of the tracers through the system. This self diffusion coefficient may be thought of as a measure of the frictional forces which exist between the atoms as a result of their relative motion.

In the above it was assumed A and B have similar interatomic forces. That is, the force pairs A-B, A-A, and B-B are indistinguishable. This is a good assumption for isotopes of an element. However, it is usually not good for cases where the species have significantly different chemical properties. If the force pairs are not similar and if a concentration gradient exists within the system, then a given atom will not have an equal probability of moving in all possible directions as was assumed above. Certain atomic configurations will be favored. For example, if the pairs A-A and B-B are favored at the expense of forming A-B pairs then it would be expected that diffusion would proceed more slowly than for the ideal case. Herein lies the basic difference between the phenomena of self diffusion and interdiffusion. The movement of interdiffusing atoms is not random in the same sense that it is for self diffusing atoms. The presence of a concentration gradient of chemically distinguishable atoms perturbs the motion of the atoms themselves.

Self diffusion coefficients for one component of a binary alloy may be measured in the absence of an overall concentration gradient of either metal. The movement of tracers is observed in a system of otherwise uniform chemical composition. This coefficient should be identical to that obtained for interdiffusion at the same composition as the concentration gradient becomes vanishingly small.

Hartley and Crank (67) discuss the importance of selecting the appropriate frame of reference for evaluating diffusion coefficients from experimental data. Darkin (32) has shown that diffusion in any two component system can be described by a single diffusion coefficient which may be a function of composition but will be the same function for both components. This "intrinsic diffusion coefficient" is defined in terms of the rate of transfer of A or of B across a plane fixed so that no overall mass flow occurs across it. Such a section may or may not be possible to determine experimentally. Darkin's relationships have been confirmed by the use of markers in solid alloys. To this writers knowledge these relationships have never been confirmed for liquid metal systems. An experiment to accomplish this would be difficult, though in principle not impossible. One approach would be to observe the movement of an insoluble marker which is small, but still too large to diffuse. The density of this marker would be selected so that it would remain suspended at a particular composition layer in the system. Motion relative to this marker would be attributable to diffusion. Motion of the marker relative to the experimental frame of reference would be due to hydrodynamic flow resulting from expansion or contraction of the alloy during diffusion.

The volume frame of reference is usually chosen because it becomes identical with the cell or experimental frame of reference if the partial molal volumes of the components are independent of composition. This is

true for ideal solutions and is a reasonably good approximation for non-ideal systems when small concentration intervals are used. When the partial molal volumes are dependent on concentration, volume change occurs on mixing. If this volume change is large, mass transport is no longer described by Fick's second equation. Rather the expression for the flux relative to the cell must contain a term to describe the bulk or hydrodynamic flow resulting from the volume change, in addition to the usual terms which describe the diffusive motion of the components. To the writers knowledge refinements of this nature have never been included in the treatment of liquid metal diffusion data.

B. REVIEW OF EXPERIMENTAL DATA

Introduction

Recently Wilson (157) has reviewed the literature pertaining to liquid metal diffusion coefficients. He concludes self diffusion data are often subject to an error of $\pm$ 50% while data for diffusion coefficients in alloys may be as great as 100%. Yang and Derge (158) have also presented a review and tabulate diffusion coefficients for liquid metal systems. No discussion of reliability is included. Shewmon and Love (129) present a limited review of recent literature.

This writer has undertaken a critical review of the available literature concerning diffusion in liquid metals. An attempt has been made to ascertain the reliability of existing data. It appears that some of this experimental data is quite reliable, while for other measurements an estimate of $\pm$ 100% would be conservative. When available, the investigators estimate of the error is given in Tables 1, 2 and 3. This estimate is a measure only of the consistency or reproducability which was obtained. It does not include a consideration of the error in a more absolute sense, such as the validity of the experimental method chosen. Comments regarding these considerations are included in the footnotes and the discussion which accompanies each of the tables. In subsequent sections of this review, the applicability and limitations of each of the major experimental methods are discussed. Convection and

wall effects in these experiments are considered.

Tabulations of self diffusion data for pure metals and for components of binary alloys are given. Interdiffusion data for binary alloys is also tabulated. Pressure and concentration dependence of diffusion coefficients are also discussed.

Self Diffusion in Pure Liquid Metals

Self diffusion coefficients are measured by observing the movement of radioactive tracers in a pure liquid metals. The diffusing molecule observes a uniform environment and moves with equal liklihood in any direction. Self diffusion, thus, represents a purely statistical effect caused by the natural tendency toward randomness.

Concentration gradients of the bulk material are absent in self diffusion. This reduces the liklihood of convection arising from density inversions. The diffusion coefficients obtained have been found to be sensitive to such factors as the capillary diameter and material of which the capillary was made. Small effects like these are obscured in the study of interdiffusion where gross effects such as volume changes during diffusion and dependence of the diffusion coefficient on concentration are present.

Self diffusion studies have been reported for eleven liquid metals. The results of these studies are presented in Table 1. The values of D_o and E which are given refer to the pre-exponential and activation terms for the following empricial representation of the data.

$$D = D_o e^{-E/RT} \qquad (5)$$

Where more than one investigator has reported results for a metal, an asterisk (*) has been placed to the left of the result which this writer feels is preferred. This is based on a consideration of the method used, the temperature range investigated and criticism of other investigators.

Self diffusion in mercury has been studied by several investigators. Haissinsky and Cottin (64) calculated a self diffusion coefficient from data for isotopic interchange between mercury and aqueous mercurous nitrate. Their calculation was based on the assumption that diffusion in the liquid mercury was rate controlling. They obtained a coefficient which was a few orders of magnitude too low for liquids and their assumption as to the rate controlling step was apparently incorrect. Hoffmans' (73) measurements are 11 to 16% greater than those of Nachtrieb and Petit (98). Brown and Tucks' (18) results agree well with those of Nachtrieb and Petit. Brown and Tuck suggest that the rapid stirring used by Hoffman may have caused turbulence at the open end of the capillary cell. All of these investigations covered rather limited temperature ranges. Meyer (92) used an improved method of stirring and obtained data which show good internal agreement. He reports data over a large temperature range which when plotted as log D vs. 1/T, exhibits some curvature.

Lodding (87) determined self diffusion data for potassium, rubidium and indium from electrotransport experiments. The self diffusion coefficient reported for indium in this investigation was significantly greater than that reported by Careri et. al. (22) and by Lodding (86), both of which had been obtained using the capillary reservoir technique. This led Lodding to question the validity of the capillary reservoir technique. However, in a latter investigation, Rohlin and Lodding (122) conclude that the data obtained from the electrotransport experiments has a significant convective component and consequently the diffusion coefficients are too high.

Independent investigators found agreement of the self diffusion coefficients obtained for both silver and tin in the temperature regions where the experimental data overlap.

TABLE 1

SELF DIFFUSION DATA FOR PURE LIQUID METALS

Metal	$D_o \times 10^4$ units cm^2/sec	E cal/gr atom	Temp Range (°C)	Experimental Method (a)	Diffusion Path Diam. (mm.)	Reference
Hg	1.10	1150	23-60	LLC	0.75	(18)
	6.0	2400	10-60	CR	I	(127)
	0.85	1005	0-98.6	SC	0.5-1.0	(98)
	1.26	1160	0-90	CR	0.6	(73)
	*(b)		0-293.3	CR	0.5	(92)
	(c)		0-30	--	---	(64)
	3.0	1800	30-80	CR	1.5	(76)
Pb	$*9.15 \pm 0.030$	4450	333-657	CR	1.24 & 1.63	(123)
	(d)		70	TSIR	3.0	(60)
Ag	$*5.8 \pm 1.4$	7760 ± 670	975-1350	CR	I	(83)
	7.1 ± 0.06	8150 ± 1130	1002-1105	CR	0.80-1.5	(159)
Na	11.0 ± 3.7	2450 ± 200	98-226	CR	I	(93)
Ga	1.07	1122	30-98	SC	0.5-1.0	(107)
In	4.25	2200	255-492	TSIR	1.6-2.0	(20)
	1.76	1350	160-480	TSIR	1.6	(21)
	*3.02	2580	227-554	TSIR	0.83-2.0	(22)
	*2.89	2430 ± 50	175-740	CR	0.55	(86)
	4.2	(e)	430-870	ET (f)	0.6	(87)

TABLE 1 (continued)

Metal	$D_o \times 10^4$ units cm^2/sec	E cal/gr atom	Temp Range (°C)	Experimental Method (a)	Diffusion Path Diam. (mm.)	Reference
Sn	13.9	4000	299-662	TSIR	1.6-2.0	(20)
	*3.24±1.2	2760±80	267-683	TSIR	0.83-2.0	(22)
	*(g)		293-940	CR	0.5	(89)
Zn	8.2	5090	445-600	CR	1.0	(97)
K	*1.07±0.56	2550±270	340-460	CR	0.4-0.8	(172)
	12.5	(h)	340-540	ET (f)	0.6	(87)
Rb	22.0	(i)	315-615	ET (f)	0.6	(87)
Au	1.46±0.01	9710±710	1140-1260	CR	1.19-1.59	(69)

Abbreviations for Table 1

*	=	Preferred Data
CR	=	Capillary reservoir technique
ET	=	Electrotransport cell
FCSIR	=	Finite cylinder semi-infinite rod technique
I	=	Indeterminate from information given by investigator
LLC	=	Liquid-liquid contact
SC	=	Shear cell technique
TSIR	=	Two semi-infinite rod technique

Notes for Table 1

(a) The experimental techniques are described in detail in another section of this review.

(b) Meyers data shows some curvature when log D is plotted vs 1/T sample values are:

$D = 1.50 \times 10^{-5}$ cm^2/sec at 0°C
$D = 1.88 \times 10^{-5}$ cm^2/sec at 42°C
$D = 2.72 \times 10^{-5}$ cm^2/sec at 118.4°C
$D = 3.26 \times 10^{-5}$ cm^2/sec at 141°C
$D = 4.42 \times 10^{-5}$ cm^2/sec at 224.4°C

(c) Data obtained was inordinately low $D = 7 \times 10^{-8}$ cm^2/sec.

(d) $D = 2.54 \times 10^{-5}$ cm^2/sec at 70°C.

(e) Curvature on log D vs 1/T plot, Lodding reports $E/RT = 1.26$.

(f) Lodding latter concludes that results of this investigation using electrotransport data include convection component and the diffusion coefficients obtained are too high.

(g) Curvature in data, sample points are:

$D = 2.51 \times 10^{-5}$ at 282°C
$D = 4.47 \times 10^{-5}$ at 393°C
$D = 7.08 \times 10^{-5}$ at 561°C
$D = 17.8 \times 10^{-5}$ at 987°C

(h) Curvature in data, Lodding reports $E/RT = 1.26$.

(i) Curvature in data, Lodding reports $E/RT = 1.25$.

Self Diffusion in Binary Alloys

Self diffusion of one component in a binary alloy may be studied by contacting two alloys of identical composition. One of these alloys contains radioactive tracers of the metal whose self diffusion coefficient is to be studied. The other alloy is prepared from inactive metals.

As in the case of self diffusion measurements for pure alloys, good precision can be obtained due to the absence of volume changes or concentration dependence of the diffusion coefficient. The results of Paoletti and Vincentini (102, 103) show that it is possible to discern effects such as dependence of the diffusion coefficient on capillary diameter. They obtained reproducable data wherein the variation in magnitude of the diffusion coefficients was only a few percent. This gives some indication of the high precision attainable for this type of measurement.

Schadler and Grace (127) verified the applicability of Darkin's (32) theoretical relationships between self and interdiffusion coefficients for dilute zinc amalgams.

Available self diffusion data for binary alloys is summarized in Table 2. The results are tabulated in terms of the pre-exponential D_o, and the activation term E as was done for self diffusion in pure metals. When measurements were for a single temperature, this value of the diffusion coefficient is reported.

TABLE 2

SELF DIFFUSION IN BINARY LIQUID METAL ALLOYS

Binary Composition			$D_o \times 10^4$	E	Temp Range		Path Diam	
Solvent	Solute	Tracer	cm^2/sec	cal/gr atom	°C	Method	(mm.)	Reference
Bi	0.255 atom % Pb	Pb^{210}	1200	9860±1070	281-414	CR	1.16-1.53	(124)
Bi	0.255 atom % Pb	Bi^{210}	465	8100±466	281-414	CR	1.16-1.53	(124)
In	0.5 atom % Pb	In^{114}	2.64±0.18	2373±83	249-544	TSIR	1.6-0.8	(102)
In	1.5 atom % Pb	In^{114}	3.04±0.26	2550±350	249-544	TSIR	0.8	(102)
In	0.5 atom % Pb	Pb^{210}	2.10±0.15	2220±311	249-544	TSIR	1.6	(102)
In	0.5 atom % Pb	Pb^{210}	2.32±0.24	2435±127	249-544	TSIR	0.8	(102)
In	1.0 atom % Sn	In^{114}	3.35±0.36	2606±127	250-470	TSIR	1.6-0.8	(147)
In	1.0 atom % Sn	Sn^{113}	3.19±0.35	2473±129	250-470	TSIR	1.6	(147)
In	1.0 atom % Sn	Sn^{113}	2.75±0.36	2356±179	250-470	TSIR	0.8	(147)
In	47.0 atom % Sn	In^{114}	4.25±0.57	2771±158	200-450	TSIR	1.6	(103)
In	47.0 atom % Sn	Sn^{113}	1.17±0.17	1380±156	200-450	TSIR	1.6	(103)
Sn	1.0 atom % In	Sn^{113}	3.74±0.54	2909±172	250-470	TSIR	1.6-0.8	(147)

TABLE 2 (continued)

Binary Composition				$D_o \times 10^4$					
Solvent	Solute		Tracer	cm^2/sec	E cal/gr atom	Temp Range °C	Method	Path Diam (mm.)	Reference
Pb	0.1 wt. % Zn		Zn^{65}	4.0 ± 1.0	3200 ± 730	343-550	CR	1.5	(76)
Pb	0.5 wt. % Zn		Zn^{65}	11.0 ± 0.3	4600 ± 730	343-550	CR	1.5	(76)
Pb	1.0 wt. % Zn		Zn^{65}	19.0 ± 1.0	4900 ± 1370	343-550	CR	1.5	(76)
Pb	1.5 wt. % Zn		Zn^{65}	13.0 ± 1.0	4000 ± 740	343-550	CR	1.5	(76)
Hg	0.103 wt. % Zn		Zn^{65}	1.1	1000	0-60	CR	I	(127)
Hg	0.488 wt. % Zn		Zn^{65}	1.8	1500	0-60	CR	I	(127)
Hg	1.163 wt. % Zn		Zn^{65}	3.4	1900	0-60	CR	I	(127)
Hg	0.104 wt. % Zn		Hg^{203}	7.8	2500	0-60	CR	I	(127)
Hg	0.437 wt. % Zn		Hg^{203}	2.7	1900	0-60	CR	I	(127)
Hg	1.456 wt. % Zn		Hg^{203}	1.5	1600	0-60	CR	I	(127)
Hg	0.75 atom % Tl		Tl^{204}	$*D = 0.98 \pm 0.12 \times 10^{-5}$		25	CR	1.0	(51)
Hg	7.13 atom % Tl		Tl^{204}	$*D = 0.85 \pm 0.021 \times 10^{-5}$		25	CR	1.0	(51)

TABLE 2 (continued)

Binary Composition				$D_o \times 10^4$	E	Temp Range		Path Diam	
Solvent	Solute		Tracer	cm^2/sec	cal/gr atom	°C	Method	(mm.)	Reference
Hg	16.10	atom % Tl	Tl^{204}	$^*D=0.71\pm0.009 \times 10^{-5}$		25	CR	1.0	(51)
Hg	20.04	atom % Tl	Tl^{204}	$^*D=0.62\pm0.02 \times 10^{-5}$		25	CR	1.0	(51)
Hg	28.56	atom % Tl	Tl^{204}	$^*D=0.47\pm0.02 \times 10^{-5}$		25	CR	1.0	(51)
Hg	34.60	atom % Tl	Tl^{204}	$^*D=0.41\pm0.02 \times 10^{-5}$		25	CR	1.0	(51)
Hg	38.68	atom % Tl	Tl^{204}	$^*D=0.38\pm0.013 \times 10^{-5}$		25	CR	1.0	(51)
Hg	41.58	atom % Tl	Tl^{204}	$^*D=0.39\pm0.013 \times 10^{-5}$		25	CR	1.0	(51)

* Data reported only at 25°C, the units of D are cm^2/sec

** Experimental methods are described elsewhere in this review. Abbreviations as follows:

CR = Capillary reservoir technique
TSIR = Two semi-infinite rods technique

I Indeterminate from information given by the investigator

Interdiffusion in Binary Liquid Metal Alloys

The available data for interdiffusion in binary liquid metals is summarized in Table 3. Examination of this table reveals that much of the interdiffusion data has been determined using experimental conditions not nearly as favorable as those used to obtain self diffusion coefficients in pure metals and their alloys.

The occurrence of convection in liquid metal diffusion experiments is discussed elsewhere in this review. From an analysis of the data for self diffusion in liquid metals, this writer concludes that even under favorable conditions convective effects will be appreciable for experiments conducted with diffusion paths greater than a few millimeters in diameter. The magnitude of the convective effect will be dependent on other factors. For example, it is common practice to maintain the top of the diffusion path a few degrees warmer than the bottom to avoid density inversions. For metals which are very non-ideal and liberate large amounts of energy upon mixing, this superimposed temperature gradient may not be sufficient to overcome local heating which can give rise to convection. The data of Bonilla (13) for the system potassium-mercury has an order of magnitude variation in the diffusion coefficient as the amalgam composition varies. Such phenomena is not uncommon in solids though liquids usually show less variation than this. The inordinately high values may have been due to an exothermic reaction which gave rise to convection in the large diffusion path used by Bonilla.

A number of the early diffusion studies employed large diameter paths. In addition, the ratio of diameter to length of the diffusion path often was unfavorable. The data of von Wogau (150) was obtained using a pool of mercury 20 mm by 50 mm. That of Meyer (170) from a pool 17 mm in diameter. Cohen and Bruins (26) who dispute the data of von Wogau and Meyer obtained their own data in a pool 20 mm by 20 mm. It is hard to conclude much about the reliability of this early data. Often the cell geometry was very unfavorable, though fortunately most of the experiments were performed at near ambient temperatures and the concentration intervals were necessarily very small owing to the low soluability of most metals in mercury at low temperatures. Convection in these experiments, if it existed was probably due to vibration in the apparatus rather than to thermally induced density inversions.

The data of Roberts-Austin (120) leaves many questions unanswered. The experimental temperature dropped from 550 to 500°C due to a malfunction in the equipment. There is an indication that large temperature gradients existed in the alloy columns (top end warmer). The same data has been reported at three different temperatures in as many articles. Some of this data, particularly that involving the precious metals has never been checked by other investigations.

A number of the investigations noted in Table 3 were conducted utilizing concentration intervals of substantially more than a few

atom %. This introduces two problems into the experimental interpretation. First, volume changes occur which render the usual mathematical approaches invalid. Rigorous treatment requires a frame of reference other than the cell frame of reference which is normally used. Second, the diffusion coefficient often depends on the composition and a large concentration interval yields some average value. Niwa (99) used concentration intervals of 0-10 atom % to study diffusion in dilute alloys. His investigations of diffusion coefficients as a function of composition employed large concentration intervals, often 60 atom % or larger. Grace and Derge (57) studied diffusion of bismuth in lead. For measurements made with small concentration intervals they obtained results in reasonable agreement with those of Rothman and Hall (123). However, when they used large concentration intervals of approximately 50 and 100 atom % they obtained inordinately high values for the diffusion coefficient. Grace and Derge term these coefficients "effective diffusion coefficients". Morgan and Kitchner (171) and Bonilla (12) use initial concentration intervals of 100 atom % to study the diffusion of cobalt in iron and of uranium in bismuth respectively. Morachevski (95) used intervals from 12 to 39 atom % in his investigation of diffusion in the sodium-lead system.

Uremas' (143) data for solute diffusion in aluminum exhibits extreme temperature dependence of the diffusion coefficient.

Data for diffusion of non-metals in metals is not included in Table 3. The reader is referred to Yang and Derge.(158)

TABLE 3

INTERDIFFUSION DATA FOR BINARY ALLOYS

Solvent	Solute	Experimental Results (a)	Temp Range °C	Exp. Method (b)	Path Diam. (mm.)	Solute Concentration Interval (c)	V^M% (d)	Reference
Ag	Au	$D_o=8.8\pm1.2\times10^{-4}$ $E=8690\pm600$	980-1260	CR	0.75-1.0	C_o=Trace Au^{199} C_b=0.00	vs	(62)
Ag	In	$D_o=5.75\pm0.24\times10^{-4}$ $E=6760\pm900$	980-1270	CR	I	C_o=Trace In^{114} C_b-0.00		(136)
Ag	Sb	$D_o=4.06\pm0.81\times10^{-4}$ $E=5700\pm480$	980-1270	CR	I	C_o=Trace Sb^{115} C_b=0.00		(136)
Ag	Sn	$D_o=4.4\pm1.2\times10^{-4}$ $E=6030\pm760$	975-1350	CR	I	C_o=Trace Sn^{113} C_b=0.00		(83)
Al	Cu	$D=7.2\times10^{-5}$ (e)	700	FCSIR		C_1=13.4 atom % C_2=55.0 atom %	-6.7 @	(143)
		$D=15.0\times10^{-5}$	1000			C_1=23.8 atom % C_2=55.0 atom %	Cu_3Al	
Al	Fe	$D=1.4\times10^{-5}$ (e)	700	FCSIR		C_1=0.194 atom % C_2=15.8 atom %		(143)
		$D=20\times10^{-5}$	1000			C_1=7.28 atom % C_2=15.8 atom %		

TABLE 3 (continued)

Solvent	Solute	Experimental Results (a)	Temp Range °C	Exp. Method (b)	Path Diam. (mm.)	Solute Concentration Interval (c)	V^M% (d)	Reference
Al	Mg	$D=2.7 \times 10^{-5}$ (e)	700	FCSIR		C_1=7.44 atom % C_2=100.0 atom %	-2.7	(143)
		$D=6.4 \times 10^{-5}$	800			C_1=23.1 atom % C_2=100 atom %		
Al	Mg	$D=6.1 \times 10^{-5}$ $D=7.5 \times 10^{-5}$	670 700					(11)
Al	Ni	$D=1.22 \times 10^{-5}$	700	FCSIR		C_1=0.145 atom % C_2=21.0 atom %		(143)
		$D=7.7 \times 10^{-5}$	1000			C_1=4.97 atom % C_2=21.0 atom %		
Al	Zn	$D=6.2 \times 10^{-5}$	700	FCSIR		C_1=100 atom % C_2=19.4 atom %	±0	(143)
		$D=14 \times 10^{-5}$	800			C_1=100 atom % C_2=29.5 atom %		
Bi	Ag	$D_o=62.0 \times 10^{-4}$ E =6400±800	300-700	CR	0.4-0.8	C_o=Trace Ag^{110} C_b=0.00	vs	(145)

TABLE 3 (continued)

Solvent	Solute	Experimental Results (a)	Temp Range °C	Exp. Method (b)	Path Diam. (mm.)	Solute Concentration Interval (c)	V^M% (d)	Reference
Bi	Au	D=5.23 x 10-5	550 (f)	FCSIR	12	I	-0.34 @0.4 N Sn	(12)
Bi	Sn	D_o=13.0 x 10^{-4} E =1500	450-600	TSIR	3	C_1=0-10 atom % C_2=0.00	+1.1	(99)
Bi	U	D=2.60 x 10^{-5}	500	FCSIR	12.2	C_1=100 atom % C_2=0.00		(12)
Cd	U	D=1.3 x 10^{-5} D=2.3 x 10^{-5}	450 650	CR	3.4& 4.2	C_o=1.4 wt. % C_b=0.00		(71)
Fe	Co	D=4.7 x 10^{-5} D=5.3 x 10^{-5}	1538 1638	FCSIR	1.0& 2.0	C_1=100 atom % C_2=0.00		(171)
Fe	Ni	D_o=0.9 x 10^{-4} E =3900	1256-1412	CR	2.0	C_o=0.00 wt. % C_b=1.41 wt. %		(168)
Fe	Ti	D_o=3.2 x 10^{-4} E =6400	1216-1440	CR	2.0	C_o=0.00 wt. % C_b=0.63 wt. %		(168)
Hg	Ba	D=0.62±0.016x10^{-5} (i)	7.8	SC	20	0.54-0.12 wt. %		(150)

TABLE 3 (continued)

Solvent	Solute	Experimental Results (a)	Temp Range °C	Exp. Method (b)	Path Diam. (mm.)	Solute Concentration Interval (c)	V^M% (d)	Reference
Hg	Bi	$D=0.99 \times 10^{-5}$	25	P		0.00075-0.00575 wt. %		(166)
Hg	Ca	$D=0.625 \pm 0.0225 \times 10^{-5}$	10.2	SC	20	0.1 wt %		(150)
Hg	Cd	$D=1.53 \times 10^{-5}$ $D=3.05 \times 10^{-5}$	25 148	ET (g)	(h)	0-2 atom %	+0.7	(90)
Hg	Cd	$D=1.81 \times 10^{-5}$ (i)	15		17	0.1 wt %	+0.7	(170)
Hg	Cd	$D=1.68 \pm 0.1 \times 10^{-5}$ (i) $D=3.43 \pm 0.1 \times 10^{-5}$	8.7 99.1	SC	20	0.116-0.150 wt %	+0.7	(150)
Hg	Cd	$D=1.66 \pm 0.03 \times 10^{-5}$	22	P		9.957-13.93 mM/liter	+0.7	(131)
Hg	Cd	$D=1.528 \times 10^{-5}$	20		40	I	+0.7	(26)
Hg	Cd	$D=1.53 \pm 0.076 \times 10^{-5}$	20	TSIR	4	0.9-1.5 wt %	+0.7	(155)
Hg	Cd	$D=1.52 \times 10^{-5}$	25	P		0.69-2.08 mM	+0.7	(142)
Hg	Cs	$D=0.52 \pm 0.02 \times 10^{-5}$ (i)	7.3	SC	20	0.119-0.169 wt %		(150)
Hg	Cu	$D=1.06 \times 10^{-5}$	25	P		0.0027-0.00189 wt %		(53)

TABLE 3 (continued)

Solvent	Solute	Experimental Results (a)	Temp Range °C	Exp. Method (b)	Path Diam. (mm.)	Solute Concentration Interval (c)	V^M% (d)	Reference
Hg	In	$D=1.47\pm0.03\times10^{-5}$	22	P		7.50-10.25 mM/liter	vs	(131)
Hg	K	(j)	589-800		6.1& 12.2		-25.	(13)
Hg	K	$D=0.614\pm0.038\times10^{-5}$ (i)	10.5	SC	20	0.0962-0.1713 wt %		(150)
Hg	Li	$D=0.765\pm0.052\times10^{-5}$ (i)	8.2	SC	20	0.1018-0.1821 wt %		(150)
Hg	Na	$D=0.74\pm0.02\times10^{-5}$ (i)	9.6	SC	20	0.0942-0.1846 wt %		(150)
Hg	Na	$D=0.80\pm0.05\times10^{-5}$	22	P		9.54-6.32 mM/liter		(131)
Hg	Pb	$D=1.58\times10^{-5}$	15.6		17	0.1 wt %	-0.7	(170)
Hg	Pb	$D=1.74\pm0.103\times10^{-5}$ (i)	10	SC	20	0.118-0.162 wt %	-0.7	(150)
		$D=2.22\pm0.035\times10^{-5}$	99.2			0.134-0.142 wt %		
Hg	Pb	$D=1.41\pm0.05\times10^{-5}$	22	P		10 mM/liter	-0.7	(131)

TABLE 3 (continued)

Solvent	Solute	Experimental Results (a)	Temp Range °C	Exp. Method (b)	Path Diam. (mm.)	Solute Concentration Interval (c)	V^M% (d)	Reference
Hg	Pb	$D=1.28 \times 10^{-5}$	25	P		0.69mM-2.08mM	-0.7	(142)
Hg	Pb	$D=1.16 \times 10^{-5}$	25	P		0.00158-0.00304 wt %	-0.7	(53)
Hg	Rb	$D=0.532 \pm 0.008 \times 10^{-5}$ (i)	7.3	SC	20	0.132-0.193 wt %		(150)
Hg	Sn	$D=1.77 \pm 0.074 \times 10^{-5}$	9.6-14.0	SC	20	0.124-0.162 wt %	-0.9	(150)
Hg	Sn	$D=1.68 \times 10^{-5}$	25	P		0.00041-0.00402 wt %	-0.9	(53)
Hg	Sr	$D=0.544 \pm 0.041 \times 10^{-5}$ (i)	9.4	SC	20	0.123-0.174 wt %		(150)
Hg	Tl	$D=0.99 \times 10^{-5}$	25	P		0.00216-0.00278 wt %	-0.7 @N= 0.5 Tl	(53)
Hg	Tl	$D=1.01 \pm 0.087 \times 10^{-5}$ (i)	11.0-12.0	SC	20			(150)

TABLE 3 (continued)

Solvent	Solute	Experimental Results (a)	Temp Range °C	Exp. Method (b)	Path Diam. (mm.)	Solute Concentration Interval (c)	V^M% (d)	Reference
Hg	Tl	$D=1.08 \times 10^{-5}$	25	CR	1.0	C_o=0.00 atom %		(52)
						C_b=0.71 atom %		
		$D=1.37 \times 10^{-5}$				C_o=4.62 atom %		
						C_b=6.11 atom %		
		$D=1.50 \times 10^{-5}$				C_o=7.97 atom %		
						C_b=9.93 atom %		
		$D=1.37 \times 10^{-5}$				C_o=13.8 atom %		
						C_b=15.8 atom %		
		$D=1.14 \times 10^{-5}$				C_o=17.8 atom %		
						C_b=19.8 atom %		
		$D=0.83 \times 10^{-5}$				C_o=26.0 atom %		
						C_b=29.8 atom %		
		$D=0.95 \times 10^{-5}$				C_o=30.6 atom %		
						C_b=33.7 atom %		
		$D=1.11 \times 10^{-5}$				C_o=38.8 atom %		
						C_b=42.0 atom %		

TABLE 3 (continued)

Solvent	Solute	Experimental Results (a)	Temp Range °C	Exp. Method (b)	Path Diam. (mm.)	Solute Concentration Interval (c)	V^M% (d)	Reference
Hg	Tl	$D=1.6 \times 10^{-5}$	25	P		0.001 wt %		(174)
Hg	Zn	$D=2.42 \times 10^{-5}$	15		17	0.01 wt %		(170)
Hg	Zn	$D=1.67\pm0.05 \times 10^{-5}$	20	SLC	4.0	N=0.235 wt %		(155)
		$D=1.61\pm0.05 \times 10^{-5}$				N=0.475 wt %		
		$D=1.57\pm0.02 \times 10^{-5}$				N=0.675 wt %		
Hg	Zn	$D=1.52\pm0.02 \times 10^{-5}$	20	SLC	4.0	N=0.85 wt %		(155)
		$D=1.47\pm0.02 \times 10^{-5}$				N=0.90 wt %		
Hg	Zn	$D=1.21 \times 10^{-5}$	30	CR	I	C_o=2.87 atom % C_b=4.30 atom %	-1.3	(127)

TABLE 3 (continued)

Solvent	Solute	Experimental Results (a)	Temp Range °C	Exp. Method (b)	Path Diam. (mm.)	Solute Concentration Interval (c)	V^M% (d)	Reference
Hg	Zn	$D=1.39 \times 10^{-5}$	30	CR	I	C_o=1.62 atom % C_b=2.64 atom %	-1.2	(127)
		$D=1.31 \times 10^{-5}$				C_o=1.42 atom % C_b=2.79 atom %		
		$D=1.70 \times 10^{-5}$				C_o=0.00 atom % C_b=1.63 atom %		
		$D=1.53 \times 10^{-5}$				C_o=0.00 atom % C_b=2.79 atom %		
Pb	Ag	$D_o=0.826 \times 10^{-4}$ E =1925	300-506	SLC	4.2	C_1=100 atom % C_2=0.00 atom %	vs	(116)
Pb	Ag	$D=2.95 \times 10^{-5}$	350	ET (g)	0.5-0.8	I	vs	(80)
		$D=4.50 \times 10^{-5}$	450					
		$D=5.1 \times 10^{-5}$	500					
Pb	Au	$D=3.51 \times 10^{-5}$	550 (f)	FCSIR	12	0.85-7.3 wt %		(120)

TABLE 3 (continued)

Solvent	Solute	Experimental Results (a)	Temp Range °C	Exp. Method (b)	Path Diam. (mm.)	Solute Concentration Interval (c)	V^M% (d)	Reference
Pb	Bi	$D_o=3.37 \times 10^{-4}$ $E=2760$	350-550	CR	0.79-1.20	C_o=1.7 wt % C_b=0.0 wt %	+0.3	(57)
		D_o=6.5 (k) $E=8150$				C_o=52.7 wt % C_b=0.00 wt %		
		D_o=4.1 (k) $E=9500$				C_o=100 wt % C_b=0 wt %		
Pb	Bi	$D_o=9.63 \pm 0.5$ $E=4070 \pm 546$	233-657	CR	1.24-1.63	C_o=Trace Bi	+0.3	(123)
Pb	Bi	$D_o=9.6 \times 10^{-4}$ $E=4200$	450-600	TSIR	3.0	C_1=0-10 atom % C_2=0.00 atom %	+0.3	(99)
		$D=6.6 \times 10^{-5}$	500			N=0.2 (1)		
		$D=7.4 \times 10^{-5}$				N=0.4		
		$D=8.5 \times 10^{-5}$				N=0.6		
		$D=7.5 \times 10^{-5}$				N=0.8		
Pb	Cd	$D_o=11.0 \times 10^{-4}$(m) $E=4800$	450-600	FCSIR	3.0		+0.8	(99)

TABLE 3 (continued)

Solvent	Solute	Experimental Results (a)	Temp Range °C	Exp. Method (b)	Path Diam. (mm.)	Solute Concentration Interval (c)	V^M% (d)	Reference
Pb	Cu	$D_o=2.7 \times 10^{-4}$	450-767	SLC	4.2	C_1=100 atom %		(55, 56)
		E =2963				C_2=0 atom %		
Pb	Na	$D=1.21 \times 10^{-5}$	400	CR	I	C_o=22.5 atom %		(96)
						C_b=0.0 atom %		
		$D=1.53 \times 10^{-5}$	500			C_o=12.7 atom %		
						C_b=0.0 atom %		
		$D=1.42 \times 10^{-5}$				C_o=22.5 atom %		
						C_b=0.0 atom %		
		$D=1.95 \times 10^{-5}$				C_o=38.0 atom %		
						C_b=0.0 atom %		
		$D=1.97 \times 10^{-5}$	600			C_o=12.7 atom %		
						C_b=0.0 atom %		
		$D=1.79 \times 10^{-5}$				C_o=22.5 atom %		
						C_b=0.0 atom %		
Pb	Pt	$D=1.96 \times 10^{-5}$	550 (f)	FCSIR	12	0.390-9.02 wt %		(120)
Pb	Rh	$D=3.51 \times 10^{-5}$	550 (f)	FCSIR	12	I		(120)

TABLE 3 (continued)

Solvent	Solute	Experimental Results (a)	Temp Range °C	Exp. Method (b)	Path Diam. (mm.)	Solute Concentration Interval (c)	$V^M\%$ (d)	Reference
Pb	Sb	$D_o=25 \times 10^{-4}$ $E=6400$	450-600	TSIR	3	C_1=0-10 atom % C_2=0.00 atom %		(99)
Pb	Sn	$D_o=12 \times 10^{-5}$ $E=5900$	450-600	TSIR	3.0	C_1=0-10 atom % C_2=0.00 atom %		(99)
		$D=4.0 \times 10^{-5}$	510	TSIR	3.0	N=10 atom % (n)		
		$D=3.6 \times 10^{-5}$				N=20 atom %		
		$D=3.1 \times 10^{-5}$				N=30 atom %		
		$D=2.4 \times 10^{-5}$				N=40 atom %		
		$D=1.75 \times 10^{-5}$				N=50 atom %		
		$D=1.85 \times 10^{-5}$				N=60 atom %		
Sn	Ag	$D_o=2.6 \times 10^{-4}$ $E=4200$	250-500	CR	0.75 1.25	C_o=0.2-0.7 wt % C_b=0.00	-4.7 @ N= 0.25	(88)
Sn	Ag	$D=4.79 \times 10^{-5}$	550 (f)	FCSIR	12	I		(120)
Sn	Al	$D_o=19 \times 10^{-4}$ $E=5200$	250-500	CR	0.75 1.25	C_o=0.2-0.7 wt % C_b=0.00		(88)

TABLE 3 (continued)

Solvent	Solute	Experimental Results (a)	Temp Range °C	Exp. Method (b)	Path Diam. (mm.)	Solute Concentration Interval (c)	V^M% (d)	Reference
Sn	Au	$D=5.38 \times 10^{-5}$	550 (f)	FCSIR	12	I	+0.6 @ N= 0.5	(120)
Sn	Bi	$D_o=5.2 \times 10^{-4}$ $E=3200$	450-600	TSIR	3	C_1=0-10 atom % C_2=0.00	+1.1	(99)
Sn	Co	$D=2.7 \times 10^{-5}$	350	ET (g)	0.73	I		(80)
		$D=17 \times 10^{-5}$	350	ET (o)	0.73	I		
Sn	Cu	$D_o=1.8 \times 10^{-4}$ $E=4200$	250-500	CR	0.75	C_o=0.2-0.7 wt % C_b=0.00	-7.3 @ N= 0.75	(88)
Sn	Ni	$D_o=2.3 \times 10^{-4}$ $E=4530$	250-500	CR	12	I		(120)
Sn	Pb	$D=3.68 \times 10^{-5}$	550 (f)	FCSIR	12	I		(120)
Sn	Sb	$D_o=3.3 \times 10^{-4}$ $E=2800$	450-600	TSIR	3	C_1=0-10 atom %		(99)
Sn	Zn	$D_o=6.2 \times 10^{-4}$ $E=4880$	250-500	CR	0.75 1.25	C_o=0.2-0.7 wt % C_b=0.00		(88)

Abbreviations for Table 3

CR = Capillary reservoir technique

ET = Electrotransport method

FCSIR = Finite cylinder semi-infinite rod technique

I = Indeterminate from information given by investigator

P = Polarography

SC = Shear cell

SLC = Solid Liquid contacting technique

TSIR = Two semi-infinite rods

vs = very small

Notes for Table 3

(a) Results have been reported in various ways. D refers to the diffusion coefficient and has units of cm^2/sec. D_o is the pre-exponential term in the equation $D=D_o exp(-E/RT)$ and has units of cm^2/sec. E has units of cal/gr. atom.

(b) The major experimental methods are discussed elsewhere in this review. The abbreviations are listed above.

(c) Concentration intervals are given where available. For the capillary reservoir technique C_o refers to the initial concentration of solute metal in the capillary and C_b to the same in the bath. In the TSIR, FCSIR, and SLC techniques, C_1 and C_2 refer to the initial

concentrations of solute in the two phases. The concentrations noted for the polarography experiments refer to the amalgam composition of the dropping mercury electrode.

(d) Little information is available regarding the volume change on mixing of the pure components for liquid metal alloys. The values of V^M reported here were taken from Wilson (157).

(e) Urema's data (143) exhibits extreme temperature dependence.

(f) The actual experimental temperature for the Roberts-Austin (120) investigation is uncertain. It appears to have varied from 500 - 550°C during the investigation.

(g) Data obtained from electrotransport experiments in the absence of an electric field.

(h) Mangelsdorf used a rectangular channel of dimensions 0.025 mm by 2.0 mm.

(i) The data of von Wogan and Meyer have been disputed by Weischedel and Cohen and Bruins.

(j) Bonilla's results exhibit a greater variation in magnitude of the diffusion coefficient than is expected for liquids. Also, the data was not taken at constant pressure due to the large vapor pressure of potassium amalgams (the pressure varied from atmospheric to 400 psig).

(k) Grace and Derge report this data as "effective diffusion coefficients" They note that Fick's law is no longer valid for describing diffusion

since large concentration gradients existed.

(l) Niwa employed a large concentration interval to determine this data.

(m) Niwa appears to have used incorrect equation to calculate this result from experimental quantities.

(n) Niwa used concentration range of about 60 atom %.

(o) This diffusion coefficient was obtained from electrotransport experiment with field. It undoubtly contains a large convective component.

Concentration Dependency of Diffusion Coefficients

The composition dependency of diffusion coefficients has been studied for a number of binary liquid metal systems. Interdiffusion coefficient data for bismuth in tin (99), bismuth in lead (57,99,124), zinc in mercury (127), lead in tin (99), and sodium in lead (96) are presented in Table 3. The concentration dependency of self diffusion coefficients in binary alloys has also been investigated. Coefficients for indium in indium-tin alloys (22, 103, 147), zinc in zinc-lead alloys (76), zinc and mercury in zinc-mercury alloys (127), and for thallium in thallium amalgams (51) are presented in Table 2.

Darkin (32) has derived an expression relating the interdiffusion coefficient, D_{AB}, to the self diffusion coefficients of the pure components, D_A^* and D_B^*, and a thermodynamic quantity which is a function of composition.

$$D_{AB} = (N_B D_A^* + N_A D_B^*)\left[1 + \frac{d \ln a_A}{d \ln N_A}\right] \qquad (6)$$

a_A = Activity coefficient of A

N_A = Atom fraction of A

N_B = Atom fraction of B = 1 - N_A

A number of investigators have noted that an alloy exhibiting a negative deviation from Raoult's law should have a maximum in the relationship between diffusion coefficient and composition because the thermodynamic term in equation (6) has a maximum for this type deviation from

ideality. Likewise, alloys with positive deviations from Raoult's law can be expected to exhibit a minimum, while for those which behave ideally the diffusion coefficient should be nearly constant as the composition is varied. Niwa (99) has shown this to be qualitatively true for the systems lead-bismuth, lead-tin, and tin-bismuth which exhibit positive deviations from Raoult's law, negative deviations, and nearly ideal behavior respectively. Yang and Derge (158) have pointed out the above reasoning implies the term $(N_B D_A^* + N_A D_B^*)$ does not vary appreciably with composition. This is not necessarily true. Schadler and Grace (127) measured self and interdiffusion coefficients for the zinc-mercury system. Their results show that variation of the term $(N_B D_A^* + N_A D_B^*)$ accounts for two-thirds of the total variation of the interdiffusion coefficient with composition.

Foley et. al. (51, 52) have investigated self and interdiffusion coefficients for thallium in thallium amalgams. They found that at liquid compositions corresponding to the existance of compounds in the solid state the tracer diffusion coefficients were low. They attribute this to high attractive forces between constituents in solution.

Bearman (8) shows that for regular solutions the product of the diffusion coefficient and the viscosity should be constant.

Pressure Dependence of Diffusion Coefficients

Some investigations have been made to determine the effect of pressure on diffusion coefficients of liquid metals. If diffusion and

viscous flow are thought of as similar kinetic processes, then it is expected that both will be affected in a similar manner by the application of pressure. This similarity of behavior has been found experimentally.

Nachtrieb and Petit (98) investigated the decrease in the self diffusion coefficient of mercury with increasing pressure. They found a linear dependence of log D on the melting point of mercury T_m.

$$\text{Log}_{10}\ D = \frac{-0.572\ T_m}{T} - 4.343 \qquad (7)$$

For self diffusion in gallium, Nachtrieb and Petit (97) report the following relationships

$$\text{Log}_{10}\ D = \frac{1.332\ T_m}{T} - 6.104 \qquad (8)$$

$$\text{Log}_{10}\ \mathbf{D} = -4.7793 - 9.529\text{x}10^{-6}P\ \frac{kg}{cm^2} \qquad (9)$$

Cohen and Bruins (26) investigated the influence of pressure on the diffusion coefficient of cadmium in mercury. At 1 atmosphere and 20°C they found a value of 1.52×10^{-5} cm^2/sec, while at 1500 atm and 20°C the value was 1.446×10^{-5} cm^2/sec.

Each of these investigations shows that increasing the pressure caused a decrease in the diffusion coefficient. This is consistent with the theory, to be discussed later, that a liquid contains free volume. When the pressure is increased this free volume is decreased

as the atoms are forced into closer proximity with each other, their motions are more restricted and their diffusion coefficient is lowered.

Diffusion Near the Melting Point

The diffusion coefficient of a substance rises rapidly in the vicinity of its melting point. Its value often increases by a thousand-fold or more.

Meyer and Nachtrieb (93, 94) have investigated the self diffusion of both liquid and solid sodium to within 0.1°C of its melting point. They found the transition occurs just as abruptly and simultaneous with the discontinuous melting process itself.

Eckert and Drickhamer (42) investigated self-diffusion of indium near the melting point and tracer diffusion of thallium in indium near its melting point. Diffusion coefficients were obtained in three regions. First for the solid to 1°C below the melting point, second in the region from 1°C below the melting point to the melting point, and third in the liquid 1-2°C above the melting point. Diffusion in both polycrystalline and single crystals of indium was investigated. For diffusion of thallium in polycrystalline indium a rapid rise was found to begin 1°C below the melting point and continue for approximately 0.4°C after which a linear increase continued into the liquid state. For thallium diffusion in single crystals of indium the rapid rise took place near the melting point of the indium but still occurred over a finite interval of 0.1°C. This difference was interpreted as strong evidence the

grain boundaries melt below the measured melting point. For self diffusion in polycrystalline indium the rise occurs about 0.6°C below the melting point and is more sharp than that for thallium in indium. The rise for self diffusion in a single crystal occurred about 0.05°C higher than that for polycrystalline indium. Eckert and Drickhammer note that this melting phenomena may be explained by grain boundary melting but also probably includes a high degree of lattice dislocations at this temperature.

The coefficients that Eckert and Drickhammer obtained for diffusion in the liquid phase were subject to large experimental error because the method they used was not particularly suited to liquid phase measurements.

C. REVIEW OF EXPERIMENTAL METHODS

Introduction

Unlike the study of diffusion in aqueous and organic systems, it is not possible to use optical methods to study diffusion in liquid metals. The principal advantage of optical methods is that it is possible to determine the rate at which material enters the diffusion path. From this, anomalies such as disturbances during the initial part of the experiment can be detected. A method has been developed by this writer which permits observation of this rate from electrical measurements on a liquid metal concentration cell. This method is discussed in detail elsewhere in this thesis and will not be included in the discussion that follows.

A number of the methods discussed below employ a diffusion path with a diameter ranging from a half to several millimeters. Small paths are used to reduce the liklihood of convection. For purposes of mathematical analysis the interface between the solute and diffusate is taken to be planar. In reality the interface is non-planar for small diameter paths. This is due to factors such as the degree to which the solute and solvent wet the material of which the path is constructed and the manner in which the phases are brought into contact. For methods in which only the total quantity of material transferred is accessible, the existence of a non-planar interface will lead to a value of the diffusion coefficient larger than the true one.

This effect is discussed in detail elsewhere in this thesis. In experimental situations where the length of the experiment is one or two hours the error will be about 2% for a semi-spherical interface.

The principal experimental methods used to investigate diffusion in liquid metals are discussed below. The advantages and limitations of each are considered. Since, all of these methods are subject to convection, this subject is not discussed in detail here. Rather a subsequent section of this review is devoted to convection and wall effects.

Capillary-Reservoir Technique

The capillary reservoir technique was first used to measure liquid metal diffusion coefficients by Roberts-Austin (120) in the late nineteenth century. Later, Anderson and Saddington (2) introduced the use of radioactive tracers with this technique.

A capillary with one end closed is filled with a solute metal or an alloy of the solute with a solvent of known concentration. This capillary is immersed in a large bath of solvent metal, the reservoir. After a measured time the capillary is removed from the bath and the composition of the material in the capillary is determined and compared with the initial composition of metal in this capillary. The diffusion coefficient is determined from this information.

Liquid metals have high thermal conductivities and the bath serves to maintain a uniform temperature throughout the diffusion path. It

should be noted that sometimes it is desirable to maintain the top of the capillary at a slightly higher temperature than the bottom to minimize the possibility of convection initiated by thermal density inversions.

The capillary may be positioned in the bath with the open end either up or down. The lower density material must of course be on top of the higher density material to avoid density inversions. Normally the capillary is arranged vertically in the bath. Leak and Swalin (83) state that a tilted position is more desirable than a vertical position for reducing convection effects. A tilted position would, however, most surely lead to density inversions if the surfaces of constant concentration advancing in the capillary are non-planar. Such non-planar profiles are likely to result from initial disturbances near the mouth of the capillary.

Diffusion of tracers or solute may proceed either from the capillary alloy to the bath alloy or visa versa. Hesson and Burris (71) investigated diffusion of uranium in bismuth and found greater accuracy was possible when the labeled uranium diffused from the capillary to the bath.

Early investigators who used the capillary reservoir technique used Fick's first law to calculate diffusion coefficients from the slope of the concentration gradient in sections of the capillary column of metal after diffusion had been allowed to proceed for a known period of

time. The concentration gradient in the diffusion column was determined by chemical analysis. This procedure suffers from two major sources of error. First, the sections obtained are often irregular and estimation of the concentration profile based on their analysis is difficult. Second, shrinkage of the alloy during cooling and solidification distorts the concentration gradient. Careri (22) discusses corrections which may be made to compensate for alloy shrinkage upon cooling.

Anderson and Saddington (2) introduced the use of radioactive tracers in the capillary reservoir technique. Radiochemical analysis can be made to obtain both the gradient of the tracer in the diffusion path and the overall amount of tracer which has entered or left the capillary. When the tracer employed has a short half-life, corrections must be made for its decay subsequent to the diffusion experiment. The major advantage of this method is that in addition to permitting study of interdiffusion, it is possible to study self diffusion which cannot be studied without radioactive tracers.

Anderson and Saddington have described diffusion within the capillary with Fick's second law. For the case where the diffusion coefficient is constant

$$\frac{\partial C}{\partial t} = D \frac{\partial^2 C}{\partial x^2} \quad , \quad 0 < x < L \, , \quad t > 0 \qquad (10)$$

The x-axis is selected to coincide with the axis of the capillary and distance is measured from the closed end, L=0. The initial concentration of material in the capillary is C_o.

$$C(x,o) = C_o \quad , \quad 0 < x < L \tag{11}$$

Convective transfer in the bath is assumed sufficient that the concentration of the solute at the open end of the capillary is zero.

$$C(L,t) = 0 \quad , \quad t > 0 \tag{12}$$

If no appreciable concentration changes occur at the closed end of the capillary

$$\frac{\partial C(o,t)}{\partial x} = 0 \quad , \quad t > 0 \tag{13}$$

Equation (10) may be solved with initial condition (11) and boundary conditions (12) and (13) to obtain the concentration profile C(x,t) in the capillary. Since only the total amount of material transferred from the capillary to bath is calculated, C(x,t) must be integrated over the length L of the capillary. If $\bar{C}$ denotes the average concentration of the diffusing species in the capillary at time t, the integration yields the following:

$$\bar{C} = \frac{8}{\pi^2} \sum_{n=0}^{\infty} \frac{C_o}{(2n+1)^2} \exp\left[- \pi^2 (2n+1)^2 \frac{Dt}{4L^2} \right] \tag{14}$$

when $Dt/h^2 > 0.25$ the series converges rapidly and its first term gives a good approximation of $\bar{C}$. Solving this expression for D gives,

$$D = \frac{4L^2}{\pi^2 t} \ln \frac{\pi^2}{8} \frac{\bar{C}}{C_o} \qquad (15)$$

When this equation is used it is important the volume of the capillary be known accurately in order to calculate $\bar{C}$. Also, the experiment must be terminated before any appreciable concentration change occurs at the closed end of the capillary. Kassner et. al. (76) have performed experiments where significant changes did occur at the closed end of the capillary. Equation (14) is not applicable. Instead, the series solution of Carslaw and Jaeger (25) for finite geometry was used. In addition to knowing the volume of the capillary accurately when reflection at the closed end occurs it is necessary this closed end be flat and perpendicular to the axis of the capillary so as not to distort the cross-section of the diffusion path.

Grace and Derge (57) treat diffusion between the capillary and bath as a case of mass transfer through a unit area of surface on a slab of infinite thickness. They solve Fick's second law with boundary conditions similar to those used by Anderson and Saddington. The two differences between the solutions are: Grace and Derge take the origin of their coordinate system at the open end of the capillary, and they designate the concentration of the diffusate in the bath to be C_b instead of zero. Their solution yields the following expression for the

diffusion coefficient.

$$D = \frac{\pi}{t}\left[\frac{L}{2}\,\frac{C_o - \bar{C}}{C_o - C_b}\right]^2 \qquad (16)$$

Hesson and Burris (71) have presented a solution of Fick's second law with conditions similar to Anderson and Saddington. They too have taken the origin of the coordinate system at the open end of the capillary. When their solution is rearranged it is found to be identical with that of Grace and Derge. All of these solutions assume no molal volume changes occur within the capillary during diffusion.

Rastas and Kwalo (117) discuss two sources of error in the capillary reservoir technique. First, is the "immersion effect" arising from mixing of the capillary alloy and the bath alloy when the capillary is initially immersedin the bath. The initial condition $C(x,0)=C_o$ is not fulfilled when this occurs. Instead the initial condition may be approximated as $C(x,0)=\varphi(x) = C_o$. Rastas and Kwalo treat $\varphi(x)$ as a continuous function and derive an expression for $\ln \bar{C}$ possessing linear dependence on time t.

$$\ln\ \bar{C}(t) = -\frac{\pi^2 D}{4L^2} + \ln a_o \qquad (17)$$

where a_o is an integral involving the initial distribution $\varphi(x)$, which is unknown. It is possible to determine the coefficient $\pi^2 D/4h^2$ in equation (17) from a series of runs. $(t_1, \ln \bar{C}_1),\ldots(t_n,\ln \bar{C}_n)$, from

which D can be established. Brown and Tuck (18) have shown the self diffusion coefficients of mercury calculated from short runs were greater than for longer runs. This is probably due to a small amount of interfacial mixing when the two phases were first contacted and supports the existence of an immersion effect as postulated by Rastas and Kwalo.

Rastas and Kwalo discuss a second source of error which they refer to as the "Δl effect". This effect will be present if the boundary condition expressed in equation (12) is not maintained at the mouth of the capillary. This effect may better be referred to as the "end-effect". If the velocity of material in the bath moving past the mouth of the capillary is too low, there will be an accumulation of diffusate at this point which will reduce the efflux as compared with the ideal case. This will give a low value of the diffusion coefficient. Several investigators have provided for rotation of the capillaries in the bath at various speeds or have stirred the bath to aid mass transfer. However, if the velocity of the fluid moving past the mouth of the capillary becomes too great, not only is the diffusate leaving the capillary swept away by the liquid flow, but a sufficient drag force is exerted on the fluid inside to cause it to flow out. A high value of the diffusion coefficient will then be obtained. Stirring, in addition, may cause vibration in the apparatus which increases the liklihood of convection in the capillary. Borucka et. al. (14) have confirmed this effect in their experiments with aqueous dye. They point

out the difficulty in selecting the correct rotation speed which depends on the value of the diffusion coefficient. They developed a holder for their capillaries in which the mouth of the capillary was flush with the surface of the rotating disc. With this arrangement, desirable hydrodynamic patterns were obtained to sweep away the efflux at the mouth of the capillary with a minimum of flow disturbance in the proper of the capillary.

Mangelsdorf (90) discusses the end effect for diffusion from an aperture. If the efflux is not rapidly removed from the region near the aperture, the local concentration build up in the bath may be thought of as increasing the effective length of the capillary. Most of the diffusional flow will take place near the perimeter of the aperture because the concentration gradient is largest there. Mangelsdorf concludes a cylindrical capillary is the worst possible choice of geometry for end effects because the perimeter is a minimum with respect to the cross-sectional area. Mangelsdorf shows the end effect for a channel 0.025 mm thick by 2 mm in width will have only one tenth the end effect of a cylindrical capillary 0.6 mm in diameter even though the diffusive capacities are about equal.

The solutions of Fick's law above hold only for capillaries of uniform bore. It is often difficult to obtain uniform diameter capillaries of fused silica and other materials useful for the investigation of diffusion in liquid metals at very high temperatures. Talbot et. al.

(137) have solved Fick's second law for a slightly tapered capillary with initial and boundary conditions identical to those used by Anderson and Saddington. They obtain a correction factor which can be applied to data taken with slightly tapered capillaries.

The use of the capillary-reservoir technique requires the development of considerable experimental technique. Chemical and radiochemical analysis are tedious for the small concentration changes desirable to minimize volume changes during interdiffusion. The alloy and the capillary must be thoroughly outgassed to prevent the formation of small gas bubbles in the capillary which will distort the cross-sectional area of the diffusion path. Nachtrieb et. al. (97) report difficulty was encountered in filling of capillaries so traces of gas entrapped at the closed end would not force metal out of the capillary upon melting.

Shear Cell

This method has been used by Nachtrieb and Petit (98, 107) to investigate self diffusion in liquid mercury and gallium.

The shear cell consists of several discs mounted coaxially. These discs have off-center holes drilled in them which may be aligned to form the diffusion path. The solvent and solute metals are kept separated until the run is begun by aligning the holes which make up the diffusion path. At the conclusion of the run the discs are again rotated to misalign the compartments. The diffusion coefficient is obtained from the slope of the concentration gradient calculated from

analysis of the alloy composition in each compartment.

The major disadvantage of this technique is, possible stirring may occur when the discs are rotated at the conclusion of the experiment. The magnitude of this mixing is probably dependent on the length to diameter ratio of each of the compartments. The larger this ratio the less mixing will occur. This method, like the capillary-reservoir technique, keeps the solvent and solute metals separated until the actual diffusion run is begun. Unlike some of the methods to be discussed, there is no premature contacting of the phases with attendendant uncertainty in the time or temperature of the run.

A major advantage of this method is its usefullness for measuring diffusion coefficients at elevated pressures. The capillary-reservoir technique is not easily adapted to high pressure measurements. The volume of the system must be kept small and there is no room for stirring. In their determination of the self diffusion coefficient of mercury, Nachtrieb and Petit filled the pressure bomb with hydraulic silicone fluid and pumped the system up to pressure. The pressure was transmitted to the metal in the column via the thin films of hydraulic fluid between the discs.

von Wogau (150) used the shear cell technique to determine diffusion coefficients of metals in mercury at low temperature. The diameter of his path, 20 mm, and its length to diameter ratio of 2.5 are both extremely unfavorable with respect to suppression of convection. It is also hard to conceive how a path of this large diameter could be

sheared at the conclusion of the experiment without introducing significant mixing in the diffusion path.

Two Semi-Infinite Rods

This technique which has often been used to study diffusion in the solid state has been applied to liquid metals. A capillary is half filled with solute or an alloy thereof and half with the solvent metal (alternatively half may be filled with metal containing radioactive tracers of the solute metal and half with inactive metal). The capillary and metals are heated rapidly to a desired temperature and the solute or tracer metal diffused into the solvent or inactive metal. After a period of time the capillary is cooled rapidly. The diffusion coefficient can be obtained from measurements of the concentration of solute or tracer activity at various points along the rod.

Many of the experimental details which apply to the capillary reservoir technique also apply here. To reduce the possibility of convection, a capillary path is used. The top of this capillary is kept a few degrees warmer than the bottom. The same precautions with regard to radioactive counting must be observed.

This technique has its unique problems which must be considered. If the metal which is placed in the lower section of the capillary has a similar or higher melting point than the metal in the upper section it is necessary to melt the metal in the lower section before the metal in the upper section is added. Otherwise, metal from the upper section

will descend into the gap between the metal in the lower section and the wall of the capillary. Careri et. al. (21) note that care must be taken during melting and solidification of the metals to keep the strata parallel in the liquid and solid phases. They attempted to do this by allowing the change of state to occur slowly over a period of twenty minutes. Even when observing precautions like this, the interface between the two metals is likely to be non-planar if one of the metals wets the capillary wall better than the other.

Unlike the capillary reservoir technique in which the metal in the capillary and that in the reservoir can be kept separate until the experimental apparatus is at the desired temperature, the two rods of metal in this method are in contact during the heating and cooling periods as well as during the diffusion period. Diffusion will indeed occur during the heating and cooling periods and will not be limited to the so-called "diffusion period". This consideration renders the technique most useful when the two metals melt at similar temperatures and where diffusion is to be studied at temperatures not too far removed from these melting points. Careri et. al. (21) attempt to make a correction for the diffusion which occurs during heating of the system from the melting point to the desired temperature and subsequent cooling at the conclusion of the experiment. They calculate a mean temperature for diffusion which is slightly lower than the maximum temperature attained during the cycle. The estimation of this mean temperature is difficult due to two considerations. First, diffusion in liquids is

a strong function of temperature and the coefficient will be changing during the heating and the cooling periods. The solutions of Fick's law available for the geometry of this system apply to isothermal diffusion. Second, the error introduced by diffusion which occurs during the heating period is much greater than that introduced during the cooling period. During the heating period the concentration gradient is very steep and the flux is large. As much redistribution of material will occur during the first several minutes of the experiment as will occur during the remainder. Thus, in this technique a very significant portion of the diffusion occurs during a time interval when the temperature is different from that which is identified with the remainder of the run. This uncertainty in the experimental conditions may be interpreted as one of a question of the length of the run rather than of the temperature of the run. This consideration, the large amount of diffusion which occurs during the initial several minutes of the experiment, leads this writer to question Careri's procedure in allowing melting to occur over a long period of time.

The time of diffusion at the maximum temperature attained by the system must be long enough to offset the initial period. It must also, however, be kept short enough so the system is essentially infinite and significant concentration changes do not occur at the upper and lower ends of the path.

Diffusion in this type experiment can be described by Fick's second law with the following initial conditions.

$$C(x,0) = C_o \qquad x < 0 \qquad (18)$$

$$C(x,0) = 0 \qquad x > 0 \qquad (19)$$

The boundary conditions for no concentration changes at the ends of the rods are;

$$\lim_{x \to \infty} C(x,t) = C_o \qquad (20)$$

$$\lim_{x \to +\infty} C(x,t) = 0 \qquad (21)$$

The appropriate solution of Fick's law is,

$$C(x,t) = 1/2\ C_o\ \mathrm{erfc}\left(\frac{x}{2\sqrt{Dt}}\right) \qquad (22)$$

Careri et. al. (22) discuss errors involved in evaluation of the diffusion coefficient from the concentration profile. In their early experiments (20, 21), the coefficient were evaluated from the slope of the penetration curve in the concentration intervals $15\%\ C_o < C < 35\%\ C_o$ and $65\%\ C_o < C < 85\%\ C_o$. Where C_o is the initial concentration of the solute or radioactive tracer in one of the rods and its initial concentration in the other is zero. Subsequent investigation (22) of the error involved in evaluating the diffusion coefficient from different points on the curve showed the best values could be obtained in the

region 3% $C_o < C < 20\%$ C_o. Points lying in the region 20% $C_o < C <$ 30% C_o and 70% $C_o < C < 90\%$ C_o were found to give diffusion coefficients with large experimental error.

When the metals solidify contraction occurs in both the longitudinal and radial directions. Careri et. al. (22) discuss corrections which can be made to establish the true concentration profile.

Finite Cylinder and Semi-Infinite Rod

Diffusion coefficients may be obtained by allowing diffusion to occur from a finite cylinder into a semi-infinite rod. A small quantity of solute or alloy thereof is placed either on top of, or below a long rod of the solvent metal. This is heated to the desired temperature and diffusion is allowed to proceed for a known interval of time. The system is then cooled and the diffusion coefficient obtained from the concentration profile of the solute. The experiment must be terminated before appreciable concentration change occurs at the far end of the long rod.

This method is similar to the one employing two semi-infinite rods of metal. Diffusion between solute and solvent during the heating period is a problem and the method is best applied to systems where diffusion is to be investigated in the vicinity of the melting point.

Fick's second law can be solved with appropriate initial and boundary conditions. For the case where the thickness of the solute cylinder is small compared to the penetration distance for diffusion, the follow-

ing solution has been obtained by Crank (31).

$$C = \frac{M}{\sqrt{\pi Dt}} \exp\left(-\frac{x^2}{4Dt}\right) \qquad (23)$$

where M is the total quantity of solute per unit area of cross-section of the cylinder.

Niwa et. al. (99) have used this method to determine diffusion coefficients for the lead-cadmium system. Instead of the above equation for the semi-infinite system they mistakenly used the expression for diffusion in an infinite system. The difference between the two being, for the infinite system the term on the right-hand side of equation (23) is divided by two. Thus, the diffusion coefficients reported for this system is probably in error by a constant factor. The alternative is a misprint in their article.

Urema (143) has used this technique to study diffusion of solutes in aluminum. He uses the solution of Fick's law where the thickness of the finite cylinder is not negligible by comparison to the penetration distance. For a solute cylinder of thickness h_c.

$$C = \frac{C_o}{2}\left[\operatorname{erf}\left(\frac{h_c + x}{2\sqrt{Dt}}\right) + \operatorname{erf}\left(\frac{h_c - x}{2\sqrt{Dt}}\right)\right] \qquad (24)$$

The thickness of the finite cylinder was approximately 1/6th the longitudinal dimension of the diffusion path.

Solid-Liquid Contacting

Diffusate may be introduced into a liquid metal by contacting a solid metal with the liquid. The solid metal dissolves and once in solution diffuses away from the interface. The concentration of the diffusate in the liquid at the interface is equal to its solubility in the liquid at the particular temperature if no interfacial resistence exists. In this case the diffusion coefficient can be directly related to the total amount of diffusate which has entered the liquid phase during a given period of time. Gorman (55) presents mathematical solutions of Fick's law for diffusion in the liquid both with and without interfacial resistance. Analysis of Gorman's data for the diffusion of copper in lead indicates that interfacial resistance is negligible.

Since, the solid metal is located at the bottom of the path, this method is applicable to alloys where the solution of the solute metal is denser than the pure solvent metal. If the solid were located at the top, problems would be encountered due to expansion or contraction of the liquid. In the case of contraction, the liquid level would drop away from the solid phase and terminate diffusion.

This method is akin to the electrochemical concentration cell method proposed by this writer in so for that the rate of solute transfer to the diffusion path is dependent on diffusion away from the interface where this solute is introduced. The concentration cell technique has the added advantage that it is possible to observe the

rate of transfer and not just the overall transfer as is the case for this method.

Electrotransport

Diffusion coefficients may be obtained with electrotransport experiments. Basically, a current is passed through a capillary column of metal. Under the influence of the potential gradient, components of this metal migrate toward the electrodes at the ends of the capillary column of metal. Diffusion coefficients may be obtained from data obtained with the presence of the electric field, or by watching back diffusion when the field is removed.

Lodding (87) measured self diffusion coefficients for rubidium, potassium and indium. His coefficients were obtained for separation data of isotopes such as K^{39} and K^{41}.

Kuzmeynko (80) calculated diffusion coefficients for silver in lead and for cobalt in tin using electrotransport data. He reports coefficients both with and without the electric field. The coefficients obtained with the field are significantly greater than those obtained without a field. High current densities must be employed in electrotransport experiments to effect a significant separation. Density gradients in the metal arise due to the ohmic heating which accompanies these high current densities. The density gradients give rise to convection which is responsible for the high values of diffusion coefficients obtained with the field. Rohlin and Lodding (122) have

investigated self diffusion of potassium using the capillary-reservoir technique. They conclude the self diffusion coefficients obtained earlier by Lodding (87) were too large. This discrepancy was attributed by the authors to convection in the electrotransport experiments.

Angus (3) calculates diffusion coefficients for copper diffusing in bismuth from electrotransport data. The values obtained are generally larger than expected for liquids and show considerable scatter. Angus concludes convection probably affected the results.

Mangelsdorf (90) performs electrotransport experiments in a specially designed ribbon cell. The metal is contained in a channel of one thousandth of an inch thickness and one millimeter in width. The large surface area to volume ratio allows more efficient dissipation of the heat generated. After a separation has been effected the current is turned off and the rate of back diffusion observed by measurement of the resistance between probes at different points along the channel. The diffusion coefficient is calculated from this data.

Polarography

Polarography is a highly developed technique when used to determine diffusion coefficients on the solution side of a dropping mercury electrode. In order to measure diffusion coefficients in mercury that is within the drop, the technique must be modified. Instead of a pure mercury electrode, a dropping amalgam electrode is used. It is necessary to develop an expression similar to the Ilkovic equation for the current

produced by the diffusion of metal atoms as they diffuse from the interior to the surface of the drop. The major problem arises in evaluating the constants for the equation developed. Unlike the case of diffusion on the solution side, no wealth of data is available. Furman and Cooper (53) who used this technique admit there was only one piece of data reliable enough to use for evaluation of the three constants in the equation. This was a value of the diffusion coefficient for zinc in mercury at 0.235 wt% amalgam composition obtained by Weischedel (155). Furman and Cooper's coefficients for the diffusion of lead, copper and tin in mercury are therefore dependent on the accuracy of Weischedel's data. Thus, polarography is an indirect rather than a direct method of measuring diffusion coefficients in liquid metals. In view of the limited data avilable from which to evaluate the constants in the equation for the diffusion coefficient as a function of limiting current, the coefficients calculated from polarographic work are suspect.

D. CONVECTION AND SURFACE EFFECTS

Introduction

Recent investigations have shown that selection of the path diameter in experiments to measure the diffusion coefficients of liquid metals is critical. A survey of the literature reveals two opposing phenomena which must be considered. First is convection. Even with carefully controlled experimental conditions it is possible that circumstances will arise either intermittently or continuously that may lead to convection. In general it appears the smaller the diameter of the diffusion path, the less the liklihood of convection. The second consideration is that of surface or wall effects. These are not completely understood at present but are probably related to chemical or physical interaction of the metal with the material of which the wall is composed or impurities present in this wall.

It is desirable to select the optimum path diameter to minimize the influence of these effects on the values of the diffusion coefficient obtained. Careri et. al. (22) have concluded that a diameter of 1.6 mm appeared best for studying diffusion in indium. This path gave substantially the same values as a path two millimeters in diameter indicating that convection was not a problem. It also gave values of the diffusion coefficient significantly different than values obtained with paths of 0.83 and 1.0 mm diameters where wall effects seemed to be significant. Sufficient data is not available to make as critical a

choice for most other systems. However the value of 1.6 mm seems reasonable to this writer in view of the data available.

These two phenomena are discussed in detail below.

Convection

Convection is a longer range phenomena of mixing than is molecular diffusion. It results from disturbances such as density inversions (dense material on top of lighter material) and vibration in the apparatus.

A number of investigators have observed convection in diffusion experiments with liquid metals. The presence of gross convective effects will result in values of the diffusion coefficient which are much larger than is expected for liquids and usually exhibit a considerable degree of scatter. Morgan and Kitchner (171) in their study of molten iron observed convection in capillaries with diameters greater than 2 mm. Rothman and Hall (123) attempted to measure diffusion in lead with a shear cell having a path diameter of 7 mm. They were unsuccessful due to convection which produced scatter in their results. Gorman and Preckshot (56) and Preckshot and Hurdlick (116) studied diffusion of copper and of silver in lead respectively. In both cases a sharp transition was observed at which point the value of the diffusion coefficient increased by more than an order of magnitude when the temperature was increased. This was attributed to convection and is probably due to a combination of the decreasing viscosity of the metal and the

greater difficulty in eliminating thermal gradients in the cell as the temperature is increased. Careri et. al. (21) found that negative temperature gradients (bottom of diffusion column warmer than top) as small as 0.1 °C/cm were sufficient to cause turbulence. Usually the top of the diffusion path is kept warmer than the bottom to prevent this. There appears to be two cases where, even this precaution, may not eliminate density inversions leading to convection. The first, which is widly recognized, is present in electrotransport experiments where the high current density in the metal cuases local ohmic heating. The second, which to this writer's knowledge has not been pointed out by other investigators, is present in very non-ideal systems where a strong exothermic reaction accompanies diffusion. Evolution of thermal energy at a particular composition corresponding to association in the liquid can cause local density inversions. This seems to be a reasonable explanation for the inordinately high values of the diffusion coefficient which Bonilla et. al. (13) obtained for the diffusion of potassium in mercury.

There have been a number of other investigations in which the diffusion coefficients have been found to be sensitive to the path diameter. Usually the variation is limited to 5 or 10%. While this variation may be due in part to convection there is strong evidence that surface phenomena, which becomes more perceptable as the diameter of the capillary is decreased and the surface area to volume ratio rises, are responsible for this affect. Discussion of these effects is not in-

cluded here but undertaken separately.

Taylor (139) has considered the case of a density gradient where a heavier fluid is on top of a lighter one. Convection is expected, however a point will be reached where a small inverted density gradient can be supported as a result of the finite resistance of the fluid to flow. Taylor presents the following relationship as a criteria for stability of such a density inversity.

$$\frac{dC}{dx} = \frac{67.97\ \eta}{g\ \rho\ \alpha\ a^2} \qquad (25)$$

where

D = diffusion coefficient

2a = diameter of the path

g = acceleration due to gravity

η = viscosity of the fluid

α is defined by $\rho = \rho_o\ (1 + \alpha\ c)$ and is usually unity

When the value of dC/dx is greater than this convective flow will occur. This expression is similar to that obtained by Rayleigh (172) for the stability of density gradients in fluids heated from below.

An alternate approach useful to determine the factors likely to contribute to convection is to observe the form of the Grashof number for binary liquids (60).

$$Gr_{AB} = \frac{a^3 \rho^2 g \, \delta \, \Delta N_A}{\eta^2} \qquad (26)$$

where

δ = concentration coefficient of volumetric expansion

N_A = mole fraction of A

g = acceleration due to gravity

ρ = fluid density

a = characteristic length of the system, which is taken as the diameter of the capillary

η = viscosity of the fluid

The Grashof number may be thought of as the ratio of the driving force for convection to viscous drag force or the inertia of the system to fluid movement. The most noteworthy observation is the path diameter occurs to the third power in the numerator. The larger the Grashof number the more readily convection will occur if conditions become favorable. If the diameter of the diffusion path is increased from one to ten millimeters, the value of the Grashof number increases a thousand-fold.

When continuous convective mixing exists the "effective diffusion coefficient" may be thought of as

$$D_{eff} = D + D' \qquad (27)$$

where

D = component due to molecular diffusion

D' = component due to convection

Taylor (138) shows that for this case it is possible to obtain an error function type penetration curve as is obtained for molecular diffusion, the only difference being that higher values of the diffusion coefficient are obtained from this curve. Paoletti et. al. (101) discuss Taylor's results. They conclude this can occur when the time length of diffusion is much larger than the characteristic time scale of the turbulence.

Surface Effects

A number of investigators have studied diffusion of liquid metals under carefully controlled conditions. They have been able to discern small effects such as the dependence of the diffusion coefficient on path diameter or on the material of which the diffusion path is constructed. Often this variation amounts to no more than a few percent. In some cases this has been construed as an indication that convection is present in the experiment. While, in some cases, convection may be a contributing factor there is strong evidence that surface phenomena are responsible for these effects. These phenomena become noticable as the diameter of the capillary is decreased and the area to volume ratio increases.

Vincentini and co-workers (101, 102, 103) have noted that diffusion coefficients in some systems are independent of the diameter of the

capillary used, while in other systems the diameter affects the results. Some of their results are summarized in Table 4.

TABLE 4

EFFECT OF PATH DIAMETER ON DIFFUSION COEFFICIENTS IN SELECTED SYSTEMS

Alloy	Diffusion Coefficient of tracer is independent of path diameter	Diffusion Coefficient of tracer is dependent on path diameter
Sn		Sn
In	In	
In - 1% Sn	Sn	In
In-0.5% Pb	Pb	In
In-1.5% Pb		In
Sn-1% In		Sn

It is difficult to explain these results in terms of convection. Particularly in the cases of the In-1% Sn and In-0.5% Pb alloys where the coefficient for one of the tracers depends on the diameter but not that of the other. A more likely explanation, one that has been advanced by Vincentini, is that a wall effect is present in some systems. The atoms near the wall do not participate in diffusion in the same manner as do the atoms in the interior of the fluid. The wall effect becomes more pronounced as the area to volume ratio of the path increases and

and gives values of the diffusion coefficient lower than the true value. Careri et. al. (22) proved the existance of such an effect by dissolving away the external layer of a diffusion rod and showing that a higher value of the diffusion coefficient was obtained from the center section. Thus, the atoms in the interior diffused further than those near the wall.

Careri et. al. (21) notes that formation of crystallites on impurities which accumulate near the surface of an alloy may alter the properties of the liquid and lower the diffusion coefficient near the surface. This is in agreement with the results of a study of Eckert and Drickamer (42) who found a lower value of the diffusion coefficient near the surface for liquid indium near its melting point. The latter could possibly be due to the formation of liquid crystallites on traces of oxide at the surface of the indium. Paoletti et. al. (102) also found that runs made in capillaries of mullite gave lower values of the diffusion coefficient than runs using pyrex capillaries. This is a further indication that some sort of interaction with the capillary wall or reaction with the impurities present in this wall alters the fluid structure nearby. Rohlin and Lodding (122) found dependence of diffusion coefficient on the path diameter for self diffusion of potassium. Potassium is a very reactive material and may very well have reacted with the wall or impurities in this wall.

Fixman (50) has considered the hindering effect of a wall on the diffusion coefficients normal and parallel to the wall. He shows that

the coefficient parallel to the wall will have dropped to 90% of its bulk value at a distance of a few hundred angstroms from the wall. The magnitude of the variation predicted by this analysis is not large enough to explain the variation found experimentally by Vincentini and co-workers.

E. REVIEW OF THEORETICAL DEVELOPMENTS

Introduction

Of the three states of matter, the liquid state is least understood. The diffusion coefficient is a quantity which may be measured experimentally and much effort has been expended in testing various models against available diffusion coefficient data. Though, even agreement of the predictions of a model with experimental data is not conclusive proof of the validity of the assumptions underlying that model.

Some of these models picture a liquid as an aggregation of impenetrable non-interacting spheres. No order is postulated. Other models depend on structures of limited order not unlike those which exist for longer ranges in the solid state. Diffusion is conceived to occur through specific jumps to vacancies in this structure. More recently, attempts have been made to develop models which incorporate the interaction forces between atoms and the idea of cooperative movements of groups of atoms.

Often these models have been used far beyond their limitations to make predictions regarding the nature of the liquid state. Much discussion has centered about the question of what is the mobile species for diffusive transfer in liquid metals, the atom or the ion . Models have been called upon in support of both cases. To this writer, this effort seems unnecessary. There is little doubt that an atom in a

metal has given up some fraction of its electrons to the conduction band. This accounts for the stability of the metallic bond. Any statement to the effect that in order to diffuse within the metal a particular atom must become identified with a particular electron seems out of the question. But this is precisely what is implied when the radius of the diffusing species is calculated and compared with the ionic and atomic radii reported in the literature. There also exists the possibility that in metals possessing strong interactions between constituent atoms the diffusing species may be an agglomerate of ions. That is, a solute ion with several solvent ions tightly bound to it. The term ion here is taken to mean an atom which has given up some fraction of its electrons to the conduction band. The argument of Li and Chang (84) leads one to conclude that it is impossible to distinguish between diffusion of this agglomerate and diffusion of the bare ion simply from a calculation of the radius of the diffusing species.

A number of the models which have been proposed are discussed. Particular attention is given to the assumptions underlying each and the implications these have for use of the model. In view of the many simplifying and often unrealistic assumptions which have been made the reader is cautioned against attaching too great significance to the results.

Stokes-Einstein and Sutherland Equations

Einstein (43) first derived the Stokes-Einstein equation for colloidal solutions from consideration of the Brownian movement. Later he arrived at the same equation by considering the osmotic pressure gradient as the driving force for diffusion. In this latter case, the van't Hoff expression for osmotic pressure was employed.

$$p = CRT \tag{28}$$

This expression is good only for ideal solutions. The force due to this osmotic pressure gradient acting on each solvent particle is found to be,

$$f'' = - RT/NC \, (dC/dx) \tag{29}$$

If the diffusing particle is assumed to be a sphere moving through a continuous viscous medium, the drag force f' is given by Stokes law,

$$f' = 6\pi\eta \, r\vec{v} \tag{30}$$

When the diffusing particle is moving with constant velocity, $\vec{v}$, the force originating from the osmotic pressure gradient is equal to the drag force, f'' = f'.

$$6 \, \pi\eta r \, \vec{v} = - \frac{RT}{NC} \frac{dC}{dx} \tag{31}$$

the flux of the diffusing particles will be Cv. From Fick's first law $C\vec{v} = D(dC/dx)$, so

$$D = \frac{kT}{6\eta r\pi} \qquad (32)$$

where $k = R/N$.

The principal assumptions in this derivation are:

(a) The solution is ideal. This is implicit in the derivation of the van't Hoff expression for osmotic pressure which has been incorporated in the above derivation.

(b) The diffusing particles are hard spheres and move with a uniform (terminal) velocity. The sphere size is not restricted in an absolute sense except it must be of sufficient size to obey Stokes law. The application of Stokes law to spheres of atomic size is questionable. Their velocity through the medium can hardly be regarded as uniform. When the particle diameter approaches its mean free path, the particle becomes subjected to Brownian movement and a random motion is superimposed on any directed velocity. Lapple (169) notes that for this case the actual resistance to motion exerted by the viscous medium on the particle will be less than Stokes law predicts.

(c) The solvent has been assumed to be a continuous medium. For a medium composed of discrete particles this

assumption may be regarded as true only when the size of the diffusing particle is large compared to the size of the discrete particles.

(d) The spheres which make up both the medium, if this is regarded as composed of discrete particles, and the solute which is diffusing in this medium are regarded as non-interacting. This is not a good approximation for systems where there is strong interaction between the solvent and solute, or where the concentration of the solute is large and solute particles interact with each other.

Sutherland (133) presented an empirical correction to the Stokes-Einstein equation. This correction was based on an empirically modified form of Stokes law. Instead of the drag force used by Einstein, Sutherland used,

$$f' = 6\pi r\eta v \left[\frac{1 + \frac{2\eta}{\beta r}}{1 + \frac{3\eta}{\beta r}}\right] \qquad (33)$$

where β is the coefficient of sliding friction between the diffusing particle and the medium. β has meaning only for values between zero and infinity. When this drag force is used in the derivation of an expression for the diffusion coefficient, the following expression is obtained.

$$D = \frac{kT}{6\pi r\eta}\left[\frac{1 + \frac{2\eta}{\beta r}}{1 + \frac{3\eta}{\beta r}}\right] \qquad (34)$$

For large atoms of solute moving among smaller atoms of solvent, slipping is probably small and β becomes infinite. Equation (34) reduces to the Stokes-Einstein relationship. In the other extreme case where a small solute atom is moving among equal or larger solvent atoms, the small solute atoms can travel a good deal in the gaps which exist. For this case $\beta = 0$ and equation (34) takes the following form.

$$D = \frac{kT}{4\pi r\eta} \qquad (35)$$

Walls and Upthegrove (152) and Ma and Swalin (88) point out that since solute diffusion of liquid metals deals with particles of not too different dimensions, it is more likely the conditions imposed on the model used to derive equation (35) will apply. In the foregoing, equation (35) will be referred to as the Sutherland equation.

A number of investigators have used the Stokes-Einstein equation to calculate the radius of the diffusing particle for both self and interdiffusion. In view of the analysis presented above it would appear the Sutherland equation would be a better choice if this type of equation is to be used. Several investigators have calculated the radius of the diffusing particle with the Sutherland equation. In either case, the particle radii obtained have often shown close

agreement with the values of the crystallographic ionic radii of the diffusing species. This has been construed as evidence that the diffusing particles are ions. Upthegrove and Walls (152) caution against attaching too great significance to this argument. They point out the following:

(a) Crystallographic radii presented by Pauling (104) and by Goldschmidt (54) are obtained by assuming the ionic radii in oxide and halide compounds may be simply added to give the interatomic distances.

(b) It is assumed in the above that the ionic radii is identical in the solid and liquid states.

Ma and Swalin (88) investigated solute diffusion in liquid tin. They chose a series of solutes which give a range of solute-solvent interactions from repulsive to attractive. The Stokes-Einstein and Sutherland equations predict diffusion coefficients of the correct order of magnitude, however, these equations fail to predict the relative numerical order of the diffusion coefficients. This is not surprising since in the derivation of these equations it was assumed the particles are non-interacting.

Gorman (55) has calculated the radii of diffusing particles for a number of metals diffusing in mercury. The Stokes-Einstein equation was used. From a comparison of the calculated radii with the ionic and atomic radii presented by Pauling and Goldschmidt respectively,

Gorman concludes the effective radii of alkali and alkaline earth metals corresponds to the neutral atom, while those of Cd, Ag, Pb, Zn, Tl, Bi and Sn correspond to the ionic radii. This author questions the validity of this conclusion. The Stokes-Einstein equation, as has been mentioned previously, neglects interactions between solvent and solute. Examination of partial molal enthalpies at infinite dilution for solution of alkali metals in mercury indicates very large attractive interactions exist. These interactions are greater than those for amalgams of the heavier metals. Large attractive interactions between solvent and solute atoms will reduce the diffusion coefficient for the system and indiscriminate application of the Stokes-Einstein or Sutherland equations will give a value of the solute radius which is too large. Gorman has made a rather fine distinction, movement of ions vs. movement of atoms, based on the application of an equation which is hardly valid for the non-ideal systems to which is was applied.

Sobal (173) used the Stokes-Einstein equation to calculate the temperature variation of ionic and atomic radii. Much of the diffusion coefficient data he used, for example that of Roberts-Austin (120), was not reliable. Gorman et. al. (55, 56) and Preckshot (116) have also used the Stokes-Einstein equation to calculate the temperature variation of radii of solutes diffusing in liquid metals. Since liquid metals expand as the temperature is increased it is reasonable to expect the effective radius of the diffusing species to increase with

increasing temperature. The use of either the Stokes-Einstein or the Sutherland equations to predict the magnitude of this increase, however, does not seem justified. These equations are based on a hard sphere model and do not take account of holes in the liquid, free volume and thermal vibrations, all of which seem responsible in part for the relatively large temperature variation exhibited by diffusion coefficients in liquids. In all probability temperature variation for radii of diffusing particles calculated from these equations is too large.

Theory of Walls and Upthegrove

Walls and Upthegrove (152) developed a three parameter equation for prediction of diffusion coefficients similar to the Sutherland and Eyring equations. In their derivation they incorporate a geometric parameter, b, which is defined as the ratio of the atomic radius of a diffusing particle to its interatomic spacing, d_a. From the definition of viscosity and Einstein's expression for mobility they obtain the following expression.

$$D = \frac{kT}{2\pi r(2b+1)\eta} \qquad (36)$$

When the atomic diameter becomes equal to the interatomic spacing, $b = 1/2$ and equation (36) reduces to the Sutherland equation. The form of equation (36), however, is more desirable than that of the Sutherland equation. It allows for the effective radius of the diffusing particle to be something other than the ionic radius.

Walls and Upthegrove proceed to express the viscosity in the from proposed by Eyring (48).

$$\eta = \frac{Nh}{V_m} \exp\left(-\frac{\Delta S^*}{R}\right) \exp\left(\frac{\Delta H^*}{RT}\right) \tag{37}$$

A configurational constant, γ, is introduced

$$\gamma = \frac{Nd_a^3}{V_m} \tag{38}$$

V is the molar volume and N, Avagadros number. Finally they arrive at the following expression for the diffusion coefficient.

$$D = \frac{kT\gamma^{1/3}}{2\pi hb(2b+1)}\left[\frac{V_m}{N}\right]^{2/3} \exp\left(\frac{\Delta S^*}{R}\right) \exp\left(-\frac{\Delta H^*}{RT}\right) \tag{39}$$

This expression contains three parameters; a configurational constant γ which can be calculated from a specified or experimentally determined coordination number; a geometrical parameter relating particle size to interparticle spacing; and the entropy and enthalpy of activation which is postulated to be identical for diffusion and viscous flow. The entropy and enthalpy of activation can be calculated from experimental viscosity data. This author questions the introduction of equation (37) into the development. It complicates the resultant expression and simply introduces the two quantities ΔS^* and ΔH^*, which, as Walls and Upthegrove state must be evaluated from viscosity data. Rather, starting with equation (36), r may be expressed as r = bd where d is the

interatomic spacing. Then

$$D = \frac{kT}{2\pi bd(2b + 1)\eta} \qquad (40)$$

Now, $\gamma = Nd_a^3/V_m$ and

$$D = \frac{kT\gamma^{1/3}}{2\pi b(2b + 1)\eta} \left[\frac{N}{V_m}\right]^{1/3} \qquad (41)$$

Expression (41) is equivalent to the expression derived by Walls and Upthegrove provided the viscosity is represented by the Eyring relation. This expression is more convenient to use since the experimentally determined viscosity can be inserted without the necessity of first evaluating ΔS^* and ΔH^* from this same data.

To evaluate the diffusion coefficient using either Walls and Upthegrove's expression or the modified form suggested by this author requires the geometrical parameter, b, be assumed constant for a given class of liquids such as for liquid metals. Walls and Upthegrove evaluated the parameter b from the data of Meyer (92) for self diffusion in liquid mercury. This data was selected both because of the good precision of the measurements and the agreement with Swalin's theory. A value of b = 0.419 was obtained which compares favorable with the value 0.416 calculated from Pauling's univalent ion radius for mercury and interatomic spacing data available in the literature. Walls and Upthegrove found good agreement of predicted and experimentally determined self diffusion coefficients for several liquid metals.

This model does not admit consideration of interatomic potentials. Thus, like the Sutherland equation it is not in principle applicable to impurity diffusion.

Eyring Theory

Eyring et. al. (48) have treated diffusion in terms of their activation state theory. A quasi-crystalline model is adopted and diffusion is considered as involving distinct jumps of atoms from one equilibrium position to another. For this jump to occur there must be a hole available and the jumping atom must be capable of pushing its neighbors aside to reach the new equilibrium site. The energy which a diffusing atom must have to accomplish this jump, over and above the average energy a non-jumping atom has in the lattice, gives rise to the idea of an activation energy associated with diffusion. In their derivation of an expression for diffusion in a binary system the rates for the forward and reverse reactions are assumed equal. For equal rates, the net flow of atoms of one kind in one direction must be compensated for by a corresponding flow in the reverse direction. This implies, of course, that the atoms must be approximately the same size. If one species of atoms is much larger than the other, the Stokes-Einstein treatment is more appropriate. No account is taken of interaction between different species so the resulting equations can be expected to be applicable only to ideal and perhaps very dilute solutions where the solvent and solute do not interact strongly. The flux is assumed

to be proportional to the jump length also.

Eyring computed the fluxes in the forward and reverse directions and the net flux was related to the diffusion coefficient with Fick's first law. The expression obtained is then compared with Eyring's expression for viscous flow to obtain.

$$D = \frac{\lambda_1 kT}{\lambda_2 \lambda_3 \lambda_v^2 K_v} \qquad (42)$$

where

λ_1, λ_2 = interatomic distances perpendicular to the direction of motion.

λ_3 = interatomic distance in the direction of motion

λ_v = jump distance for viscous flow

K_v = specific rate constant for viscous flow

k = Boltzman's constant

T = absolute temperature

D = diffusion coefficient

For simple monatomic liquids composed of spherical molecules in a liquid which has a high degree of local order it is reasonable to assume,

$$\lambda_1 = \lambda_2 = \lambda_3 \cong 2r \qquad (43)$$

where r is the atomic radius. The mean jump distance is assumed identical to the interatomic distance. Then

$$D = \frac{kT}{2r\eta} \tag{44}$$

where $\eta = \lambda_v^2 K_v$.

Equation (44) does not predict diffusion coefficients well for liquid metals. Comparison of this equation with the Sutherland expression, equation (35), reveals they differ by a factor of 2π in the denominator. Thus, Eyring's equation can be expected to predict diffusion coefficients more than six times as large as the Sutherland equation which has been found to be a reasonable approximation for many liquid metals.

In their development of the temperature dependency of the diffusion coefficient based on activation state theory, Eyring and coworkers developed the following expression

$$D = e\lambda^2 \frac{kT}{h} \exp(\Delta S^*/R) \exp(-E/RT) \tag{45}$$

where

ΔS^* = entropy of activation

E = activation energy for diffusion

h = Planks constant

In addition to the assumptions noted above it has been assumed here that diffusion occurs at constant pressure and temperature.

A large amount of experimental data can be expressed in the form

$$D = D_o \exp(-E/RT) \tag{46}$$

which is identical to equation (45) if

$$D_o = e\lambda^2 \frac{kT}{h} \exp(\Delta S^*/R) \qquad (47)$$

Eyring points out that in the case of self diffusion the free energies of activation for diffusion and for viscous flow should be equal. Rothman and Hall (123) note that if this is so the heats of activation should also be approximately equal for the two processes. Yang and Derge (158) compare experimental activation energies for self diffusion and viscous flow for a number of liquid metals. In general, they found agreement within the limits of experimental error. This implies the mechanism of diffusion is similar to that for viscous flow.

Li and Chang (84) modify the derivation of Eyring's equation. In the original derivation the average velocity of an atom was taken relative to a fixed lattice. Li and Chang state that this is not the case for liquids and redefine and velocity to include relative motion between the diffusing atom and its neighbors. They arrive at the expression

$$D = \frac{\sigma - \tau'}{2\sigma} \frac{kT}{\eta \left(\frac{V_m}{N}\right)^{1/3}} \qquad (48)$$

where $\left(\frac{V_m}{N}\right)^{1/3} = \frac{\lambda_2\lambda_3}{\lambda_1}$ and $\left(\frac{V_m}{N}\right)^{1/3} = 2r$. Equation (48) is equivalent

to the Sutherland equation if $\frac{\sigma - \tau'}{2\sigma} \backsimeq 2\pi$. This is true for simple cubic packing of molecules $\sigma = 6$, $\tau' = 4$.

Eyring et. al. (45, 46, 47) have recently presented a modified activation model and mechanism of diffusion. The diffusing atom is considered to advance a distance λ_3 between neighboring lattice positions. A shear stress ζ is exerted on the advancing atom by the closest neighboring molecules in a plane perpendicular to its direction of motion. Eyring obtains the expression

$$D = \frac{\lambda_1 kT}{\zeta \lambda_2 \lambda_3 \eta} \frac{d \ln a}{d \ln c} \qquad (49)$$

where a is the activity of the diffusing component and c its concentration. For self diffusion $d \ln a / d \ln c = 1$. Also $(\lambda_1/\lambda_2\lambda_3) = (N/V)^{1/3} \backsimeq 2r$ and equation (49) becomes,

$$D = \frac{kT}{2\zeta r \eta} \qquad (50)$$

As noted earlier ζ is the effective number of neighbors of the diffusing atom lying in the plane perpendicular to its motion. For close packed structure $\zeta = 6$ and

$$D = \frac{kT}{12r\eta} \qquad (51)$$

This is approximately equal to the Sutherland equation which provides a reasonable approximation of some liquid metal diffusion data.

Cohn-Turnbull Theory

In developing their free-volume theory of liquids, Cohen and Turnbull (27) adopt a model in which liquids are conceived of as an aggregation of impenetrable non-interacting spheres. The Cohen-Turnbull theory is a version of hole theory in which diffusion is postulated to occur by movement of atoms into voids with a size greater than some critical value. An atom may be thought of as being contained in a cage formed by its nearest neighbors. Fluctuations in density open up holes in this cage large enough to permit displacement of the atom. Diffusive motion occurs when another atom jumps into the hole created by movement of the first atom before this first atom can return to its original position. The essential difference between the Cohen-Turnbull mechanism and the activated state mechanism proposed by Eyring is that in the former isoenergetic redistribution of the available free volume is responsible for the origin of voids, whereas activation state theory assumes a local energy fluctuation creates a void of atomic dimensions and a neighboring atom jumps into the gap. Since, in the Cohn-Turnbull theory diffusion is treated simply as translation of an atom across a void within its cage caused only by redistribution of the free volume it is not necessary to postulate an activation energy for this model. Walls and Upthegrove (152) remark, that in the sense of stipulating a critical void size necessary for diffusion to occur, the theory may be regarded as an activated volume analog of the more conventional Boltzman activation energy concept.

Cohen and Turnbull calculate the average distribution of free volume for a system of hard spheres in which no energy change is associated with redistribution of the free volume. The volume available for redistribution is taken as the change in volume upon melting plus volume increases due to expansion of the liquid when heated to the temperature in question. They obtain the following expression for the diffusion coefficient.

$$D = g'a^* u \exp\left[-\gamma v^*/v_f\right] \qquad (52)$$

where,

g' = a geometric factor, taken as 1/6

a^* = the atomic diameter at 0°K

γ = a parameter between 0.5 and 1.0 introduced to account for overlap of free volume

v^* = critical free volume for movement of a particle

v_f = average free volume of a solvent cell

u = velocity of a particle in a cell and is taken as $(3kT/m)^{1/2}$

Lodding (87) expresses equation (52) in the following form

$$D = 6.8 \times 10^{-9} r_a T^{1/2} m^{-1/2} \exp\left[-\left(\frac{r_i}{r_a}\right)^3 \frac{1}{\alpha_v T}\right] \qquad (53)$$

where

r_a = atomic radius of the diffusing particle

r_i = ionic radius of the diffusing particle

m = mass of the diffusing particle

α_v = coefficient of volume expansion

Thus, the Cohn-Turnbull model relates the diffusion coefficient of a system to measurable or calculable properties of the liquid.

Leak and Swalin (83) state that the assumption of hard spheres in this model is equivalent to the assumption that in metallic solution all atoms are identical. They conclude while the model may be applied to self diffusion it should not be applied to make quantitative calculations of solute diffusion. Strictly speaking, the assumption of hard spheres is not equivalent to the assumption that all atoms are identical. The size of the spheres may vary. Rather, the assumption of non-interacting spheres is where difficulty is encountered when this model is applied to solute diffusion.

Kassner et. al. (76) note that for dilute alloys each of the solute atoms may be regarded as being surrounded by solvent atoms. If the distribution of free volume is random, a reasonable assumption for non-interacting spheres, the free volume of an impurity cell may be regarded as

$$V_{fi} = \varphi v_f \qquad (54)$$

where

V_{fi} = average free volume of impurity cell

v_f = average free volume of solvent cell

φ = quotient formed by dividing the volume of the solute ion by that of the solvent ion.

Then, v_f in equation (52) should be replaced by $\varphi\ v_f$, and

$$D_i = g' a_i^* \vec{v}_i \exp\left(-\gamma\ v_i / \varphi\ v_f\right) \qquad (55)$$

where the subscript i refers to the solute or impurity atom.

Leak and Swalin (83) point out that in this model the diffusion of solute particles is governed by their size. If the solute particle is smaller than the solvent particle it will diffuse at about the same rate as the pure solvent since diffusive transport is complete in this model only when a neighboring solvent particle jumps into the void left by the diffusing solute particle. If the solute particle is larger than the solvent particles, the critical void volume must be correspondingly larger and the impurity should diffuse slower than the pure solvent.

Cohen and Turnbull (27) discuss the applicability of their model to self diffusion of liquid metals. Experimental data for several metals indicates that when γ is arbitrarily set equal to unity and the experimental values of the self diffusion coefficient are inserted in

equation (52) the radii of critical voids is found to be close to the ion core radii of the highest valence state of the metal. Kassner et. al. (76) calculated the radii of critical voids for self diffusion in several pure metals, and for self diffusion of solute atoms in dilute indium, lead and mercury solution. They also found the critical void sizes of the order of ionic core sizes. Nachtrieb et. al. (97) conclude the same for self diffusion of zinc. These findings agree with those of the Sutherland Eyring equations, that ion cores are the mobile species during diffusion in liquid metals.

On the basis of a free-volume theory of diffusion it would seem reasonable to expect the diffusion coefficient to decrease markedly when the system is subjected to high pressures thus reducing the amount of free-volume available for diffusion. Cohen and Turnbull note that the self diffusion coefficients of gallium and of mercury are relatively insensitive to pressure. As a possible explanation for the discrepancy which appears to exist here they suggest that expansion of liquid metals which occurs on heating is primarily due to the introduction of free volume while contraction upon the application of pressure is largely due to a uniform shrinkage of the electron gas.

Swalin's Fluctuation Theory

Swalin (134) developed a theory for self diffusion from a model of the liquid state in which it is postulated that diffusion occurs by cooperative movements of five atom assemblages. These cooperative

motions give rise to time dependent density fluctuations with respect to a given atom and its four nearest neighbors in a plane. The jump distance is not discrete as it is in quasi-crystalline theories, rather a continuous distribution of fluctuation distances is permitted. There is little difference between an atom participating in such a cooperative motion and one which is not, consequently no activation energy arises.

A local density fluctuation gives rise to a void which Swalin treats as a section of a prolate spheroid. The energy associated with a fluctuation is that energy necessary to elongnate bonds between the atom under consideration and its four nearest neighbors in a plane. Evaluation of this energy requires an expression for the energy as a function of separation of the atoms. Swalin chose the Morse function to represent this separation energy. The Morse function is commonly used for solids and was chosen on the premise that bonding energy in liquid metals is similar to metallic binding in the solid phase. The energy expended in increasing the distance between two nearest neighbors a value j over their equilibrium spacing is

$$\epsilon = \epsilon_d \left[1 + \exp\left(- 2\alpha_m j_m\right) - 2 \exp\left(-\alpha_m j_m\right) \right] \qquad (56)$$

ϵ_d is the energy of dissociation of a bond and α_m is related to the curvature of the potential-distance curve. ϵ_d can be estimated from quasi-chemical theory and is related to the heat of vaporization of the

liquid ΔH_v,

$$\epsilon_d = \frac{2\Delta H_v}{Z_c N} \tag{57}$$

Diffusive motion is treated as a random walk phenomena and the following expression is obtained for the diffusion coefficient.

$$D = \frac{3Z_c^2 N k^2 T^2}{96h \Delta H_v \alpha_m^2} \tag{58}$$

α is related to the Waser-Pauling force constant (153) as follows

$$\alpha_m = \left(\frac{Z_c N k'}{4 \Delta H_v}\right)^{1/2} \tag{59}$$

This force constant, k', was obtained from compressibility data for crystalline structures. Waser and Pauling state their determination of this force constant was based on central forces acting along a bond and that this may not be a good approximation for metals wherein the free electrons and the lattice of residual ion cores requires the use of non-central forces. When equations (58) and (59) are combined an expression of the following form is obtained.

$$D = A' \frac{T^2}{k'} \tag{60}$$

The basis for postulating an activated process for diffusion phenomena in liquids is, the Arrhenius equation

$$D = D_o \exp(-E/RT) \tag{61}$$

seems to represent experimental data well over small temperature intervals. If equation (60) is differentiated to obtain $\partial \log D/\partial(1/T)$

$$\frac{\partial \ln D}{\partial(1/T)} = -\frac{2}{2.3} T \tag{62}$$

and now if equation (61) is differentiated in similar manner

$$\frac{\partial \log D}{\partial(1/T)} = \frac{E}{2.3R} \tag{63}$$

Comparison of equations (62) and (63) indicated that for the fluctuation process an "apparent activation energy" can be defined as follows, regardless of the physical significance or lack of significance of the term.

$$E = 2RT \tag{64}$$

This implies the higher the temperature, the higher the activation energy will be. Swalin (134) examined self diffusion data for several metals and found this trend to exist.

Swalin shows that activation volume for his fluctuation model represents the effect of pressure on the size distribution of the fluctuations. This is different from its definition for an activated process where it represents the excess volume associated with an atom in the activated state.

Gordon (167) questions the small average jump distances predicted by fluctuation theory. He notes that to obtain significant values of the diffusion coefficient with small jump distances the jumping frequencies required may exceed the maximum atomic vibration frequency. Gordon suggests that both activated jumps and local density fluctuations may make significant contributions to diffusion in liquids. It should be noted that experimental data seems to confirm the idea that diffusion occurs by a mechanism incorporating a series of small jumps. Nachtrieb and Petit (98) found an activation volume of 0.98 Å for self diffusion in liquid mercury. This is significantly smaller than the atomic volume of mercury which is 24.7 Å. From this consideration the average jump length would be 0.17 Å.

Lodding (87) has investigated self diffusion for rubidium, potassium and indium. When his results, which he obtained from electrotransport experiments, are plotted as log D vs. 1/T the resultant curves are linear for low values of temperature and show curvature consistant with Swalin's theory for higher temperatures. Lodding suggests this may be an indication that the melt undergoes a phase transformation as the temperature is raised and the diffusion mechanism varies. This explanation is reasonable, at low temperatures the structure of the liquid can be expected to be more like the quasi-crystalline structures which have been postulated and for which a linear relationship is predicted by theory. At higher temperatures a greater degree of randomness arises from increased thermal motions. Diffusion can be expected to occur

more by the cooperative mechanism suggested by Swalin for which a curved relationship is expected. It should be noted however, that further investigation by Rohlin and Lodding (122) who re-measured the self diffusion coefficient of potassium by the capillary reservoir technique indicated that convective effects were present in the original data obtained from electrotransport experiments. Thus, the curvature of log D vs. 1/T at elevated temperatures could be due to increased convective effects at elevated temperatures rather than a change in the mechanism of diffusion.

Meyer (92) found that both Swalin's theory and the modified Eyring theory represent the self diffusion data of mercury well over a wide temperature range. Ma and Swalin (89) investigated self diffusion of tin over a temperature interval of 700°C. They found the type of curvature in log D vs. 1/T predicted by Swalin's theory. Paoletti et. al. (103) note that Swalin's theory predicts values of the diffusion coefficient for indium which are three times larger than the experimental values they obtained. Also, Yang and Derge (158) report that fluctuation theory predicts values of the self diffusion coefficient for sodium which are two times too large. In general, sufficient self diffusion data for wide temperature ranges is not available to allow a more critical evaluation of the model on which fluctuation theory is based. It appears this theory predicts the self diffusion coefficients for some metals rather well while in other

cases it may be in error by a factor of two or three.

Fluctuation theory has also been applied to solute or impurity diffusion. In the following it is assumed the solution is dilute enough so only interactions between the solute atom and its nearest neighbors need be considered. No account is taken of solute-solute atom interactions in solutions this dilute. The probability and magnitude of local density fluctuations will be influenced by the binding energy between the solute and solvent atoms.

For the case of strong coulombic attraction between solute and solvent atoms the diffusing cluster may be thought of as one solute atom surrounded by several tightly bound solvent atoms. This cluster has a large radii, and from consideration of the general form of the Sutherland equation it might be thought that it will diffuse at a rate slower than the solvent atoms. Ma and Swalin (88) have noted, however, according to the derivation of Li and Chang (84) the Eyring and Sutherland equations may be written as

$$D = \frac{\sigma - \tau'}{2\sigma} \frac{kT}{\eta} \left(\frac{N}{V_m}\right)^{1/3} \qquad (65)$$

where σ is the number of nearest neighbors surrounding the diffusing particle and τ' is the number of nearest neighbors in a single plane. A large cluster would have larger values of σ and τ'. Ma and Swalin show that for solute diffusion in liquid tin the expression for diffusion of the cluster is approximately equal to the Sutherland expression for diffusion of a single atom, $D=kT/4\pi\eta\, r$. Thus, for

strong attractive interactions between solute and solvent atoms the solute can be expected to diffuse at a rate similar to that of the pure solvent.

For the case of coulombic repulsion between solute and solvent atoms a reduction of the shear moduli will result in the vicinity of the solute atom and the solute will diffuse at a rate faster than the pure solvent atoms. Ma and Swalin (88) have examined the diffusion of a number of solutes in liquid tin and conclude the above relationships are true. That is, for diffusion in liquid alloys which exhibit large negative partial molal enthalpies impurities diffuse at about the same rate as the pure solvent atoms, while impurities in systems which exhibit large positive partial molal enthalpies diffuse at rates much greater than the pure solvent atoms.

Quantitative calculation of solute diffusion is difficult because of the lack of potential energy vs. distance curves for unlike pairs of atoms in solution. Leak and Swalin (83) show that for systems where the solute and solvent atoms are similar in size and where the only significant difference is their valence, their interaction potential may be approximated by first order perturbation theory. A coulombic repulsion term is superimposed on the Morse potential function. The following form is used for the coulombic repulsion term.

$$E_c = \frac{\beta' z' e^2}{d_a} \exp(-q\, d_a) \qquad (66)$$

where

E_c = the repulsive contribution of this interaction to the total lattice energy.

z' = relative valence of the solute with respect to the solvent, it may be positive or negative.

d_a = the distance between ion centers

q = a screening constant

β' = a constant depending upon the particular solvent solute pair.

Leak and Swalin derive the following expression

$$\frac{D_{impurity}}{D_{self,\ solvent}} = \left[1 - \frac{q^2\epsilon_o}{k_f} - \frac{2q\epsilon_o}{d_o k_f} - \frac{2\epsilon_o}{d_o^2 k_f}\right] \qquad (67)$$

where k_f is the appropriate force constant and ϵ_o is obtained by evaluating expression (66) for the value of d, i.e. d_o, corresponding to the interionic distance.

Leak and Swalin note the fluctuation model is probably more accurate for calculating relative quantities where many of the terms difficult to evaluate cancel out.

Swalin's fluctuation model may be modified by postulating a critical volume fluctuation j* which implies that diffusion is an activated process. The activation energy for impurity diffusion may

be expressed as

$$\Delta H_i = \Delta H_s - \Delta H_c \qquad (68)$$

where

ΔH_i = activation energy for impurity diffusion

ΔH_s = activation energy for pure solvent diffusion

ΔH_c = coulombic interaction contribution to the activation energy

The value of ΔH_c may be either positive or negative depending on whether the interaction is repulsive or attractive. This equation is simply a statement that the presence of a solute atom will affect the energy necessary to form a void next to that atom. ΔH_s is evaluated from self diffusion data for the solvent and ΔH_c by calculating the value of the critical fluctuation j* for the pure solvent.

Leak and Swalin (83) show that

$$\frac{D_{impurity}}{D_{self,\ solvent}} = \exp\left[\frac{\Delta H_s - \Delta H_i}{RT}\right] \qquad (69)$$

an expression which is analogous to equation (67). Gupta (62) has tested this relation for solute diffusion in liquid silver and found good agreement with experimental data.

Hoffman and Turnbull (141) proposed a thermodynamic relationship

between the activation energy for solute diffusion and the solute binding energy in solid metals.

$$Q_i - Q_s = 1/2\, Q_s \left[\frac{E_i - E_s}{E_s} + \frac{\overline{\Delta E}_{is}}{E_s} \right] \qquad (70)$$

where

Q_i = activation energy for diffusion of solute i in solvent s

Q_s = Activation energy for self diffusion of solvent s

E_i = bond energy of pure i

E_s = bond energy of pure s

$\overline{\Delta E}_{is}$ = partial molal energy of solution of i in s

Implied in the derivation of this expression is the assumption that activation energies for diffusion of solute and solvent are directly proportional to their binding energies. This is likely to be a good assumption only in very dilute solutions. Gupta (62, 63) has investigated the validity of this expression for solute diffusion in liquid metals. Bond energies were evaluated from the Waser-Pauling constants. Good agreement found for solute diffusion in liquid silver and tin.

Quasi-Crystalline Theory of Careri and Paoletti

Careri and Paoletti (21) treat liquid metal diffusion as a quasi-crystalline phenomena. Diffusion in a crystalline substance can be

thought of as resulting from two possible mechanisms:

a. Diffusion via vacancies where an energy fluctuation allows movement of an atom into an adjacent void.

b. Diffusion by direct interchange of neighbors. The existance of a ring which can rotate must be postulated for this mechanism.

For solids the latter mechanism is extremely improbable due to the high activation energy required to interchange neighbors in a lattice. In liquids this interchange mechanism is more probable, though, due to thermal agitation the existance of rings incorporating more than two atoms is improbable. Careri and Paoletti investigated the possibility of describing self diffusion in liquid indium and liquid tin in terms of a vacancy mechanism and of a direct interchange mechanism. Their analysis of the latter mechanism is based on quantum mechanical calculations for a hindered rigid rotator. They conclude that a model of the liquid state wherein couples of atoms rotate in random fashion can be used to describe diffusion in the liquid metals noted above. The probability of having complete cycles of these rotators is so small that random mixing will occur. Also, the occurence of rotations is small enough so the quasi-crystalline structure which was assumed in the derivation is not destroyed. Careri and Paoletti point out the data used to evaluate this model is for self diffusion reasonably close to the melting point. As the temperature is raised, it is reasonable to

expect the number of rings to increase but steric hinderances will also increase with the overall result of increased randomness of the motions.

In a series of investigations, Vincentini and co-workers (22, 102) studies activation energies for self diffusion of both indium and lead in pure indium and dilute alloys of lead in indium. They note that the activation energy for diffusion of lead in these dilute indium alloys is close to the activation energy for self diffusion of pure indium. The activation energy for pure lead is significantly higher. Thus, the activation energy for impurity diffusion in dilute solution is determined primarily by the nature of the solvent rather than that of the impurity. Paoletti and Vincentini construe this to support the validity of their quasi-crystalline model though the connection is not obvious to this writer.

Peter's Equation

Peter (106) develops an expression for diffusion from a model which considers a liquid to be a homogenous aggregation of hard spheres. Each sphere is postulated to have twelve nearest neighbors (most dense spherical structure for equal sized spheres) and the binding forces are imagined to be identical for all spheres. For a particle to move from one position to another it must possess a minimum energy ϵ. From a consideration of the probability of a particle possessing this energy, the square of the average displacement of each jump, and the free volume

of the liquid Peter obtains the following relationship.

$$D = 5.17 \times 10^{-16} \nu(\Delta V)^2 \left(\frac{E}{RT}\right)^{5/2} \exp(-E/RT) \qquad (71)$$

where

ΔV = volume change per gr atom on melting

E = ΔH

ν = vibrational frequency of the atoms, sec^{-1}

D = diffusion coefficient, cm^2/sec

Peter evaluates ν, the vibrational frequency for liquids as nine-tenths of the Debye frequency for solids. Equation (71) will predict the self diffusion coefficients of several liquid metals to better than an order of magnitude though good agreement is not obtained.

III. EXPERIMENTAL INVESTIGATION

A. EXPERIMENTAL DESIGN

General Considerations

Several investigators (1, 65, 70, 75, 91, 154) have demonstrated the feasibility of operating concentration cells with fused salt electrolytes and liquid metals for anodes and cathodes at high current densities. Most of these investigations have been directed toward the development of cells capable of producing high power densities for space power systems. These works were, however, the impetus for the present investigation.

In this section the concept of a liquid metal concentration cell and its utilization to measure diffusion coefficients in binary liquid metal alloys is discussed.

A liquid metal concentration cell has three major components: an anode, a cathode, and an electrolyte. If the anode is composed of pure alkali metal A, and the cathode of an alloy of A with a heavier metal B, written as A(B), the cell may be represented schematically as

anode	electrolyte	cathode
A	A^+	A(B)

The half-cell reaction at the anode-electrolyte interface is

$$A \rightleftharpoons A^+ + e^- \qquad \varphi = \varphi_a \qquad (72)$$

while at the cathode-electrolyte interface it is

$$B + A^+ + e^- \rightleftharpoons A(B) \qquad \varphi = \varphi_c \qquad (73)$$

A is univalent. The flow of one electron from the anode to the cathode is accompanied by a transfer of one atom of A from the anode, through the fused salt as the ion A^+, to the cathode where it alloys with B. The overall reaction is the sum of the half-cell reactions

$$A + B \rightleftharpoons A(B) \qquad (74)$$

When metals react to form alloys an exchange of energy takes place. The energy associated with the cell can be expressed as

$$\Delta \bar{G} = \Delta \bar{G}^\circ + RT \ln \frac{a_2}{a_1} \qquad (75)$$

where

$\Delta \bar{G}$ = partial molal free energy of species A [The energy associated with the assimilation of one mole of A by a large amount of A(B)].

$\Delta \bar{G}^\circ$ = partial molal standard free energy

a_1 = activity of A in the anode

a_2 = activity of A in the cathode alloy

By definition a_1 is unity since the anode is pure A. Equation (75) becomes

$$\Delta \bar{G} = \Delta \bar{G}^\circ + RT \ln a_2 \qquad (76)$$

at equilibrium

$$\Delta \bar{G} = 0 \tag{77}$$

$$\Delta \bar{G}^{\circ} = n_e F E \tag{78}$$

A is univalent so $n_e = 1$. The reversible potential of the cell is obtained by combining (76), (77) and (78)

$$\varphi^{\circ} = \frac{RT}{F} \ln a_2 \tag{79}$$

The activity is defined as

$$a_2 = \gamma_A N_A \tag{80}$$

where

γ_A = activity coefficient of A in the alloy

N_A = atomic fraction of A in alloy A(B)

The expression for the reversible cell potential becomes

$$\varphi^{\circ} = \frac{RT}{F} \ln (\gamma_A N_A) \tag{81}$$

From this equation it is apparent that the reversible cell potential (open-circuit potential) for the concentration cell shown depends only on the temperature and the atomic fraction of A in the cathode alloy.

When current flows in the external circuit reversible conditions no longer exist. The cell potential differs from its equilibrium value due to resistance, concentration, and activation polarization. Resistance polarization arises from the finite resistance the electrolyte offers to ionic movement of A^+. Activation polarization is associated with the charge transfer reactions (72) and (73). Concentration polarization results from a difference in the concentration of the transferred species at the interface from its concentration in the bulk of the phase. In the cell described, the anode is pure A and the electrolyte contains only cations of A. Concentration polarization occurs with respect to A in the cathode.

The diffusion of A in the alloy A(B) can be determined from the current time relationship of the liquid metal concentration cell when it is discharged at constant potential if concentration polarization of A in the cathode is the rate limiting step. This means the magnitude of this effect must be considerably larger than any other polarization due to diffusion. Convective transfer is limited by the capillary dimensions of the cathode.

Briefly, the operation of a diffusion cell to measure diffusion coefficients is as follows: the initial composition of the cathode alloy is $\left[A(B)\right]_o$. If the potential-composition relationship for the alloy A(B) is given by the curve shown in Figure 1 , the open-circuit potential of the cell will be φ_o. The potential shown in Figure 1 is for a cell with a pure A anode and a cathode of alloy A(B). If the cell is discharged at the constant potential φ_s where $\varphi_s > \varphi_o$, the

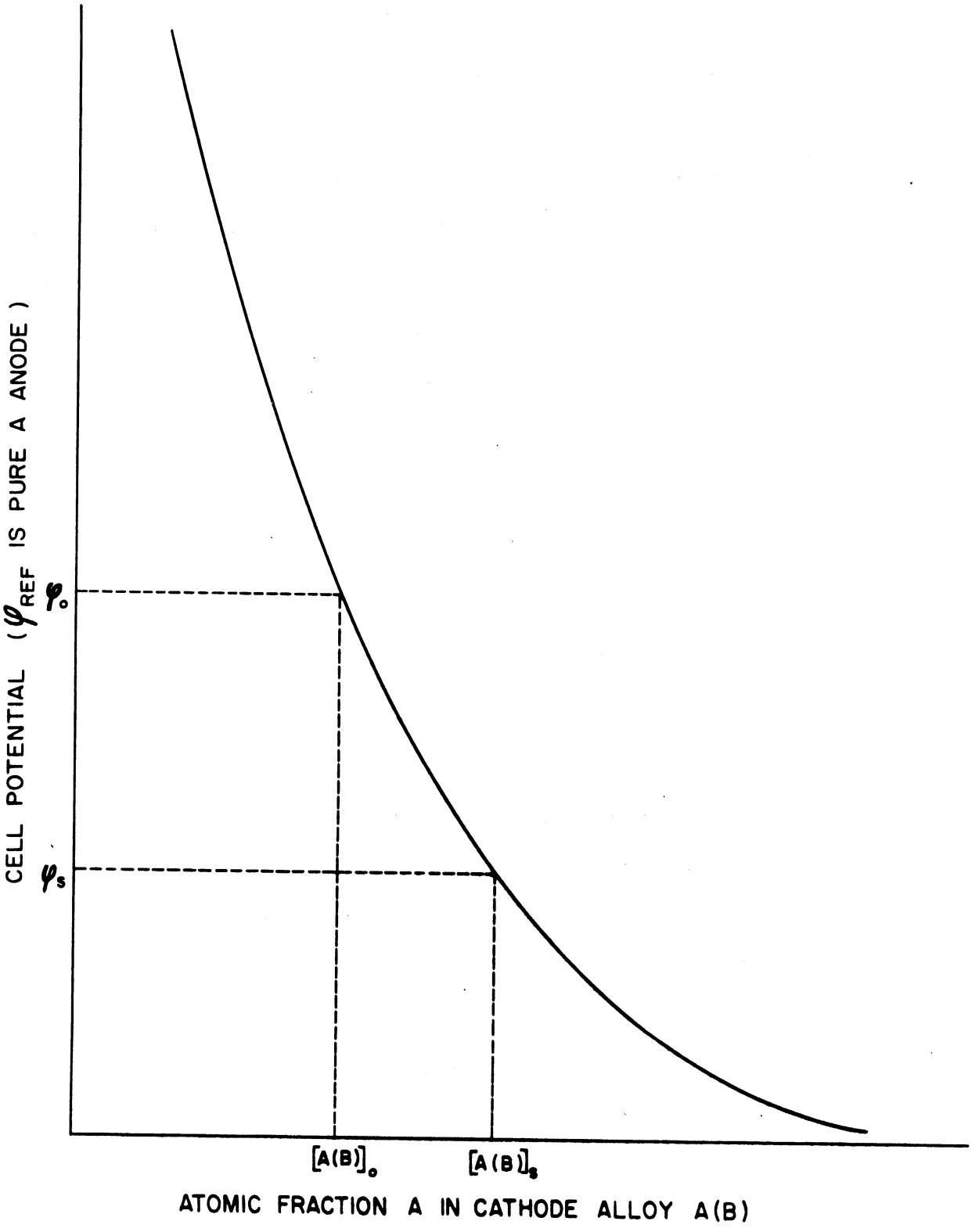

Figure 1. Cell Potential vs. Cathode Composition

concentration of A will remain constant at the cathode-electrolyte interface (assuming negligible IR losses in the electrolyte). A concentration gradient of A will be established in the cathode causing A to diffuse from the cathode-electrolyte interface into the bulk of the alloy.

It is only noted here that a solution of Ficks' laws for diffusion with the boundary and initial conditions corresponding to the surface and initial concentrations discussed above is possible. The detailed mathematical analysis and solution are given in a subsequent section.

For successful measurement of diffusion coefficients by the aforementioned method, the following constraints must be placed on the design and operation of the concentration cell.

(a) The activity of A in the alloy A(B) must be known as a function of the composition of the alloy for the temperature ranges over which diffusion is to be studied.

(b) All phases, the anode, cathode, and electrolyte must be liquids at the cell operating temperature. In addition phases in contact with one another must be mutually insoluble and chemically unreactive.

(c) The current in the external circuit during discharge of the cell must be a true indicator of the quantity of A which is transferred from the anode to the cathode.

(d) Transfer of A from the cathode-electrolye interface to the bulk of the cathode alloy must be the rate controlling step and occur only by the mechansim of diffusion.

(e) Resistance of the electrolyte to ionic movement of A^+ must be sufficiently low so resistance polarization does not signficantly influence cell operation.

(f) The charge transfer reactions occuring at the electrodes must occur fast enough so activation polarization is not significant in determing the discharge rate of the cell.

The remainder of this section is devoted to discussion of the specific systems investigated and to those electrochemical and physical phenomena which must be considered when designing cells consistent with the constraints above.

Systems Investigated

A summary of the systems which were investigated and the components of the cells employed in these investigations is given in Table 5.

TABLE 5

SUMMARY OF SYSTEMS INVESTIGATED

Diffusion Couple	Anode	Electrolyte	Cathode
K in K (Hg)	K	KOH-KI-KBr (E)	K (Hg)
Na in Na (Pb)	Na	NaOH or, NaI-NaCl (E)	Na (Pb)
Na in Na (Sn)	Na	NaOH or, NaI-NaCl (E)	Na (Sn)

In the Na-Sn and Na-Pb cells the choice of electrolyte depended upon operating temperature. For lower temperatures NaOH was used, while for elevated temperature NaI-NaCl was employed. (E) denotes a eutectic composition.

Hultgren et. al. (74) has tabulated activities for these systems based on the results of several investigators and methods for each. Curves for cell voltage as a function of cathode alloy composition and temperature based on Hultgren's tabulation are presented for K-Hg, Na-Sn, and Na-Pb cells in Figures C-1, C-2 and C-3 of Appendix C. Each of these curves represents the open-circuit voltage for a cell with a pure alkali metal anode and a cathode of an alloy of this alkali metal with the heavier metal indicated.

Current Efficiency

If the current flowing in the external circuit is to be a true indicator of the alkali metal transferred from the anode to the cathode, cell discharge must occur at, or close to, 100% current efficiency. The current efficiency will be influenced by:

(a) The occurrence of electrode reactions other than those indicated by equations (72) and (73).

(b) Solubility of the alkali metal in the fused salt electrolyte.

Each of these factors is discussed below.

Electrode Reactions:

A 1:1 relationship between the electron flow in an external circuit and the alkali metal atoms transferred from anode to cathode is indicated by the half cell reactions given in (72) and (73). This implies that no other charge transfer reactions occur. Only cations of the alkali metal are present and the only other reaction which need be considered here is the oxidation of the fused salt anion at the anode

$$2X^- \rightleftharpoons X_2 + 2e^- \qquad (82)$$

where $X = OH^-, Cl^-, Br^-$ or I^-.

Reaction (82) will not occur as long as the potential across the cell does not exceed the decomposition potential for any of the fused salts in the electrolyte. Cambi and Devoto (19) determined the decomposition potentials of NaCl, NaI, KI and KBr as 3.20, 2.295, 2.525 and 2.98 volts respectively. Baur (7) investigated the NaOH-Na_2O system and reports a decomposition potential of 2.18 for Na_2O at 340°C. From examination of the potential concentration relationships for the three systems of interest, Figures C-1, C-2 and C-3 of Appendix C, it is apparent the cell potentials during discharge will never exceed a volt. Therefore, liberation of gas at the anode according to reaction (82) will not occur. Examination of the ionization potentials (163) for sodium and potassium indicated oxidation state greater than +1 will not occur.

Solubility of Alkali Metals in Fused Salts:

Solubility of alkali metal anode in the fused salt electrolyte may affect current efficiency in two ways. These are discussed in detail below.

First, solution of alkali metal at the anode-electrolyte interface may be followed by diffusive transport of this metal through the electrolyte and its dissolution in the alloy at the cathode-electrolyte interface. There is no electron transfer associated with this mechanism of alkali metal transport. The result is that more alkali metal will be transferred from the anode to the cathode than is indicated by the cell discharge current. Retention of the electrolyte in a porous matrix limits transport of this nature since convection is unlikely in the matrix pores.

Bredig et. al. (15) investigated the solubility of sodium in sodium halide salts. He reports a solubility of 0.08 mole % sodium in sodium chloride at 750°C, while its solubility in sodium iodide is 3.3 mole % at 674°C. The solubility is a strong function of temperature, at 1000°C the solubility of sodium in sodium chloride is 33 mole %. This places an upper limit on operating temperature for cells with fused alkali-halide electrolytes.

The only published data for the solubility of sodium in sodium-hydroxide is by von Hevesy (149). At 600°C the solubility is 10 mole % sodium in sodium hydroxide. The data show a decreasing solubility relationship with respect to increasing temperature and

neglect the reaction of sodium with its hydroxide to produce the monoxide and hydride as reported by Williams (156). This casts doubt on the validity of the data.

Heyman and Weber (72) note, when sodium dissolves in its halide salts the solutions formed are deep violet or black. This is attributed to formation of complexes and may have been the source of darkening observed by Weaver et. al. (154) in previous investigations with liquid metal concentration cells. Weaver attributed this darkening to I_2 coloration caused by electrolyte decomposition in the Na-Sn cell. Such decomposition, as discussed earlier, is unlikely.

A second possibility involves the transfer of alkali metal from anode to cathode by the expected mechanism described by equations (72) and (73). However, upon discharge of alkali atoms at the cathode-electrolyte interface some fraction of these atoms may re-enter the salt phase due to their solubility therein. This results in a net transfer of alkali metal to the cathode which is less than the cell discharge current indicates. Heyman and Weber (72) have investigated the distribution equilibrium of sodium between molten sodium halides and molten heavy metal phases (including Pb and Sn). Calculations are presented in Appendix I to illustrate the effect of this equilibrium on the current efficiency of the hypothetical cell Na/NaI/Na(Pb) discharged at 690°C. About 2% of the sodium discharged at the cathode re-enters the salt phase.

The percentage is probably less for the cells operated in this investigation since in general temperatures were lower, and the other fused salts present exhibit lower sodium solubilities than do iodide salts.

Delimarskii and Markov (35) and Reddy (118) review the fused salt literature. They conclude that deposition of metal on a liquid metal cathode will occur at near 100% current efficiency for small current densities.

Activation Polarization

Reddy (118) and Baimakov et. al.(6) note that exchange currents in metal-metal ion systems are high due to the elevated temperatures. Often they are 1 - 4 amps/cm^2. A high exchange current implies little resistance is offered to the electron transfer reaction at the electrode-electrolyte interface. The transfer reaction proceeds rapidly and is not likely to be rate controlling.

Piontelli and co-workers (109-115 inc.) have investigated the overpotentials for a large number of metal-metal ion couples with fused salt systems. They conclude the overpotential they measure is entirely due to IR drop in the electrolyte for current densities as high as 2 amps/cm^2.

In view of these experimental findings it was concluded that activation polarization would not be rate controlling in this investigation. Current densities no greater than 1 amp/cm^2 occur.

Fused Salt Electrolyte

Molten salts have a specific conductivity about 100 times greater than moderately concentrated aqueous solutions. It is this high specific conductivity which results in low values of resistance polarization for fused salt concentration cells.

Agruss and co-workers (1, 75) measured the conductance of the KOH-KI-KBr eutectic salt employed in this investigation. A value of 1 ohm^{-1} cm^{-1} was obtained at 543°K. They also reported a formation factor of about 10 when this electrolyte is impregnated in an alumina matrix of 45% porosity. The formation factor is defined as the resistivity of the electrolyte impregnated in the matrix to the resistivity of the pure electrolyte.

Weaver et. al. (154) measured the conductivity of the fused salt NaI-NaBr (E) and found it to be 4.3 ohm^{-1} cm^{-1} at 625°C.

It was noted earlier the alkali metal anode is partially soluble in the fused salts employed as electrolytes. Bronstein and Bredig (16, 17) have studied the influence of dissolved sodium and potassium on the specific conductances of their halide salts. In all cases, the specific conductance increases with increasing metal concentration. Specific conductances in the range 4 - 10 ohm^{-1} cm^{-1} were reported for these salts at temperatures of 700 - 800°C. This effect would cause the resistance of the cells to decrease with time during discharge, though, the effect in most cases would be less than 10% in cell resistance.

It is important that phases of a concentration cell in direct contact with each other do not react chemically. Williams (156) has investigated the reaction of sodium metal with fused sodium hydroxide. It appears this reaction preceeds at temperatures above 300°C according to the following mechanism

$$2Na + NaOH \longrightarrow Na_2O + NaH \qquad (83)$$

$$NaH \rightleftharpoons Na + 1/2\ H_2 \qquad (84)$$

Dissolution of sodium hydride is suppressed by an inert gas blanket indicating it must vaporize or sublime before it can dissociate. Investigation of the reaction of potassium with potassium hydroxide reveals that it occurs to a much smaller extent, probably due to higher solubility of the hydride in the KOH-K_2O melt.

Doan (38) notes that reaction of the cathode alloy with the electrolyte can occur with the evolution of hydrogen gas. This gas forms voids in the electrolyte and can increase the cell resistance. Analysis of his results indicates the reaction occurring is probably that of the cathode metal, M, with residual water in the electrolyte.

$$M + H_2O \rightarrow M(OH) + H_2 \qquad (85)$$

This illustrates the importance of removing all traces of water from fused salt electrolytes prior to their use in cells.

Interfacial Phenomena

At an electrode-electrolyte interface a charge separation will exist which is often referred to as the Helmholtz double layer. This charge influences the surface energy of the system and the shape of the electrolyte-cathode interface is dependent on electrical potential. Antropov (4) presents data for the electrocapillary zero potential of sodium amalgams. In general little data is available for other liquid metal alloys. Furthermore, once a faradic current is introduced the electrocapillary curves break down due to fluctuations which disturb the surface energy.

The shape of the cathode-electrolyte interface also depends on the ease with which the electrolyte and the cathode alloy wet the cathode compartment. Gul'din and Buzhinskaya (61) have investigated the system, quartz-lead-KCl, NaCl. They report the contact angle of a lead drop on quartz covered with the fused salt varied irregularly with time with a general tendency to decrease to a stable contact angle of 127°. Based only on this latter consideration the shape of the cathode-electrolyte interface would tend to be convex with respect to the cathode alloy as shown in Figure 2 a and b. Which case prevails depends on how much the alloy recedes from the matrix.

In the following section a mathematical model for diffusion in the cathode is presented. The effects of perturbation of the interface from the idealized planar shape due to surface energy effects are considered.

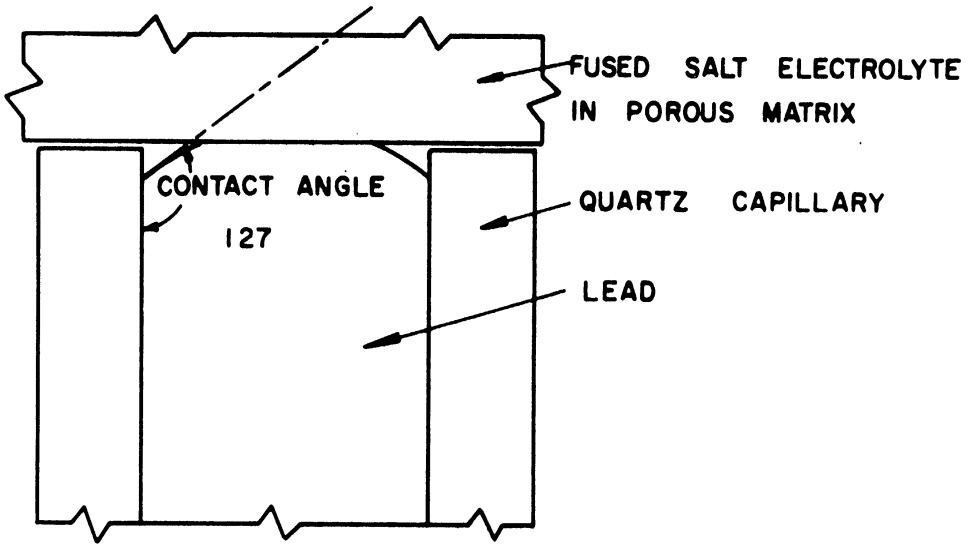

(a) LEAD IN CONTACT WITH ELECTROLYTE MATRIX

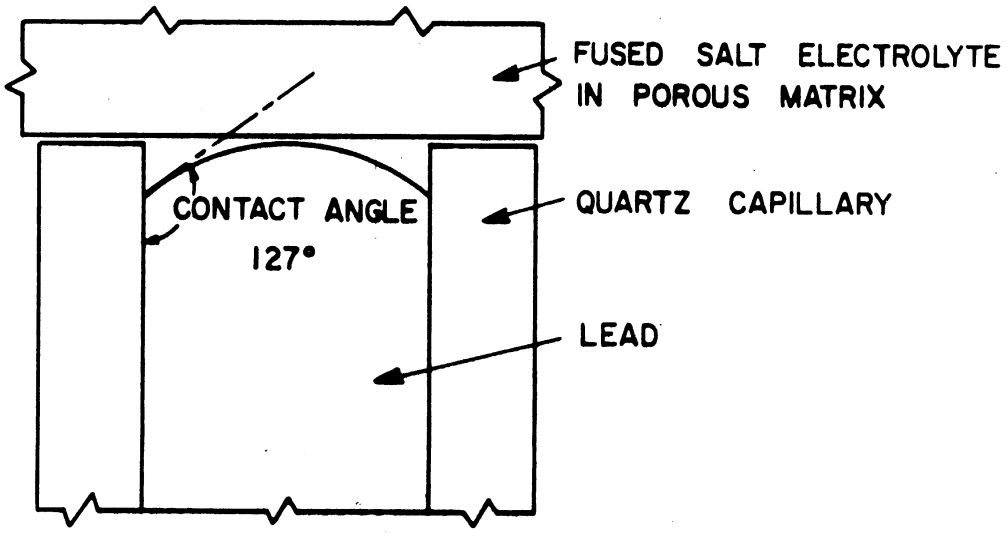

(b) LEAD RECESSED FROM ELECTROLYTE MATRIX

Figure 2. Interfacial Phenomena for System, Quartz-Lead-Equimolar KCl NaCl

B. MATHEMATICAL ANALYSIS

Diffusion in a One Dimensional System

In a cell where concentration polarization of the cathode is the rate limiting process, the cathode may be taken as the system for purposes of mathematical analysis. Other processes occurring in the cell such as ionic transfer in the salt will not influence the equations governing diffusion in the cathode. The capillary cathode of the cell may be treated as a one-dimensional, semi-infinite diffusion path. The semi-infinite criteria applies only if significant concentration gradients are not established at the lower end of the diffusion path. Approximation of the system as one-dimensional applies only if no concentration gradients exist perpendicular to the capillary axis. If, furthermore, the diffusion coefficient is considered to be concentration independent, and no volume change occurs as the components diffuse, Ficks' first and second laws can be expressed as follows

$$J(x,t) = - D A_s \frac{\partial C}{\partial x} \tag{86}$$

$$\frac{\partial C}{\partial t} = D A_s \frac{\partial^2 C}{\partial x^2} \tag{87}$$

The origin of the system, x=0, is taken as the cathode-electrolyte interface. If the cathode alloy has a uniform initial concentration C_o,

the initial condition for equation (87) is

$$C\,(x,0) \;=\; C_o \tag{88}$$

Diffusion is terminated before any significant concentration gradient is established at the lower end of the capillary. The boundary condition at this end of the capillary is

$$\lim_{x \to \infty} C(x,t) \;=\; C_o \tag{89}$$

Discharging the cell at constant potential constrains the concentration at the cathode-electrolyte interface to be a constant and known value since the cell potential is a monatonic function of cathode composition. The IR drop in the cell is assumed negligible by comparison to the potential maintained across the cell. It is also assumed that no resistance to mass flow exists at the boundary x=0. If this constant concentration at the boundary is designated as C_s, the boundary condition at x=0 is

$$C(0,t) \;=\; C_s \tag{90}$$

The solution of equation (87) subject to the conditions specified in equations (88), (89) and (90) is presented in Appendix G. The concentration profile is

$$C(x,t) \;=\; \left[C_o + (C_s - C_o)\ \mathrm{erfc}\ \frac{x}{2\sqrt{Dt}}\right] \tag{91}$$

The flux at the interface x=0 is

$$J(0,t) = A_s(C_s - C_o)\left(\frac{D}{\pi t}\right)^{1/2} \qquad (92)$$

and the total quantity of alkali metal which has been transferred from anode to cathode at any time is

$$Q = 2(C_o - C_s)\sqrt{\frac{Dt}{\pi}} \qquad (93)$$

Equations (91), (92) and (93) are, at best, approximations of the actual diffusion phenomena in the cathode. The approximative nature of these solutions may be attributed to the following:

(1) Non-ideality of the cathode alloy. There may exist both a concentration dependence of the diffusion coefficient, and a volume change during diffusion. Wagner (28, 29) discusses transformations of equation (87) to account for volume changes. Concentration dependence of the diffusion coefficient may be dealt with by use of small concentration gradients to measure differential diffusion coefficients.

(2) Variations in geometry of the system from the one-dimensional idealization. The existence of surface energy at the cathode-electrolyte interface leads to a non-planar surface. Flux vectors

perpendicular to the x-direction will be appreciable, particularly for small x and t.

(3) Cell limitations. The equation for flux (92) indicates as $t \rightarrow 0$, $J \rightarrow \infty$, that is, the rate becomes extremely large for small times. This is unlikely, for very large rates either ionic transport in the salt or the electron transfer reaction at the cathode-electrolyte interface will be rate limiting.

Concentration dependence of the diffusion coefficients measured in this investigation is dealt with by employing small concentration gradients and measuring differential diffusion coefficients. Items (2) and (3) indicate, for small times the mathematical analysis presented above is not a good model for diffusion in the cathode. To supplement this analysis, solutions of the diffusion equation for a few applicable cases are obtained and these solutions pieced together to obtain an overall solution from consideration of time intervals for which each is applicable. Three cases are considered; diffusion at very small times, diffusion in a semi-infinite one-dimensional system with a time dependent boundary condition, and diffusion into a spherical surface.

Diffusion at Very Small Times

At very small times the concentration gradient in the cathode will

be very large. The flux which is, according to Ficks' first law, directly proportional to the concentration gradient will also be large. Under these conditions the iR drop in the electrolyte will be rate limiting. The open-circuit cell-potential is φ_o. This potential corresponds to that for a cell with unit activity in the anode and a cathode alloy of uniform initial concentration C_o. The cell-discharge potential is fixed at a value φ_d such that $\varphi_d < \varphi_o$. For discharge the available potential drop across the electrolyte is $(\varphi_o - \varphi_d)$. The maximum current which can flow in the cell is obtained from Ohms' law

$$i_m = \frac{\varphi_o - \varphi_d}{R_c} \qquad (94)$$

where R is resistance to ionic transport in the fused salt electrolyte. For very small times this resistance to ionic transport will be rate limiting and the discharge current will be constant with time.

Diffusion in a Semi-Infinite One-Dimensional System with a Time Dependent Boundary Condition

For times larger than those considered in case I, but still relatively small, both resistance polarization and concentration polarization in the cathode will be significant. During this time interval the concentration at the cathode-electrolyte interface will not remain constant, rather the surface concentration will increase with time. The potential relationship for the cell can be expressed as

$$\varphi_o - \varphi_s = \varphi_o - (\varphi_d - iR) \tag{95}$$

where φ_s is the potential corresponding to surface concentration at the cathode-electrolyte interface, φ_d the discharge potential and φ_o the open-circuit potential of the cell. The quantity iR decreases rapidly as concentration polarization which is initially absent is established in the cathode.

Ficks' second law must be solved for a one-dimensional semi-infinite system with uniform initial concentration C_o, and time dependent surface concentration $C(0,t)=F(t)$. An exponential decay function was chosen to represent time dependency of the surface concentration

$$C(0,t) = C_o + (C_s - C_o)(1 - e^{-kt}) \tag{96}$$

C_s is the equilibrium value of surface concentration which the system approaches at large t. This function satisfies the necessary conditions, at $t=0$ $C(0,t)=C_o$, and as $t \to \infty$ $C(0,t) \to (C_s - C_o)$. K is a positive constant and chosen so the solution will approach the solution for a constant surface concentration at a particular time. The solution of Fick's law with appropriate boundary conditions for this case is presented in Appendix G. The flux at the surface x=0 is

$$J(0,t) = 2KA_s (C_s - C_o) \sqrt{\frac{Dt}{\pi}}\, e^{-kt} \sum_{n=0}^{\infty} \frac{(kt)^n}{(2n+1)\, n!} \tag{97}$$

Only the flux is considered here since this is the quantity of interest and can be directly related to the electrical current which is measured

during cell discharge.

Diffusion into a Spherical Surface

Surface energies at the cathode-electrolyte interface lead to a non-planar surface. The solutions for diffusion in a one-dimensional system are applicable only when a planar interface exists. The extreme case of a non-planar interface is diffusion into a spherical surface. A solution of Ficks' second law for diffusion into a sphere with uniform initial concentration C_o, and uniform surface concentration is presented in Appendix G. The flux of material across the boundary r=a of a hemisphere is found to be

$$J_{r=a} = 4\pi aD\,(C_s - C_o) \sum_{n=1}^{\infty} \exp\left(\frac{Dn^2\pi^2 t}{a^2}\right) \qquad (98)$$

Here it is assumed no mass flow occurs across the base of the hemisphere. This assumption, of course, limits the applicability of equation (98) to small times.

In Figure 3 values of $J/\pi a^2(C_s - C_o)$ are compared for each of the following cases.

I. Diffusion in a one-dimensional semi-infinite system with uniform initial concentration C_o, and constant surface concentration C_s. The surface area A_s is πa^2 and taken perpendicular to the x-axis.

II. Diffusion in a one-dimensional semi-infinite system with uniform initial concentration C_o,

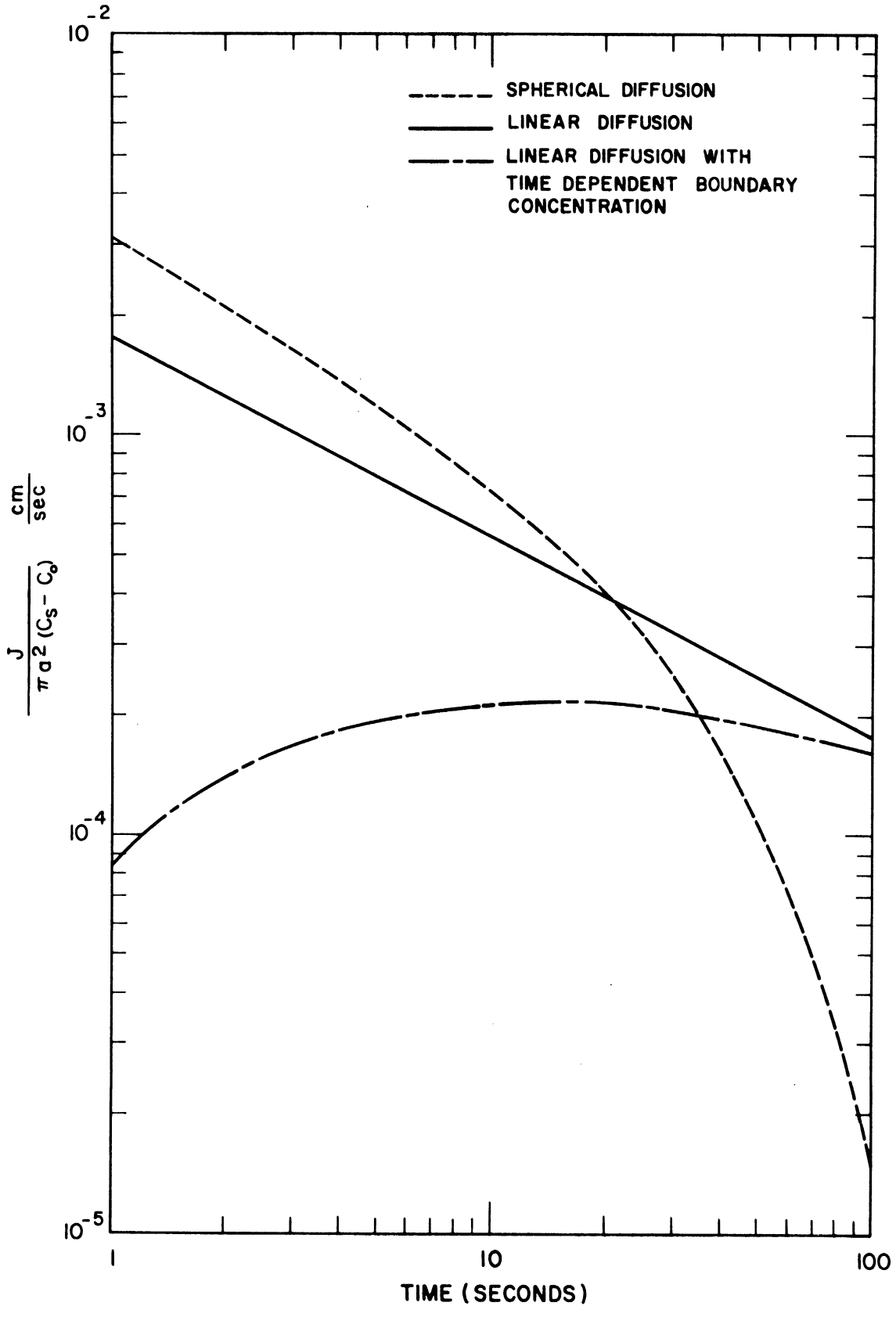

Figure 3. Solutions of Diffusion Equation for Small Time

and surface concentration $C(0,t)\ F(t)$

where, $F(t)$ is defined in equation (96).

Again, the area A_s is πa^2.

III. Diffusion into a hemisphere with uniform initial concentration C_o, and constant surface concentration C_s. No mass is transferred across the base of the hemisphere. The area A_s is $2\pi a^2$, which is the area of a hemispherical surface whose base has area πa^2.

The flux for case I is linear on log-log coordinates and has slope -1/2. Values for the flux in case II have been obtained from equation (97) where K = 0.023. This value of K has been selected so at 100 seconds $C(0,t) - C_o(t,o)$ will be nine tenths of its equilibrium value for large time. A maximum is expected from the form of equation (97). The independent variable is present in both the numerator and denominator of the right-hand expression. Case III for diffusion into a hemispherical surface yields a larger flux at small times. At larger times when reflection at the center point becomes significant the value of the flux drops rapidly to less than that in either of the other cases. Reflection, of course, is not as marked when mass is permitted to cross the base of the hemisphere.

It is possible to piece these solutions to obtain an idea of the general behavior which may be expected for the current-time curve where

diffusion occurs in a semi-infinite cylinderical diffusion path with mass transfer into this path occurring only across the hemispherical surface at the bounded end. This curve is shown in Figure 4 . At small time the value of J increases as the surface concentration C(0,t) increases at the cathode-electrolyte interface. It passes through a maximum and slowly approaches the linear case.

Numerical Solution of Diffusion Equation

As noted above the diffusion path may be approximated geometrically as a semi-infinite cylinder with a hemispherical surface at the bounded end. The flux of material into this path all passes through the hemispherical surface. At small times the flux may be approximated as spherical while at larger times much of the diffusion is taking place in the cylinderical region and the one-dimensional solution is applicable. This tells little about the rate at which the spherical solution approaches the linear one for the coupled problem. An analytic solution is difficult. The boundary conditions in the hemispherical section are manageable only if spherical coordinates are employed. Polar coordinates are required to deal with the cylinderical section. Simultaneous solution of the differential equations describing diffusion in each of these sections is complicated by the transformation of coordinate systems which must be made and the difficulty of expressing the boundary condition at the plane formed by intersection of the end of the cylinder and base of the hemisphere. In this plane the concentration is time dependent and a function of position.

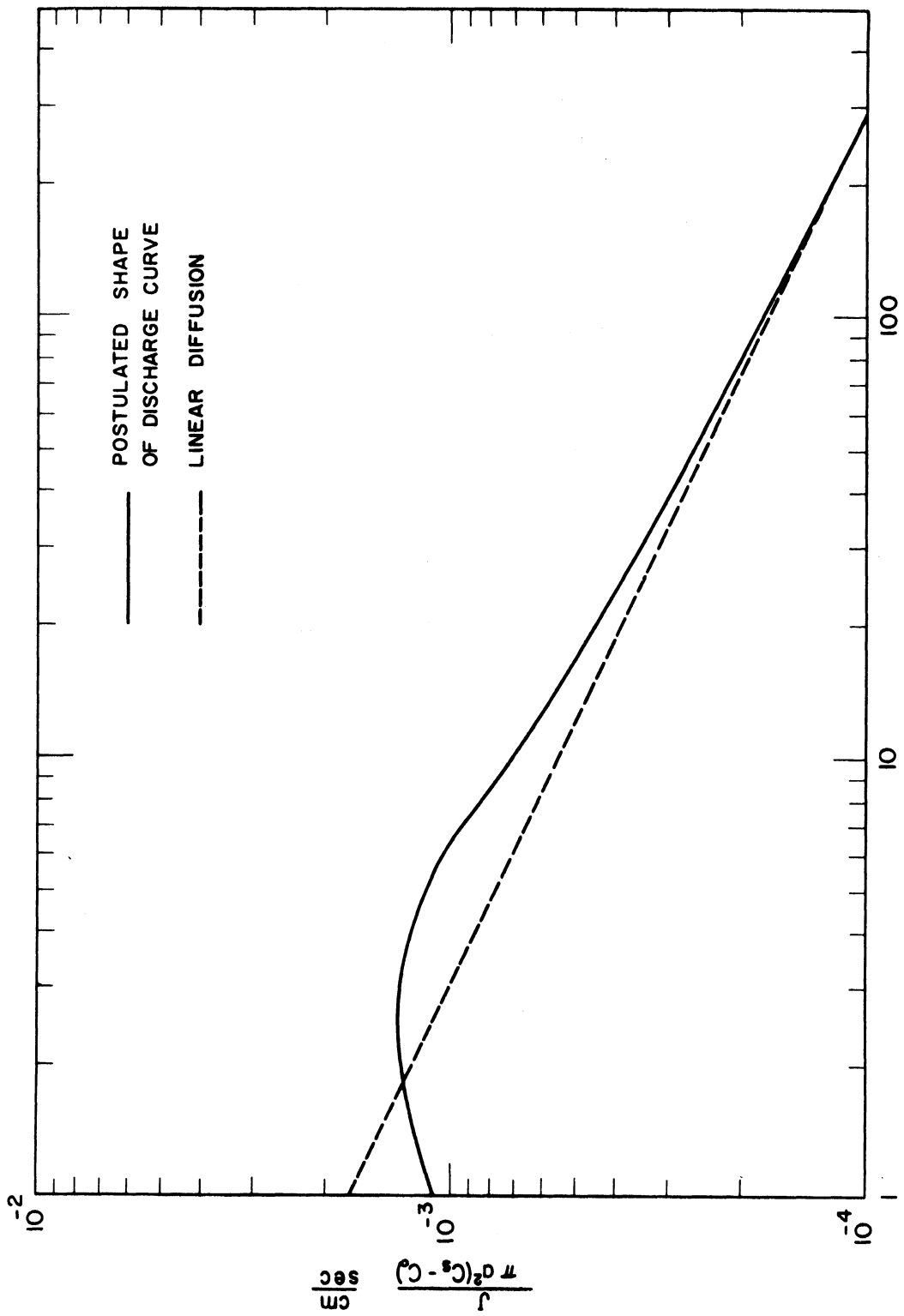

Figure 4. Postulated Shape of Discharge Curve for Cell with Capillary Cathode from Piecing of Solutions

A numerical solution of Fick's second law for this geometry is presented in Appendix H. The results of this solution are shown in Figures 5, 6 and 7. In Figure 7 the shapes of the concentration profiles at 1 second and at 100 seconds are shown. At small times the profiles are very non-planar while at larger time they approach the planar case. In Figure 5 the non-planar flux is compared to the ideal or planar case. Again the greatest deviations occur for small times and the two converge for large time. The concentration gradient is large at small times when the concentration profiles are non-planar. Consequently, a larger quantity of material is transferred to the diffusion path than the solution for the ideal case predicts. This excess diffusate decreases with increasing time. Figure 6 shows the relationship between the percentage of excess diffusate transferred, over and above the ideal case, and the duration of the experiment.

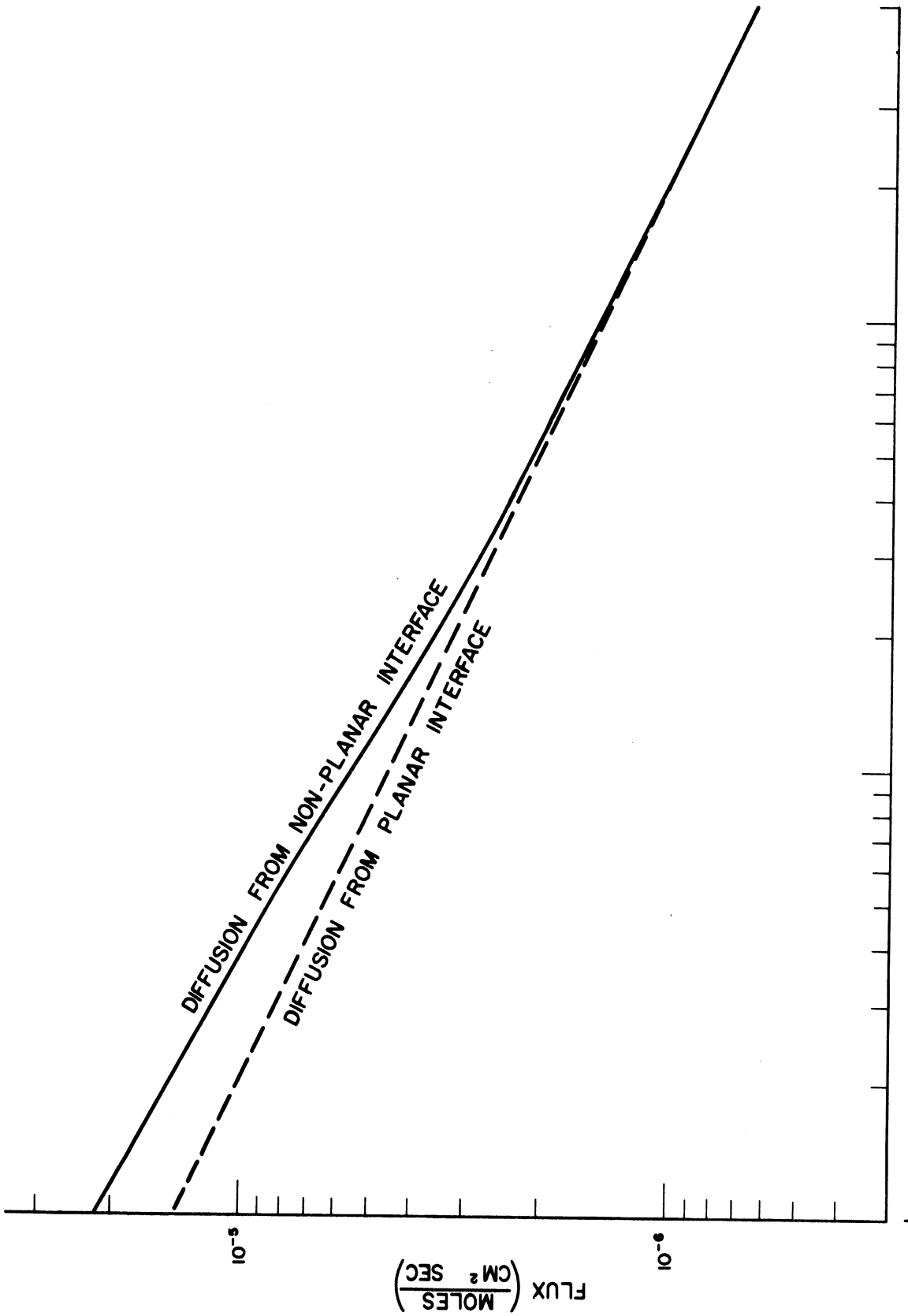

Figure 5. Flux for Coupled Diffusion Problem

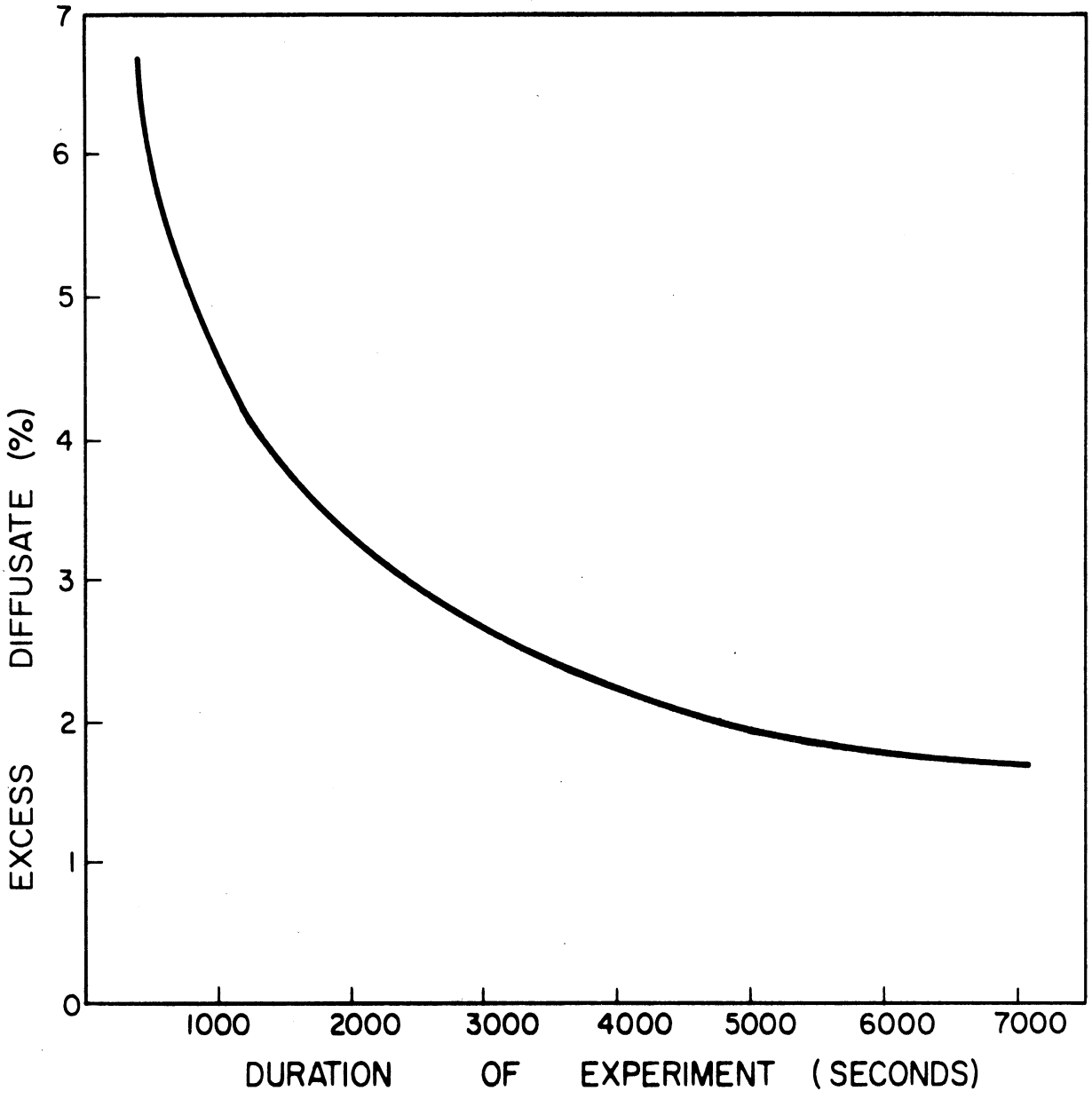

Figure 6. Excess Diffusate Due to Non-Planar Interface

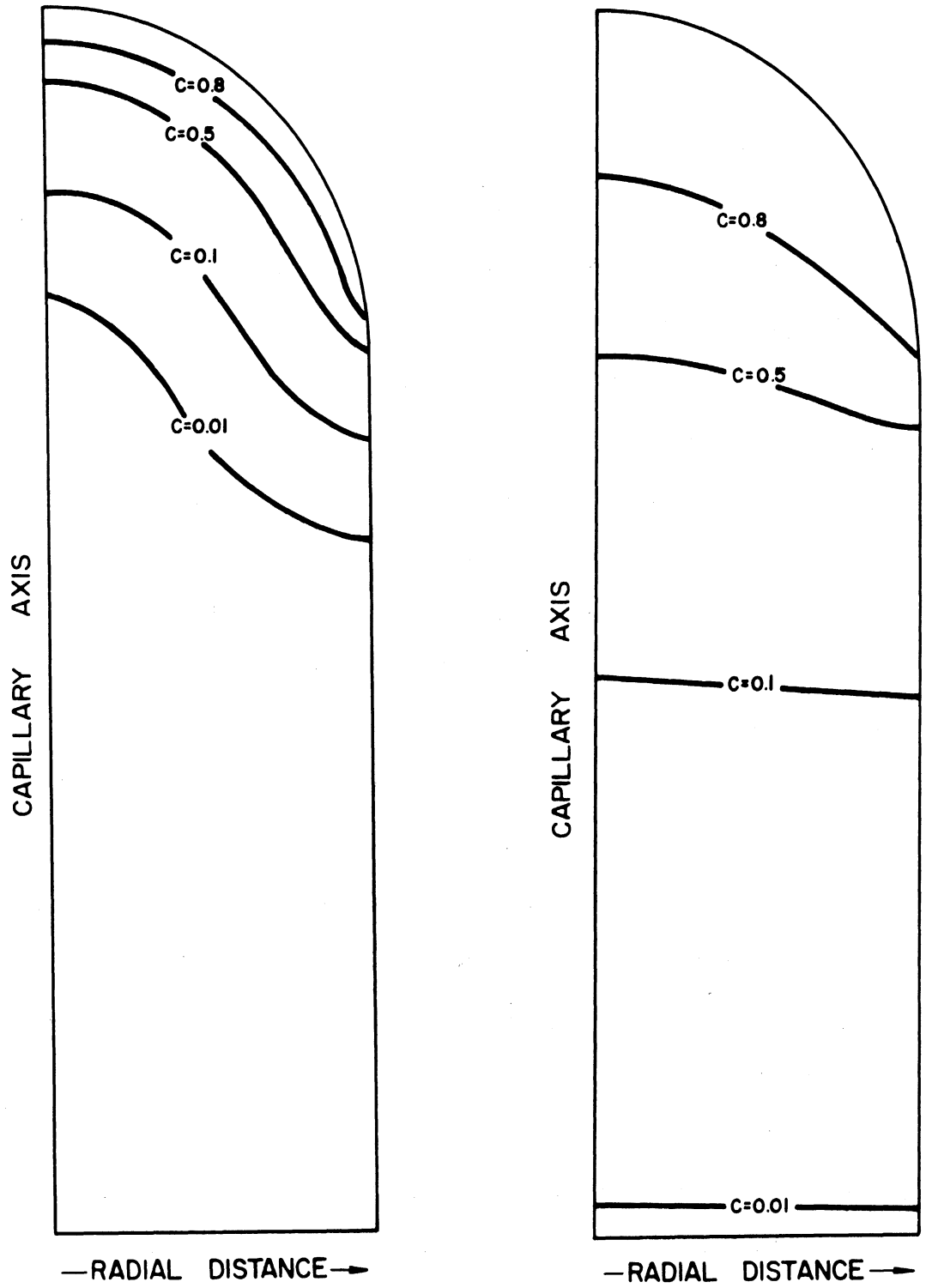

Figure 7. Non-Planar Concentration Profiles for Coupled Diffusion Problem

C. EXPERIMENTAL EQUIPMENT

Diffusion Cell

The basic cell design is that of a differential density concentration cell. The lightest phase, the alkali metal, is on top. The heaviest phase, the cathode alloy, is located on the bottom. The fused salt electrolyte which is intermediate in density is located in the middle. This design precludes any gross density inversion within the cell. The only case where a density inversion would be possible is for cathode alloys very rich in alkali metal content. This case is of no interest because the voltage of such a cell would be too low for stable discharge. During discharge of the cell the highest concentration of alkali metal in the cathode alloy will occur at the top of the cathode. This leads to a stable density gradient in the cathode alloy, the density decreasing in the upward direction.

The components of a diffusion cell are shown in Figure 8 . The anode body is constructed from a sleeve of impervious recrystalized alumina ($99.7^{+}\%$ Al_2O_3). Impervious alumina is used to withstand contact with the pure alkali metal anode.

The matrix which supports the electrolyte must be electrically non-conducting. It was constructed of Coors AHP-99 high purity porous alumina. The pores are 2 - 3 microns in size and the apparent porosity of the material is 40 - 43%. The matrix, in addition to containing the fused salt electrolyte, provides a fixed separation of approximately

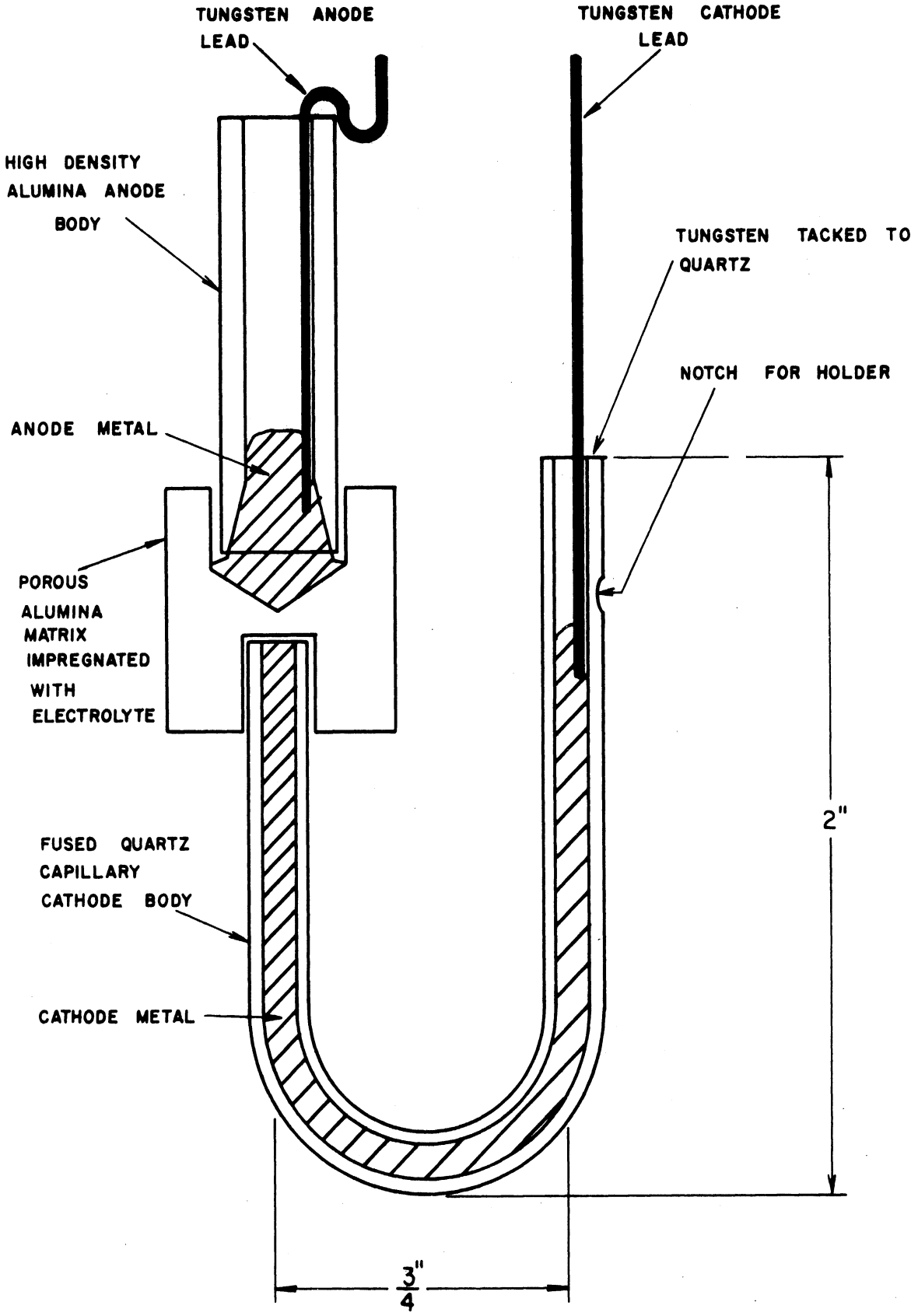

Figure 8. Diffusion Cell

1/16" between the anode and cathode metal. The upper compartment is left with the "V" bottom which it receives from drilling. This provides a larger area of contact for the anode metal than does a flat-bottomed compartment. The face of the lower compartment in the matrix is ground flat and perpendicular to the axis of the matrix.

The "U" tube cathode compartment is constructed from precision bore clear fused quartz tubing. Two sizes of tubing were used, one with a nominal I. D. of 1 mm. and O. D. of 3 mm. and another with a nominal I. D. of 1.6 mm. and O. D. of 4 mm. Quartz tubing was employed for two reasons, first it can easily be bent into the desired "U" shape, and second, it is transparent and small bubbles may be observed in the cathode metal. The lowered activity of the alkali metal in the cathode alloy permits use of a quartz diffusion path. Quartz, however, was not found satisfactory for use as an anode compartment material which must withstand direct contact with the pure alkali metal. The leg of the cathode which is inserted in the matrix is cut square so that its face will be perpendicular to the face of the matrix which it contacts. The other leg of the cathode is left open to allow for expansion of the cathode alloy. When the capillaries are formed from quartz tubing care is taken to leave the legs long enough so the diffusion path is not distorted in making the "U" bend. The leg must also be long enough so the concentration gradient does not extend into the bent section of the capillary. This would lead to convection due to density inversions within the alloy in the bent section.

Tungsten wires of 0.020" diameter are employed as leads for both the anode and cathode compartments. The wire which enters the open leg of the cathode is tacked to the quartz to prevent movement during cell operation. Tungsten was chosen because of its inert characteristics toward all of the metals employed as well as toward the fused salt electrolytes. A new cell was constructed for each experimental run. The dimensions shown in Figure 8 are only approximate and vary from cell to cell. The cell design described above was arrived at after many experiments with preliminary designs. These preliminary designs are discussed in Appendix L, along with an analysis of why they failed and what aspects each contributed to the present cell design.

Furnace Vessel and Superstructure

The vessel used to contain the cell in the furnace was constructed from a 57 mm O. D. Vycor sleeve closed at one end and flared at the other to fit a 3" modified Dressler Coupling. The sleeve was approximately 24" in length and allowed positioning of the cell at any desired height in the furnace.

Two furnace heads were used. One for fusing salts and filling capillary compartments. The second for operation of diffusion cells.

The furnace head for fusing salts and filling the capillaries is shown in Figure 9 . The upper section is machined from a piece of 3" brass rod stock. This was drilled and tapped to accept a Conax vacuum sealing gland through which a 25 BWG 1/4" O.D. stainless steel tube

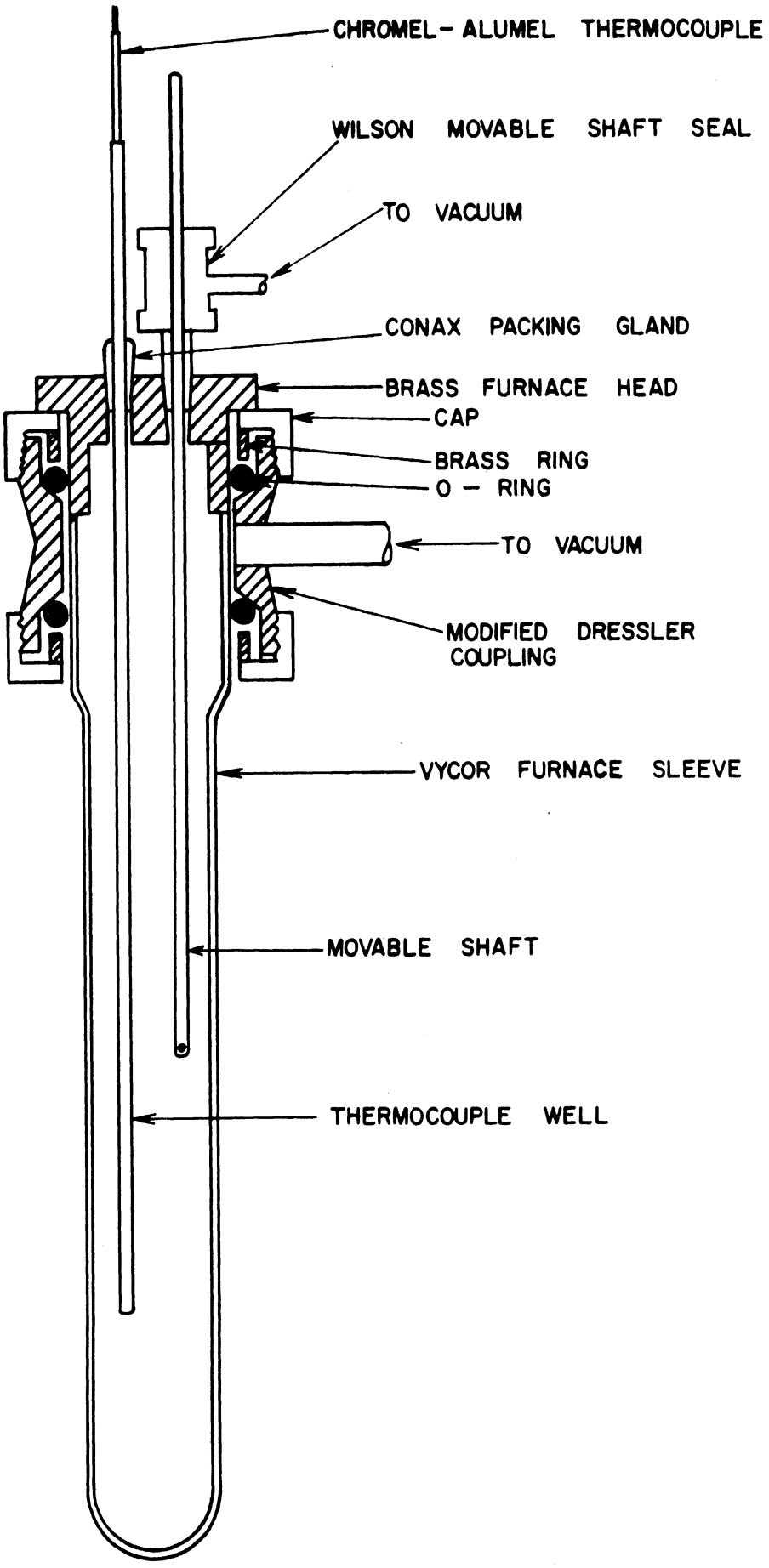

Figure 9. Furnace Arrangement for Fusing Salts and Preparing Alloys

was passed. The lower end of this tube, which served as a thermocouple well, was sealed. A second moveable shaft was also passed through this head. The Wilson fitting which supported this shaft was provided with a separate connection to the vacuum system. Evacuation of the intermediate compartment in the Wilson fitting reduces contamination within the furnace which otherwise results as the shaft is moved up and down. The moveable shaft is provided with a hole hear the bottom to allow connection of stirring devices etc.

The furnace head employed for discharge of the concentration cell is shown in Figure 10. The upper section, like the previously described head, was machined from a section of 3" brass rod stock. The electrical leads for the cell entered the furnace through a three wire Conax high-vacuum sealing gland. These wires are sheathed in teflon for good electrical insulation. They are connected to 1/16" bare stainless steel busses which carry the current down to the tungsten cell leads. Connection of the tungsten leads to the busses is accomplished by tacking stainless hypodermic tubing to the busses near their lower ends. If the tungsten leads are bent slightly a good electrical connection is obtained when they are inserted in the hypodermic tubing. Care is taken to insure both stainless-tungsten connections are made at the same height in the furnace to avoid thermal emf's. The insulated copper wires at the top of the busses are coiled into helixes to prevent transmission of undue stresses to the fragile

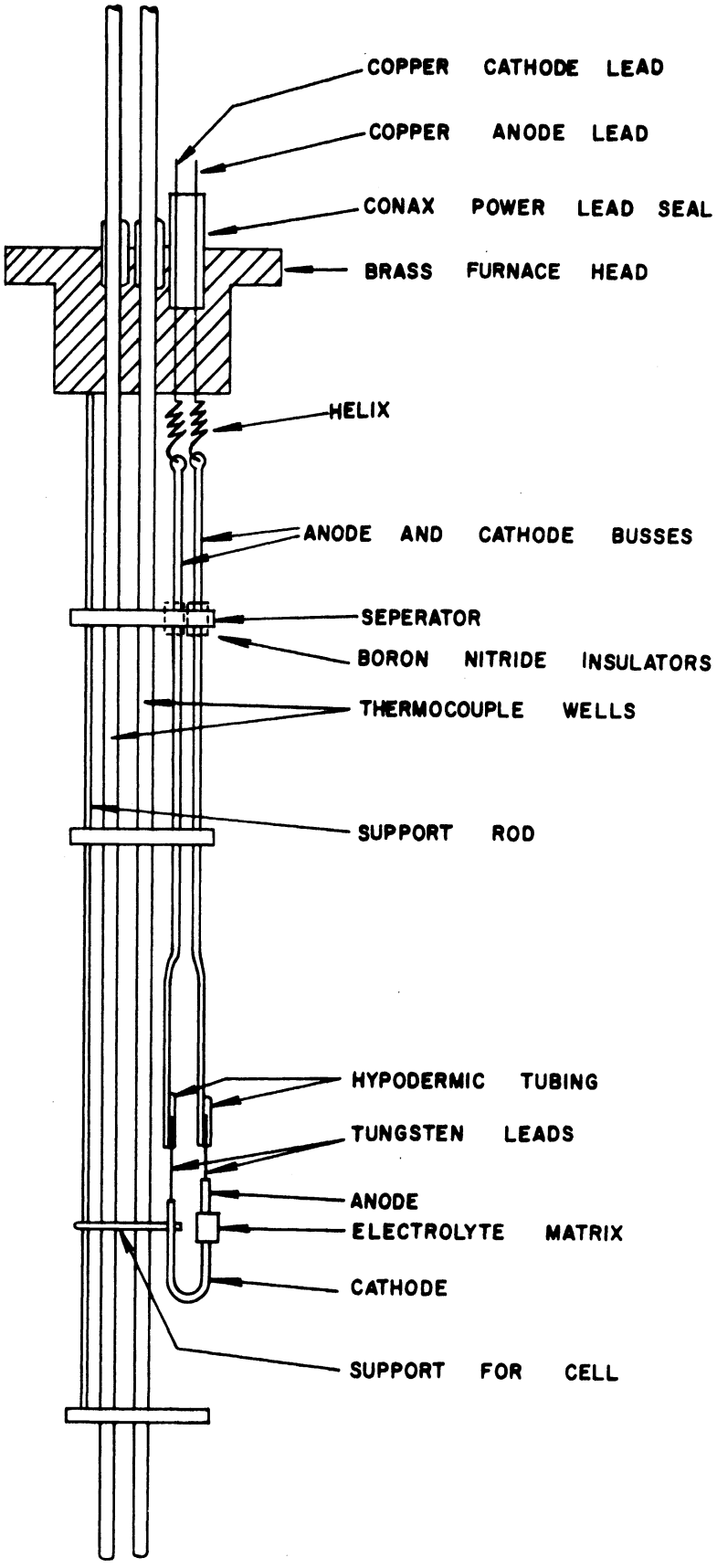

Figure 10. Furnace Head and Superstructure for Discharge of Concentration Cell

cell. The coil expansion can be adjusted to apply sufficient pressure to hold the cell together but not so much as to shear the quartz cathode compartment.

Two thermocouple wells constructed from 25 BWG 1/4" O. D. type 304 stainless steel are provided. One contains the control thermocouple, the bead of which is positioned even with the cathode-electrolyte interface of the cell. The second contains a thermocouple which can be moved up and down to measure axial thermal gradients in the furnace.

A 1/2" stainless rod supports three stainless spacer plates. These spacers guide the current busses to the cells and insure they will not become shorted by contacting each other or the thermocouple wells. Boron nitride sleeves are used to insulate the spacers from the current busses. Boron nitride is an excellent high temperature electrical resistor, 5×10^{8} ohm at 1000°C (161). It is easily shaped by conventional machining methods, and according to Norante (100) is not attacked by alkali metals or fused salts under the conditions of these experiments. Boron nitride also has surface characteristics which retard formation of continuous films of moisture or oil, thus it provides excellent electrical resistance even under adverse conditions.

As discussed above, high electrical resistance materials were employed throughout the furnace superstructure to insure low leakage current for the concentration cell. Figure B-1 of Appendix B, shows the resistance measured between the electrical leads external to the furnace for the furnace superstructure and a dummy cell (no electrolyte

impregnated in the matrix). At 800°K the resistance is 10^8 Ω . For a cell voltage of 1.0 volts and current of 0.01ma, the error in the discharge current due to leakage current would be 0.01%.

The diffusion cell was mounted with a stainless steel jig as shown in Figure 10. The cell was held from the free end of the capillary body by a set screw which fits into a notch in the capillary body. It was not possible to support the cell from below because excess fused salt from the electrolyte runs down the outside of the capillary compartment. If a film of this salt makes direct contact with the stainless steel furnace superstructure, which is at system ground, it will disturb the electrical circuit of the concentration cell.

It is important the diffusion cell be mounted so the diffusion path is vertical. If it is inclined convection currents may result from density inversions which are particularly likely to occur when the surfaces of constant concentration advancing in the axial direction of the capillary are not planar.

Neoprene "O" rings are used to seal the furnace where the Vycor sleeve and brass furnace head meet the Dressler coupling. All threaded connections in the furnace head are sealed with teflon tape. Stainless steel is used for those sections of the furnace superstructure exposed to high temperatures. Corrosion, primarily pitting, was apparent when working with fused salts containing NaCl.

Potentiostat

The cell voltage was maintained constant with the potentiostat circuit shown in Figure 11. This circuit is often referred to as a voltage follower. It incorporates a differential input direct current operational amplifier (P-2) and a current booster amplifier (P-5). Both amplifiers are solid state and were manufactured by Philbrick Researches, Inc.

The experimental cell is bucked with a reference voltage which in turn is connected to the negative input of the amplifier. The positive input of the amplifier and the cathode of the cell are grounded. The differential amplifier functions to keep both of its inputs at the same potential by regulating the cell current via a negative feedback circuit. Briefly, the operation of the circuit is as follows. If the voltage of the diffusion cell exceeds the reference voltage the amplifier will have a negative voltage (relative to system ground) on the floating input. The output of the amplifier will be a positive voltage causing electrons to flow from the anode of the cell through the feedback circuit and to the amplifier. These electrons, of course, are returned to the cell cathode via the system ground. An increase in electron flow from the cell is accompanied by an increase in the alkali metal transferred to the cathode. Since diffusion in the cathode is limiting, the concentration of alkali metal at the cathode-electrolyte interface will rise thereby decreasing the

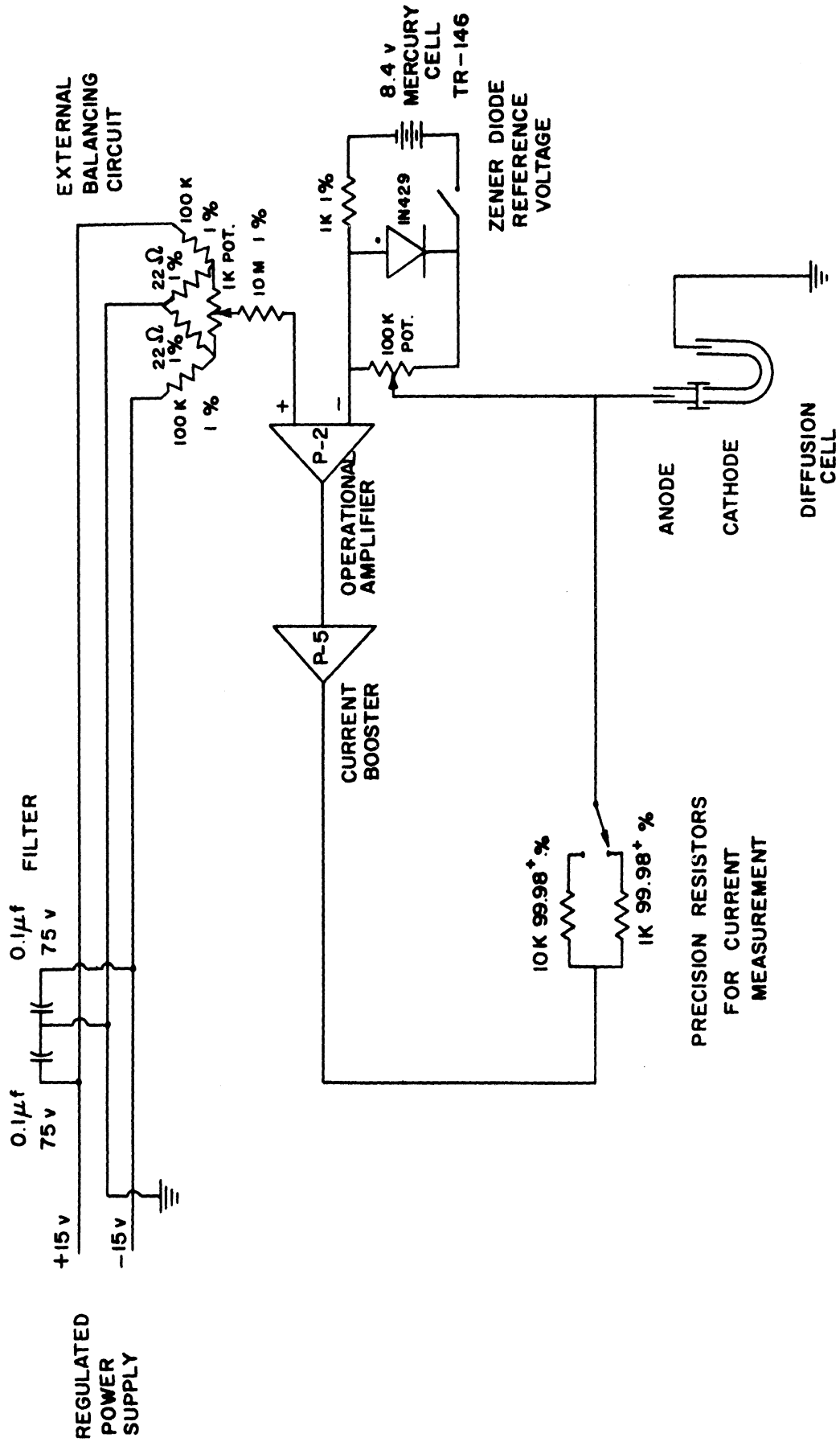

Figure 11. Potentiostat Circuit

cell voltage until it is equal to the reference voltage. If the cell voltage drops below the reference voltage, the output of the amplifier will be negative and the rate of cell reaction decreased until the voltage rises to the reference value.

The current booster amplifier serves only to increase the range of current attainable from the potentiostat circuit. Unlike the differential amplifier, the booster amplifier does not invert the input signal, nor does it change its amplitude.

The input impedence of the P-2 amplifier is extremely high ($>10^{12}$ Ω), virtually all of the output current flows through the experimental cell. Current was measured by determining voltage drop across a Leeds and Northrup precision resistor placed in the feedback circuit. Two resistors, one of 10,000 Ω and the other of 1,000 Ω were used. This allows measurement of a wide range of cell currents. The maximum voltage drop across the resistor is limited by the maximum output voltage of the amplifier, $\pm$ 11 volts in this case. Since the output voltage of the amplifier floats with respect to ground, neither end of these resistors can be at ground potential. Therefore, measurement of voltage drop across the resistor cannot be accomplished with an instrument having one of its inputs grounded. It is necessary to use an instrument such as a battery operated electrometer to measure the voltage drop.

The Zener reference voltage circuit was constructed from a 1N429 Hoffman diode and an 8.4 volt TR-146 primary mercury cell. A 10 turn 100 K potentiometer with a linearity of 0.025% provides fine selection

of reference voltage. The 1 K resistor in this circuit as well as the 100 K and the 22 K resistors employed in the external amplifier balancing circuit discussed below are all precision 1% half watt wire wound resistors.

The positive input of the operational amplifier was connected to an external balancing circuit. A 20 turn micro-pot provided finer balancing control than did the rough balancing potentiometer on the amplifier body. With this external balancing circuit it was possible to correct for drift in the inputs by floating the positive input $\pm$ 3.5 mv. from ground. Each revolution of the adjustment screw represents 0.35 mv. During the balancing operation the amplifier was connected as a power of 2000 multiplier and the input adjusted to give zero output.

All electrical connections were made with Amphenol 21-537 coaxial cable. Only one end of the sheaths was grounded to avoid ground loops which can in turn induce currents in the central conductors. The entire circuit was shielded by enclosure in an aluminum chasis. External connections were made with Amphenol BNC coaxial connectors.

The current source for the P-2 and P-5 amplifiers was a Philbrick PR-30 Regulated Dual Power Supply. It was located outside of the shielded chasis so no alternating current would enter the enclosure.

The circuit was tested and found to function well. When the impedence of a dummy cell was changed by a thousand-fold in step-like fashion, the potentiostat maintained the potential across the dummy cell to better than 10 microvolts. The response time was less than a second for this test.

Instrumentation

The voltage drop across the precision resistors in the potentiostat circuit was measured with a Keithley Model 600A Electrometer. This instrument has overlaping scales and an accuracy of 2% of full scale when used to measure voltage.

The reference and cell potentials were measured with a Keithley Model 660 Guarded D.C. Differential Voltmeter and a Curtis Wright Model NA101A Dynamic Capacitor Electrometer.

The cell conductivity was measured with an Industrial Instruments Conductivity Bridge Model RC-18. This instrument applies an alternating potential to the cell when it is measuring conductivity. The accuracy of the bridge was found to be satisfactory when checked against a 1% precision carbon resistor.

Furnace and Temperature Controller

A Hevi-Duty resistance wound hinged furnace was used to maintain the desired temperature for these experiments. The furnace has a three inch inner diameter and three independently controlled windings. The center winding is 12" in length and each of the end windings are 3" in length. The current ratios in these windings can be regulated to compensate for thermal losses at the furnace ends and to establish a desired temperature gradient in the center zone. It was possible to maintain a stable temperature gradient of 0.5°C per inch in the center section of the furnace. The top and bottom of the furnace were insulated with fiberfrax wool to minimize thermal losses.

A Barber Coleman Model 407 Capitrol provided proportional control of the current supplied to the furnace windings. All three windings were regulated by this Capitrol, however, each had a separate variac in series to provide current ratio control. Power to the furnace was supplied from a Lindberg 1.5KVA saturable core reactor. This minimized fluctuations originating from excursions of line voltage.

The furnace temperature was measured with a 20 gauge chromel-alumel thermocouple. An ice bath was maintained for the reference junction. Output from the thermocouple was read on a Leeds and Northrup indicating potentiometer.

Vacuum System

A schematic diagram of the vacuum system is shown in Figure 12. A Welsch Duo-Seal Pump was employed for roughing. A CVC Oil Diffusion Pump, Model VHF 21 was used to obtain low pressures in the furnace. Dow Corning #705 diffusion pump oil was used in the pump. The diffusion pump was by-passed until the pressure was less than 20 microns, it was then cut in and was capable of lowering the pressure in the system to below 1 micron.

Piping between the furnace and the roughing pump was 7/8" OD Seamless Copper Tubing. Jamesbury Double Seal 1/2" Ball Valves were used in the foreline and high vacuum line to the furnace. These valves gave considerably less pressure drop than diaphram type valves. The combination of large diameter tubing, ball valves, and compact piping

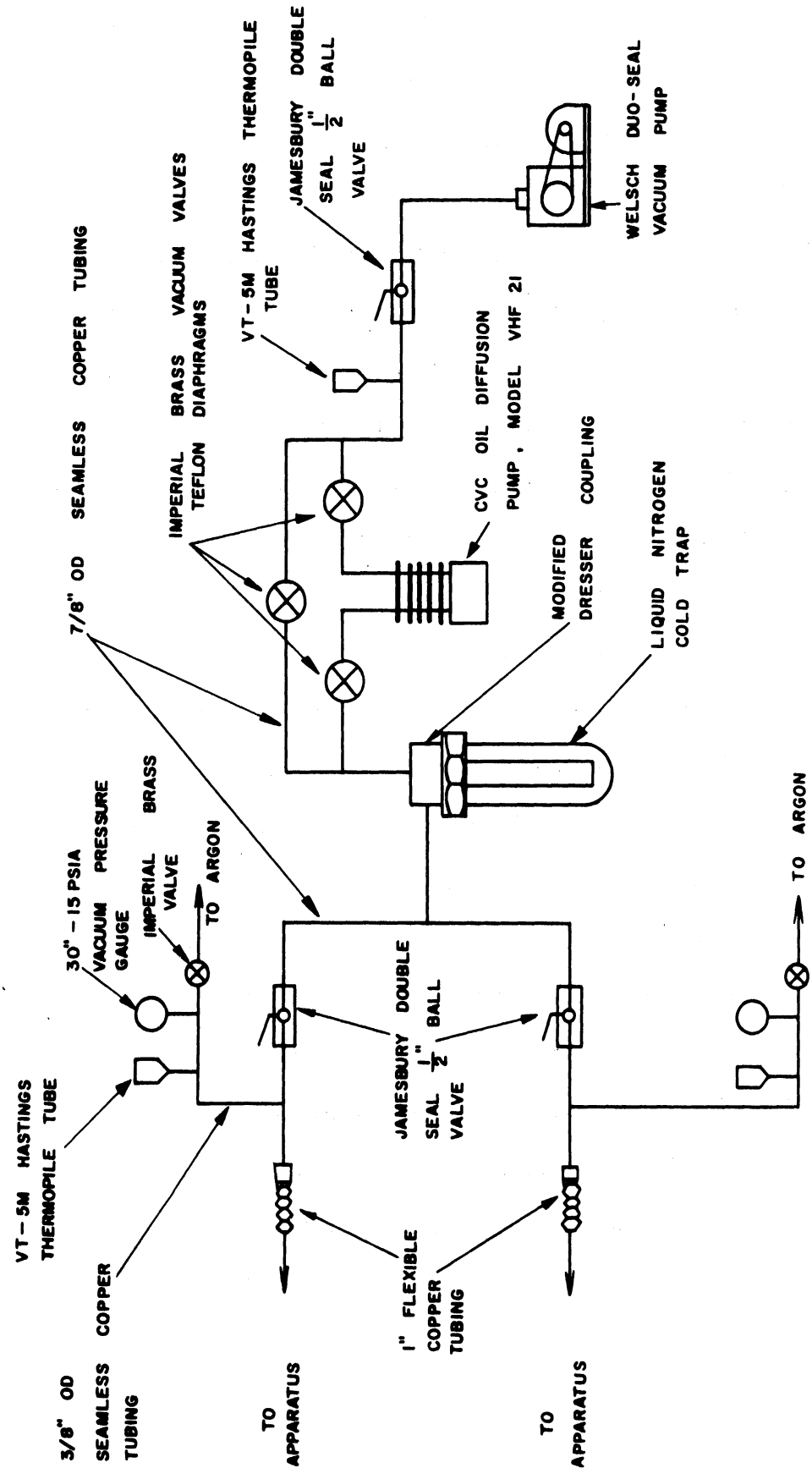

Figure 12. Vacuum System

gave a system capable of being evacuated rapidly.

A modified Dresser coupling was used for construction of a liquid nitrogen trap to remove condensables from the furnace. This is particularly important for fusing salts where the moisture from the salts corrodes the pumps.

Piping in the system which leads to the argon supply was constructed of 3/8" seamless copper tubing. Pressure drop was not crucial here.

Two vacuum lines to the apparatus were provided. Only one was used during discharge of the cell. However, during fusion of the salts and preparation of the alloys one was used for evacuation of the furnace while the other was used to evacuate the chamber of the Wilson moveable shaft seal. Each vacuum line to the apparatus was provided with a 30"-15 psig vacuum-pressure gauge.

Three factory matched VT-5M Hastings Thermopile Tubes were located in the system. One on the foreline and one on each of the high vacuum lines. A three station VT-SB Hastings Vacuum Gauge allowed rapid and successive measurements of the vacuum in different parts of the system. The scale of this gauge is non-linear and can be read accurately in the range 1-100 microns. This multiple gauge arrangement was useful when removing condensables from a melt in the furnace.

The Duo-Seal pump was mounted on springs to reduce vibrations transmitted to the equipment. It was connected to the piping via a flexible hose. One inch flexible copper tubing was used to connect the furnace head and the Wilson seal to the vacuum piping.

D. EXPERIMENTAL PROCEDURE

Preparation of Cathode Alloys and Filling Cathode Compartments

The procedures for the preparation of the cathode alloys varied somewhat, depending on the chemical properties of the metals incorporated in each alloy. The purity, source of supply, and lot numbers for all metals employed in this investigation are given in Table A-4 of Appendix A.

For the cases of sodium-tin and sodium-lead alloys the procedure was as follows. First the lead or the tin was melted in a graphite crucible (National Carbon ATJ Graphite). This produced an ingot of metal convenient for handling in latter steps of the preparation. Since the graphite crucible serves to maintain a slight atmosphere of CO over the melt, it also removed any oxide from the melt which had formed on the large surface area of the metal which was supplied in granular form. The metal was heated to approximately 100°C above the anticipated operating temperature of the diffusion cell for which it was intended. The furnace was then evacuated to outgas the metal. It was found helpful to agitate the metal during outgasing. The high surface tension of liquid metals prevents some entrapped gases from escaping, agitation helps to release these gases. A tungsten agitator shaped from a 0.030" wire was used. Effective outgasing of the cathode metal was found requisite for successful operation of the diffusion cells. If dissolved

gases remain in the alloy they may coalese and form bubbles in the diffusion path during operation of the cell. This will distort the diffusion path by changing its area perpendicular to the direction of diffusion. In some cases it may cause a complete separation of the metallic capillary producing an open circuit. The reason for thorough outgasing of the cathode base metal (lead or tin) at this point in the alloy preparation is as follows. After alloying this base metal with the alkali metal, attempts to outgas at elevated temperatures produced metallic deposits on the cooler sections of the furnace. These deposits proved to be metallic sodium and oxides thereof. This indicated part of the sodium vaporized from the alloy during outgasing with a resultant change in alloy composition. Therefore, outgasing of the cathode metal was limited to the base metal and no attempt was made to outgas the alloy at temperatures above the cell operating temperature.

After outgasing of the pure lead or tin, the metal was cooled under vacuum to below its solidification temperature. Then an inert blanket of argon was admitted to the furnace which hastened cooling to room temperature.

The ingot of metal was accurately weighed, then it and the graphite crucible were placed in the dry box for addition of the proper amount of sodium. The dry box was equipped with a vacuum lock which was evacuated twice each time it was opened to the atmosphere. An inert atmosphere of oil pumped nitrogen was maintained in the dry box. This

gas was dried by passage through a calcium chloride column prior to its entry to the dry box. In addition five trays of indicating and plain calcium chloride were placed in the dry box and changed as required.

Sodium metal was cut from the center of a block of lump sodium and accurately weighed on a balance in the dry box. It was then charged to the crucible, sodium on the bottom and lead or tin on top. To protect the sodium from oxidation while it was being transferred from the dry box to the furnace, a layer of high purity n-pentane was placed over it. This n-pentane had been previously dried by storage over sodium metal. It is easily removed from the charge when the furnace is evacuated.

The charge was placed in the furnace together with several cathode bodies. The latter were attached to the tungsten stirrer with the open ends of the legs up. The furnace was evacuated until a pressure of less than 1 micron was attained and argon admitted to bring the pressure to about 10 psia. The charge was rapidly heated to a few degrees above the melting point of the lead or the tin and the melt agitated with a tungsten stirrer for about an hour to insure uniformity of composition. The furnace was then evacuated to about 100 microns pressure and the melt agitated for a few moments to release any entrapped gas. At a pressure of 100 microns, no vaporization from the melt was noticed. The "U" tube capillaries attached to the stirring rod were immersed in the melt. A positive pressure of 2 or 3 psig of argon was placed over the melt to aid flow of alloy into the capillary. After a few minutes immersion, the melt was cooled and the capillaries removed just as the alloy started

to solidify. By allowing the capillaries to remain in the melt until this time the shrinkage which occurred upon solidification of the metal was minimized. Also, the high surface tension of liquid metals makes a thin column a very unstable shape. By allowing the metal to cool to the solidification point, there is less chance it will escape from one of the legs.

All of the capillary cathodes needed for diffusion runs at a particular alloy composition were prepared during a single filling operation. This is important because, as discussed earlier, it is difficult to thoroughly outgas the alloy. If the alloy is heated and cooled for several successive filling operations it will absorb enough gas in the process so that the capillaries filled toward the end of these filling operations will contain metal with enough absorbed gases to present problems in the diffusion cell runs.

After the filling operation is completed the cathodes were stored under argon in a desiccator.

Preparation of the potassium-mercury alloys differed from the above procedure in the following ways. The use of graphite crucibles was not possible. Dzurus and Henning (41) note that graphite readily forms lamellar compounds with potassium, whereas with sodium a catalyist is required. Therefore, potassium-mercury alloys were prepared in quartz glassware.

The mercury was heated to 200°F and outgased. It was not possible to outgas the mercury above cell operating temperatures because of the

high vapor pressure of mercury. Instead outgasing was allowed to proceed at the lower tmperature for about an hour with intermittent stirring. Argon was then admitted to the furnace, the charge cooled and transferred to the dry box. Both the mercury and the potassium were weighed in this dry box. n-Pentane was added to the charge to cover the potassium which floated on top of the mercury. The charge was transferred to the furnace which was evacuated to remove the pentane. It was found the potassium floated on top of the mercury with little apparent reaction at room temperature. This was probably due to a thin oxide film which formed on the potassium even in the controlled atmosphere of dry box. It was necessary to hold the potassium under the surface of the mercury with the tungsten stirrer while the charge was heated slowly until all of the potassium was dissolved and the resultant alloy was fluid. An argon blanket of 14 - 16 psia was maintained above the alloy at all times while it was being heated. This alloy had to be heated slowly instead of rapidly as was done in the cases of sodium-lead and sodium-tin because solution of potassium in mercury is accompanied by a large evolution of heat. If the charge is heated rapidly and solution of the entire lump of potassium occurs instantaneously, part of the mercury will be vaporized and the alloy splashed out of the crucible. On one occasion a geyser of alloy several inches high was observed.

Filling and storage of the capillaries was accomplished in a manner identical to that described earlier for the sodium-lead and sodium-tin alloys.

Table A-2 in Appendix A lists the compositions of alloys prepared for this investigation. It should be noted each alloy was prepared from the pure metals instead of preparing the less concentrated alloys by successive dilution of the most concentrated one. Again this procedure was used because of the tendency for the alloys to absorb gas when heated and cooled several times.

Electrolyte Preparation

The electrolyte for a diffusion cell is a fused salt or a mixture of fused salts impregnated in a porous alumina matrix. Table A-4 in Appendix A lists the supplier, purity, and lot numbers for all the fused salts used in this investigation.

The fused salts were prepared by weighing the individual components in the dry box. Use of the dry box was essential because of the deliquesent nature of the salts, particularly the hydroxides. It is impossible to obtain accurate weights if the operation is performed in air of normal humidity.

The procedure for fusing salt mixtures depended on the composition of the system.

Fusion of the sodium hydroxide was first attempted in a high density alumina crucible. This was unsuccessful, upon solidification of the melt stresses were set up in the crucible which would invariably cause it to crack upon re-heating. A crack in the crucible would allow the salt to run into the bottom of the Vycor furnace sleeve which proved

even more susceptable to cracking upon solidification of the salt. Graphite crucibles were found suitable for the fusion of sodium hydroxide, they did not crack as did the alumina. Pellets of sodium hydroxide contained in a covered graphite crucible were heated in an argon atmosphere to a few degrees below the melting point of the salt. The furnace was evacuated to remove any traces of water from the charge. The temperature was then raised slowly (over a period of approximately a half hour) to a few degrees above the melting point of the salt. A vacuum was maintained in the furnace during this heating period. Argon was admitted and the melt heated to about 100°C above its melting point, held there for 10 minutes, and then cooled back down to a few degrees above the melting point of the salt. The furnace was evacuated for approximately an hour after which period the pressure had usually been reduced to 2 - 4 microns. This removed most of the water from the fused salt. Removal of virtually all of the moisture was found essential to successful operation of the diffusion cells. Sodium hydroxide holds water tenaciously. By slowly approaching the fusion temperature of the salt under vacuum and by never evacuating the system when the temperature is more than a few degrees above the fusion temperature it is possible to remove most of the water without causing the salt to foam out of the crucible.

The KOH-KI-KBr eutectic salt mixture was prepared in the dry box and heated in an alumina crucible under an argon atmosphere to 735°C.

This temperature is above the melting point of the highest melting salt present (KI, m.p. 730°C) and insures all of the salt will be in solution. The temperature of the melt was lowered to 240°C, a few degrees above the eutectic solidification point of the system and furnace evacuated for an hour to remove any water present. Some foaming of the electrolyte occurred but this was not as severe as in the case of pure sodium hydroxide. The fused salt was then cooled to room temperature. No cracking of the crucible occurred upon reheating with this salt.

The NaI-NaCl salt mixture was heated in an alumina crucible and under an argon atmosphere to 810°C. Little water of crystallization was removed when the furnace was evacuated at this temperature. Foaming was not a problem with this system.

All three salt systems were stored under an argon atmosphere in a desiccator.

No attempt was made to impregnate the matricies during the same runs in which the salts were fused. The reason for this is to prevent the moisture released by the salts upon fusion from entering the pores of the matricies. Such water would no doubt be hard to remove and might remain entrapped when the matricies are impregnated. In addition, to prevent the salts containing hydroxides from spattering during fusion it was necessary to place a cover on the crucible. This would complicate any scheme for lowering a matrix into the melt.

The procedure for impregnation of the porous matricies is similar for all of the salt mixtures. A group of 3 to 6 matricies cradled with tungsten wire were placed in the furnace along with the salt and the furnace evacuated until the pressure was reduced to 2 or 3 microns. This removed any traces of moisture the salts had acquired during handling and storage. Argon was admitted, and the furnace heated to the impregnation temperature, (NaCl-NaI 680°C, NaOH 375°C, and KOH-KI-KBr 300°C). In each case this temperature was at least 50°C above the melting point of the fused salt. This insured the melt would have sufficient fluidity to readily permeate the pores of the matrix. The pressure in the furnace was reduced to 100 microns and the matricies were totally submerged in the salt. An argon atmosphere was placed above the salt to help force the salt into the pores of the matrix. After a few minutes the matricies were withdrawn from the melt and the pressure again reduced to about 100 microns of mercury. Immersion followed by pressurizing was repeated three times. On the final time the matricies were allowed to remain submerged in the salt for approximately an hour. After impregnation the matricies were stored under argon until required for use in a diffusion cell.

Assembly and Operation of a Diffusion Cell

When the cathode compartments are filled as described previously, it is common for the alloy to recede from the ends of the capillary tube.

This is due both to contraction of the metal upon solidification and escape of a portion of the metal which can lower its surface energy by leaving the capillary. The capillary leg which contacts the fused salt must be cut off perpendicular to the axis of the capillary. It is important this surface meet the matrix in a parallel fashion. If these surfaces are not parallel it will be possible for a portion of the alloy in the capillary to flow into the gap between the cathode compartment and matrix. If this does not result in an open circuit by breaking the metallic column in the cathode compartment, it will at least present a distorted path to the diffusing metal. The cut is made at a point so the metal in the other leg of the capillary will have a head of about 1/64" above the surface of the metal contacting the salt. This very slight head was found to give the most stable and reproducable cell operation. If the head is too large, metal will be forced out of the capillary at the cathode-electrolyte interface, while if the head is a negative one the metal may drop away from the matrix and an open circuit result.

As discussed earlier the cathode compartments were fabricated from precision bore tubing. Close examination reveals that the tubing may vary in diameter by a few thousandths of an inch. This variation is significant for diffusion paths with a diameter of approximately one millimeter. Each finished cathode was examined with a Bausch and Lomb binocular microscope equipped with a scale calibrated in thousandths of an inch superimposed on the field of vision. The diameter could be

measured by focusing on the end of the capillary. Any variation in diameter over the section where diffusion occurs could be detected by sliding the capillary under the microscope. Only those capillaries with uniform diameter were selcted for diffusion runs.

The finished cathode and the matrix impregnated with fused salt were placed in the dry box along with an empty anode compartment.

A matrix which has been impregnated retains considerable salt in the anode and cathode cavities. If this is not removed it can cause failure during cell operation. The unsupported salt upon melting will cause shifts in the cell components relative to each other. Due to the deliquesent nature of the salts it was necessary to perform this operation in the dry box. It was accomplished by rough drilling with a carbide drill bit held in an ordinary tap holder. The surfaces were finished with a hand-held high-speed electric drill equipped with diamond tipped dental bits. Special care was taken to insure the contact surfaces of the matrix and the cathode would be parallel.

The anode compartment was filled with alkali metal by pressing the sleeve into the center of a block of alkali metal. In this manner a slug of approximately 1/4" of metal could be collected. Best results were obtained by grinding the lower section of the sleeve to a knife edge prior to the filling operation. The anode cavity of the matrix was compacted with alkali metal by use of a Surgident Amalgam Carrier. This allowed the cavity to be filled with a minimum of voids. The anode

compartment was then pressed into the anode cavity of the matrix to insure good mechanical fit and a continuous phase of alkali metal.

The tungsten lead was inserted in the anode compartment until the pre-formed bend rested on the alumina anode compartment. This bend insures the tungsten wire will be at the right position in the anode compartment relative to the matrix. If the wire is too long and makes direct contact with the fused salt contained in the matrix an erronious potential will be obtained. If, on the other hand, the end of the tungsten wire is too far from the fused salt it may fail to make contact with the anode metal as it recedes during cell operation. This decrease in anode metal during cell operation is due, at least in small part, to the metal which is transferred from the anode to the cathode. It is, however, primarily due to slow vaporization of the alkali metal at cell operating temperature. This latter effect is reduced by using an anode compartment several times the length of the slug of alkali metal. This retards the rate of vaporization. The proper height of the tungsten anode lead appears to be about 1/16" above the bottom edge of the anode compartment.

A few drops of n-pentane are injected into the top of the anode compartment with a hypodermic syringe prior to transferring it from the dry box to the furnace. The cell was transferred to the furnace and the pressure quickly reduced to about 1 micron to remove the n-pentane and any traces of moisture which the cell may have picked up during handling.

Argon is admitted to bring the pressure to about 12 psia and the temperature rapidly raised to the cell operating temperature. Thermal gradients in the zone of the furnace containing the cell are measured with the sliding thermocouple and the three heaters are adjusted to give a slight temperature gradient with the top of the cell about two degrees hotter than the bottom. This gradient reduces the possibility of convection gradients in the diffusion column arising from thermally induced density inversions.

The conductivity of the cell is measured with an AC bridge prior to the diffusion run. Cell resistance is also checked at the conclusion of the diffusion run.

The discharge potential for the experiment was selected from the relationship of cell potential to composition of the cathode alloy for the particular system. See Figures C-1, C-2, and C-3 of Appendix C. It was found necessary to select the discharge potential φ_s so that it was at least 0.05 volts below the potential corresponding to the initial composition of the cathode alloy φ_o.

After the desired temperature profile had been obtained and the cell resistance determined, the cell was discharged at constant potential for a period of 1 to 2 hours. Current readings were taken at frequent intervals during the initial portion of the run, usually every 5 to 10 seconds for the first minute or so. The frequency of current readings was reduced as time progressed to one every 5 or 10 minutes after the

first half hour. The majority of the runs were terminated at the discretion of the operator, but a few were terminated by cell instability.

After completion of an experiment the cell was examined for any indications of irregularity such as bubbles in the cathode.

E. DISCUSSION OF EXPERIMENTAL RESULTS

General

Diffusion of potassium in potassium-amalgams, of sodium in sodium-lead alloys, and of sodium in sodium-tin alloys has been investigated. In each case a range of temperature and alloy composition was studied. For the potassium-mercury and the sodium-lead systems the diffusion coefficients obtained are compared with those of other investigators which have been reported in the literature.

A summary of the experimental investigations is presented in Tables A-1, A-2 and A-3 of Appendix A. Table A-1 shows the experimental conditions for each of the diffusion cells operated in the course of this study. Included are the temperature, the diameter of the diffusion path and the duration of the discharge period. The compositions of the alloys utilized in these cells is presented in Table A-2 and that of the fused salt electrolytes in Table A-3. The raw data for each of the successful runs is tabulated in Appendix B.

Four typical current-time discharge curves are shown in Figures 13, 14, 15, and 16. The general shape of the curves conforms to that predicted from the mathematical analysis, see Figures 4 , and 5 . The dashed line in each of these figures has a slope of -1/2. For times larger than about 200 seconds the experimental discharge curve appears to have a slope of -1/2 also. The slight cycling evident at long times is probably due to

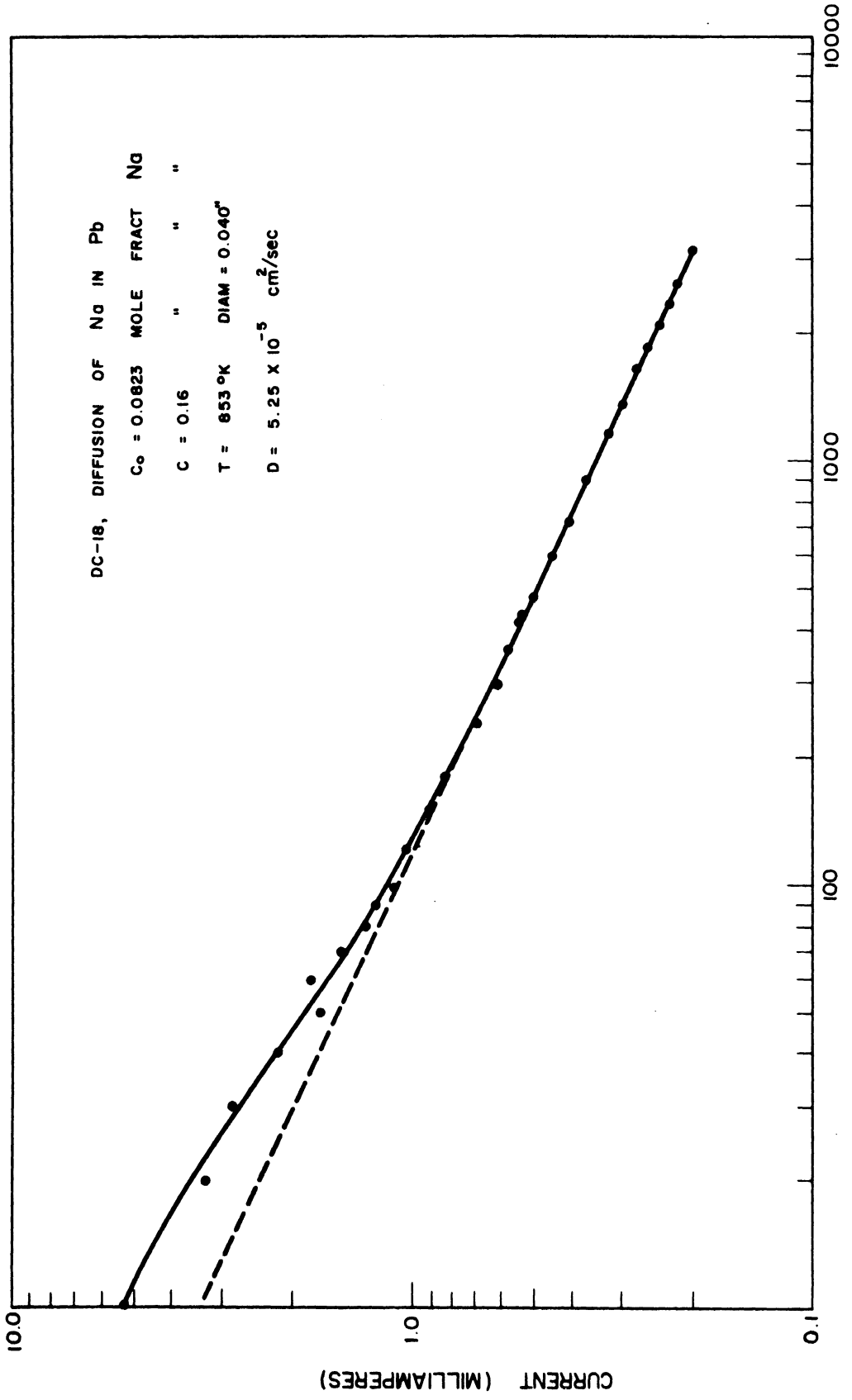

Figure 13. Discharge Curve for DC-18

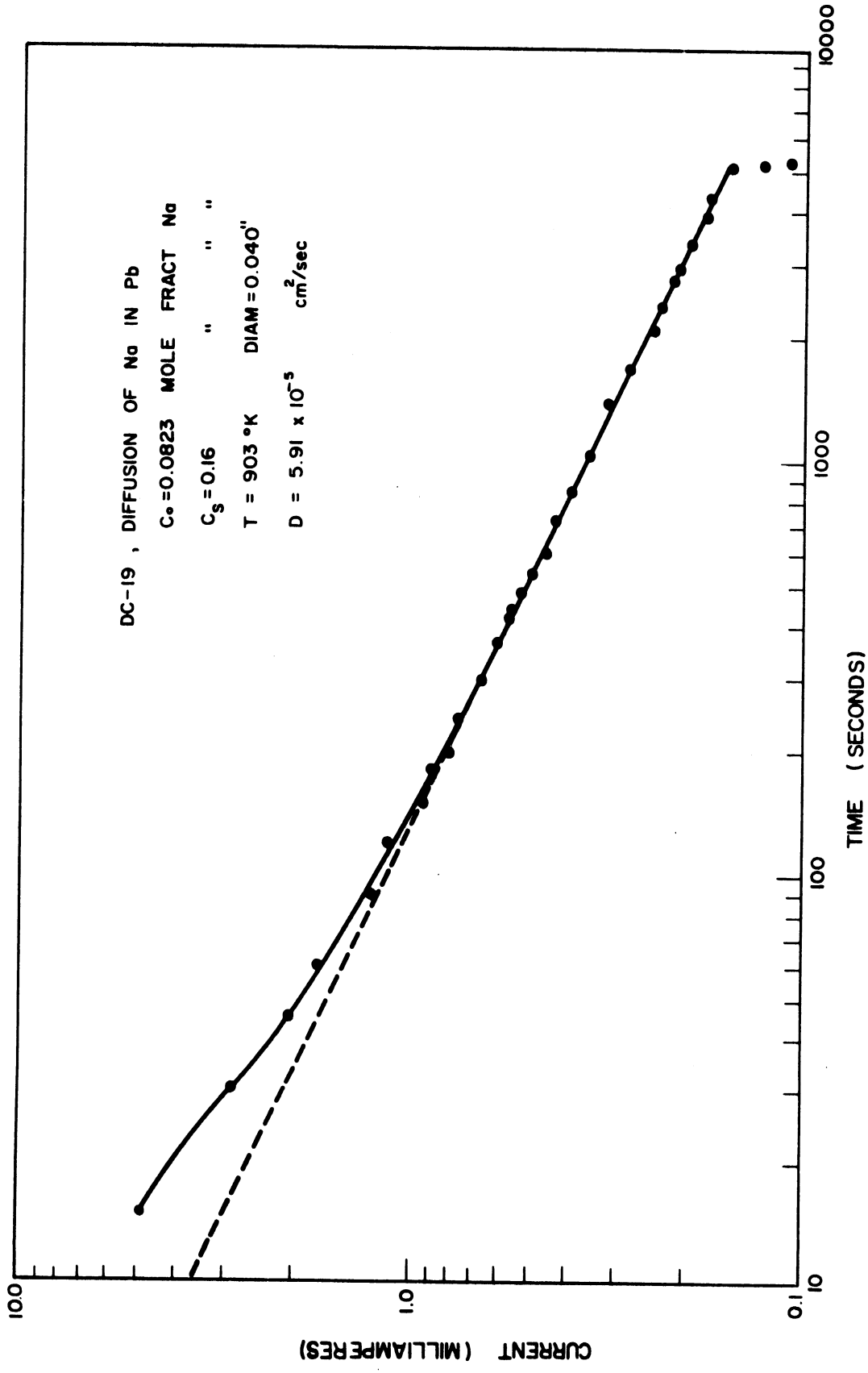

Figure 14. Discharge Curve for DC-19

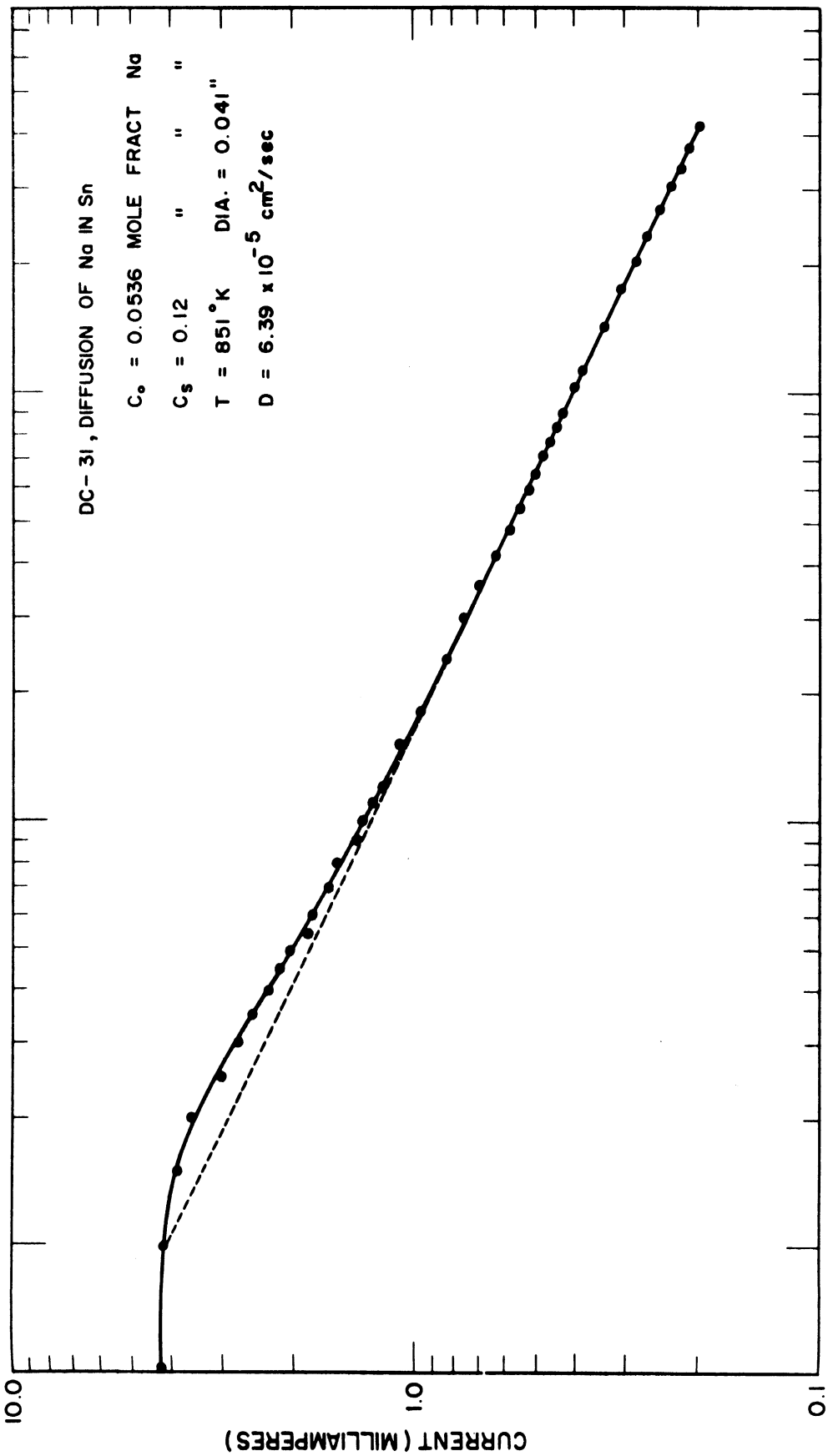

Figure 15. Discharge Curve for DC-31

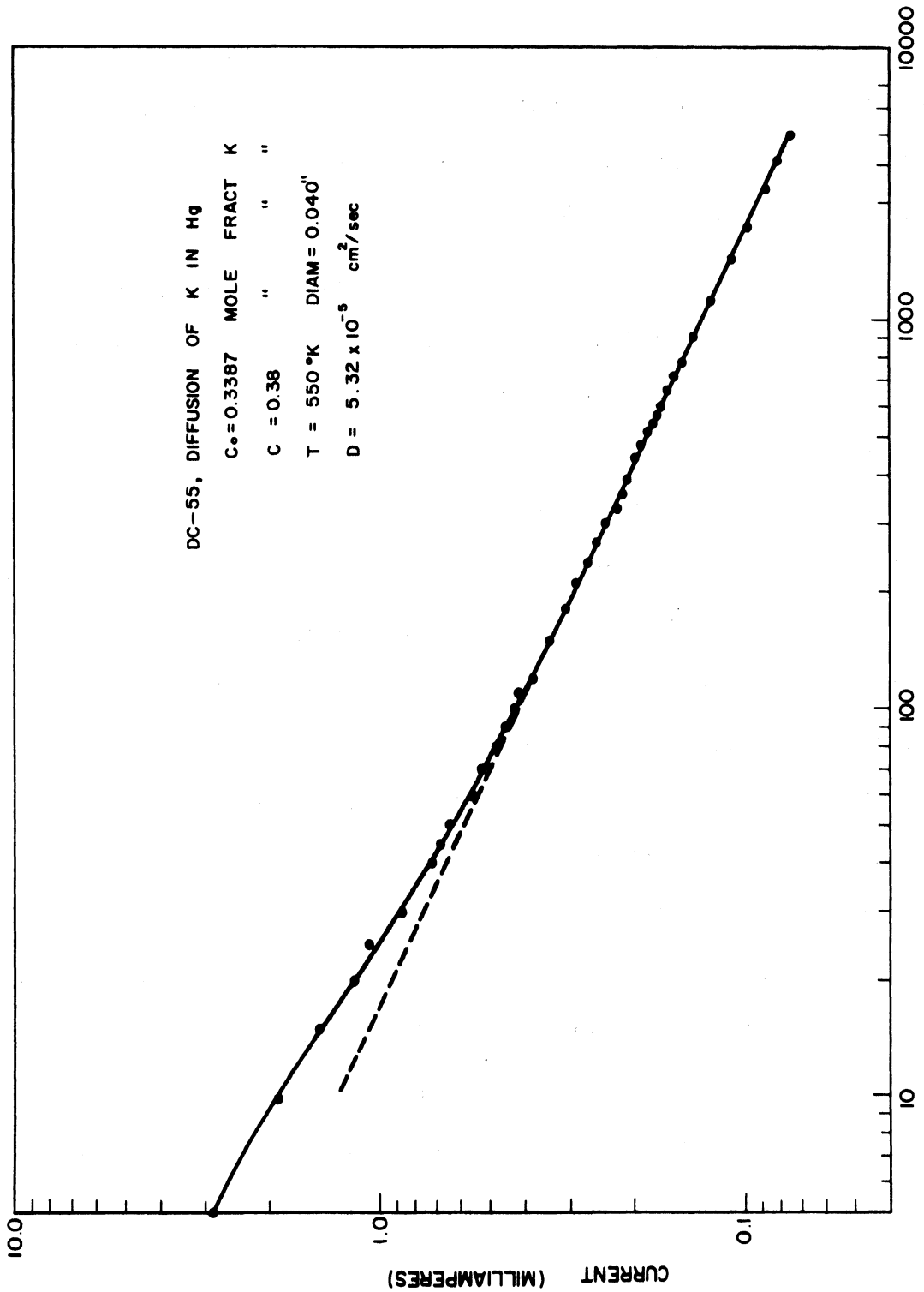

Figure 16. Discharge Curve for DC-55

slight variations in the cross-sectional area of the diffusion path. With the exception of an occasional point, there is very little scatter in the data for times greater than about 200 seconds. At small times the flux is larger than is predicted by linear extrapolation of the data for large values of time. This is attributed to the existence of a non-planar cathode-electrolyte interface. Examination of the cells at the conclusion of each run indicated the cathode alloy had usually receded from the surface for the matrix in a manner similar to that shown in Figure 2 . This behavior is reasonable for the systems investigated since the salts used appear to wet the quartz cathodes better than did the cathode alloys.

The general shapes of the discharge curves obtained in this investigation are similar, however, there is still considerable variation from experiment to experiment. More scatter occurs in the data for small times. Also at small times there is less reproducability in the shape of the curves than exists at larger times. It appears the current at small times is sensitive to such factors as surface films which may have formed at the interface and variations in contact pressure between cathode alloy and the matrix.

It would be difficult to make any quantitative predictions about the shape of the cathode-electrolyte interface on the basis of the discharge curves obtained. First, as discussed above, reproducability at small times is poor. Second, the existence of a non-planar interface gives

rise to a diffusion flux component perpendicular to the axis of the capillary. Slight inclination of the capillary will result in convection due to density inversions at the non-planar surfaces of constant concentration. This convection will tend, both to increase the flux into the diffusion path and to damp out the non-planar concentration surfaces which themselves gave rise to the convection.

Calculation of diffusion coefficients was done by use only of that portion of the data in the linear region of the discharge curves. Equation (92) for the flux in a semi-infinite one-dimensional system with uniform initial composition and constant surface concentration was used. This equation may be rearranged to give the diffusion coefficient as a function of current, surface and bulk concentrations of the cathode alloy, and time.

$$D = \left[\frac{J}{A_s (C_s - C_o)}\right]^2 \pi t \qquad (99)$$

The units of concentration used throughout this investigation are gram atoms of alkali metal per centimeter cubed of alloy. A sample calculation utilizing data from Experiment DC-55 is presented in Appendix J. Corrections are made for iR drop in the electrolyte and for thermal expansion of the diffusion path at elevated temperatures. Activation polarization has been assumed negligible, and current efficiency has been assumed to be 100%. This latter assumption appears reasonable for the current densities attained in this investigation. Calculations based on the equilibrium

distribution of Weber and Heymann (72) are presented in Appendix I and indicate the current efficiency will be close to 100%.

The semi-infinite boundary condition utilized in the solution of the differential equation from which equation (99) was obtained requires no significant concentration gradient be established at the lower boundary of the diffusion path if this solution is to alloy. If the diffusion process is allowed to proceed until such a gradient is established, convection attributed to density inversions in the "U" bend at the bottom of the capillary can be expected. The presence of convection should alter the shape of the discharge curve, though the time necessary for the gradient caused by this anomality to influence the gradient at the interface may be appreciable. Calculation of the dimensionless concentration change for experiment DC-55 indicates this change is not appreciable at the conclusion of the experiment. This calculation is presented in Appendix J. The total quantity of alkali metal transferred from the anode to the cathode has also been calculated in this appendix. 1.898×10^{-4} grams of potassium were transferred from the anode to the cathode during the experiment. One can appreciate the value of the experimental method developed in this investigation when the difficulty of analyzing chemically for this small change in potassium content of the cathode amalgam is considered. The electrical measurements of discharge current and potential are made with much greater ease and precision. This technique also is not subject to the error in the quantity of potassium transferred which is inherent in methods which measure only overall potassium transferred during

a given period of time.

The concentration intervals used in this investigation, $(C_s - C_o)$, were selected as small as possible to minimize volume changes during diffusion. To obtain stable discharge characteristics it was found necessary to apply a potential at least 0.05 volts below the open circuit potential of the cell. The lower limit on the concentration interval which could be used was determined by this factor. Concentration intervals from 4 to 8 mole % of the alkali metal were employed. Smaller concentration gradients could be used when studying the potassium-mercury system since the gradient $d\varphi/dc$ is greater for this system than for sodium-lead and sodium-tin alloys. Differential diffusion coefficients were obtained for these small concentration intervals and their values are reported as corresponding to the average value of concentration for the interval.

At small times the concentration profile in the capillary is not uniform with respect to the radial direction. The values of concentration in the axial direction cannot be described by an error function profile. This perturbation of the concentration profile for small time can be expected to cause some alteration of the shape of the profiles for the remainder of the experiment. Anomalities of this nature cannot be avoided at small times and their effect on later conditions can be expected to decrease with time. For this reason the duration of the runs was long compared to the initial period during which anomalities were significant.

The probable errors in the diffusion coefficients were calculated in Appendix K. These calculations were based on the error for a single

measurement. The estimate of probable error in each of the three systems investigated was found to be approximately 25% due, in most part, to uncertainties in the thermodynamic data used to calculate the voltage of the cell as a function of composition. The time required for preparation of cells was sufficiently long that it was not practical to make several runs at each set of experimental conditions and determine the error from statistical analysis. In those few cases where duplicate runs were made the reproducability was $\pm$ 6% for K-Hg, $\pm$ 9.5% for Na-Pb and $\pm$ 4.6% for Na-Sn.

The experimental results for each of the three systems investigated are now considered independently.

Potassium - Mercury System

The coefficients obtained for diffusion of potassium in potassium amalgams are shown in Figure 17. The concentration intervals employed to determine these values are noted at the top of the figure. A series of three cells, DC-42, DC-43 and DC-44 illustrate the reproducability of the method. Cells DC-42 and DC-43 were identical in all respects and gave values of D differing by 12%. The cell in experiment DC-44 differed from the preceding two only in that it had a diffusion path with a diameter of 1 1/2 mm compared to the 1 mm path used in the others. The similar values of D for different diameter diffusion paths indicates gross convective effects are not present in either diameter capillary.

Diffusion coefficients were obtained at three different temperatures

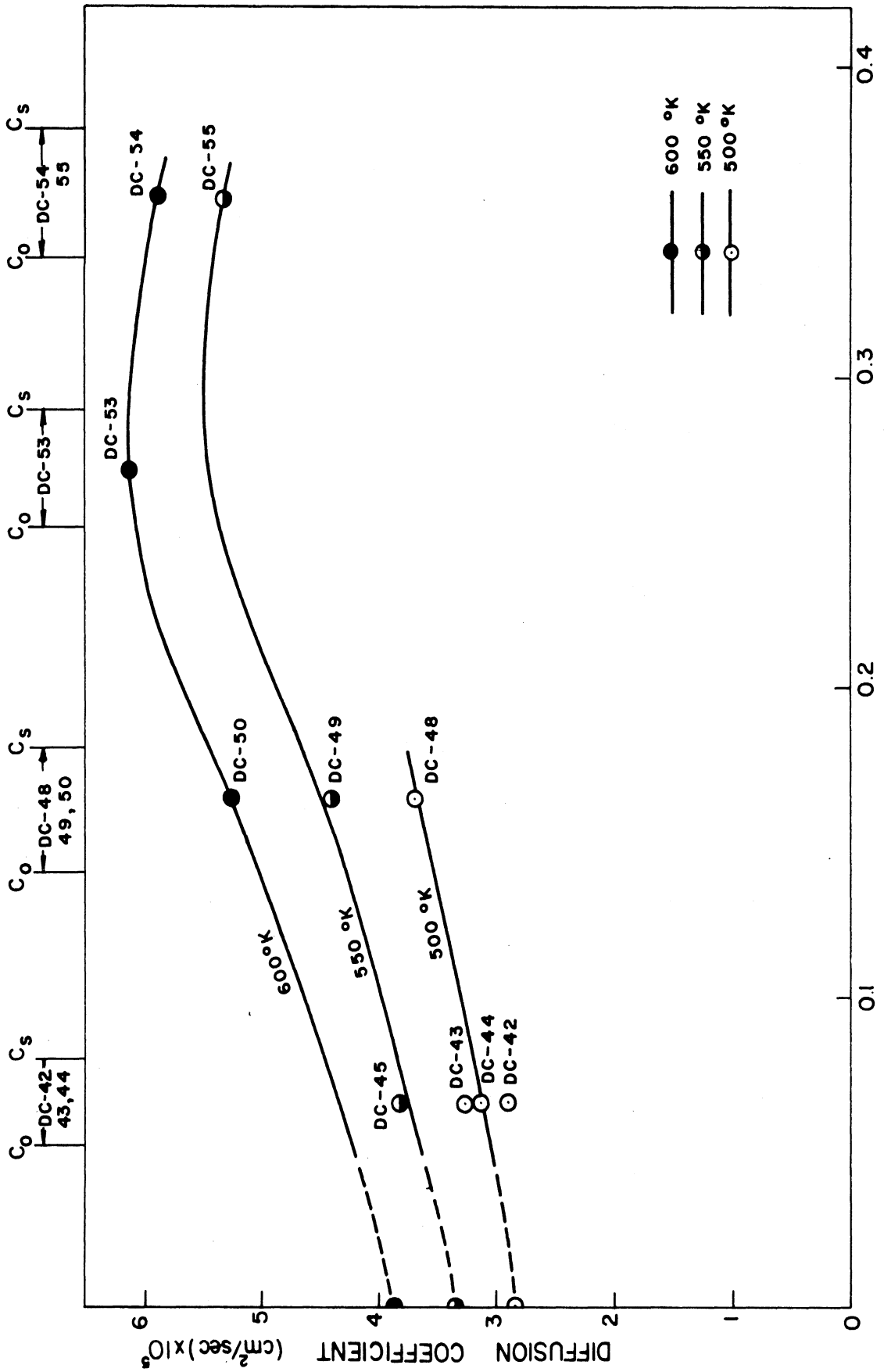

Figure 17. Diffusion Coefficients for Potassium in Potassium-Amalgams

500, 550, and 600°K and over four concentration intervals. The phase diagram for the potassium-mercury system is shown in Figure E-1 of Appendix E. The average composition and temperature corrdinates for each of the runs is indicated by an "X" on this phase diagram. The lower temperature limit was imposed by the melting point of the KOH-KI-KBr(E) fused-salt electrolyte (493°K). Thus, measurements for temperatures below 500°K and low potassium concentrations were not possible. Operation of potassium-amalgam cells above 600°K was also not feasible due to the high vapor pressure of the amalgam. Attempts to measure the diffusion coefficient of potassium in an amalgam with low potassium content, N_K=0.066 at 600°K (see DC-46, DC-47 in Table A-1) failed due to gas fomration at the cathode-electrolyte interface. This gas formation was due, no doubt, to vaporization of the low-boiling potassium-lean amalgam. An attempt to operate a cell with a cathode alloy composition greater than N_K=0.40 (see DC-56 and DC-57 in Table A-1) also failed. The open-circuit potential for these cells was below 0.10 volt and erratic operation was experienced. The value of $d\varphi/dc$ decreases rapidly with increasing potassium concentration in the cathode alloy (see Figure C-1 of Appendix C). This unstable operation may have been due to the large concentration gradient obtained under these conditions.

Experimental values of the diffusion coefficient were not obtained for value of $N_K < 0.06$. Wetting difficulties in the cathode were experienced with pure mercury and with amalgams very lean in potassium. The values of the diffusion coefficient at infinite dilution were obtained from the

Stokes-Einstein equation $D = kT/6\pi\eta r$. Values of viscosity were taken from Grosse (59) and the ionic radius of potassium calculated by Pauling (104) was used.

The values of concentration used in equation (99) to calculate the experimental diffusion coefficients were taken from Figure D-3 of Appendix D.

In Figure 18 the results of this investigation are compared with the smoothed data reported by Bonilla et. al. (13) for diffusion of potassium in potassium-amalgams. Both investigations report a maximum in the diffusion coefficient close to $N_K = 0.30$. The phase diagram for this system shows a congruently melting compound (Hg_2K) at $N_K=0.333$. Examination of thermodynamic data for the system shows that large negative deviations from Raoult's law exist. The only other liquid metals for which diffusion coefficients have been measured as a function of composition and which exhibit negative deviations from Raoult's law are Hg-Tl (52) and Bi-Pb (99). In both these cases a maximum is found to exist. Figure F-1 of Appendix F shows the relationship between viscosity and the composition of potassium amalgams. A maximum exists at $N_K = 0.25$. The viscosity and diffusion coefficient are closely related properties. On the basis of the shape of the viscosity curve it is reasonable to believe a maximum exists in the relationship between diffusion coefficient and composition.

The major discrepancy between the results of the present investigation and those of Bonilla is that of the value of the diffusion

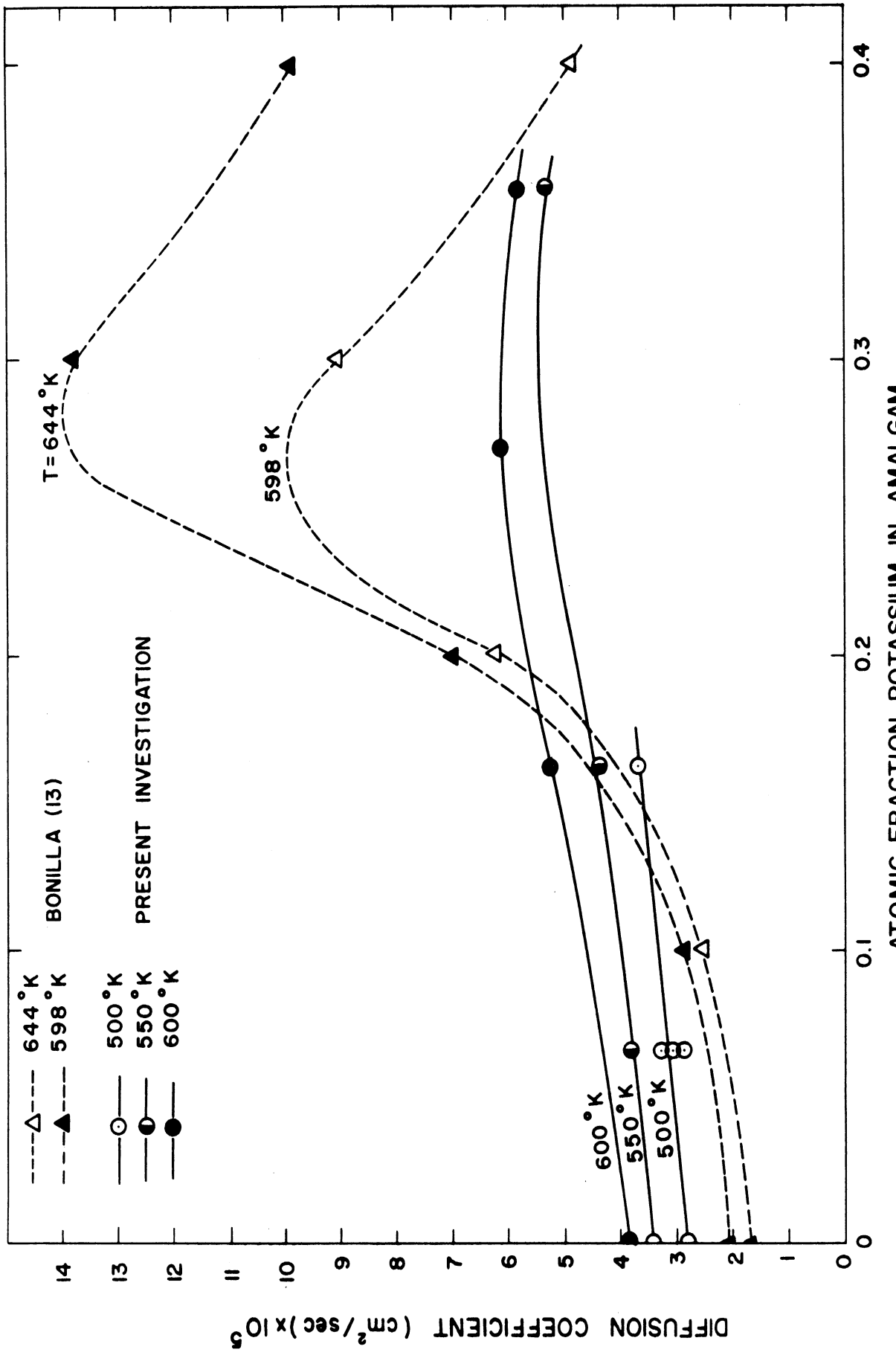

Figure 18. Comparison of Experimental Results of Present Investigation with Smoothed Results Presented by Bonilla

coefficient in the range $0.25 < N_K < 0.35$. Bonilla reports much larger coefficients in this range than were found in the present investigation. The relationships between diffusion coefficient and composition have been reported for the following systems: Hg-Tl (52), Bi-Sn (99), In-Sn (22, 103, 147), Bi-Pb (57, 99, 124), Zn-Hg (127), Pb-Sn (99), Na-Pb (96, this investigation), and Na-Sn (this investigation). With the exception of Bi-Pb (57), in no case did the diffusion coefficient vary in magnitude by more than a factor of 2.2 over the range of composition investigated. In the single exception noted the magnitude of the diffusion coefficient did vary by more than an order of magnitude. However, the investigators noted that large concentration gradients inherent in their experimental method probably gave rise to convection currents and they reported their results as effective diffusion coefficients. Large variations in the value of the diffusion coefficient with composition are common in solids where marked structure changes may occur. In liquids the atoms are less rigidly bound and variations in orientation will not be as pronounced as can exist in the solid state. Variations an order of magnitude and larger are not expected for diffusion coefficients of liquids. Bonilla used diffusion paths of 1/2 and 1/4 inch diameter to obtain the coefficients he reports. The likelihood of convection is much greater for paths this large because the ratio of the wall area to the fluid volume decreases rapidly with increasing path diameter. Convection may arise from vibrations or from

temperature induced density inversions. Bonilla maintained a small positive temperature gradient in his diffusion apparatus, as was done in the present investigation, to reduce the possibility of density inversions. The potassium-mercury system, however, is strongly exothermic and heat generation occurs during diffusion of the components. Temperature gradients may be set up due to heat liberated in the alloy. This effect is pronounced at the composition where a compound exists. The experimental conditions here are analogous to those existing in electromobility experiments where internal heat generation arises from ohmic heating. Several investigators have acknowledged the existance of convection currents arising from density inversions due to heat liberated by ohmic heating (3, 87, 122, 146). On the basis of these considerations, it appears the large values of diffusion coefficients obtained by Bonilla in the range $0.25 < N_K < 0.35$ are not expected for liquid metals and may be due to the presence of convection resulting from the combination of a large diffusion path diameter and the highly exothermic reaction associated with the formation of the compound Hg_2K. The shape of the curve obtained in the present investigation appears consistant with phase, and thermodynamic data for the system potassium-mercury.

An Arrhenium diagram for diffusion of potassium in potassium-amalgams is shown in Figure 19. A linear relationship exists between ln D and 1/T, the data may be expressed as

$$D = D_o \exp(-E/RT) \qquad (100)$$

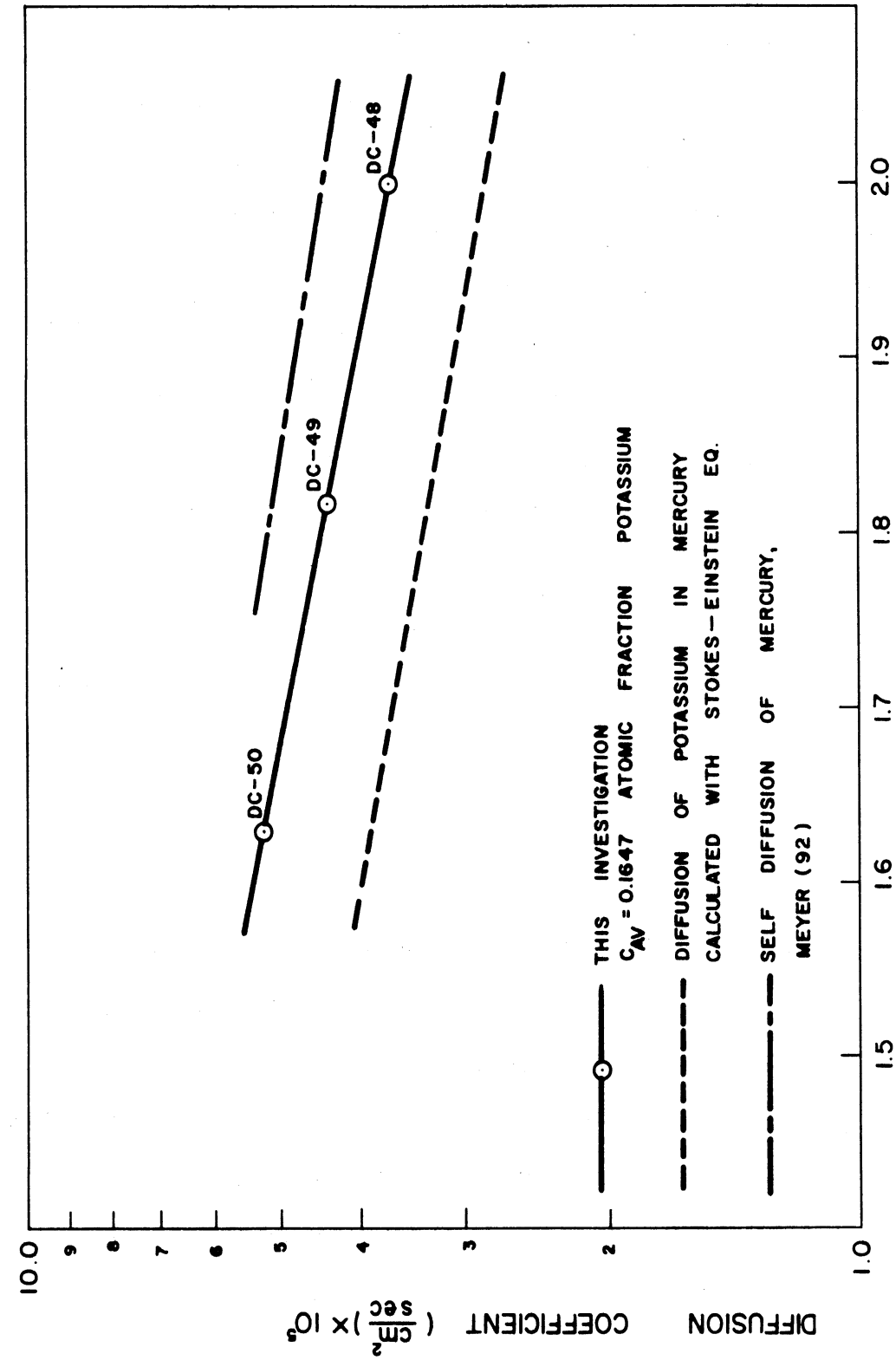

Figure 19. Arrhenius Plot for Diffusion of Potassium in Potassium-Amalgams

where E is the activation energy for diffusion. For an average amalgam concentration of $N_K = 0.1647$, $D_o = 3.715 \times 10^{-4}$ and E = 2090 cal/gr. atom. The dashed line was obtained from the Stokes-Einstein equation for the diffusion of potassium in mercury at infinite dilution. The broken line represents the self diffusion coefficient of the solvent mercury as obtained by Meyer (92). The ratio between the magnitude of the diffusion coefficient of potassium in mercury and the self diffusion coefficient of mercury is in agreement with the theory of Swalin (134). Swalin predicts that $D_{solute}/D_{self,\ solvent}$ will be close to unity for systems with large negative partial enthalpies ($\Delta\bar{H}_K = -24{,}900$ for K-H_g at $x_K = 0.00$) due to the affinity of the solvent and solute molecules.

The temperature range over which measurement have been made is not large enough to determine if any curvature exists in the relationship between ln D and 1/T.

Sodium-Lead System

The coefficients obtained for diffusion of sodium in sodium-lead alloys are shown in Figure 20. The concentration intervals employed in the determination of these values are noted at the top of the figure. Three cells were run at a concentration $N_{Na} = 0.1211$ and temperature 625°K. DC-15 and DC-17 were identical in all respects and gave values of D differing by 18.75%. The third cell DC-16 differed only in that the diameter of the capillary was about 1 1/2 times greater than the capillaries of the preceding two. This run gave similar results

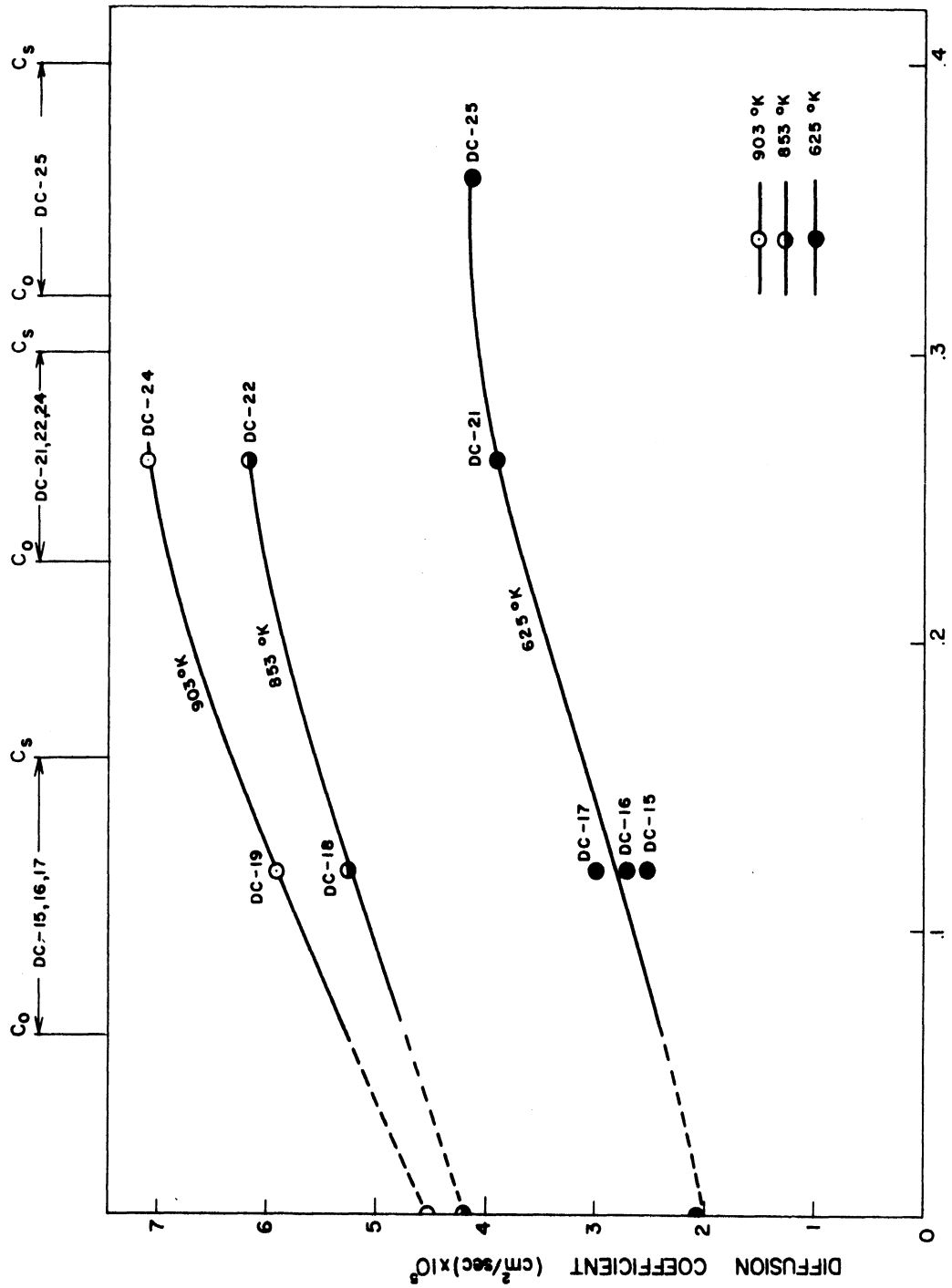

Figure 20. Diffusion Coefficients for Sodium in Sodium-Lead Alloys

indicating convective effects were not significant.

Diffusion coefficients were obtained at three temperatures, 625, 853 and 903°K and for three different concentration intervals. The phase diagram for the sodium-lead system is shown in Figure E-2 of Appendix E. The average composition and temperature coordinates for each of the experimental runs are noted on this phase diagram. The lower temperature limit is imposed by the solidus of the cathode alloy. The gap in the temperatures investigated is due to two factors. First, use of the low temperature electrolyte, sodium hydroxide, above 625°K is not possible due to reaction of sodium with the sodium hydroxide. For high temperature, 853 and 903°K, a NaCl-NaI(E) electrolyte was used. The melting point of this electrolyte is 850°K. No suitable fused salt was found for use between 625°K and 853°K. The upper temperature limit of 903°K was imposed by the increasing tendency of the sodium to vaporize from the anode compartment as the temperature was increased.

An attempt to operate a cell at 853°K and a cathode alloy composition $N_{Na} = 0.3605$ failed due to gas evolution in the cathode. Examination of the cell revealed that sodium in the cathode alloy had attacked the fused quartz cathode compartment. The activity of sodium in lead increases rather rapidly in the vicinity of this concentration and use of a quartz cathode is no longer feasible. Since no other suitable cathode material had been developed further experiments at elevated

temperatures with sodium rich alloys were not undertaken. An attempt to operate a cell with a cathode alloy initial composition $N_{Na} = 0.0118$ (see DC-28 in Table A-1) also failed. Erratic operation was attributed to wetting difficulties in the cathode. The values of the diffusion coefficients at infinite dilution which are shown in Figure 20 were calculated from the Stokes-Einstein equation. The viscosity of pure lead was obtained from Rothwell (125) and the value of the ionic radius for sodium calculated by Pauling (104) was used in the above calculation.

The results of the present investigation are compared with those reported by Morachevsky et. al. (95) in Figure 21. Morachevsky used the capillary reservoir technique and sectioned the alloy after diffusion occurred. His results show considerable scatter. The dashed line is passed through the smoothed points he reports. A standard solution of Fick's second law was used in the calculation of the diffusion coefficients. The concentration gradients in Morachevsky's experiments were as large as 40 atom % sodium. With concentration gradients this large it is necessary to modify Fick's second law as noted by Wagner (151), a modification which was not made by Morachevsky. The system sodium-lead exhibits large negative deviations from Raoult's law. The minimum in Morachevsky's data is not consistent with this, rather a maximum as was obtained in the present investigation is expected.

An Arrhenius diagram for the diffusion of sodium in sodium-lead alloys is shown in Figure 22. For an average concentration $N_{Na} = 0.1213$,

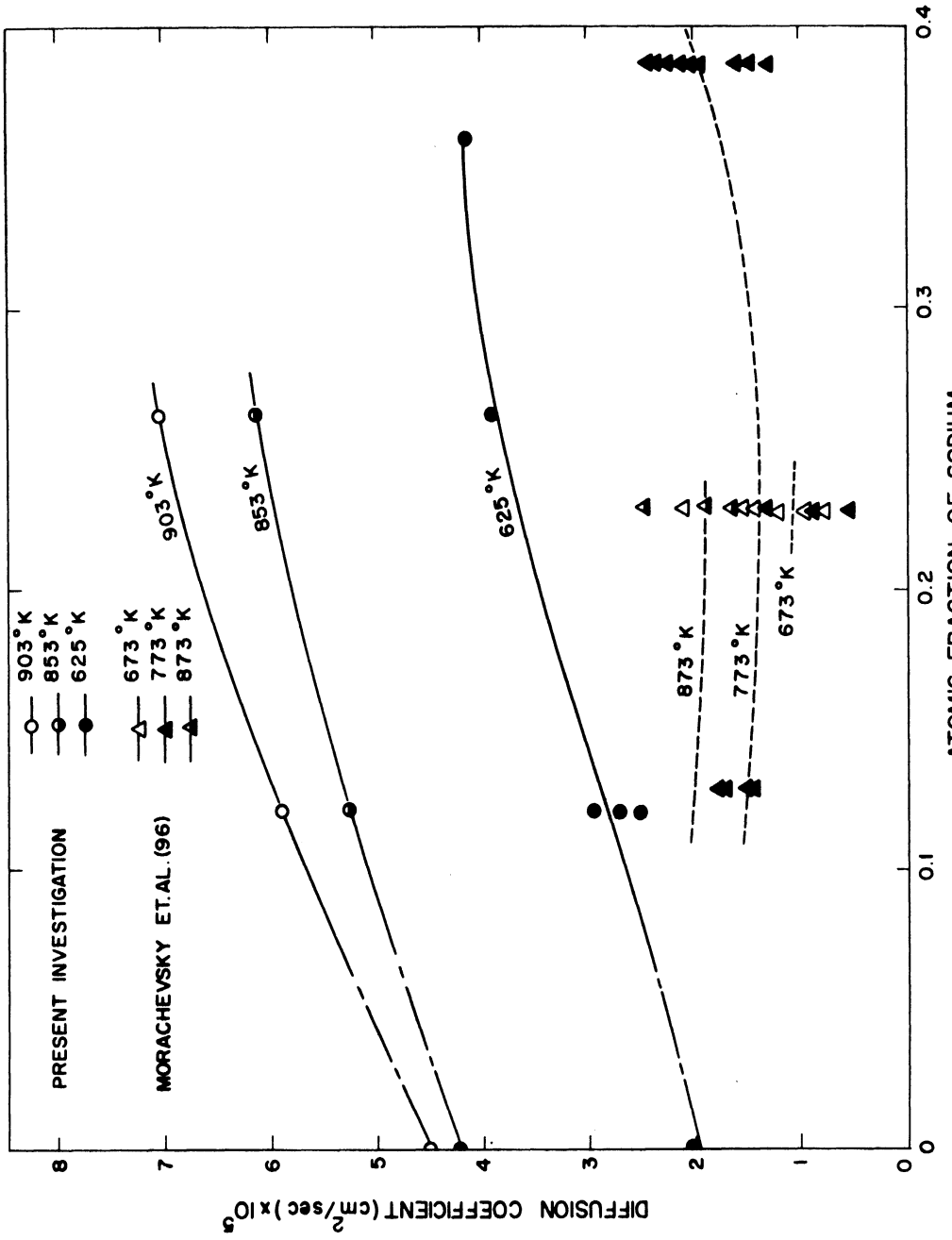

Figure 21. Comparison of Experimental Results of Present Investigation with Results Reported by Morachevsky

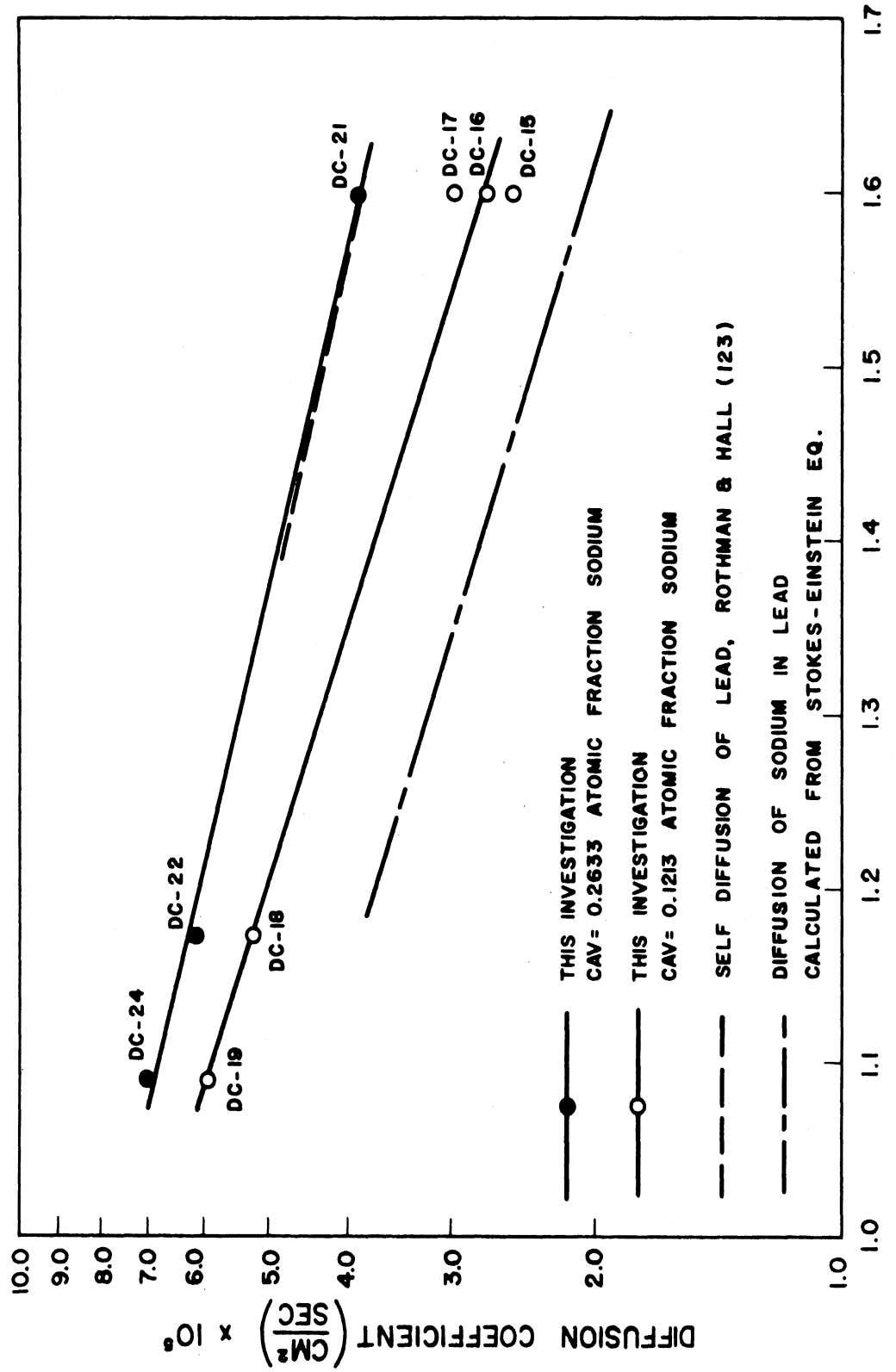

Figure 22. Arrhenius Plot for Diffusion of Sodium in Sodium-Lead Alloys

$D_o = 1.99 \times 10^{-4}$ and E = 2530 cal/gr atom. The diffusion coefficients for sodium in lead at infinite dilution are given by the dashed line which was calculated from the Stokes-Einstein equation. Self diffusion coefficients for the solute lead as measured by Rothman and Hall (123) are shown with a broken line. The ratio of magnitude of the diffusion coefficient for sodium in lead to the self diffusion coefficient of lead is in good agreement with the theory of Swalin (134). The large gap in the temperatures investigated makes it impossible to determine if any curvature exists for ln D vs. 1/T.

Sodium-Tin System

The coefficients obtained for diffusion of sodium in sodium-tin alloys are shown in Figure 23. The concentration intervals employed in the determination of these coefficients are noted at the top of the figure. Two cells were discharged at an average cathode alloy composition of $N_{Na} = 0.0868$ and 625°K. DC-33 had a diffusion path 0.040" in diameter while DC-29 had one 0.060" in diameter. These cells were identical in all other respects and yielded diffusion coefficients differing in value by 9.1%.

Diffusion coefficients were obtained at three different temperatures 625, 853, and 903°K and for three different concentration intervals. The phase diagram for this system is shown in Figure E-3 of Appendix E. The average composition and temperature coordinates for each run are noted by an "X" on this phase diagram. The gap in

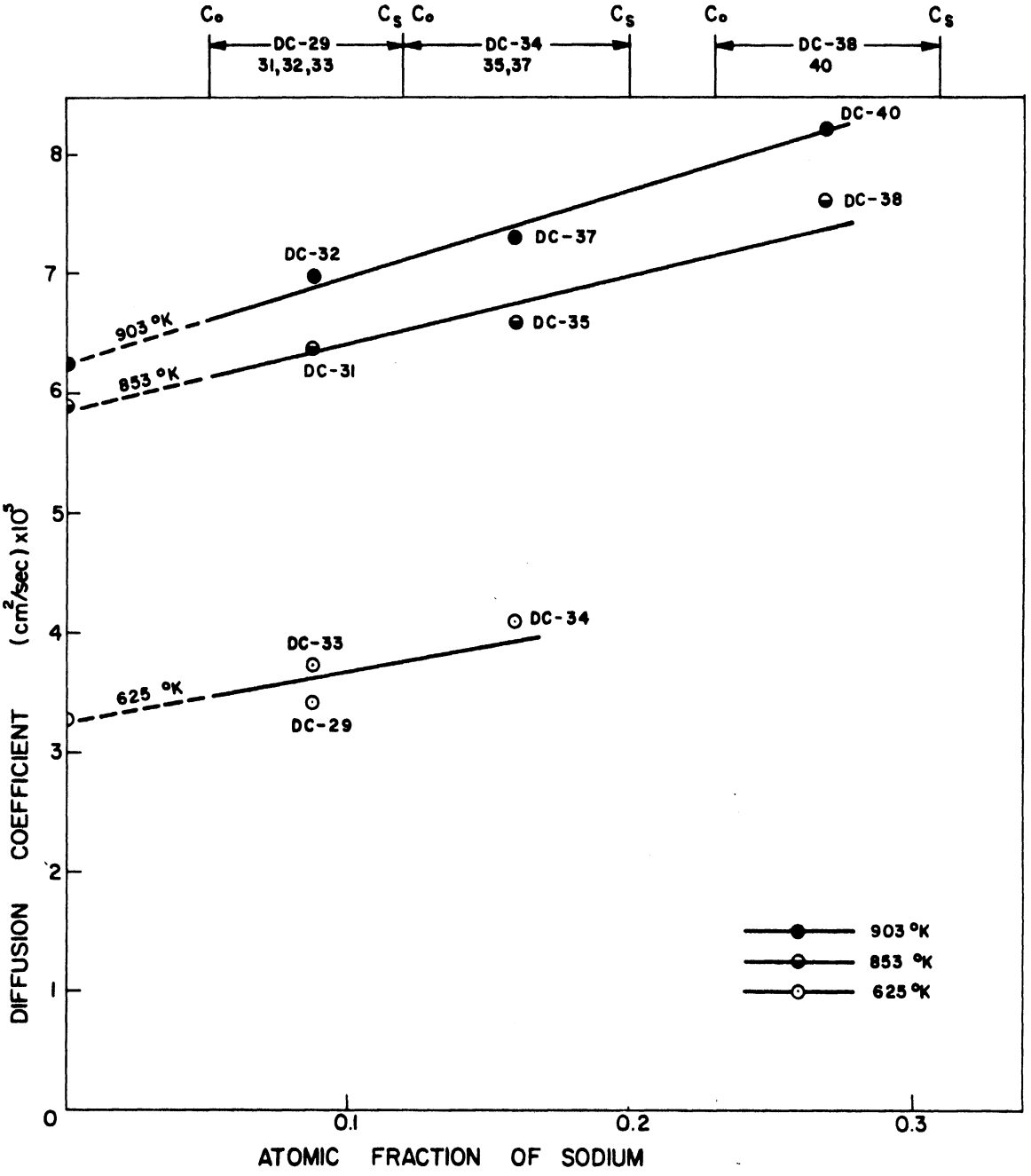

Figure 23. Diffusion Coefficients for Sodium in Sodium-Tin Alloys

the temperature range investigated was due to the unavailability of a suitable fused salt for use in this region. The lower temperature limit of the experimental investigation is determined by the solidus of the sodium-tin system. The upper limit is imposed by the high vapor pressure of sodium above 903°K. Remarks in the previous section concerning the reactivity of sodium rich alloys at elevated temperatures with the fused quartz cathodes apply as well to this system. Values of the diffusion coefficient at infinite dilution were calculated from the Stokes-Einstein equation. The viscosity of pure tin was obtained from Rothwell (125), and Pauling's (104) value of the ionic radius for sodium was used.

No other investigators have reported diffusion coefficients for this system.

An Arrhenius diagram for the diffusion of sodium in sodium-tin alloys is shown in Figure 24. At an average concentration $N_{Na} = 0.1601$, $D_o = 1.92 \times 10^{-4}$ and $E = 1865$ cal/gr atom. The diffusion coefficients for sodium in tin at infinite dilution were calculated from the Stokes-Einstein equation and are shown as a broken line in Figure 24. The self diffusion coefficients of tin measured by Careri et. al. (20) are shown as a dashed line. Again, $D_{solute}/D_{self,\ solvent} \simeq 1$ which is in agreement with the theory of Swalin (134).

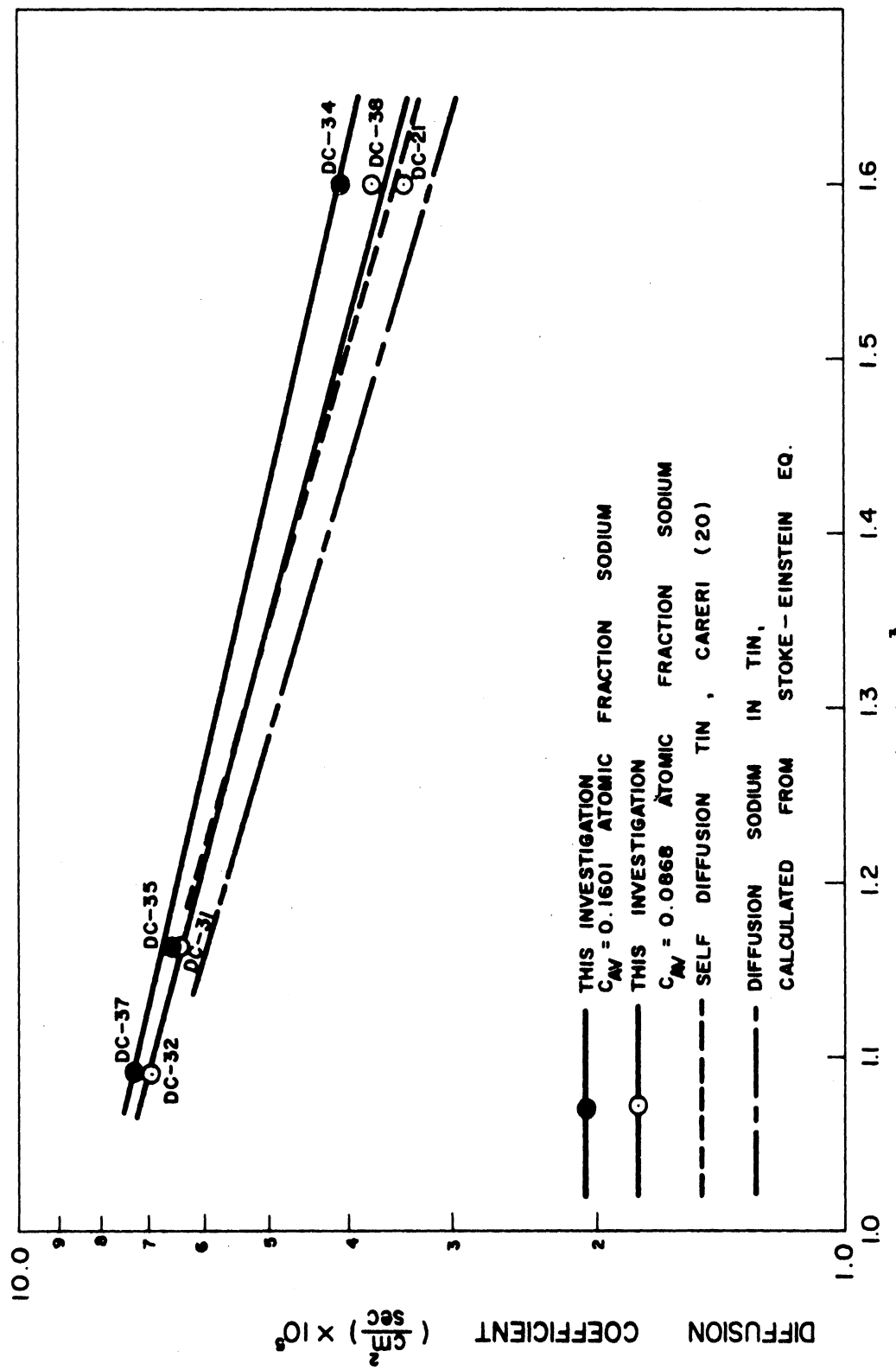

Figure 24. Arrhenius Plot for Diffusion of Sodium in Sodium-Tin Alloys

F. CRITIQUE AND RECOMMENDATIONS CONCERNING EXPERIMENTAL METHOD

The major advantages of the experimental method developed in this investigation to measure diffusion coefficients of binary liquid metal alloys are:

1. The rate of solute transfer to the diffusion path may be observed. Calculation of the diffusion coefficient can be based on that portion of the experimental data for which initial effects are not significant. The capillary reservoir technique, by way of comparison, allows measurement only of the overall concentration change. It is not possible to separate that part of change due to anomalities at the open end of the capillary, which are present initially, from the concentration change due to a diffusional mechanism during the remainder of the experiment. With the capillary reservoir technique, diffusion coefficients calculated from the overall concentration change (measured either by chemical or radiochemical analysis) will be greater than the actual coefficient due to the excess mass transferred at small times.
2. In the capillary reservoir technique, a capillary of one metal must be dipped into a bath of another. Convection undoubtly occurs when the two metals are first

contacted. This has been referred to as the "immersion effect" by Rastas and Kwalo (117). Such an effect is not present in the method developed for this investigation and more precise values of the diffusion coefficient should be obtained all other things being equal.

3. The method developed for this investigation substitutes measurement of the electrical quantities, current and voltage, for the chemical or radiochemical analysis required in other techniques. This is particularly important when small concentration intervals are used, a condition desirable for accurate representation of the diffusion process by ordinary solution of Fick's second law. Calculations presented in Appendix J show the total mass transferred may be of the order of 10^{-4} grams. Determination of quantities this small in liquid metal systems is, at best, a very difficult task. However, the current corresponding to this same transfer of mass over a period of a few hours is in the milliamp range, a quantity which is easily and accurately measured.

The major disadvantages associated with the method developed in the present investigation are:

1. The number of liquid metal alloys to which the method may be applied is limited. It is necessary

that the cell have a reasonably large open circuit potential (at least 0.10 volt) to obtain stable discharge characteristics. Alloys of alkali metals with heavier metals may satisify the conditions necessary for large cell potentials, but many other systems often do not. In addition, thermodynamic data must be available for the system to enable the calculation of cell potentials and the temperature coefficient of these potentials.

2. The concentration range of a particular alloy system which may be investigated is also limited by this requirement that the potential be greater than about 0.10 volts. As the concentration of alkali metal in the cathode alloy increases the potential developed by the cell drops off rapidly.

3. The lack of suitable fused salt electrolytes is a further limitation. Only pure salts or eutectic mixtures with a common cation were employed in this investigation. The use of salts with mixed cations would increase the number of available salt systems. However, care would be necessary to insure only the desired cation was discharged at the cathode-electrolyte interface. Delimarski and Markov (35)

report mixed cation salts form complexes which reduce the solubility of alkali metals in them. Use of such systems at elevated temperatures would be advantageous since the solubility of alkali metals in fused salts increases rapidly with temperature. A further restriction imposed on selection of fused salt electrolytes is, the cation being transferred from anode to cathode must exhibit a single valence in the salt. If this is not true, the current in the external circuit will not be a good measure of the material transferred from anode to cathode.

4. The calculations in Appendix K show the equation used to calculate the diffusion coefficient is particularly sensitive to errors in thermodynamic data needed to make the calculation. The difficulty of obtaining precise thermodynamic data for liquid metal systems at elevated temperatures limits the usefulness of this method.

All diffusion coefficient measurements reported in this investigation were determined from discharge currents of liquid metal concentration cells. It would be possible to determine these coefficients equally well from the charging current of a cell with an initial uniform concentration of alkali metal in the cathode alloy. The cell

potential would be maintained at a value greater than the open-circuit cell potential. Concentration polarization of alkali metal in the cathode alloy would be rate limiting as alkali metal diffuses from the bulk of the cathode to the cathode-electrolyte interface. The only change in the mathematical analysis is the sign of the concentration gradient in Fick's first law. The characteristic form of the solution is not altered. It is recommended that in future work both charge and discharge operation of the cells be used to provide an additional check on reliability of the method.

IV. SUMMARY AND CONCLUSIONS

The two-fold objectives of this thesis were:

(1) To develop a method useful for the measurement of diffusion coefficients in liquid metals which in addition to these diffusion coefficients yields information from which the flux of material to the path can be calculated.

(2) To utilize this method to obtain diffusion coefficients for diffusion of potassium in potassium-amalgams, and of sodium in sodium-lead and sodium-tin alloys.

In order to achieve the first goal a concentration cell was designed which utilizied liquid metals for the anode and cathode. Diffusion in the cathode alloy was rate limiting. This proved successful, the method yielded both the diffusion coefficient and the rate of transfer of metal to the diffusion path.

Diffusion coefficients were obtained for the systems noted above. The values of these coefficients are reproducible and internally consistant with values reasonable for diffusion in liquid metals. Where possible the coefficients have been compared with data available in the literature for diffusion in these metals.

An anomoly has been observed in the flux of material transferred to the diffusion path during the initial few minutes of the experiment.

This has been attributed to a non-planar cathode-electrolyte interface. This phenomena has not been recognized by other investigators. In some methods, notably the capillary-reservoir technique, this effect is probably not present because hydrodynamic mixing occurs when the metals are initially contacted, this would tend to destroy any non-planar interface. However, in other methods where two phases initially in contact are melted, it is entirely possible the difference in surface energy will produce a non-planar interface. Calculations show, this effect is most severe at small times when the flux of material is very large. When calculation of the diffusion coefficient is based on the total quantity of material transferred, a value two or three percent above the true value will be obtained.

The method developed, while feasible for the systems investigated, is severely limited in its applicability to many other alloy systems due to lack of necessary thermodynamic data, and/or a suitable fused salt electrolyte. It is, of course, not applicable to the study of self diffusion or interdiffusion in nearly ideal alloys where the cell potential developed would be zero or nearly so.

REFERENCES

1. Agruss, B., Karas, H. R. and Decker, V. L., "Design and Development of a Liquid Metal Fuel Cell," Technical Documentary Report No. ASD-TRD-62-1045, Dec. 1962.

2. Anderson, J. S. and Saddington, K., "The Use of Radioactive Isotopes in the Study of the Diffusion of Ions in Solution," Journal of the Chemical Society, Supplement S381, (1949).

3. Angus, J. C., "The Electrolysis of Some Liquid Metal Alloys," Ph.D. Thesis, the University of Michigan, pg. 112, (1960).

4. Antropov, L. I., "Kinetics of Electrochemical Reactions and the Electrocapillary Zero of Metals," Soviet Electrochemistry, Vol. 1, Kinetics and Polarography, Consultants Bureau, New York, 1961.

5. Arden, B., Galler, B. and Grahm, R., "The Michigan Algorithmic Decoder," The University of Michigan Computing Center, Jan. 1963.

6. Baimakov, Y. V. and Nikitenko, N. S., "Investigation of Ion Exchange Between a Molten Metal and Its Salt with the Aid of Radioactive Tracers," Soviet Electrochemistry, Vol. 1, Kinetics and Polarography, Consultants Bureau, New York, 1961.

7. Baur, E., "Study of Sodium Oxygen System (in German)," Zeitschrift fur Elektrochemie, Vol. 27, 194 (1921).

8. Bearman, R. J., "On the Molecular Basis of Some Current Theories of Diffusion," Journal of Physical Chemistry, Vol. 65, N. 11, 1961 (1961).

9. Bernal, J. D., "A Geometrical Approach to the Structure of Liquids," Nature, Vol. 183, N 4685, 141 (1959).

10. Bernal, J. D., "Geometry of the Structure of Monatomic Liquids," Nature, Vol. 185, N. 4706, 68 (1960).

11. Belosevsky, H. A., "Diffusion of Magnesium in Molten Aluminum (in Russian)," Journal of Light Metals (USSR), Vol. 6, N. 10, 18 (1937).

12. Bonilla, C. F., "Mass Transfer in Molten Metal and Molten Salt Systems," Proceedings of the International Conference on the Peaceful Uses of Atomic Energy, Vol. 9, 331 (1956) United Nations, New York.

13. Bonilla, C. F., Do-ik Lee and Foley, P. J., "The Electrical Resistivity of the K-Hg and Na-Hg Systems and the Diffusivity of the K-Hg System at High Temperatures," Advances in Thermophysical Properties at Extreme Pressures and Temperatures, 3rd Symposium, Mar. 22-25, 1965, p. 207-15.

14. Borucka, A. Z., Bockris, J. O'M. and Kitchner, J. A., "Self-Diffusion in Molten Sodium Chloride: A Test of the Applicability of the Nerst Einstein Equation," Proceedings of the Royal Society (London), Vol. 241A, N. 1227, 554 (1957).

15. Bredig, M. A., Johnson, J. W. and Smith, W. T., Jr., "Miscibility of Liquid Metals with Salts, I The Sodium-Sodium Halide Systems," The Journal of the American Chemical Society, Vol. 77, N. 1, 307 (1955).

16. Bronstein, H. R. and Bredig, M. A., "The Electrical Conductivity of Solutions of Alkali Metals in Their Molten Halides," Journal of the American Chemical Society, Vol. 80, N. 5, 2077 (1958).

17. Bronstein, H. R. and Bredig, M. A., "The Electrical Conductivity of Solutions of Metals in Their Molten Halides, II Sodium-Sodium Iodide, Potassium-Potassium Iodide, and Potassium-Potassium Fluoride," Journal of Physical Chemistry, Vol. 65, N. 7, 1220 (1961).

18. Brown, D. S. and Tuck, D. G., "New Method for Studying Self-Diffusion in Liquids: Self-Diffusion in Liquid Mercury," Transaction of the Faraday Society, Vol. 145, 1230 (1964).

19. Cambi, L. and Devoto, G., "The Decomposition Potential of Alkali and Alkaline Earth Fused Salts (in Italian)," Gazz. Chimica Hal., Vol. 57, 836 (1927).

20. Careri, G. and Paoletti, A., "Self-Diffusion in Liquid Indium and Tin," IL Nuovo Cimento, Vol. II, N. 3, 575 (1955).

21. Careri, G., Paoletti, A. and Salvetti, F. L., "Self-Diffusion in Liquid Indium," IL Nuovo Cimento, Vol. X, N. 4, 399 (1954).

22. Careri, G., Paoletti, A. and Vicentini, M., "Further Experiments on Liquid Indium and Tin Self-Diffusion," IL Nuovo Cimento, Vol. X, N. 6, 1088 (1958).

23. Carlson, C. M., Eyring, H. and Ree, T., "Singificant Structures in Liquids, V. Thermodynamic and Transport Properties of Molten Metals," Proceedings, National Academy of Sciences, Vol. 46, 649 (1960).

24. Carnahan, B., Luther, H. A. and Wilkes, J. O., Applied Numerical Methods, Preliminary Edition, Vol. II, Chap. 7, Wiley, 1964.

25. Carslow, H. S. and Jaeger, J. C., Conduction of Heat in Solids, Second Edition, Oxford, 1959.

26. Cohen, E. and Bruins, H. R., "The Potentiometric Determination of Diffusion Coefficients of Metals in Mercury (in German)," Zeitschrift fur Physikalische Chemie, Vol. 109, 397 (1924): "Pizochemical Studies XXV. The Influence of Pressure on the Diffusion Coefficient of Metals in Mercury (in German)," Zeitschrift fur Physikalische Chemie, Vol. 109, 422 (1924).

27. Cohen, M. H. and Turnbull, D., "Molecular Transport in Liquids and Glasses," Journal of Chemical Physics, Vol. 31, N. 5, 1164 (1959).

28. Cohen, M., Wagner, C. and Reynolds, J. E., "Calculation of Interdiffusion Coefficients when Volume Changes Occur," Transactions A.I.M.E., Journal of Metals, Vol. 5, N. 11, 1534 (1953).

29. Cohen, M., Wagner, C. and Reynolds, J. E., "Authors Supplement to Calculation of Interdiffusion Coefficients When Volume Changes Occur," Transactions A.I.M.E., Journal of Metals, Vol. 6, N. 6, 702 (1954).

30. Cooper, W. C. and Furman, N. H., "The Diffusion Coefficients of Certain Metals in Mercury," Journal of the American Chemical Society, Vol. 74, 6183 (1952).

31. Crank, J., Mathematics of Diffusion, Oxford University Press, Fair Lawn, New Jersey, 1956.

32. Darken, L. S., "Diffusion, Mobility and Their Interrelation through Free Energy in Binary Metallic Systems," Transactions of A.I.M.E., Vol. 175, 185 (1948).

33. Darken, L. S. and Gurry, R. W., Physical Chemistry of Metals, McGraw-Hill, New York, 1953.

34. Degenkolbe, J. and Sauerwald, F., "On the Internal Friction of Molten Potassium and Sodium Amalgams (in German)," Zeitschrift fur anorganische und allgemeine Chemie, Vol. 270, 317 (1952).

35. Delimarski, Iu. K. and Markov, B. F., Electrochemistry of Fused Salts, Sigma Press, Washington, D. C., 1961.

36. Delimarski, Iu. K. and Kolomi, A. A., "An Electrochemical Investigation of the System Sn-Na(in Russian)," Zhurnal Fisitcheskoi Khimi, Vol. 28, 1169 (1954).

37. Doetsch, G., Guide to the Applications of Laplace Transforms, D. Van Nostrand Co. Ldt., London, 1961.

38. Doran, D. J., "Characteristics of Zinc-Silver Oxide Molten Electrolyte Cell Systems," Proceedings of the Eleventh Annual Battery Research and Development Conference, pg. 64, May 1957.

39. Duda, J. L. and Vrentas, J. S., "Analysis of Free Diffusion Experiments in Binary Systems," Industrial and Engineering Chemistry Fundamentals, Vol. 4, N. 3, 301 (1965).

40. Dunlop, P. J., "Relation Between the Mutual and Tracer Diffusion Coefficients Associated with Isothermal Systems of Two Nonelectrolytes in an Un-ionized Solvent for the Limiting Case When the Physical and Chemical Properties of the Solutes Become Indistinguishable," Journal of Physical Chemistry, Vol. 69, N. 5, 1693 (1965).

41. Dzurus, M. L. and Henning, G. R., "Catalyzed Lamellar Reactions of Graphite," Carbon - Proceedings of the Fifth Conference, Vol. 1, pg. 139, Pergamon Press, 1962.

42. Eckert, R. E. and Drickamer, H. G., "Diffusion in Indium Near the Melting Point," Journal of Chemical Physics, Vol. 20, N. 1, 13 (1952).

43. Einstein, A., "Elementary Theory of the Brownian Movement (in German)," Zeitschrift fur Elektrochemie, Vol.17, 235 (1908): "The Movement of Particles Suspended in Stationary Liquids as Demanded by Kinetic Theory (in German)," Annalen der Physik, Vol. 17, 549 (1905): "A New Determination of Molecular Dimensions (in German)," Annalen der Physik, Vol. 19, 289 (1906): "The Theory of the Brownian Movement (in German)," Annalen der Physik, Vol. 19, 371 (1906).

44. Ewell, R. H. and Eyring, H., "Theory of the Viscosity of Liquids as a Function of Temperature and Pressure," Journal of Chemical Physics, Vol. 5, N. 9, 726 (1937).

45. Eyring, H., "Viscosity, Plasticity and Diffusion as Examples of Absolute Reaction Rates," Journal of Chemical Physics, Vol. 4, N. 4, 283 (1936).

46. Eyring, H., and Ree, T., "Significant Liquid Structures, VI. The Vacant Theory of Liquids," Proceedings of the National Academy of Sciences, Vol. 47, 526 (1961).

47. Eyring, H., Ree, T., Grant, D. M. and Hirst, R. C., "IX. Significant Structures and Relaxations," Zeitschrift fur Elektrochemie, Vol. 64, N. 1, 146 (1960).

48. Eyring, H., Glasstone S. and Laidler, K. J., Theory of Rate Pressures, McGraw Hill, New York (1941).

49. Fisher, J. C. Hollomon, J. H. and Turnbull, D., "Absolute Reaction Rate Theory for Diffusion in Metals," Transactions A.I.M.E., Vol. 175, 202 (1948).

50. Fixman, M., "Theory of Diffusion Near Walls," Journal of Chemical Physics, Vol. 29, N. 3, 540 (1958).

51. Foley, W. T. and Liu, M. T., "Tracer Diffusion of Thallium in Thallium Amalgams," Canadian Journal of Chemistry, Vol. 42, 2602 (1964).

52. Foley, W. T. and Reid, L. E., "Interdiffusion in Thallium Amalgams," Canadian Journal of Chemistry, Vol. 41, 1782 (1963).

53. Furman, N. H. and Cooper, W. C., "A Study of the Polarographic Behavior of Dropping Amalgam Electrodes," Journal of the American Chemical Society, Vol. 72, 5667 (1950).

54. Goldschmidt, V. M., "Crystal Structure and Chemical Composition (in German)," Berichte der Deutschen Chemischen Gesellschaft, Vol. 60, 1263, (1927).

55. Gorman, J. W., "Molecular Diffusion and Interphase Transfer in the Solid Cooper-Molten Lead System," Ph.D. Thesis, University of Minnesota, 1955. (University Microfilms, Inc., Ann Arbor, Michigan, Doctoral Dissertation Series, Publications No. 13,782).

56. Gorman, J. W. and Preckshot, G. W., "Molecular Diffusion and Interphase Transfer in the Solid Cooper-Molten Lead Systems," Transactions of the Metallurgical Society of A.I.M.E., Vol. 212, 367 (1958).

57. Grace, R. E. and Derge G., "Diffusion in Liquid Lead-Bismuth Alloys," Transactions A.I.M.E., Journal of Metals, Vol. 26, 839 (1955).

58. Greenway, H. T., "The Surface Tension and Density of Lead-Antimony and Cadmium-Antimony Alloys," Journal, Institute of Metals, Vol. 74, N. 11, 133 (1947).

59. Grosse, A. V., "Viscosity of Metallic Mercury (and Its Saturated Vapor) over Its Entire Liquid Range, i.e., from Its Melting Point (234.2°K) to Its Critical Point (1733°K), and an Estimate of Its Critical Viscosity," Journal of Physical Chemistry, Vol. 68, N. 11, 3419 (1964).

60. Groh, J. and Hevesy, G. V., "The Self-Diffusion Coefficient of Molten Lead (in German)," Annals Physik (Lepsig), Vol. 63, 85 (1920).

61. Gul'din, I. T. and Buzhinskaya, A. V., "Wettability of Some Minerals by Liquid Lead Under a Layer of Molten Salts," Surface Phenomena in Metallurgical Processes, Proceedings of an Inter-institute Conference, Edited by A. I. Belgaev, Consultants Bureau, New York, 1965, pg. 177.

62. Gupta, Y. P., "Diffusion of Gold in Liquid Silver," Acta Metallurgica, Vol. 14, N. 3, 297 (1966).

63. Gupta, Y. P., "On Solute Diffusion In liquid Tin," Acta Metallurgica, Vol. 14, N. 8, 1008 (1966).

64. Haissinsky, M. and Cottin, M., "Determination of the Self-Diffusion Coefficient of Mercury by the Method of Isotope Exchange (in French)," Le Journal de Physique et le Radium, Vol. 11, 611 (1950).

65. Hamby, D. C., Steller, B. W. and Chase, J. B., "Alkali Metal Voltaic Cells," Journal of the Electrochemical Society, Vol. 111, N. 8, 998 (1964).

66. Hansen, M. and Anderko, K., Constitution of Binary Alloys, Second Edition, McGraw-Hill, New York, 1963.

67. Hartley, G. S. and Crank, J., "Some Fundamental Definitions and Concepts in Diffusion Processes," Transactions of the Faraday Society, Vol. 45, 801 (1949).

68. Hauffe, K. and Vierk, A. L., "Activity Measurements on Liquid Sodium Alloys with Extremely Strong Deviations From Ideal Behavior (in German)," Zeitschrift fur Elektrochemie, Vol. 53, N. 5, 156 (1949).

69. Henderson, J. and Ling Yang, "Self-Diffusion of Copper in Molten Copper," Transactions of the Metallurgical Society of A.I.M.E., Vol. 72, N. 2, 72 (1961).

70. Henderson, R. E. and Hietbrink, E. H., "Mercury Space Power Systems," Pacific Energy Conversion Conference Proceedings, American Institute of Electrical Engineers, 1962.

71. Hesson, J. C. and Burris, L., "Uranium Diffusivity in Liquid Cadmium," Transactions of the Metallurgical Society of A.I.M.E., Vol. 227, 571 (1963).

72. Heymann, E. and Weber, H. P., "The Distribution Equilibrium of Sodium Between Molten Halides (NaI and NaBr) and a Molten Metal Phase (Cd, Pb, Tl, Sn, Bi, Sb, Au)," Transactions of the Faraday Society, Vol. 34, N. 12, 1492 (1938).

73. Hoffman, R. E., "The Self-Diffusion of Liquid Mercury," Journal of Chemical Physics, Vol. 20, N. 10, 1567 (1952).

74. Hultgren, R., Orr, R. L., Anderson, P. D. and Kelly, K. K., Selected Values of Thermodynamic Properties of Metals and Alloys, John Wiley, New York, (1963).

75. Karas, H. R. and Mangus, J. D., "First Quarterly Technical Progress Report on Research and Development of an Advanced Laboratory Liquid Metal Regenerative Fuel Cell," Allison Division of General Motors Corp., Indianapolis, Ind., EDR 3344, May 1963.

76. Kassner, T. F., Russell, R. J. and Grace, R. E., "Self-Diffusion of Zinc in Liquid Lead-Zinc Alloys," Transactions of the ASM, Vol. 55, 858 (1962).

77. Kirkwood, J. G., "Flow Equations and Frames of Reference for Isothermal Diffusion in Liquids," The Journal of Chemical Physics, Vol. 33, N. 5, 1505 (1960).

78. Kirshenbaum, A. D. and Cahill, J. A., "The Density of Liquid Tin from Its Melting Point to Its Normal Boiling Point and an Estimate of Its Critical Constants," American Society of Metals Quarterly Transactions, Vol. 55, 849 (1962).

79. Kubaschewski, O. and Caterall, J. A., Thermochemical Data of Alloys, Pergamon Press, London, 1956.

80. Kuzmeynko, P. P., Kapkov, E. I. and Lozovi, V. I., "The Electrotransport of Silver in Liquid Lead and of Cobalt in Liquid Tin (in Ukranian)," Ukrains'kyi Fizichnyi Zhurnal, Vol. 9, 881 (1964).

81. Lantratov, M. F., "The Thermodynamic Properties of Liquid Metal Solutions in the Sodium-Lead System," Russian Journal of Inorganic Chemistry, Vol. 4, N. 9, 927 (1959).

82. Lantratov, M. F. and Tsarenko, E. V., "Investigation of the Thermodynamic Properties of Liquid Metallic Solutions in the Potassium-Mercury System," Journal of Applied Chemistry of the U.S.S.R., Vol. 33, 1527 (1960).

83. Leak, V. G. and Swalin, R. A., "Diffusion of Silver and Tin in Liquid Silver," Transactions of the Metallurgical Society of A.I.M.E., Vol. 230, 426 (1964).

84. Li, J. C. M. and Pin Chang, "Self-Diffusion Coefficient and Viscosity in Liquids," Journal of Chemical Physics, Vol. 23, N. 3, 518 (1955).

85. Livingston, R. S., Physio-Chemical Experiments, Third Edition, MacMillan, New York, 1957, pp. 22-24.

86. Lodding, A. R. E., "Self-Diffusion in Molten Indium (in German)," Zeitschrift fur Naturschforchung, Vol. 11 a, 200 (1956).

87. Lodding, A. R. E., "Isotope Transport Phenomena in Liquid Metals," Gothenburg Studies in Physics, Nils Ryde - Editor. Acta Universitatis Gothoburgensis, 1961.

88. Ma, C. H. and Swalin, R. A., "A Study of Solute Diffusion in Liquid Tin," Acta Metallurgica, Vol. 8, 388 (1960).

89. Ma, C. H. and Swalin, R. A., "Self-Diffusion in Liquid Tin," Journal of Chemical Physics, Vol. 36, N. 11, 3014 (1962).

90. Mangelsdorf, P. C., Jr., "Transport Processes in Liquid Alloys. I. A.Transport Cell for Liquid Alloys," Journal of Chemical Physics, Vol. 30, N. 5, 1170 (1959).

91. Mangus, J. D., "Research and Development of an Advanced Laboratory Liquid Metal Regenerative Fuel Cell," Technical Documentary Report No. APL-TDR-64-41, April 1964.

92. Meyer, R. E., "Self-Diffusion of Liquid Mercury," Journal of Physical Chemistry, Vol. 65, 567 (1961).

93. Meyer, R. E. and Nachtrieb, N. H., "Self-Diffusion in Sodium Near the Melting Point," Journal of Chemical Physics, Vol. 23, 405 (1955).

94. Meyer, R. E. and Nachtrieb, N. H., "Self-Diffusion of Liquid Sodium," Journal of Chemical Physics, Vol. 23, 1851 (1955).

95. Morachevski, A. G., "On the Activity of Potassium in Alloys of Potassium-Ruthenium and Potassium-Lead in the Liquid State (in Russian)," Zhurnal Prikladnoi Khimii, Vol. 30, 1239 (1957).

96. Morachevsky, A. C., Cherespanova, E. A. and Alabysher, A. F., "Diffusion of Sodium in Lead (in Russian)," Izvestiia. VUZ-Tsventnaya Metallurgiya, 70, (1960).

97. Nachtrieb, N. H., Fraga, E. and Wahl, C., "Self-Diffusion in Liquid Zinc," Journal of Physical Chemistry, Vol. 67, 2353 (1963).

98. Nachtrieb, N. H. and Petit, J., "Self-Diffusion in Liquid Mercury," Journal of Chemical Physics, Vol. 24, N. 4, 746 (1956).

99. Niwa, K, Shimoji, M., Kado, S., Watanabe, Y. and Yokokawa, T., "Studies on Diffusion in Molten Metals," Transactions of A.I.M.E., Journal of Metals, Vol. 9, 96 (1957).

100. Norante, N. J., The Carborundum Company, Personal Communication July, 1964.

101. Paoletti, A. and Vicentini, M., "Some Examples of Turbulent Diffusion in Liquid Metals," Physics of Fluids, Vol. 1, 453 (1958).

102. Paoletti, A. and Vicentini, M., "Self-Diffusion in Liquid In-Pb Alloys," IL Nuovo Cimento, Vol. XIV, N. 4, 748 (1959).

103. Paoletti, A. and Vicentini, M., "Diffusion in a Liquid Indium-Tin Alloy at the Eutectic Concentration," Journal of Applied Physics, Vol. 32, N. 1, 22 (1961).

104. Pauling, L., "The Sizes of Ions and the Structure of Ionic Crystals," Journal of the American Chemistry Society, Vol. 49, N. 3, 765 (1927).

105. Peaceman, D. W. and Rachford, H. H., Jr., "The Numerical Solution of Parabolic and Elliptic Partial Differential Equations," Journal Society Industrial Applied Math, Vol. 3, 28-41 (1955).

106. Peter, S., "Concerning Viscosity and Self-Diffusion in Liquids (in German)," Zeitschrift fur Naturforschung, Vol. 9a, 98, (1954).

107. Petit, J. and Nachtrieb, N. H., "Self-Diffusion in Liquid Gallium," Journal of Chemical Physics, Vol. 24, N. 5, 1027 (1956).

108. Pfann, W. F., "An Electrolytic Method for Pointing Tungsten Wires," Technical Publication No. 2210, Class E, Metals Technology, American Institute of Mining and Metallurgical Engineer, Chicago Meeting, October 1947.

109. Piontelli, R., "Considerations in Measuring Polarization Potential, Part I (in Italian)," Gazzetta Chimica Italian, Vol. 83, 357 (1953).

110. Piontelli, R., "Consideration in Measuring Polarization Potential, Part II (in Italian)," Gazzetta Chimica Italian, Vol. 83, 370 (1953).

111. Piontelli, R, Rivolta, B. and Montanelli, C., "Measurement Methods for Polarization Voltage (in German)," Zeitschrift fur Elektrochemie, Vol. 51, N. 1, 64 (1955).

112. Piontelli, R and Sternheim, G., "Overvoltages at the Electrode Melted Pb/$PbCl_2$," Journal of Chemical Physics, Vol. 23, N. 7, 1358 (1955).

113. Piontelli, R., Sternheim, G., Francini, M. and Montanelli, G., "Investigation of the Phenomena of Overvoltage in Molten Salts," Soviet Electrochemistry, Vol. 1, Kinetics and Polarography, Consultants Bureau, New York, 1961.

114. Piontelli, R. and Sternheim, G., "Overvoltages in Melted Electrolytes," Journal of Chemical Physics, Vol. 23, N. 10, 1971 (1955).

115. Piontelli, R., Sternheim, G. and Francini, M., "Overvoltage and Passivity in Melted Electrolytes," Journal of Chemical Physics, Vol. 24, N. 5, 1113 (1956).

116. Preckshot, G. W. and Hudrlik, R. E., "Diffusion in the Solid Silver-Molten Lead System," Transactions of the Metallurgical Society of A.I.M.E., Vol. 212, 516 (1960).

117. Rastas, J. and Kwalo, P., "Diffusion Measurements with Open End Capillary Technique," Acta Polytech Scandanivian Chem-Met Series, Vol. 35, pg 1 (1964).

118. Reddy, T. B., "The Electrochemistry of Molten Salts," Electrochemical Technology, Vol. 1, N. 11-12, 325 (1963).

119. Reharge, G. and Ernst O., "The Influence of Thermodynamic Factors on the Activation Energy of Diffusion," Zeitschrift fur Naturforschung, Vol. 19a, N. 6, 823 (1964).

120. Roberst-Austen, W. C., "On the Diffusion of Metals," Phil. Trans. Royal Society (London), Vol. A 187, 383 (1896); "On the Diffusion of Metals," Proc. Ryal Society (London), Vol. 59, 281 (1896); "The Diffusion of Metals," Nature, Vol. 55 (1896).

121. Robinson, R. A. and Stokes, R. H., "The Measurement of Diffusion Coefficients," Electrolyte Solutions, Chapter 10, Academic Press, New York, 1955.

122. Rohlin, J. and Lodding, A., "Self-Diffusion in Molten Potassium (in German)," Zeitschrift fur Naturforschungen, Vol. 17a, 1081 (1962).

123. Rothman, S. J. and Hall, L. D., "Diffusion in Liquid Lead," Transactions A.I.M.E., Journal of Metals, Vol. 8, 199 (1956).

124. Rothman, S. J. and Hall, L. D., "Diffusion in a Molten Bi-0.225 Atomic Pct Pb Alloy," Transactions A.I.M.E., Journal of Metals, Vol. 8, 1580 (1956).

125. Rothwell, E., "A Precise Determination of the Viscosity of Liquid Tin, Lead, Bismuth, and Aluminium by an Absolute Method," Journal of the Institute of Metals, Vol. 90, N. 6, 389 (1961-62).

126. Sandler, S. I. and Dahler, J. S., "Nonstationary Diffusion," The Physics of Fluids, Vol. 7, N. 11, 1743 (1964).

127. Schadler, H. W. and Grace, R. E., "Self and Interdiffusion in Liquid Zinc Amalgams," Transactions of the Metallurgical Society of A.I.M.E., Vol. 215, 559 (1959).

128. Schwartz, K., "Regarding the Theory of Electrolytic Separations in Metallic Systems (in German)," Zeitschrift fur Physikalische Chemie, Vol. 164, 223 (1933).

129. Shewmon, P. G. and Love, G. R., "Diffusion in Metals," Industrial and Engineering Chemistry, Vol. 53, N. 4, 325 (1961).

130. Sittig, M., Sodium, Its Manufacture, Properties, and Uses, Chap. 3, American Chemical Society Monograph Series, Reinhold Publishing Co., New York, 1956.

131. Stackelberg, M. V. and Toome, V., "Determination of Diffusion Coefficients of Metals in Mercury with a Dropping Amalgam Electrode (in German)," Zeitschrift fur Elektrochemie, Vol. 58, 226 (1954).

132. Stark, J. P., "An Invarient of Diffusion in Binary Systems," Acta Metallurgica, Vol. 14, N. 2, 228 (1966).

133. Sutherland, W., "A Dynamical Theory of Diffusion for Non-Electrolytes and the Molecular Mass of Albumen," London Philosophical Magazine, Vol. 9, 781 (1905).

134. Swalin, R. A., "On the Theory of Self-Diffusion in Liquid Metals," Acta Metallurgica, Vol. 7, 736 (1959).

135. Swalin, R. A., "Concerning the Mechanism of Diffusion in Liquids," Acta Metallurgica, Vol. 9, 379 (1961).

136. Swalin, R. A. and Leak, V. G., "Diffusion of Heterovalent Solutes in Liquid Silver," Acta Metallurgica, Vol. 13, N. 5, 471 (1965).

137. Talbot, A. and Kitchner, J. A., "Diffusion (or Conduction) Along a Slightly Tapered Tube and Its Application to the Determination of Diffusion Coefficients," British J. Applied Physics, Vol. 7, Suppl. 5, N. 3, 96 (1956).

138. Taylor, G. I., "Diffusion by Continuous Movements," Proceedings London Mathematical Society, Vol. A20, 196 (1920).

139. Taylor, G. I., "Diffusion and Mass Transport in Tubes," Proceedings of Physical Society (London) Vol. B67, 857 (1954).

140. Trimble, L. E., Finn, D. and Cosgarea, A., Jr., "A Mathematical Analysis of Diffusion Coefficients in Binary Systems," Acta Metallurgica, Vol. 13, N., 5, 501 (1965).

141. Turnbull, D. and Hoffman, R. E., "A Correleation of Data on Diffusion of Solutes in Face-Centered Cubic Metals," Acta Metallurgica, Vol. 7, N. 6, 407 (1959).

142. Turner, R. C. and Winkler, C. A., "Dropping Amalgam Electrodes," Canadian Journal of Chemistry, Vol. 29, 469 (1951).

143. Uemura, K., "The Diffusion of Various Elements into Aluminium in Molten State (1)," Iron and Steel Institute of Japan, Journal (Tetsu-to-Hagne), Vol. 25, 24 (1939).

144. Uemura, K., "The Diffusion of Various Elements into Aluminium in the Molten State (II)," Iron and Steel Institute of Japan, Journal (Tetsu-to-Hagne), Vol. 26, 813 (1940).

145. Vasrlenko, T. V. and Kharkov, E. I., "Diffusion of Silver in Bismuth," Ukranins'kyi Fizichnyi Zhurnal, Vol. 7, 525 (1962) (in Ukranian).

146. Verhoeven, J. D., "Electrotransport as a Means of Purifying Metals," Metals, Vol. 1, N. 1, 26 (1966).

147. Vicentini, M. and Paoletti, A., "Self-Diffusion in Liquid In-Sn Alloys," IL Nuovo Cimento, Vol. XIV, N. 6, 1373 (1959).

148. Vierk, A. L. and Hauffe, K., "Activity Measurements on Liquid Potassium Mercury Alloys (in German)," Zeitschrift fur Elektrochemie, Vol. 54, 382 (1950).

149. von Hevesy, G., "The Melt-Electrolytic Precipitation of Alkali Metals from Caustic Alkali and the Solubility of These Metals in the Melt (in German)," Zeitschrift fur Elektrochemie, Vol. 15, 529 (1909).

150. von Wogau, M., "The Diffusion of Metals in Mercury (in German)," Annels Physik (Lepsig), 23/4, 345 (1907).

151. Wagner, C., "On the Solution of Diffusion Problems Involving Concentration-Dependent Diffusion Coefficients," Transactions of the A.I.M.E., Journal of Metals, Vol. 4, N. 1, 91, (1952).

152. Walls, H. A. and Upthegrove, W. R., "Theory of Diffusion Phenomena," Acta Metallurgica, Vol. 12, N. 5, 461 (1964).

153. Waser, J. and Pauling, L., "Compressibilities, Force Constants, and Interatomic Distances of the Elements in the Solid State," Journal of Chemical Physics, Vol. 18, N. 5, 747 (1950).

154. Weaver, R. D., Smith, S. W. and Willmann, N. L., "The Sodium-Tin Liquid-Metal Cell," Journal of the Electrochemical Society, Vol. 109, N. 8, 653 (1962).

155. Weischedel, F., "Diffusion of Metals in Mercury (in German)," Zeitschrift fur Physik, Vol. 85, 29 (1933).

156. Williams, D. D., "A Study of the Sodium-Hydrogen-Oxygen System," Naval Research Laboratory Report No. 33, June 1952, Washington, D. C.

157. Wilson, J. R., "The Structure of Liquid Metals and Alloys," Metallurgical Reviews, Vol. 10, N. 40, 381 (1965).

158. Yang, Ling and Derge, G., "General Considerations of Diffusion in Melts of Metallurgical Interest," Physical Chemistry of Process Metallurgy, Pt. 1, Interscience, New York, 1661, pg. 503.

159. Yang, Ling, Kado, Satoski and Derge, G., "Self-Diffusion of Silver in Molten Silver," Transactions of the Metallurgical Society of A.I.M.E., Vol. 212, 628 (1958).

160. Zener, C., "Theory of D_o for Atomic Diffusion in Metals," Journal of Applied Physics, Vol. 22, N. 4, 372 (1951).

161. "Boron Nitride Catalog Section H-8745 GD" Union Carbide Corp. New York, 1964.

162. "Fused Quartz Catalog No. Q-6," The General Electric Company, Cleveland, 1957, page 18.

163. Handbook of Chemistry and Physics, 40th Edition, C. D. Hodgeman, Editor, Chemical Rubber Publishing Co., Cleveland, 1958.

164. Liquid Metals Handbook, 2nd Edition, U. S. Government Printing Office, Washington, D. C., 1952.

165. Bird, R. B., Stewart, W. E., and Lightfoot, E. N., Transport Phenomena, New York, John Wiley (1960).

166. Cooper, W. C. and Furman, N. H., "The Diffusion Coefficients of Certain Metals in Mercury," Journal of the American Chemical Society, Vol. 74, 6183 (1952).

167. Gordon, R. B., "Hole Model for Diffusion in Liquids," Acta Metallurgica, Vol. 7, N. 10, 681 (1959).

168. Grace R. E. and Derge G., "Diffusion of Third Elements in Liquid Iron Saturated with Carbon," Transactions of the Metallurgical Society of A.I.M.E., Vol. 212, 331 (1958).

169. Lapple, C. E., "Particle Dynamics," Chemical Engineering Handbook, J. H. Perry, Editor, New York, McGraw-Hill (1950), pg. 1020.

170. Meyer, G., "Diffusion Coefficients of Metals in Mercury (in German)," Annalen der physik und chemie, Vol. 61, N. 6, 225 (1897).

171. Morgan, D. W. and Kitchner, J. A., "Solution in Liquid Iron. Part 3: Diffusion of Cobalt and Carbon," Transactions of the Faraday Society, Vol. 51, 51 (1954).

172. Rayleigh, O. M., "On convection Currents in a Horizontal Layer of Fluid, When the Higher Temperature is on the Under Side," Philosophical Magazine, Series 6, Vol. 32 (1916).

173. Sobal, C., "On the Magnitude of Effective Ionic Radii of Elements In Molten and Solid Phases at High Temperature," Zhurnal Prikladnoi Khimi, Vol. 24, 710 (1951).

174. Stromberg, I., "Diffusion of Thallium in Mercury (in Russian)," Dokl. Akad. Nauk., SSSR, Vol. 85, 831 (1952).

175. Turnbull, D., "The Liquid State and the Liquid-Solid Transition," Transactions of the Metallurgical Society of the A.I.M.E., Vol. 221, N. 6, 422 (1961).

176. Nachtrieb, N. H., "Transport Properties in Pure Liquid Metals," Seminar on Liquid Metals and Solidification, Chicago 1957, American Society for Metals, Cleveland (1958).

177. Arden, B., Galler, B. and Grahm, R., "The Michigan Algorithmic Decoder," University of Michigan Computing Center (Jan. 1963).

APPENDICIES

APPENDIX A SUMMARY OF EXPERIMENTAL INVESTIGATIONS

TABLE A-1

SUMMARY OF DIFFUSION CELLS

Exp.	Anode Metal	Cathode Alloy	Electrolyte Matrix and Salt		Temp. °K	Path Diam. (in.)	Run Dur. (sec)	Diffusion Coefficient or Comments
DC- 1	Na	A- 2	M- 3	FS- 2	625	0.040	0	Structural failure, cathode
DC- 2	Na	A- 2	M- 4	FS- 2	625	0.040	0	Gas evolution in cathode
DC- 3	Na	A- 2	M- 4	FS- 2	625	0.041	60	Break in cathode alloy
DC- 4	Na	A- 2	M- 4	FS- 3	624	0.040	300	Vaporization of anode
DC- 5	Na	A- 2	M- 5	FS- 3	625	0.060	0	Gas evolution in cathode
DC- 6	Na	A- 2	M- 5	FS- 3	625	0.040	0	Structural shifting of comp.
DC- 7	Na	A- 2	M- 5	FS- 3	625	0.040	0	Break in cathode alloy
DC- 8	Na	A- 2	M- 1	FS- 3	625	0.040	0	Leak in furnace head
DC- 9	Na	A- 2	M- 6	FS- 3	624	0.039	240	Gas evolution in cathode
DC-10	Na	A- 2	M- 7	FS- 3	625	0.040	0	High electrolyte resistance
DC-11	Na	A- 2	M- 8	FS- 3	625	0.040	5	Gas evolution in cathode
DC-12	Na	A- 2	M- 9	FS- 3	625	0.040	0	Structural failure, cathode

TABLE A-1 (continued)

Exp.	Anode Metal	Cathode Alloy	Electrolyte Matrix and Salt		Temp. °K	Path Diam. (in.)	Run Dur. (sec)	Diffusion Coefficient or Comments
DC-13	Na	A- 2	M-11	FS- 3	625	0.040	20	Gas evolution in cathode
DC-14	Na	A- 2	M-11	FS- 3	625	0.040	300	Gas evolution in cathode
DC-15	Na	A- 7	M-14	FS- 5	625	0.040	4200	$D=2.51 \times 10^{-5}$ cm^2/sec
DC-16	Na	A- 7	M-15	FS- 5	625	0.063	3800	$D=2.70 \times 10^{-5}$ cm^2/sec
DC-17	Na	A- 7	M-14	FS- 5	625	0.040	4500	$D=2.98 \times 10^{-5}$ cm^2/sec
DC-18	Na	A- 7	M-14	FS- 6	853	0.040	3100	$D=5.25 \times 10^{-5}$ cm^2/sec
DC-19	Na	A- 7	M-14	FS- 6	903	0.040	5040	$D=5.91 \times 10^{-5}$ cm^2/sec
DC-20	Na	A- 7	M-14	FS- 5	675	0.039	100	Failure, electrolyte decomp.
DC-21	Na	A- 8	M-14	FS- 5	625	0.040	4320	$D=3.90 \times 10^{-5}$
DC-22	Na	A- 8	M-16	FS- 6	853	0.039	4860	$D=6.15 \times 10^{-5}$
DC-23	Na	A- 8	M-16	FS- 6	903	0.040	0	Failure, break in cathode
DC-24	Na	A- 8	M-16	FS- 6	903	0.040	5100	$D=7.08 \times 10^{-5}$
DC-25	Na	A- 9	M-16	FS- 5	625	0.040	4640	$D=4.12 \times 10^{-5}$
DC-26	Na	A- 9	M-16	FS- 5	675	0.039	300	Failure, decomp of electrolyte

TABLE A-1 (continued)

Exp.	Anode Metal	Cathode Alloy	Electrolyte Matrix and Salt		Temp. °K	Path Diam. (in.)	Run Dur. (sec)	Diffusion Coefficient or Comments
DC-27	Na	A- 9	M-17	FS- 6	853	0.040	5	Failure, gas evolution at cathode
DC-28	Na	A-10	M-15	FS- 6	625	0.040	900	Failure, erratic operation
DC-29	Na	A-11	M-17	FS- 5	625	0.063	3780	$D=3.41 \times 10^{-5}$
DC-30	Na	A-11	M-17	FS- 5	675	0.040	10	Failure, electrolyte decomp.
DC-31	Na	A-11	M-17	FS- 6	853	0.041	4250	$D=6.39 \times 10^{-5}$
DC-32	Na	A-11	M-18	FS- 6	903	0.040	6480	$D=6.98 \times 10^{-5}$
DC-33	Na	A-11	M-18	FS- 7	625	0.040	3960	$D=3.72 \times 10^{-5}$
DC-34	Na	A-13	M-18	FS- 7	625	0.040	5040	$D=4.09 \times 10^{-5}$
DC-35	Na	A-13	M-18	FS- 8	853	0.039	4620	$D=6.60 \times 10^{-5}$
DC-36	Na	A-13	M-18	FS- 8	903	0.040	0	Failure, break in cathode
DC-37	Na	A-13	M-19	FS- 8	903	0.040	5280	$D=7.30 \times 10^{-5}$
DC-38	Na	A-14	M-19	FS- 8	853	0.041	4080	$D=7.62 \times 10^{-5}$
DC-39	Na	A-14	M-19	FS- 8	903	0.040	0	Failure, break in cathode
DC-40	Na	A-14	M-19	FS- 8	903	0.040	4380	$D=8.22 \times 10^{5}$

TABLE A-1 (continued)

Exp.	Anode Metal	Cathode Alloy	Electrolyte Matrix and Salt		Temp. °K	Path Diam. (in.)	Run Dur. (sec)	Diffusion Coefficient or Comments
DC-41	Na	A-15	M-19	FS- 8	903	0.040	0	Failure, gassing in cathode
DC-42	K	A-16	M-19	FS- 9	500	0.040	7020	$D=2.90 \times 10^{-5}$
DC-43	K	A-16	M-20	FS- 9	500	0.040	5460	$D=3.25 \times 10^{-5}$
DC-44	K	A-16	M-15	FS- 9	500	0.062	4680	$D=3.12 \times 10^{-5}$
DC-45	K	A-16	M-20	FS- 9	550	0.040	4860	$D=3.82 \times 10^{-5}$
DC-46	K	A-16	M-20	FS- 9	600	0.040	0	Failure, gassing in cathode
DC-47	K	A-16	M-20	FS- 9	600	0.039	0	Failure, gassing in cathode
DC-48	K	A-17	M-21	FS-10	500	0.040	5040	$D=3.68 \times 10^{-5}$
DC-49	K	A-17	M-21	FS-10	550	0.041	4020	$D=4.40 \times 10^{-5}$
DC-50	K	A-17	M-21	FS-10	600	0.040	6060	$D=5.23 \times 10^{-5}$
DC-51	K	A-18	M-21	FS-10	550	0.040	0	Failure
DC-52	K	A-18	M-21	FS-10	550	0.041	0	Failure
DC-53	K	A-18	M-21	FS-10	600	0.041	4320	$D=6.11 \times 10^{-5}$
DC-54	K	A-19	M-22	FS-11	600	0.039	5280	$D=5.86 \times 10^{-5}$

TABLE A-1 (continued)

Exp.	Anode Metal	Cathode Alloy	Electrolyte Matrix and Salt		Temp. °K	Path Diam. (in.)	Run Dur. (sec)	Diffusion Coefficient or Comments
DC-55	K	A-19	M-22	FS-11	550	0.040	3000	$D=5.32 \times 10^{-5}$
DC-56	K	A-20	M-22	FS-11	500	0.041	240	Failure, erratic operation
DC-57	K	A-20	M-22	FS-11	550	0.040	180	Failure, erratic operation

TABLE A-2

SUMMARY OF ALLOY PREPARATIONS

Alloy	Date	Component A		Component B	
		A	Mole Fract A	B	Mole Fract B
A- 1	6-30-65	Na	0.208	Sn	0.792
A- 2	7-26-65	Sn	1.000	--	-----
A- 3	1- 6-66	Na	0.405	Sn	0.593
A- 4	1-28-66	Na	0.1965	Sn	0.8035
A- 5					
A- 6					
A- 7	4- 1-66	Na	0.082	Pb	0.918
A- 8	4-15-66	Na	0.226	Pb	0.774
A- 9	4-20-66	Na	0.320	Pb	0.680
A-10	4-25-66	Na	0.011	Sn	0.989
A-11	4-26-66	Na	0.053	Sn	0.947
A-12	4-27-66	Na	0.093	Sn	0.907
A-13	4-28-66	Na	0.120	Sn	0.880
A-14	5-12-66	Na	0.230	Sn	0.770
A-15	5-12-66	Na	0.402	Sn	0.598
A-16	5-18-66	K	0.052	Hg	0.948
A-17	5-29-66	K	0.146	Hg	0.854
A-18	6- 4-66	K	0.251	Hg	0.749
A-19	6-10-66	K	0.338	Hg	0.662
A-20	6-17-66	K	0.451	Hg	0.549

TABLE A-3

SUMMARY OF FUSED SALT PREPARATIONS

Salt	Date	Composition (mole fractions)
FS- 1	1-27-65	NaI (0.625), NaCl (0.375)
FS- 2	7- 2-65	NaI (0.625), NaCl (0.375)
FS- 3	8-25-65	NaI (0.625), NaCl (0.375)
FS- 4	8-28-65	NaCl
FS- 5	4- 2-66	NaOH
FS- 6	4- 2-66	NaI (0.625), NaCl (0.375)
FS- 7	4-23-66	NaOH
FS- 8	4-24-66	NaI (0.625), NaCl (0.375)
FS- 9	5-19-66	KOH (0.70), KBr (0.15), KI (0.15)
FS-10	5-20-66	KOH (0.70), KBr (0.15), KI (0.15)
FS-11	6-11-66	KOH (0.70), KBr (0.15), KI (0.15)

TABLE A-4

SUMMARY OF METALS AND SALTS USED IN EXPERIMENTAL INVESTIGATION

	Form	Grade	Assay (wt %)	Supplier	Lot #
Sodium	Lump	Reagent	----------	Baker & Adamson	W 273
Potassium	Lump	Purified	----------	J. T. Baker	26,418
Tin	Granular 20 Mesh	Reagent	Min. 99.0	Baker & Adamson	X 282
Lead	Granular	Reagent	100.0	J. T. Baker	------
Mercury	Vacuum Triple Distilled	Instrument	non-volatile residue 0.025 ppm	Bethelem Apparatus Co.	A 280
Sodium Hydroxide	Pellets	Reagent	Min 97.0	Mallinckrodt	PGD X
Sodium Iodide	Crystal	Reagent	99.6	J. T. Baker	------
Sodium Chloride	Crystal	Reagent	Min. 99.5	Baker & Adamson	X 287
Potassium Hydroxide	Pellets	Reagent	Min. 85.0	Merk	60,583
Potassium Iodide	Granular	Reagent	99.8	J. T. Baker	------
Potassium Bromide	Crystal	Reagent	Min. 99.5	Baker & Adamson	V 299 S 258

APPENDIX B

EXPERIMENTAL DATA

The data for each of the successfully discharged cells is tabulated in this appendix. Those cells which were not successful are noted in Table A-1 of Appendix A.

φ_s refers to the voltage maintained across the cell during discharge. φ_o is the open-circuit voltage of the cell. The value of φ_s for a particular cell was obtained from the appropriate potential-composition curve in Appendix C. The value of C_s was obtained from the curves in Appendix D. C_o, the initial composition of the cathode alloy, was known.

A small positive temperature gradient was maintained in the region of the furnace where diffusion occurred. This gradient was usually no more than 2°C from the top of the path to the bottom, and served to reduce the possibility of convection in the alloy. The temperature reported is an average value.

Initial and final resistances, R_i and R_f respectively are reported. No cell resistance measurements were made during the discharge period.

The diameter of the diffusion path reported corresponds to room temperature.

Finally, the discharge current is tabulated as a function of time. An "f" to the right of the discharge current means pronounced fluctuations were observed.

TABLE B-1

DATA FOR DISCHARGE OF DIFFUSION CELLS

DC-15 Na-Pb

φ_o = 0.490 v. C_o = 0.0823
φ_s = 0.432 v. C_s = 0.1600
T = 625°K
R_i = 11 ohm, R_f = 15 ohm
d = 0.041"

t (sec)	I_c (ma)
0	0.000
15	2.98
30	1.75
45	1.48
60	1.18
90	0.97
120	0.781
180	0.644
240	0.558
300	0.501
480	0.430
660	0.340
900	0.289
1200	0.251
1620	0.218
1980	0.200
2460	0.176
2880	0.168
3300	0.155
4200	0.134

DC-16 Na-Pb

φ_o = 0.490 v. C_o = 0.0823
φ_s = 0.432 v. C_s = 0.1600
T = 625°K
R_i = 10 ohm, R_f = 18 ohm
d = 0.063"

t (sec)	I_c (ma)
0	0.000
20	6.6
30	5.05
40	4.48
50	3.61
60	3.09
90	2.26
120	2.04
180	1.57
240	1.32
300	1.18
360	1.09
480	0.955
600	0.855
900	0.690
1260	0.565
1560	0.521
1800	0.485
2160	0.445
2400	0.420
2700	0.399
2940	0.382
3240	0.365
3600	0.350
3780	0.335

TABLE B-1 (continued)

DC-17 Na-Pb

φ_o = 0.490 v. C_o = 0.0823
φ_s = 0.432 v. C_s = 0.1600
T = 624°K
R_i = 08 ohm, R_f = 09 ohm
d = 0.040"

t (sec)	I_c (ma)
0	0.000
10	4.2
20	2.86
30	1.69
40	1.66
50	1.40
60	1.35
90	1.03
120	0.835
180	0.790
240	0.608
300	0.550
360	0.492
480	0.421
600	0.371
720	0.338
840	0.320
1080	0.282
1380	0.248
1740	0.225
2040	0.203
2400	0.190
2700	0.178
3120	0.155
3540	0.144
3840	0.138
4500	0.138

DC-18 Na-Pb

φ_o = 0.52 v. C_o = 0.0823
φ_s = 0.442 v. C_s = 0.1600
T = 853°K
R_i = 10 ohm, R_f = 12 ohm
d = 0.040"

t (sec)	I_c (ma)
0	0.000
10	5.38
20	3.28
30	2.81
40	2.18
50	1.7
60	1.8 f
70	1.5
80	1.31
90	1.24
120	1.11
150	0.915
180	0.825
240	0.698
300	0.610
360	0.575
420	0.541
480	0.500
600	0.448
720	0.408
900	0.367
1140	0.326
1280	0.298
1620	0.273
1860	0.258
2100	0.241
2340	0.225
2640	0.218
3120	0.199

TABLE B-1 (continued)

DC-19 Na-Pb

φ_o = 0.525 v. C_o = 0.0823
φ_s = 0.448 v. C_s = 0.1600
T = 903°K
R_i = 12 ohm, R_f = 13 ohm
d = 0.040"

t (sec)	I_c (ma)
0	0.000
15	4.85
30	2.87
45	2.03
60	1.73 f
90	1.27
120	1.14
150	0.94
180	0.895
240	0.760
300	0.665
360	0.610
420	0.565
480	0.530
540	0.495
600	0.460
720	0.432
840	0.395
1020	0.358
1380	0.320
1680	0.271
2100	0.246
2400	0.233
2760	0.218
2940	0.210
3360	0.196
3900	0.180
4320	0.175
5040	0.156
5160	0.130
5220	0.100

DC-21 Na-Pb

φ_o = 0.380 v. C_o = 0.2265
φ_s = 0.330 v. C_s = 0.3000
T = 625°K
R_i = 15 ohm, R_f = 11 ohm
d = 0.040"

t (sec)	I_c (ma)
0	0.000
20	2.61
30	1.82
40	1.59
50	1.43
60	1.21
90	0.98
120	0.825
150	0.750
180	0.690
240	0.610
300	0.520
360	0.475
480	0.428
600	0.374
900	0.308
1200	0.269
1620	0.233
2100	0.198
2520	0.180
2940	0.171
3480	0.158
3900	0.146
4320	0.141

TABLE B-1 (continued)

DC-22 Na-Pb

φ_o = 0.378 v. C_o = 0.2265
φ_s = 0.318 v. C_s = 0.3000
T = 852°K
R_i = 14 ohms, R_f = 16 ohms
d = 0.039"

t (sec)	I_c (ma)
0	0.000
20	2.64
30	2.42
40	1.82
50	1.78
60	1.58
90	1.21
120	1.03
150	0.865
180	0.785
240	0.664
300	0.582
360	0.531
600	0.412
900	0.338
1260	0.285
1620	0.258
2040	0.217
2340	0.207
2760	0.191
3300	0.174
3780	0.162
4320	0.153
4860	0.142

DC-24 Na-Pb

φ_o = 0.375 v. C_o = 0.2265
φ_s = 0.316 v. C_s = 0.3000
T = 903°K
R_i = 11 ohm, R_f - 16 ohm
d = 0.040"

t (sec)	I_c (ma)
0	0.000
15	4.28
30	2.78
45	1.95
60	1.71
90	1.31
120	1.11
150	1.00
180	0.870
240	0.761
300	0.675
420	0.575
540	0.501
660	0.458
900	0.376
1200	0.340
1560	0.288
1860	0.276
2220	0.244
2580	0.230
3120	0.211
3840	0.235
4200	0.226
4680	0.221
5100	0.213

TABLE B-1 (continued)

DC-25 Na-Pb

φ_o = 0.315 v. C_o = 0.3209
φ_s = 0.262 v. C_s = 0.4000
T = 625°K
R_i = 10 ohm, R_f = 16 ohm
d = 0.040"

t (sec)	I_c (ma)
0	0.000
20	2.72
30	2.08
40	1.78
50	1.55
60	1.35
90	1.09
120	0.921
150	0.825
180	0.725
240	0.630
300	0.561
540	0.419
720	0.362
1020	0.297
1380	0.261
1680	0.240
2160	0.208
2520	0.142 f
3000	0.176
3540	0.162
4640	0.149

DC-29 Na-Sn

φ_o = 0.512 v. C_o = 0.0536
φ_s = 0.470 v. C_s = 0.1200
T = 624°K
R_i = 16 ohm, R_f = 15 ohm
d = 0.063"

DC-29 continued

t (sec)	I_c (ma)
0	0.000
20	6.95
30	5.45
40	4.45
50	4.10
60	3.40
90	2.72
120	2.32
180	1.71
240	1.55
300	1.40
360	1.24
420	1.15
480	1.08
540	1.01
720	0.87
900	0.78
1080	0.675
1260	0.665
1440	0.61
1740	0.558
2100	0.505
2460	0.475
2820	0.440
3300	0.410
3780	0.375

DC-31 Na-Sn

φ_o = 0.500 v. C_o = 0.0536
φ_s = 0.455 v. C_s = 0.1200
T = 852°K
R_i = 15 ohm, R_f = 18 ohm
d = .041"

TABLE B-1 (continued)

DC-31 continued

t (sec)	I_c (ma)
0	0.000
5	4.12
10	4.10
15	3.88
20	3.58
25	3.04
30	2.73
35	2.55
40	2.33
45	2.18
50	2.04
55	1.85
60	1.80
70	1.65
80	1.55
90	1.38
100	1.35
110	1.29
120	1.21
150	1.09
180	0.967
240	0.837
300	0.760
360	0.690
420	0.631
480	0.580
540	0.552
600	0.519
720	0.478
780	0.462
840	0.444
900	0.430
1020	0.402
1140	0.381
1440	0.340
1740	0.310

DC-31 continued

t (sec)	I_c (ma)
2040	0.282
2340	0.265
2700	0.246
3060	0.230
3360	0.221
3720	0.210
4200	0.198

DC-32 Na-Sn

φ_o = 0.495 v. C_o = 0.0536

φ_s = 0.448 v. C_s = 0.1200

T = 902°K

R_i = 10 ohm, R_f = 12 ohm

d = 0.040"

t (sec)	I_c (ma)
0	0.000
20	4.81
30	3.62
40	2.80
50	2.25
60	1.90
90	1.42
120	1.19
240	0.781
300	0.700
360	0.628
420	0.588
480	0.552
600	0.492
720	0.441

TABLE B-1 (continued)

DC-32 continued

t (sec)	I_c (ma)
840	0.420
1020	0.383
1200	0.355
1440	0.321
1680	0.296
1920	0.270
2280	0.248
2580	0.232
2940	0.220
3240	0.212
3540	0.203
3840	0.193
4200	0.184
4500	0.178
4800	0.172
5160	0.168
6000	0.155
6480	0.150

DC-33 Na-Sn

φ_o = 0.512 v. C_o = 0.0536

φ_s = 0.470 v. C_s = 0.1200

T = 625°K

R_i = 16 ohm, R_f = 15 ohm

d = 0.040"

t (sec)	I_c (ma)
0	0.000
10	4.15
20	2.95
30	2.20
40	1.82
50	1.58

DC-33 continued

t(sec)	I_c (ma)
60	1.35
90	1.16
120	0.91
180	0.78
240	0.655
300	0.55
360	0.508
480	0.46
600	0.382
720	0.36
900	0.318
1140	0.285
1380	0.261
1740	0.228
1980	0.216
2280	0.200
2520	0.188
3180	0.177
3600	0.158
3960	0.150

DC-34 Na-Sn

φ_o = 0.470 v. C_o = 0.1201

φ_s = 0.416 v. C_s = 0.2000

T = 624°K

R_i = 12 ohm, R_f = 14 ohm

d = 0.040"

t (sec)	I_c (ma)
0	0.000
10	5.49
20	4.16
30	3.24

TABLE B-1 (continued)

DC-34 continued

t (sec)	I_c (ma)
40	2.65
60	1.91
90	1.40
120	1.13
150	0.92
180	0.87
240	0.74
300	0.662
360	0.608
420	0.561
600	0.469
780	0.410
1080	0.350
1440	0.305
1740	0.265
2160	0.248
2460	0.235
2960	0.214
3360	0.198
3840	0.178
4260	0.165
4560	0.162
5040	0.154

DC-35 Na-Sn

φ_o = 0.455 v. C_o = 0.1201

φ_s = 0.403 v. C_s = 0.2000

T = 853°K

R_i = 15 ohm, R_f = 16 ohm

d = 0.039"

t (sec)	I_c (ma)
0	0.000
10	5.39

DC-35 continued

t (sec)	I_c (ma)
20	3.99
30	3.31
40	2.85
50	2.53
60	2.25
90	1.70
120	1.38
180	1.04
240	0.841
300	0.752
360	0.690
600	0.535
900	0.431
1140	0.378
1560	0.328
1980	0.291
2460	0.260
2820	0.243
3300	0.211
3660	0.201
4020	0.188
4620	0.180

DC-37 Na-Sn

φ_o = 0.448 v. C_o = 0.1201

φ_s = 0.399 v. C_s = 0.2000

T = 903°K

R_i = 12 ohm, R_f = 15 ohm

d = 0.040"

t (sec)	I_c (ma)
0	0.000
15	4.38
30	2.98

TABLE B-1 (continued)

DC-37 continued

t (sec)	I_c (ma)
45	2.71
60	1.98
90	1.58
120	1.32
150	1.18
180	1.03
240	0.928
300	0.836
420	0.700
540	0.618
660	0.561
780	0.508
960	0.460
1140	0.428
1500	0.371
1860	0.332
2280	0.301
2760	0.280
3180	0.255
3780	0.235
4320	0.221
4800	0.209
5280	0.200

DC-38 Na-Sn

φ_o = 0.382 v. C_o = 0.2305

φ_s = 0.340 v. C_s = 0.3100

T = 852°K

R_i = 13 ohm, R_f = 17 ohm

d = 0.041"

t (sec)	I_c (ma)
0	0.000
10	6.78
20	4.40

DC-38 continued

t (sec)	I_c (ma)
30	3.31
40	2.69
50	2.30
60	2.01
90	1.64
120	1.38
180	1.11
240	0.955
300	0.87
360	0.778
420	0.721
480	0.660
540	0.640
600	0.600
660	0.576
900	0.485
1080	0.447
1260	0.410
1500	0.377
1800	0.351
2220	0.312
2340	0.308
2760	0.280
3480	0.250
4080	0.231

DC-40 Na-Sn

φ_o = 0.380 v. C_o = 0.2305

φ_s = 0.341 v. C_s = 0.3900

T = 903°K

R_i = 12 ohm, R_f = 13 ohm

d = 0.040"

TABLE B-1 (continued)

DC-40 continued

t (sec)	I_c (ma)
0	0.000
5	5.41
10	4.8
15	4.1
20	3.75
25	3.31
30	3.0
40	2.68
50	2.19
60	2.02
90	1.60
120	1.39
240	0.91
300	0.825
360	0.76
540	0.605
900	0.482
1260	0.395
1620	0.355
2100	0.315
2400	0.280
2700	0.281
3120	0.254
3900	0.231
4380	0.217

DC-42 K-Hg

φ_o = 0.860 v. C_o = 0.0521

φ_s = 0.800 v. C_s = 0.0800

T = 500°K

R_i = 8 ohm, R_f = 7 ohm

d = 0.040"

DC-42 continued

t (sec)	I_c (ma)
0	0.000
5	1.82
10	1.55
15	1.41
20	1.10
25	1.07
30	0.935
35	0.87
40	0.80
45	0.75
50	0.70
55	0.645
60	0.60
70	0.56
80	0.516
90	0.481
100	0.45
110	0.425
120	0.41
150	0.46
180	0.432
240	0.28
300	0.255
360	0.288
420	0.21
540	0.186
660	0.167
900	0.148
1080	0.131
1320	0.120
1680	0.105
2040	0.095
2400	0.088
3000	0.0785
3540	0.0725
4080	0.067

TABLE B-1 (continued)

DC-42 continued

t (sec)	I_c (ma)
4560	0.065
5400	0.058
6360	0.054
7020	0.051

DC-43 K-Hg

φ_o = 0.860 v. C_o = 0.0521

φ_s = 0.080 v. C_s = 0.0800

T = 500°K

R_i = 6 ohm, R_f = 12 ohm

d = 0.040

t (sec)	I_c (ma)
0	0.000
5	3.25
10	2.31
15	1.7
20	1.48
25	1.14
30	1.05
35	0.921
40	0.845
45	0.750
50	0.720
60	0.645
70	0.582
80	0.572
90	0.49
100	0.48
110	0.455
120	0.435
150	0.38
180	0.351

DC-43 continued

t (sec)	I_c (ma)
240	0.30
300	0.265
360	0.244
420	0.235
480	0.21
540	0.20
600	0.187
720	0.175
840	0.16
960	0.151
1080	0.141
1200	0.13
1320	0.127
1440	0.12
1500	0.115
1800	0.109
2160	0.095
2520	0.0900
2880	0.085
3600	0.0755
3960	0.072
4440	0.0675
4800	0.065
5100	0.063
5460	0.060

DC-44 K-Hg

φ_o = 0.860 v. C_o = 0.0521

φ_s = 0.800 v. C_s = 0.0800

T = 500°K

R_i = 6 ohm, R_f = 10 ohm

d = 0.063"

TABLE B-1 (continued)

DC-44 continued

t (sec)	I_c (ma)
0	0.000
5	5.05
10	4.19
15	3.78
20	3.32
25	2.97
30	2.63
35	2.39
40	2.18
50	1.86
60	1.63
70	1.46
80	1.34
90	1.24
120	1.03
150	0.902
180	0.801
240	0.695
300	0.618
360	0.565
480	0.491
600	0.439
720	0.400
840	0.371
1260	0.298
1620	0.264
1980	0.240
2400	0.218
2760	0.203
3240	0.188
3660	0.175
4080	0.166
4620	0.156
4680	0.151

DC-45 K-Hg

$\varphi_o = 0.859$ v. $C_o = 0.0521$

$\varphi_s = 0.790$ v. $C_s = 0.0800$

$T = 550°K$

$R_i = 12$ ohm, $R_f = 13$ ohm

$d = 0.040"$

t (sec)	I_c (ma)
0	0.000
5	3.22
10	2.52
15	2.10
20	1.81
25	1.58
30	1.42
35	1.28
40	1.17
45	1.08
50	0.996
55	0.921
60	0.843
70	0.744
80	0.672
90	0.618
100	0.570
110	0.532
120	0.501
150	0.433
180	0.385
210	0.349
240	0.322
300	0.284
360	0.261
420	0.242

TABLE B-1 (continued)

DC-45 continued

t (sec)	I_c (ma)
480	0.225
540	0.214
600	0.202
900	0.164
1260	0.139
1820	0.116
2040	0.109
2400	0.102
2880	0.0905
3300	0.0861
3840	0.0798
4320	0.0770
4860	0.0701

DC-48 K-Hg

φ_o = 0.630 v. C_o = 0.1467

φ_s = 0.550 v. C_s = 0.1800

T = 500°K

R_i = 8 ohm, R_f = 9 ohm

d = 0.040"

t (sec)	I_c (ma)
0	0.000
5	2.61
10	1.78
15	1.43
20	1.19
25	1.04
30	0.921
35	0.839
40	0.772
45	0.703
50	0.662

DC-48 continued

t (sec)	I_c (ma)
60	0.598
70	0.542
80	0.498
90	0.472
120	0.392
150	0.346
180	0.315
240	0.269
300	0.239
360	0.218
420	0.202
480	0.189
600	0.168
960	0.135
1140	0.123
1500	0.107
1740	0.0995
1920	0.0937
2340	0.0825
2640	0.0801
3060	0.0751
3600	0.0688
4080	0.0655
4620	0.0602
5040	0.0580

DC-49 K-Hg

φ_o = 0.615 v. C_o = 0.1467

φ_s = 0.530 v. C_s = 0.1800

T = 550°K

R_i = 6 ohm, R_f = 9 ohm

d = 0.041"

TABLE B-1 (continued)

DC-49 continued

t (sec)	I_c (ma)
0	0.000
10	2.22
20	1.62
30	1.23
40	1.05
50	0.891
60	0.798
90	0.590
120	0.522
150	0.420
180	0.385
240	0.330
300	0.295
360	0.260
480	0.232
600	0.211
720	0.188
900	0.172
1080	0.148
1440	0.134
1680	0.129
2100	0.109
2400	0.103
2820	0.097
3360	0.088
4020	0.0805

DC-50 K-Hg

φ_o = 0.605 v. C_o = 0.1467

φ_s = 0.518 v. C_s = 0.1800

T = 600°K

R_i = 7 ohm, R_f = 9 ohm

d = 0.040"

DC-50 continued

t (sec)	I_c (ma)
0	0.000
5	1.0
10	1.4
15	1.6
20	1.48
25	1.4
30	1.25
45	1.05
60	0.81
90	0.61
120	0.510
150	0.44
180	0.41
240	0.342
300	0.295
360	0.270
420	0.245
480	0.232
540	0.220
600	0.210
720	0.188
840	0.175
960	0.166
1080	0.155
1380	0.137
1620	0.129
1860	0.120
2100	0.111
2400	0.104
2700	0.098
3000	0.0921
3300	0.0871
3600	0.0824
3080	0.0703
4400	0.0758
5100	0.0718
5580	0.0668
6060	0.0652

TABLE B-1 (continued)

DC-53 K-Hg

φ_o = 0.348 v. C_o = 0.2513
φ_s = 0.270 v. C_s = 0.2900
T = 600°K
R_i = 8 ohm, R_f = 10 ohm
d = 0.041"

t (sec)	I_c (ma)
0	0.000
5	2.6
10	2.2
15	1.88
20	1.78
25	1.36
30	1.26
40	0.98
50	0.84
60	0.75
70	0.658
80	0.62
90	0.581
120	0.501
150	0.436
180	0.404
240	0.34
300	0.298
420	0.25
540	0.231
660	0.211
840	0.185
1020	0.166
1320	0.148
1620	0.131
1980	0.129
2280	0.124
2640	0.0941
3240	0.086

DC-53 continued

t (sec)	I_c (ma)
3900	0.084
4320	0.082

DC-54 K-Hg

φ_o = 0.193 v. C_o = 0.3387
φ_s = 0.140 v. C_s = 0.3800
T = 600°K
R_i = 10 ohm, R_f = 12 ohm
d = 0.039"

t (sec)	I_c (ma)
0	0.000
5	2.18
10	1.63
15	1.38
20	1.17
25	1.05
30	0.915
45	0.718
60	0.605
70	0.558
80	0.501
90	0.472
120	0.398
180	0.325
240	0.266
300	0.233
360	0.218
420	0.194
480	0.186
540	0.174
600	0.166

TABLE B-1 (continued)

DC-54 continued

t (sec)	I_c (ma)
900	0.137
1200	0.115
1500	0.104
1680	0.0991
2040	0.0880
2345	0.0845
2940	0.0735
3600	0.0661
4920	0.0565
5280	0.0439

DC-55 K-Hg

$\varphi_o = 0.205$ v. $C_o = 0.3387$

$\varphi_s = 0.146$ v. $C_s = 0.3800$

$T = 550°K$

$R_i = 13$ ohm, $R_f = 15$ ohm

$d = 0.040$

t (sec)	I_c (ma)
0	0.000
5	2.85
10	1.91
15	1.47
20	1.17
25	1.07
30	0.871
35	0.785
40	0.718
45	0.68
50	0.642
60	0.55
70	0.52
80	0.481
90	0.448

DC-55 continued

t (sec)	I_c (ma)
100	0.425
110	0.418
120	0.378
150	0.340
180	0.310
210	0.290
240	0.266
270	0.252
300	0.241
330	0.222
360	0.215
390	0.210
420	0.199
450	0.197
480	0.191
510	0.182
540	0.178
570	0.172
660	0.168
720	0.155
780	0.149
840	0.143
900	0.138
1140	0.124
1440	0.108
1740	0.0983
2140	0.0878
2580	0.0811
3000	0.0751

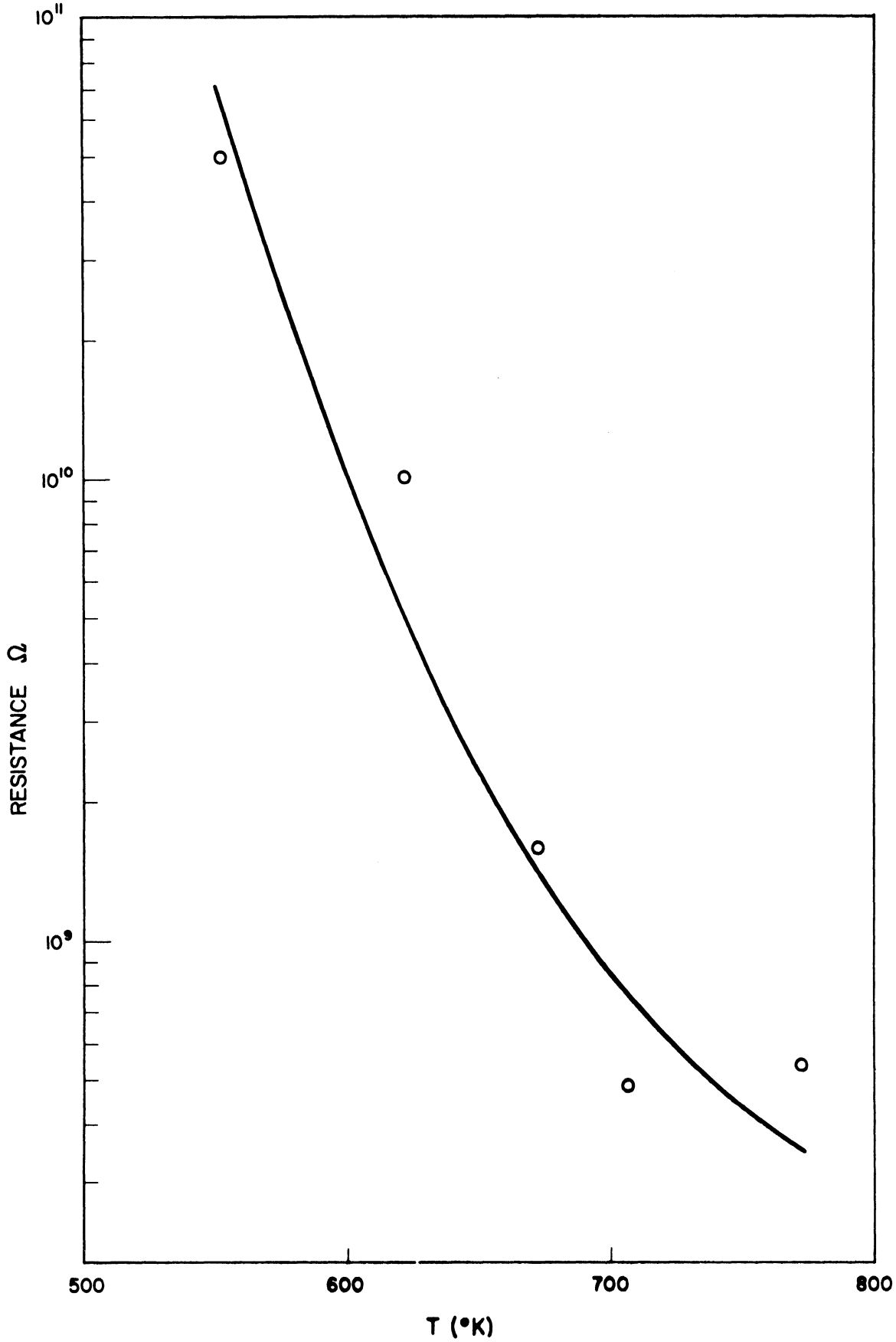

Figure B-1. Cell Resistance as a Function of Temperature

APPENDIX C

CELL VOLTAGE AS A FUNCTION OF CATHODE COMPOSITION FOR LIQUID METAL CELLS

Electromotive force measurements for the systems potassium-mercury, sodium-lead, and sodium-tin are shown in Figure C-1, C-2 and C-3 respectively. These potentials refer to cells of the type

$$A \;\Big|\; A^{+}\ (\text{solid}) \;\Big|\; A(B)$$

where the anode is a pure alkali metal and the cathode an alloy of this metal with a heavier metal. A solid electrolyte containing cations of A^{+} is used in most equilibrium cells.

The curves were calculated from the smoothed partial free energies and partial entropies tabulated by Hultgren et. al. (74). Cell potentials were calculated from the relation

$$\Delta \bar{G}^{\circ} = - n_e F E \qquad (101)$$

The temperature coefficients of the voltage was calculated from

$$\Delta \bar{S}^{\circ} = n_e F \frac{\partial E}{\partial t} \qquad (102)$$

The values used in these calculations are presented in Table C-1 along with Hultgrens estimate of the error involved in each. The uncertainties shown correspond roughly to the 95% confidence limit of the associated values.

Electromotive force measurements for cells with a wide range of cathode alloy compositions (vs. pure alkali metal anodes) are available for each of the systems. The measurements of Lantratrov and Tsarenko (82) agree well with those of Vierk and Hauffe (148) for potassium-mercury alloys. Measurements for sodium-lead are reported by Lantratrov (81) and by Hauffe and Vierk (68). Hauffe and Vierk (68) and Delimarsky and Kolomi (36) have investigated the sodium-tin system. In each of these cases the measurement of EMF was made with a glass electrode. Activities calculated from the above data agree well with those obtained from independent vapor pressure measurements. Hultgrens values were arrived at by an analysis of the existing vapor pressure and emf data available for each system.

TABLE C-1

THERMODYNAMIC PROPERTIES

System	T(°K)	N_{alkali}	$\Delta \bar{G}^{\circ}_{alkali}\left(\frac{cal}{gr\ mole}\right)^{*}$	$\Delta \bar{S}^{\circ}_{alkali}\left(\frac{cal}{gr\ mole}\right)^{*}$
K - Hg	600	0.0	$-\infty$	$+\infty$
		0.1	-16,680	-6.0
		0.2	-10,750	-6.9
		0.3	- 5,770	-6.3
		0.4	- 1,260 $\pm$ 200	-2.5 $\pm$ 2.5
Na - Pb	698	0.0	$-\infty$	$+\infty$
		0.1	-11,130	+2.55
		0.2	- 9,240	0.00
		0.3	- 7,550	-1.28
		0.4	- 6,000	-1.78
		0.5	- 4,520 $\pm$ 200	-1.75 $\pm$ 0.6
Na - Sn	773	0.0	$-\infty$	$+\infty$
		0.1	-10,950	-1.50
		0.2	- 9,450	-1.60
		0.3	- 8,340	-1.53
		0.4	- 7,060	-2.68
		0.5	- 5,640 $\pm$ 150	-4.87 $\pm$ 0.4

*For the units given, F = 23,066 cal/volt and n_e = 1 in equations (72) and (73).

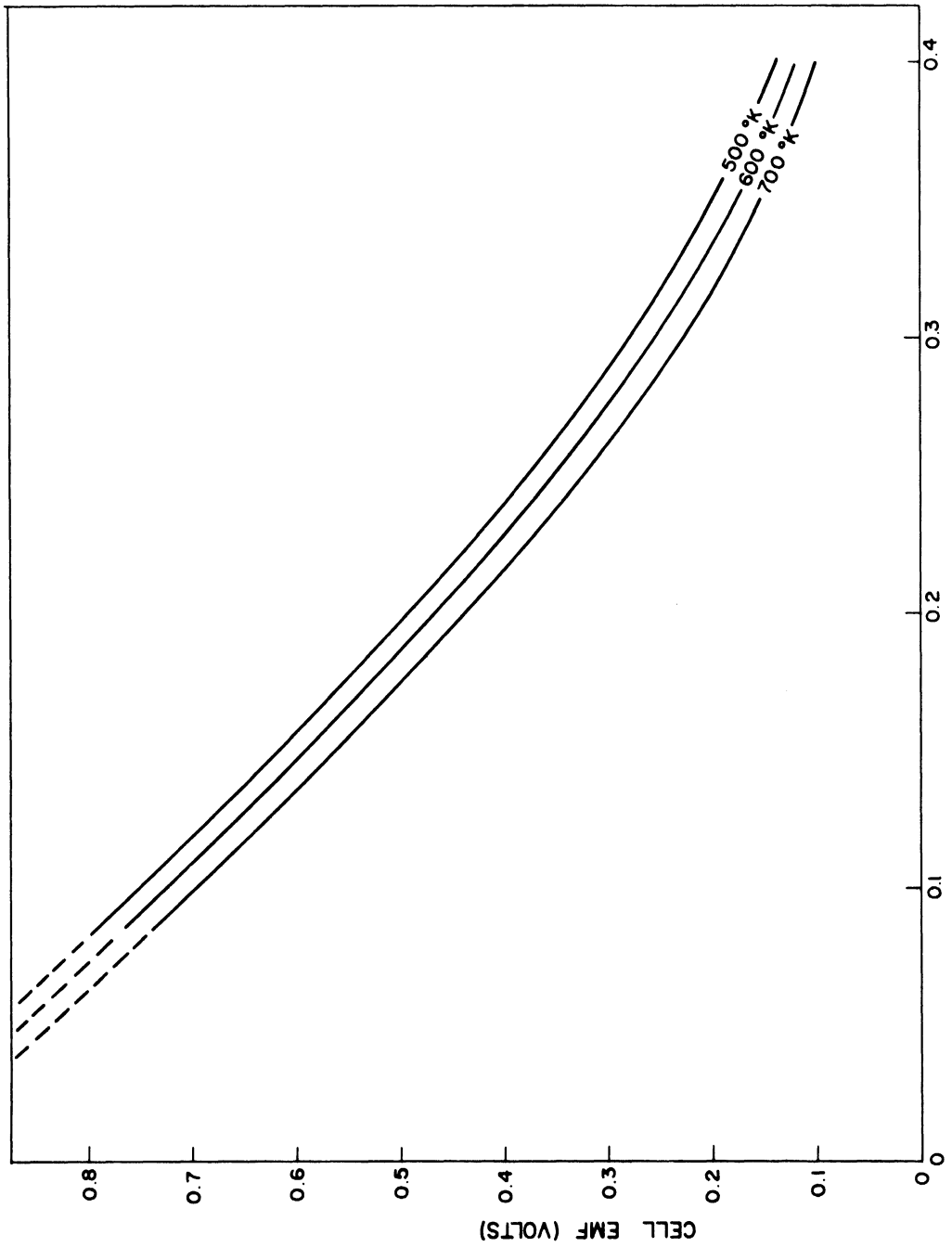

Figure C-1. Cell Potential for K-Hg System

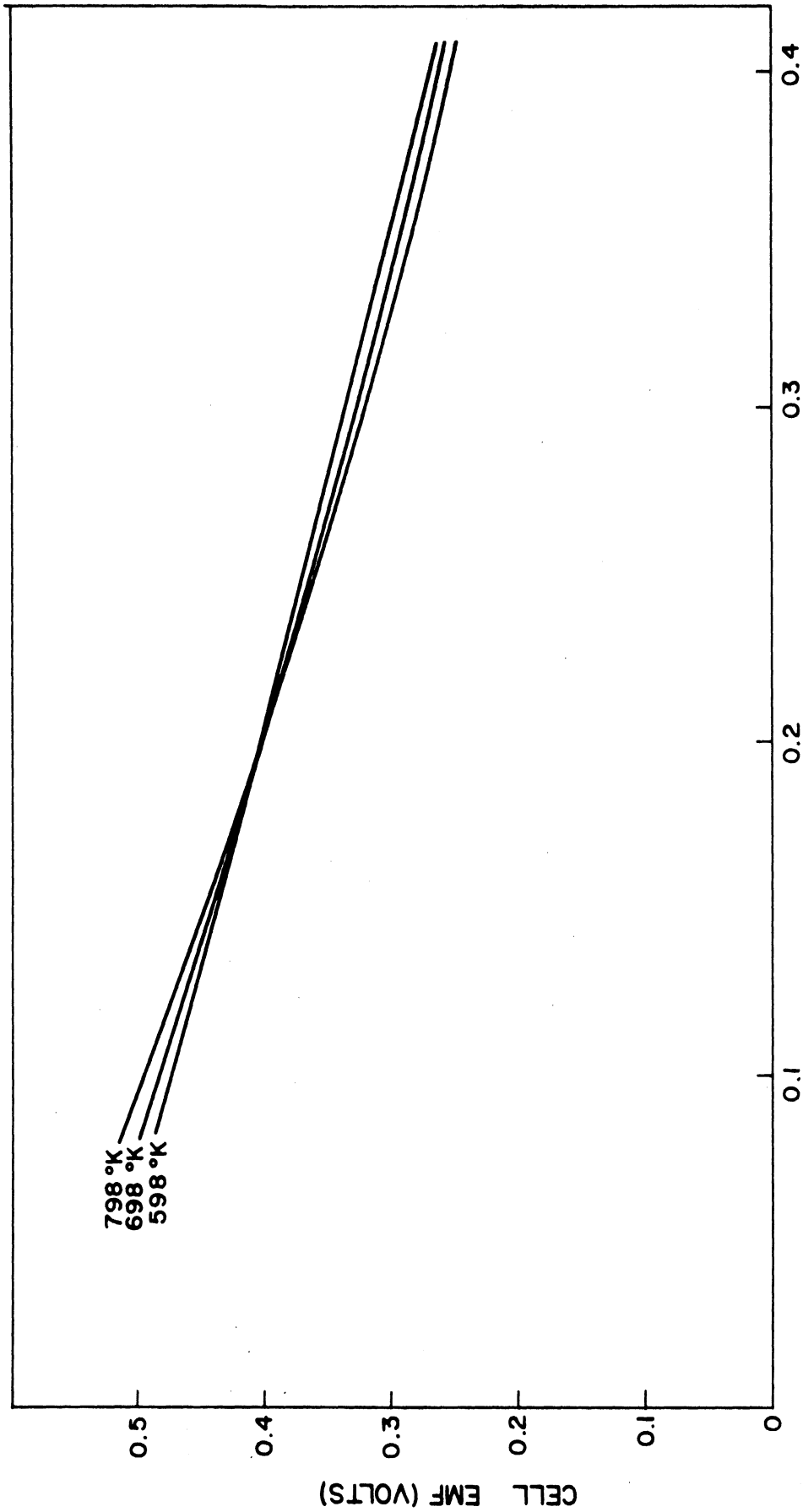

Figure C-2. Cell Potential for Na-Pb System

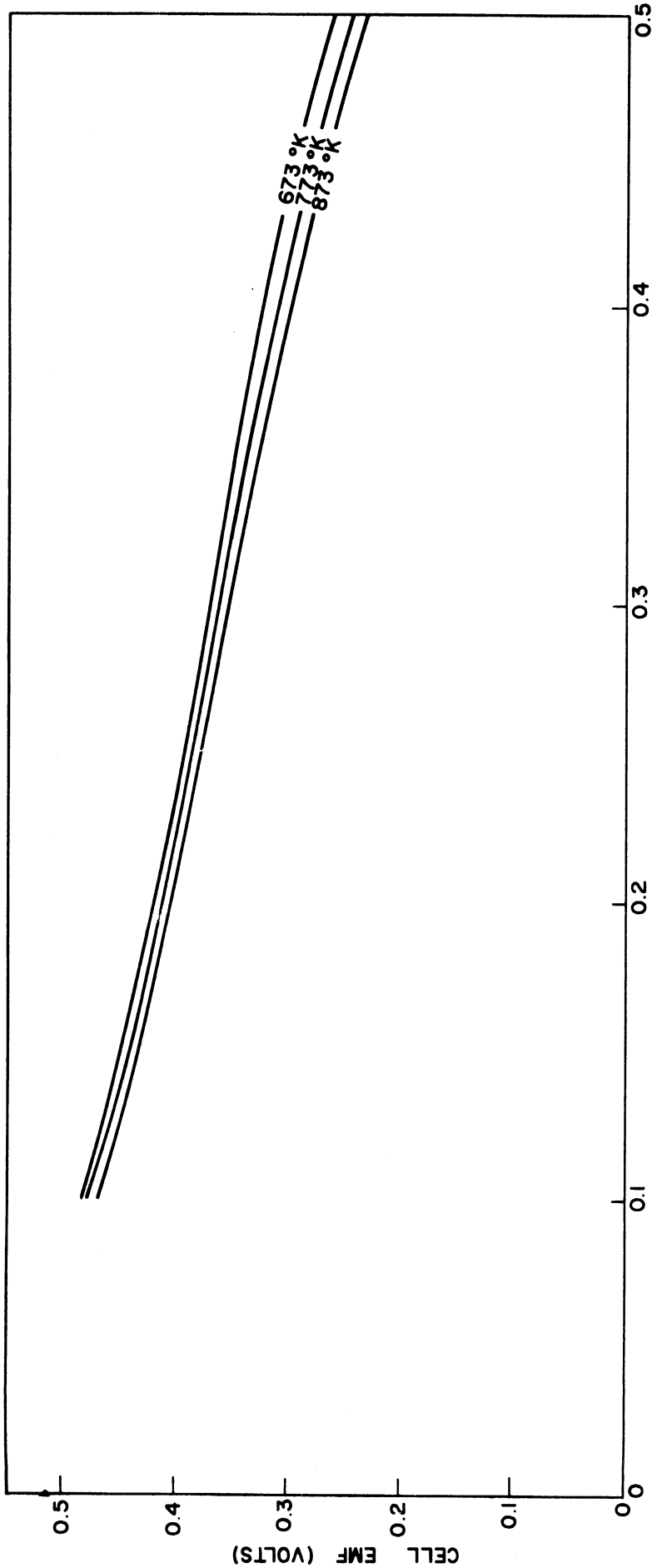

Figure C-3. Cell Potential for Na-Sn System

APPENDIX D

ALLOY DENSITIES

Alloy density data for potassium amalgams is given in Table D-1. The atomic densities, ρ_A, were taken from Bonilla et. al. (13) who obtained them from the experimental data of Degenkolbe and Sauerwald (34) by linear extrapolation of values at 573 and 643°K. The molar volume V_m, and the potassium density ρ_K, were calculated from ρ_A.

The atomic volume of the amalgam is plotted against the mole fraction of potassium in Figure D-1. The negative deviation from Raoults law is expected since addition of potassium to mercury is highly exothermic. The linear relation indicated by the dashed line is true only for ideal solutions where no volume change on mixing occurs.

The atomic density of the alloy is plotted against the mole fraction of potassium in the amalgam in Figure D-2. The linear dashed line in this case represents the case where the molecules are of the same diameter but have differing densities.

Finally, potassium density is plotted against the mole fraction of potassium in the amalgam in Figure D-3.

Comparison of Figures D-1 and D-2 indicates that estimation of alloy densities for the potassium-mercury system could best be done by linear interpolation of the pure component densities on a plot of atomic density vs. the mole fraction of potassium.

Like potassium-mercury, the sodium-tin, and sodium-lead systems exhibit negative deviations from Raoults law. Experimental density data, however, is unavailable for either of these systems. The density of sodium in the alloy (gr. atoms Na/cm^3) as a function of alloy composition was estimated by linear interpolation of the pure component densities on a plot of density vs mole fraction. The results are shown in Figures D-4 and D-5.

TABLE D-1

DENSITY OF POTASSIUM AMALGAMS

	T = 533°K			T = 588°K		
Mole Fraction K	ρ_A $\frac{\text{gr atoms}}{\text{cm}^3}$	V_m $\frac{\text{cm}^3}{\text{gr atom}}$	ρ_K $\frac{\text{gr atoms K}}{\text{cm}^3}$	ρ_A $\frac{\text{gr atoms}}{\text{cm}^3}$	V_m $\frac{\text{cm}^3}{\text{gr atom}}$	ρ_K $\frac{\text{gr atoms K}}{\text{cm}^3}$
0.0	0.0646	15.48	0.00000	0.639	15.66	0.00000
0.1	0.0601	16.62	0.00601	0.0590	17.00	0.00590
0.2	0.0555	18.01	0.01110	0.0549	18.21	0.01098
0.3	0.0508	19.70	0.01524	0.0502	19.90	0.01098
0.4	0.0459	21.80	0.01836	0.0452	22.15	0.01808
0.5	0.0406	24.62	0.02030	0.0398	25.25	0.01990
0.6	0.0347	28.80	0.02082	0.0342	29.25	0.02052
0.7	0.0298	33.55	0.02086	0.0294	34.00	0.02058
0.8	0.0259	38.60	0.02072	0.0256	39.05	0.02048
0.9	0.0226	44.25	0.02034	0.0195	51.30	0.01950

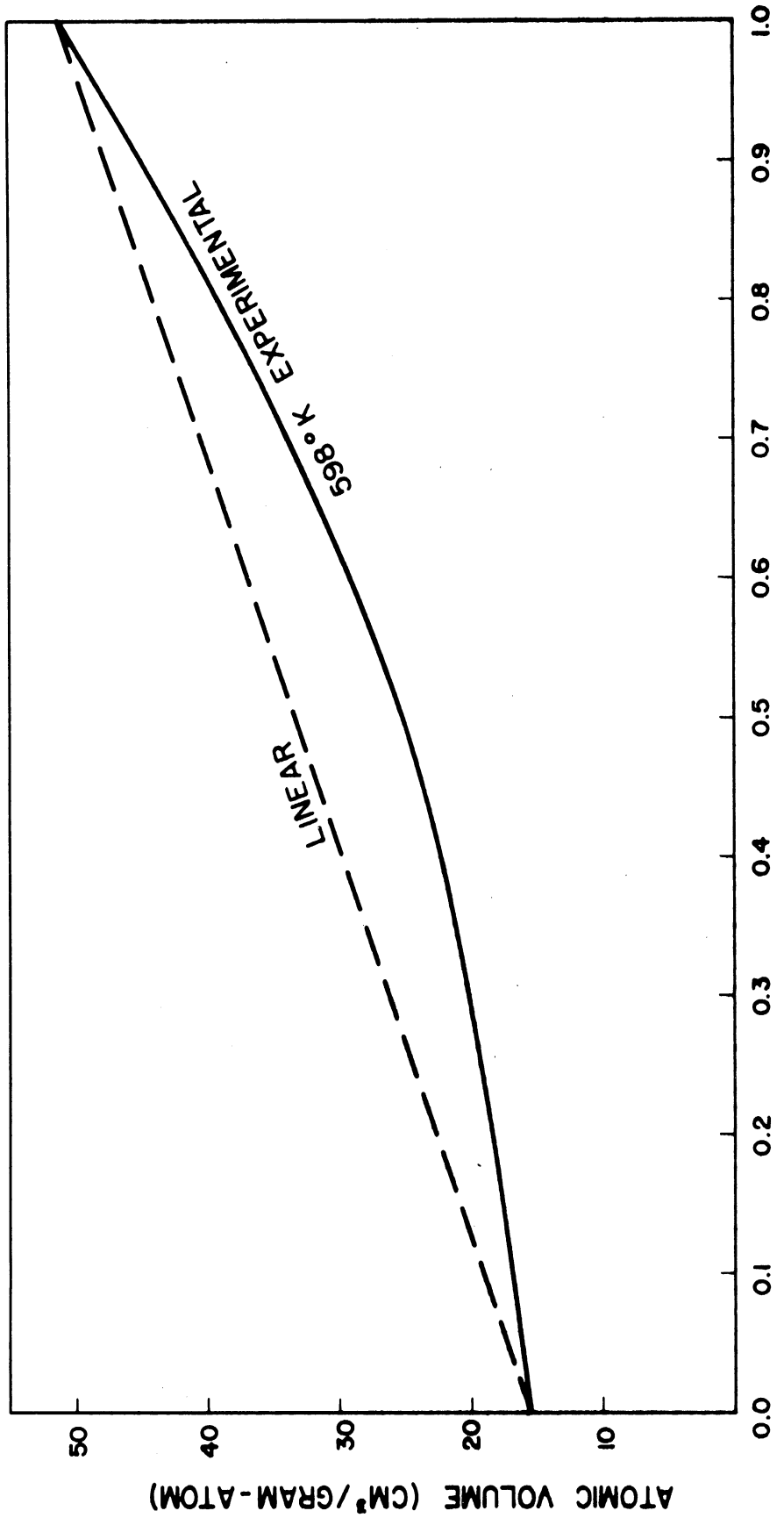

Figure D-1. Atomic Volume vs. Mole Fraction Potassium for Potassium Amalgams

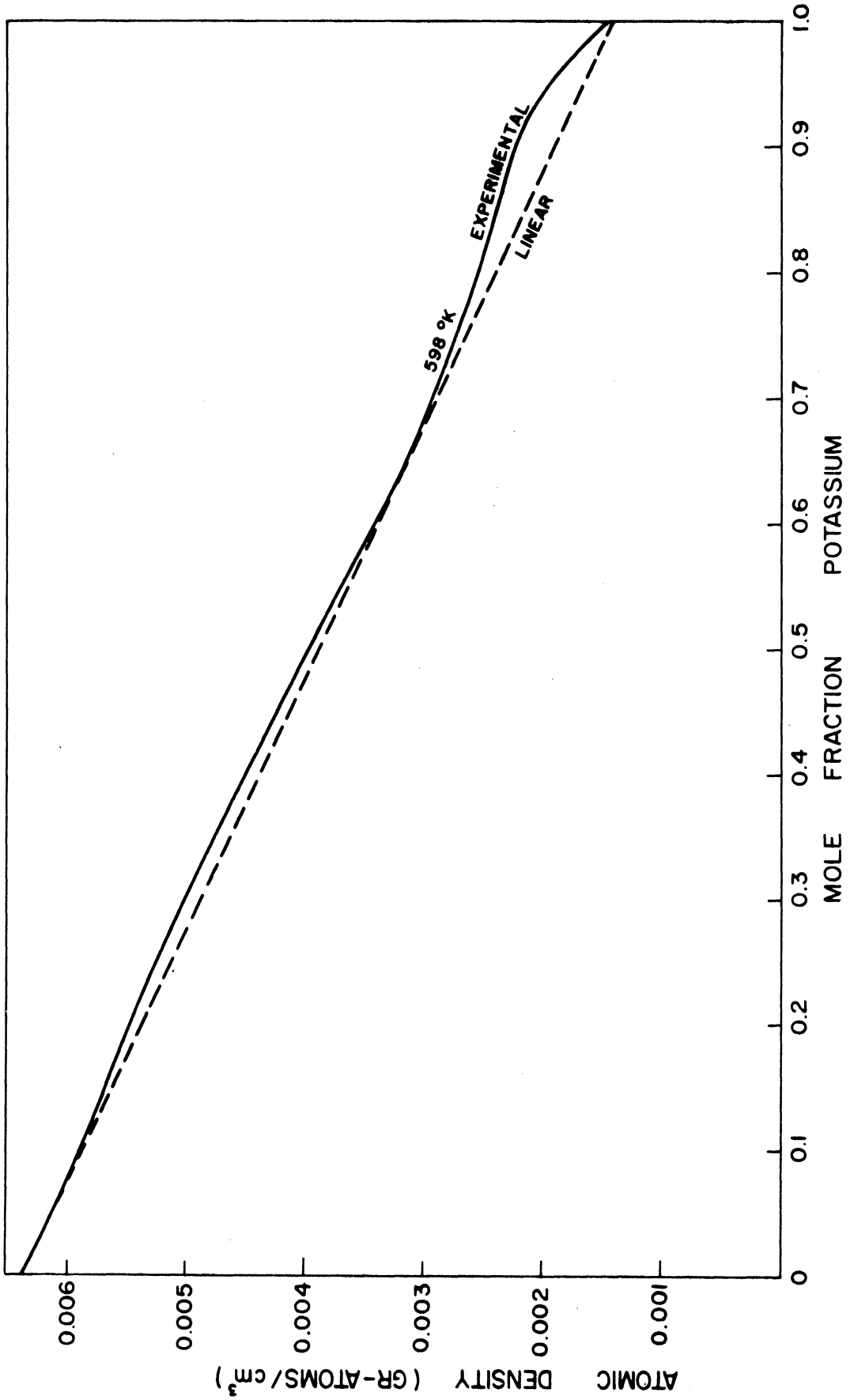

Figure D-2. Atomic Density vs. Mole Fraction Potassium for Potassium Amalgams

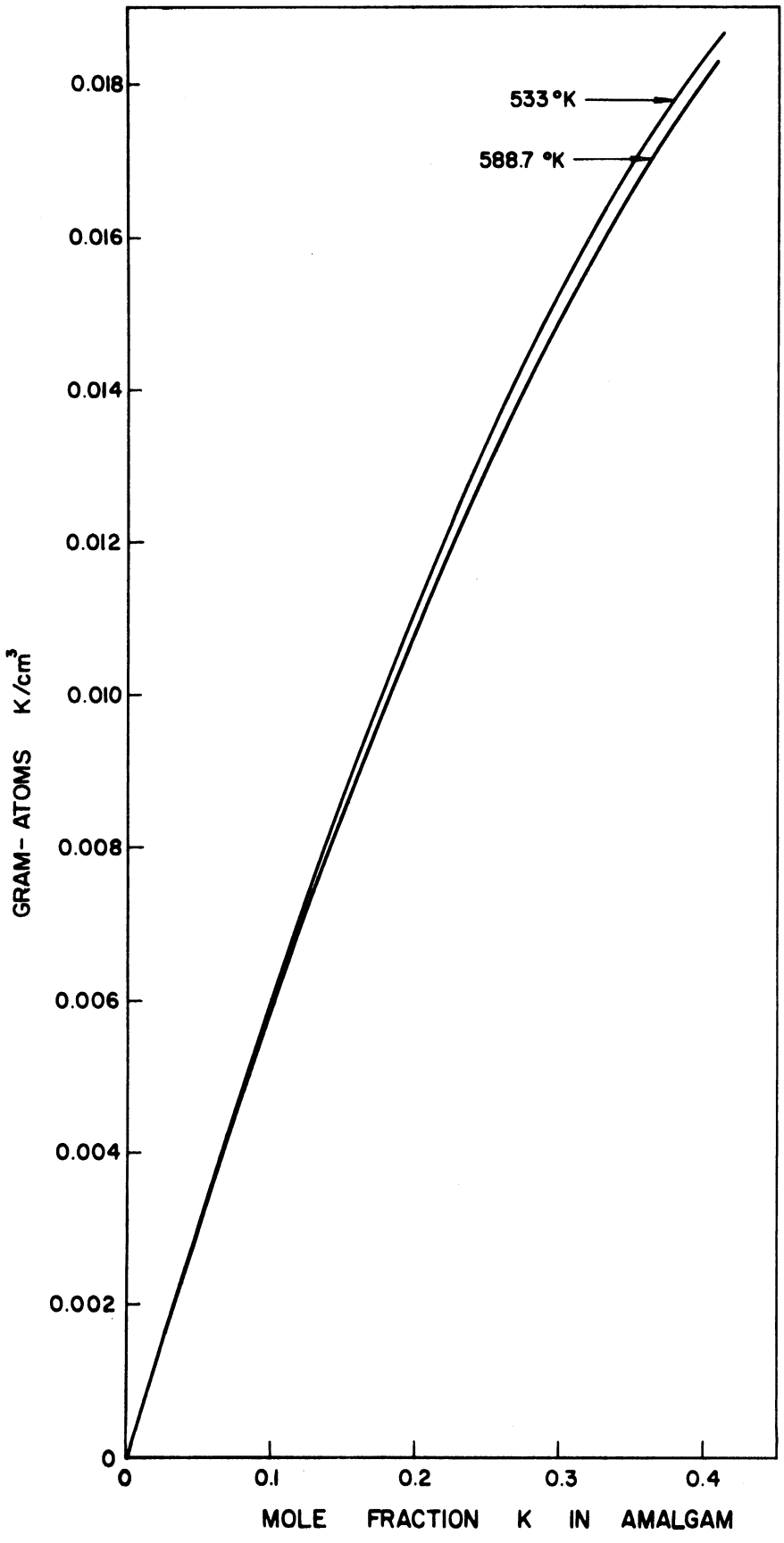

Figure D-3. Potassium Density of Amalgams

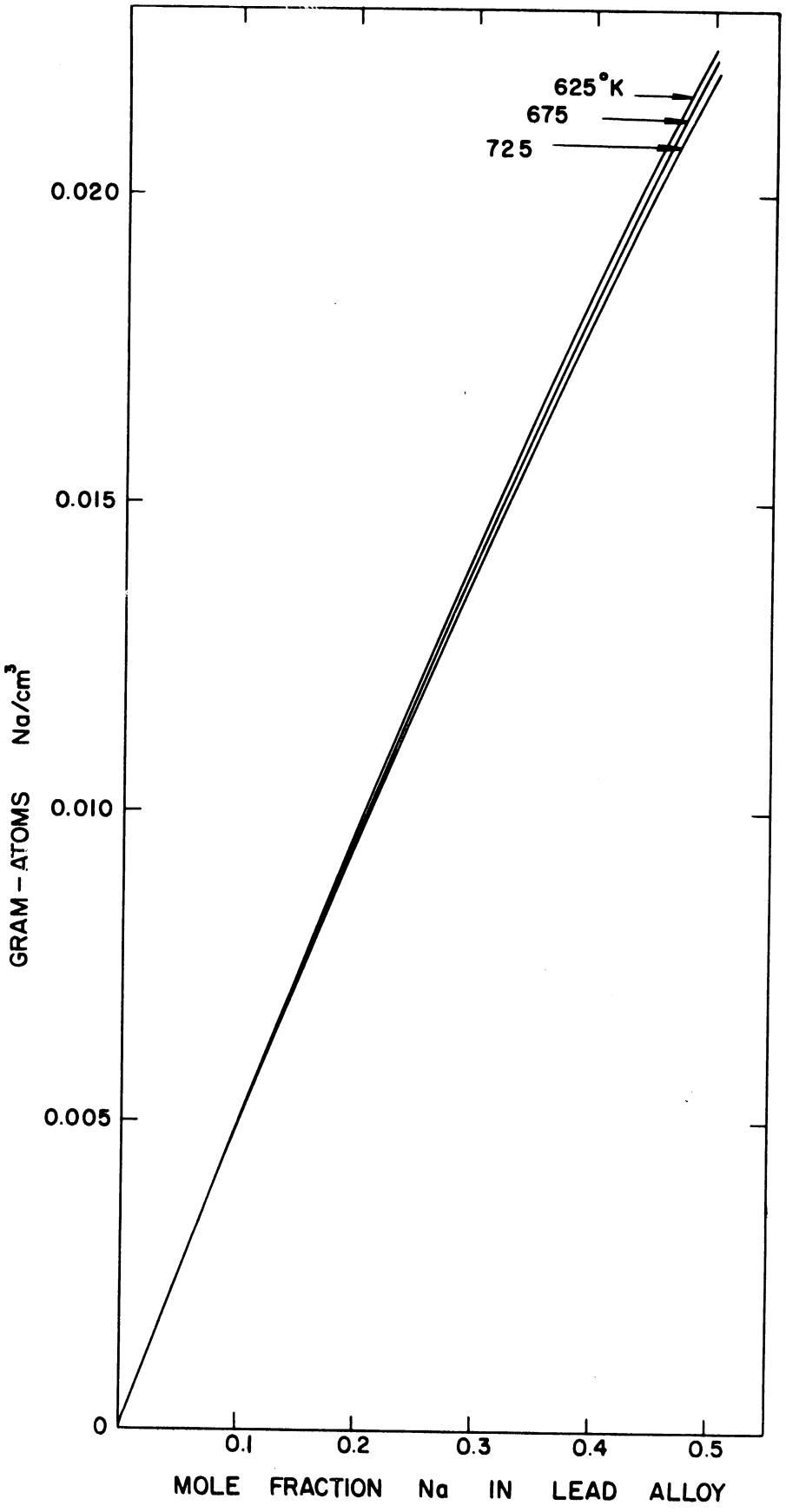

Figure D-4. Sodium Density of Sodium-Lead Alloys

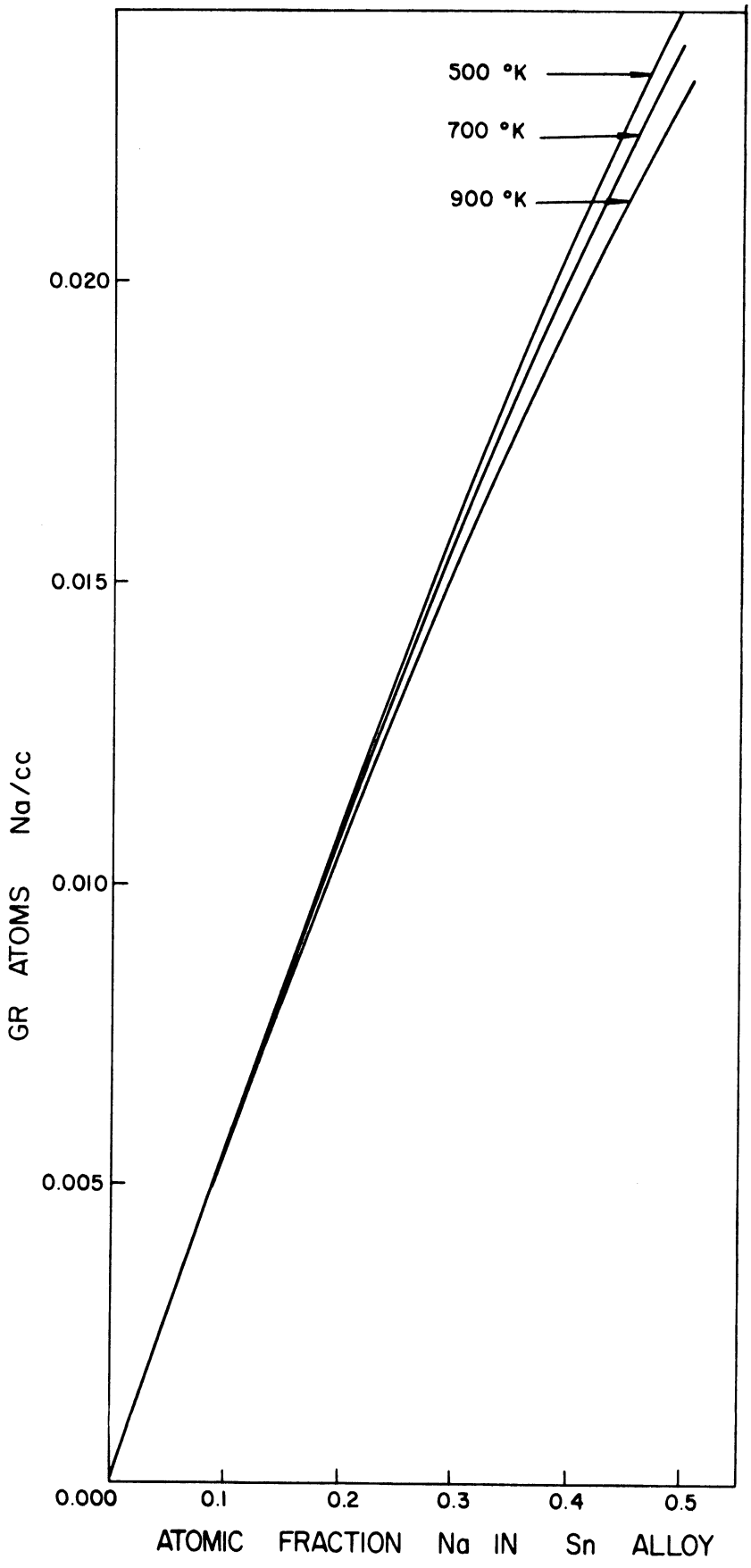

Figure D-5. Sodium Density of Sodium-Tin Alloys

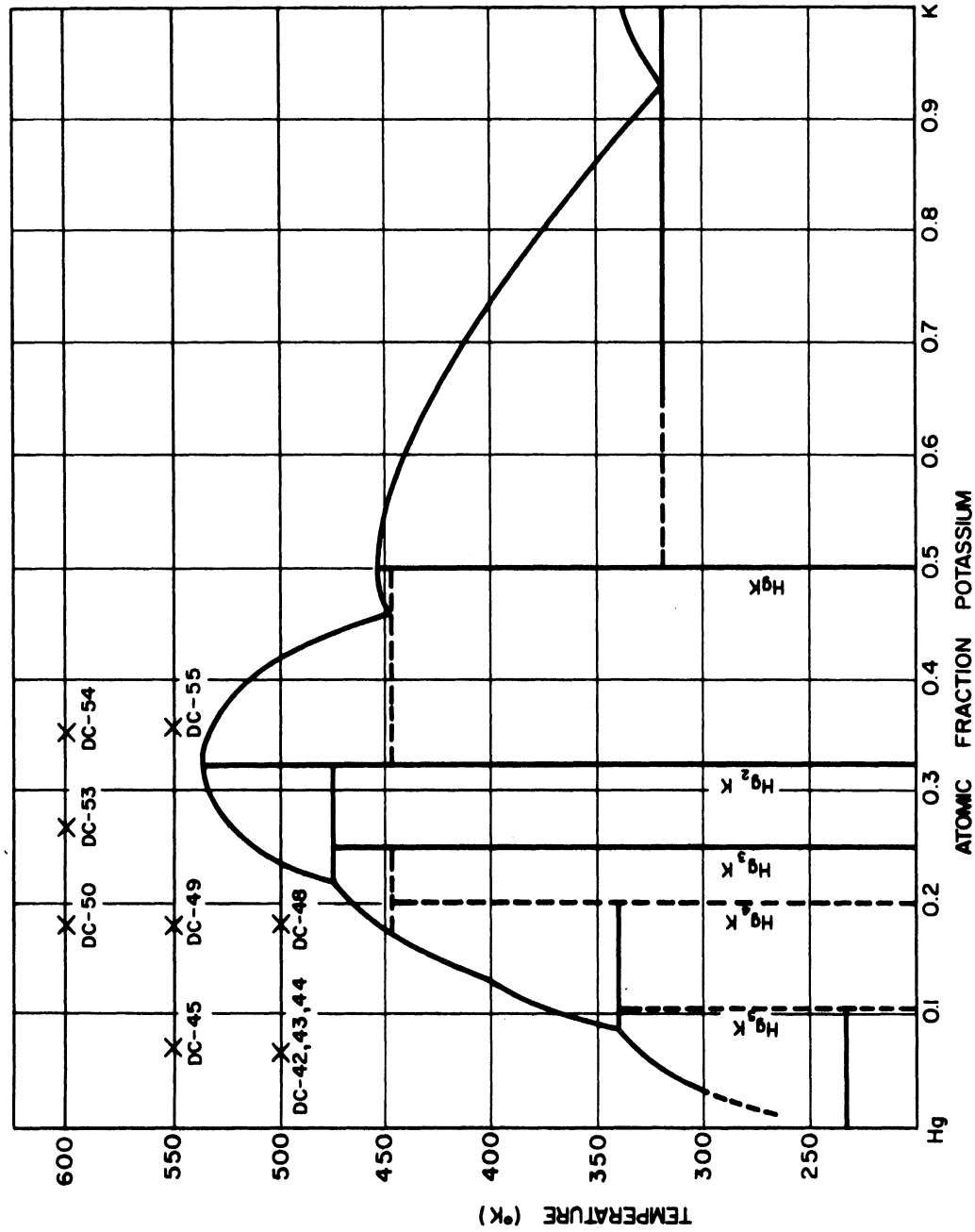

Figure E-1. Phase Diagram for K-Hg System

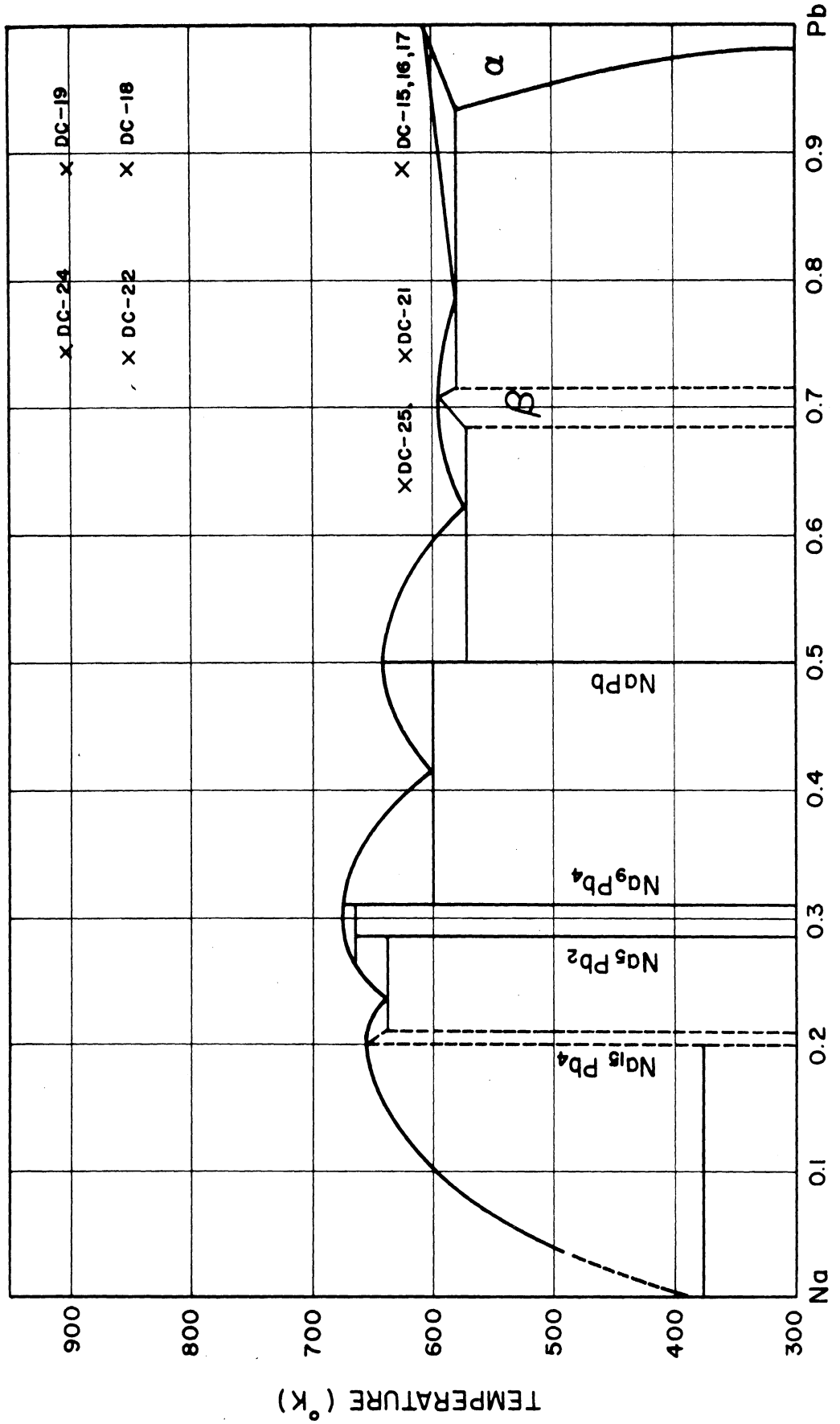

Figure E-2. Phase Diagram for Na-Pb System

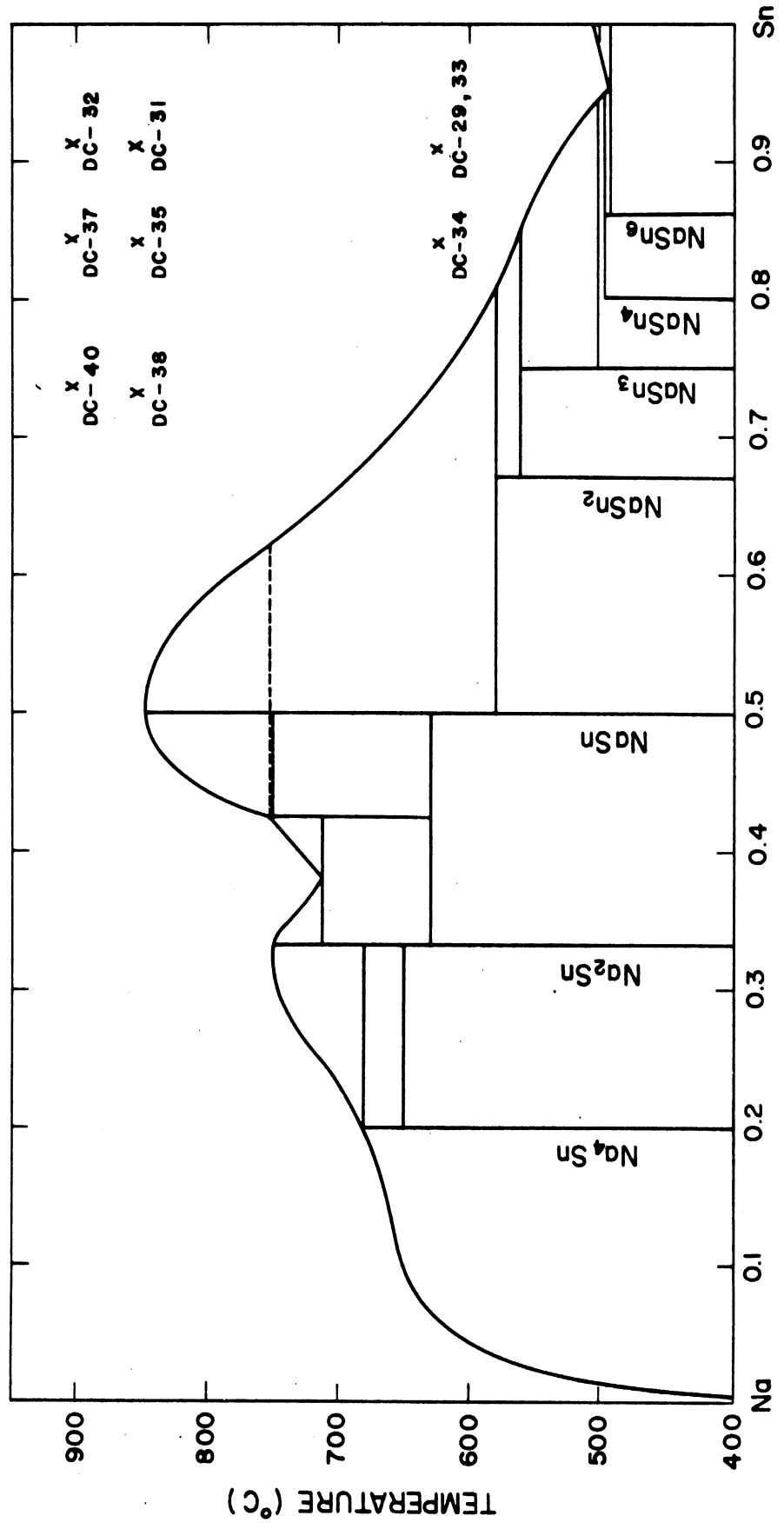

Figure E-3. Phase Diagram for Na-Sn System

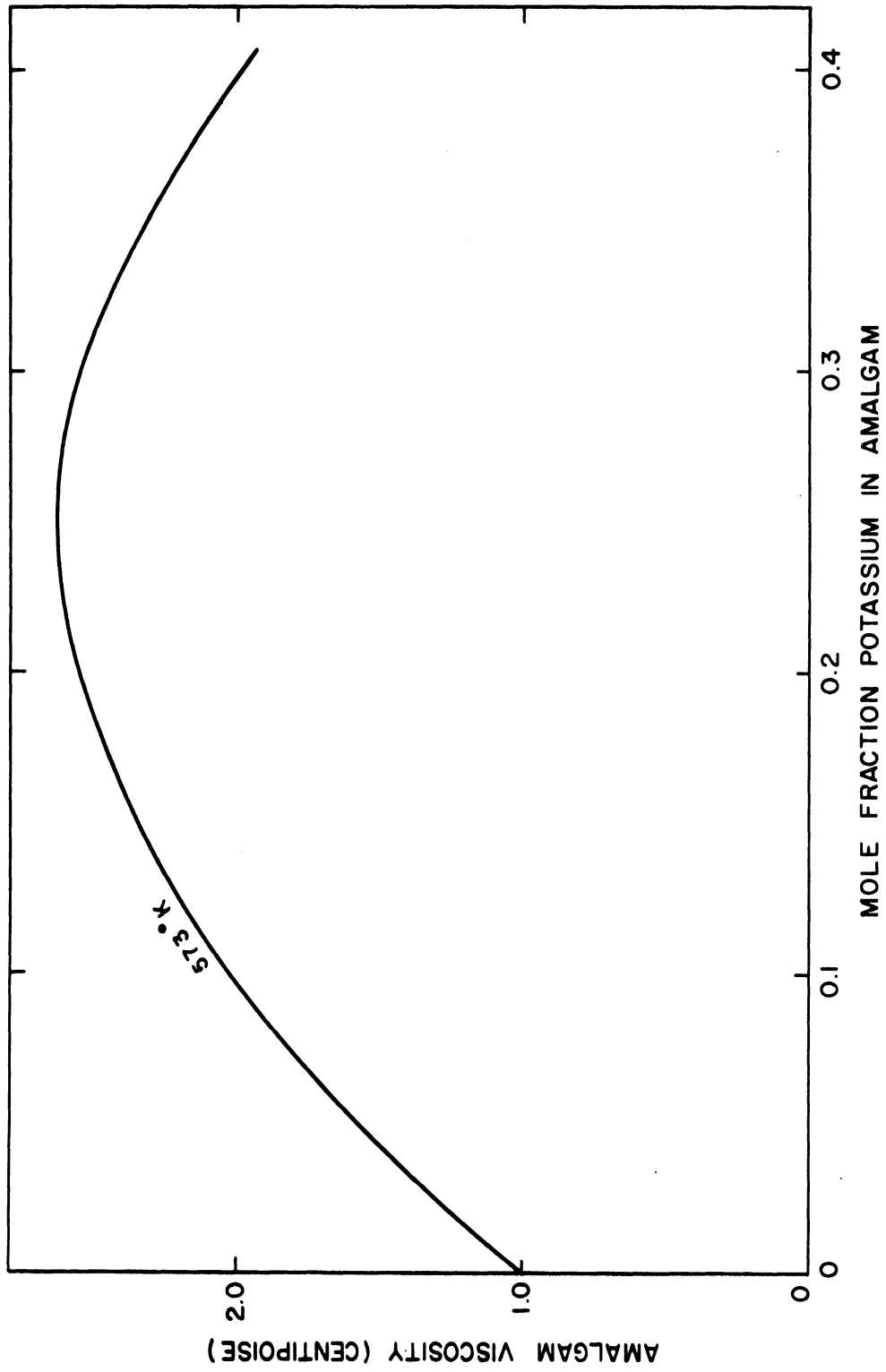

Figure F-1. Viscosity of Potassium Amalgams

APPENDIX G

ANALYTIC SOLUTION OF DIFFUSION EQUATION

Case I.

Diffusion in a one-dimensional semi-infinite plane with uniform initial concentration C_o, and constant surface concentration C_s. Fick's second law for the one-dimensional case is

$$\frac{\partial C}{\partial t} = D \frac{\partial^2 C}{\partial x^2} \tag{103}$$

If the initial composition is uniform and has the value C_o,

$$C(x,0) = C_o \tag{104}$$

The boundary condition at infinity is

$$\lim_{x \to \infty} C(x,t) = C_o \tag{105}$$

If at $t=0^+$ the concentration at x=0 is raised to C_s and if there is no resistance to mass flow across the boundary x=0, then

$$C(0,t) = C_s \tag{106}$$

The solution of equation (103) subject to (104), (105), and (106) is obtained by use of the operational methods of Laplace transforms. Transforms and inverse transforms are taken from Doetsch (37).

The transform of (103) with respect to t is,

$$s \bar{C}(x,s) - C(x,0) = D \bar{C}_{xx}(x,s) \tag{107}$$

substituting (104) into (107) and rearranging

$$\overline{C}_{xx}(x,s) - \frac{s}{D}\overline{C}(x,s) = -C_o \tag{108}$$

Equations (105) and (106) transform to give

$$\lim_{x \to \infty} \overline{C}(x,s) = \frac{C_o}{s} \tag{109}$$

$$\overline{C}(0,s) = \frac{C_s}{s} \tag{110}$$

The roots of (108), $\pm s/D$ indicate a solution of the form

$$\overline{C}(x,s) = f\, e^{-x\sqrt{\frac{s}{D}}} + g\, e^{+x\sqrt{\frac{s}{D}}} + \overline{C}_p \tag{111}$$

the particular solution $\overline{C}_p$ is found by inspection

$$\overline{C}_p = \frac{-C_o/D}{-s/D} = \frac{C_o}{s} \tag{112}$$

The boundary condition (109) indicates G=0 since $\overline{C}(x,s)$ must be bounded.

$$\overline{C}(x,s) = f\, e^{-x\sqrt{\frac{s}{D}}} + \frac{C_o}{s} \tag{113}$$

From equations (111) and (113)

$$f = \frac{C_s - C_o}{s} \tag{114}$$

Then

$$\overline{C}(x,s) = \frac{C_s - C_o}{s}\, e^{-x\sqrt{\frac{s}{D}}} + \frac{C_o}{s} \tag{115}$$

The inversion of (115) is

$$C(x,t) = C_o + (C_s - C_o)\left[\operatorname{erfc}\frac{x}{2\sqrt{Dt}}\right] \qquad (116)$$

The flux at the origin can be obtained from the derivative of (115)

$$\frac{\partial C(x,s)}{\partial x} = -\frac{C_s - C_o}{\sqrt{D}}\,\frac{1}{\sqrt{s}}\,e^{-x\sqrt{\frac{s}{D}}} \qquad (117)$$

Inversion of (117) gives

$$\frac{\partial C(x,t)}{\partial x} = \frac{C_s - C_o}{\sqrt{\pi Dt}}\,e^{-\frac{x^2}{4Dt}} \qquad (118)$$

at x=0

$$\frac{\partial C(0,t)}{\partial x} = \frac{C_s - C_o}{\sqrt{\pi Dt}} \qquad (119)$$

Ficks' first law of diffusion for x=0

$$J(0,t) = -D\,A_s\left[\frac{\partial C(0,t)}{\partial x}\right] \qquad (120)$$

thus

$$J(0,t) = -A_s\,(C_s - C_o)\left(\frac{D}{\pi t}\right)^{1/2} \qquad (121)$$

The total amount of alkali metal that has been transferred from the anode to the cathode, Q, at any time t, is the area under the concentration

profile

$$Q = \int_0^\infty (C - C_o)\, dt \tag{122}$$

this can be written as

$$Q = 2\sqrt{Dt} \int_0^\infty (C - C_o)\, d\left(\frac{x}{2\sqrt{Dt}}\right) \tag{123}$$

Substituting the value of $(C - C_o)$ obtained in equation (116)

$$Q = 2\sqrt{Dt}\ (C_s - C_o) \int_0^\infty \left(1 - \operatorname{erf} \frac{x}{2\sqrt{Dt}}\right) d\left(\frac{x}{2\sqrt{Dt}}\right) \tag{124}$$

The definite integral has the value $1/\pi$

$$Q = \frac{2}{\sqrt{\pi}}\ \sqrt{Dt}\ (C_s - C_o) \tag{125}$$

Case II.

Diffusion in a sphere with uniform initial composition C_o, and constant surface concentration C_s.

Consider diffusion in a sphere where the spherical surfaces of constant concentration are concentric. Ficks' second law, equation (103), becomes

$$\frac{\partial C}{\partial t} = D \frac{\partial^2 C}{\partial r^2} + \frac{2}{r} \frac{\partial C}{\partial r} \tag{126}$$

If the initial concentration C_o is constant throughout the sphere

$$C(r,0) = C_o \qquad 0 \leq r \leq a \tag{127}$$

and if at $t > 0$, the surface concentration is raised to and maintained at a constant value C_s

$$C(a,t) = C_s \qquad t > 0 \tag{128}$$

The following transformation is introduced to linearize equation (126).

$$U = Cr \tag{129}$$

then

$$\frac{\partial C}{\partial t} = \frac{1}{r} \frac{\partial U}{\partial t} \tag{130}$$

$$\frac{\partial C}{\partial r} = \frac{1}{r} \frac{\partial U}{\partial r} - \frac{U}{r^2} \tag{131}$$

$$\frac{\partial^2 C}{\partial r^2} = -\frac{2}{r} \frac{\partial U}{\partial r} + \frac{1}{r} \frac{\partial^2 U}{\partial r^2} - \frac{U}{r^3} \tag{132}$$

Equation (126) becomes

$$\frac{\partial U}{\partial t} = D \frac{\partial^2 U}{\partial r^2} \tag{133}$$

and the boundary and initial conditions become

$$U(a,t) = a\,C_s \tag{134}$$

$$U(r,0) = r\,C_o \tag{135}$$

An additional boundary condition is needed. If the concentration C is bounded at r=0, then a valid boundary condition is

$$U(0,t) = 0 \tag{136}$$

It is useful to make the further transformations

$$a\,x = r \qquad 0 \leq x \leq 1 \tag{137}$$

$$t_o\,\tau = t \tag{138}$$

$$t_o = a^2/D \tag{139}$$

Equation (133) now becomes

$$\frac{\partial^2 U}{\partial x^2} = \frac{\partial U}{\partial \tau} \tag{140}$$

the corresponding initial and boundary conditions are

$$U(1,\tau) = a\,C_s \tag{141}$$

$$U(x,0) = a\,x\,C_o \tag{142}$$

$$U(0,\tau) = 0 \tag{143}$$

The Laplace transform of equation (140) with respect to t is

$$S\bar{U}(x,s) - U(x,0) = \bar{U}_{xx}(x,s) \tag{144}$$

the initial condition, equation (142) is inserted to give

$$S\bar{U}(x,s) - a\,x\,C_o = \bar{U}_{xx}(x,s) \tag{145}$$

Transforming equations (141) and (143) yields

$$\bar{U}(1,s) = \frac{a\,C_s}{s} \tag{146}$$

$$\bar{U}(0,s) = 0 \tag{147}$$

The solution of equation (145) takes the following form

$$\bar{U} = f\,e^{-\sqrt{s}\,x} + g\,e^{+\sqrt{s}\,x} + \bar{U}_p \tag{148}$$

The particular solution, $\bar{U}_p$, is obtained by inspection

$$\bar{U}_p = \frac{a\,x\,C_o}{s} \tag{149}$$

The constants are evaluated from

$$0 = f + g \tag{150}$$

$$f = -g \tag{151}$$

and

$$\frac{a}{s}(C_s - C_o) = -f\,e^{-\sqrt{s}} + f\,e^{+\sqrt{s}} \tag{152}$$

$$f = \frac{2a(C_s - C_o)}{s \sinh\sqrt{s}} \tag{153}$$

Therefore

$$\bar{U} = \frac{a(C_s - C_o)}{s} \frac{\sinh \sqrt{s}\, x}{\sinh \sqrt{s}} + \frac{axC_o}{s} \tag{154}$$

at r=a

$$\bar{U} = \frac{aC_s}{s} \tag{155}$$

The derivative of equation (154) with respect to dimensionless distance is

$$\frac{\partial \bar{U}}{\partial x} = \frac{a(C_s - C_o)}{\sqrt{s}} \frac{\cosh \sqrt{s}\, x}{\sinh \sqrt{s}} + \frac{aC_o}{s} \tag{156}$$

at r=a, x=1 by its definition in equation (137) and

$$\left.\frac{\partial \bar{U}}{\partial x}\right|_{r=a} = \frac{a(C_s - C_o)}{\sqrt{s}} \frac{\cosh \sqrt{s}}{\sinh \sqrt{s}} + \frac{aC_o}{s} \tag{157}$$

Equations (155) and (157) are inverted to give

$$U|_{r=a} = a\, C_s \tag{158}$$

and

$$a \left.\frac{\partial U}{\partial r}\right|_{r=a} = a(C_s - C_o) \left[1 + 2 \sum_{n=1}^{\infty} e^{-n^2\pi^2\tau}\right] + aC_o \tag{159}$$

since $\tau = t/t_o$ and $t_o = a^2/D$, then $\tau = Dt/a^2$ and equation (159) becomes

$$\left.\frac{\partial U}{\partial r}\right|_{r=a} = (C_s - C_o) \left[1 + 2 \sum_{n=1}^{\infty} e^{-\frac{Dn^2\pi^2 t}{a^2}}\right] + C_o \tag{160}$$

Now

$$U = Cr \tag{161}$$

and

$$\nabla C = \frac{1}{r}\frac{\partial U}{\partial r} - \frac{U}{r^2} \tag{162}$$

at r=a

$$\nabla C_{r=a} = \frac{2(C_s - C_o)}{a} \sum_{n=1}^{\infty} e^{-\frac{Dn^2\pi^2 t}{a^2}} \tag{163}$$

Ficks first law of diffusion is

$$J_{r=a} = - D A_s \nabla C_{r=a} \tag{164}$$

For a hemisphere

$$A_s = 2\pi a^2 \tag{165}$$

and the flux J becomes

$$J_{r=a} = -4\pi a D(C_s - C_o) \sum_{n=1}^{\infty} e^{-\frac{Dn^2\pi^2 t}{a^2}} \tag{166}$$

Case III.

Diffusion in a one-dimensional semi-infinite plane with uniform initial concentration C_o, and surface concentration a function of time $C(0,t) = F(t)$.

Ficks' law for one dimensional diffusion is

$$\frac{\partial C}{\partial t} = D \frac{\partial^2 C}{\partial x^2} \tag{167}$$

The initial concentration is C_o

$$C(x,0) = C_o \tag{168}$$

as $x \to \infty$

$$\lim_{x \to \infty} C(x,t) = C_o \tag{169}$$

At $x = 0$

$$C(0,t) = C_o + (C_s - C_o)(1 - e^{-Kt}) \tag{170}$$

This function satisfies the conditions that at t=0, $C(0,t) = C_o$, and as $t \to \infty$, $C(0,t) \to (C_s - C_o)$. K is a constant and is chosen so the diffusion flux will approach the linear case at a prescribed time.

The transform of equation (167) with respect to t is

$$s\overline{C}(x,s) - C(x,0) = D\overline{C}_{xx}(x,s) \tag{171}$$

Incorporating the initial condition into this equation and rearranging

$$\overline{C}_{xx}(x,s) - \frac{s}{D}\overline{C}(x,s) = -\frac{C_o}{D} \tag{172}$$

The boundary conditions transform as follows

$$\lim_{x \to \infty} C(x,s) = \frac{C_o}{s} \tag{173}$$

$$\overline{C}(0,s) = \frac{C_s}{s} - \frac{C_s - C_o}{s + K} \tag{174}$$

The solution of equation (172) takes the form

$$\bar{C}(x,s) = f\, e^{-\sqrt{\frac{s}{D}}\, x} + g\, e^{+\sqrt{\frac{s}{D}}\, x} + \bar{C}_p \qquad (175)$$

The particular solution, $\bar{C}_p$, is found by inspection

$$\bar{C}_p = \frac{-C_o/D}{-s/D} = \frac{C_o}{s} \qquad (176)$$

The constant G in equation (175) is zero since $\bar{C}(x,s)$ must be bounded as $x \to \infty$. F is evaluated from the other boundary equation.

$$f = (C_s - C_o)\left[\frac{1}{s} - \frac{1}{s+K}\right] \qquad (177)$$

Thus

$$\bar{C}(x,s) = (C_s - C_o)\left[\frac{1}{s} - \frac{1}{s+K}\right] e^{-\sqrt{\frac{s}{D}}\, x} + \frac{C_o}{s} \qquad (178)$$

The derivative of equation (178) with respect to distance is

$$\frac{\partial \bar{C}(x,s)}{\partial x} = \frac{(C_s - C_o)}{\sqrt{D}}\left[\frac{1}{\sqrt{s}} - \frac{\sqrt{s}}{s+K}\right] e^{-\sqrt{\frac{s}{D}}\, x} \qquad (179)$$

At $x = 0$

$$\left.\frac{\partial \bar{C}}{\partial x}\right|_{x=0} = \frac{C_s - C_o}{\sqrt{D}}\left[\frac{1}{\sqrt{s}} - \frac{\sqrt{s}}{s+K}\right] \qquad (180)$$

The inversion of equation (180) is

$$\left.\frac{\partial C}{\partial x}\right|_{x=0} = \frac{(C_s - C_o)}{\sqrt{D}} \quad \frac{2\sqrt{K}}{\sqrt{\pi}} \quad e^{-Kt} \quad \int_o^{\sqrt{Kt}} e^{\lambda^2} \, d\lambda \tag{181}$$

e^{λ^2} can be expressed as a power series

$$\left.\frac{\partial C}{\partial x}\right|_{x=0} = \frac{2(C_s - C_o)\sqrt{K}}{\sqrt{D\pi}} \quad e^{-Kt} \quad \int_o^{Kt} \frac{\lambda^{2n}}{n!} \, dn \tag{182}$$

The Weirstrauss M-test reveals the series is uniformly convergent so that the order of summation and integration can be interchanged and the series integrated term by term.

$$\left.\frac{\partial C}{\partial x}\right|_{x=0} = \frac{2(C_s - C_o)\sqrt{K}}{\sqrt{D\pi}} \quad e^{-Kt} \left[\frac{\lambda^{2n+1}}{(2n+1)\, n!} \right]_0^{\sqrt{Kt}} \tag{183}$$

$$\left.\frac{\partial C}{\partial x}\right|_{x=0} = 2(C_s - C_o)\, K\sqrt{\frac{t}{D\pi}} \quad e^{-Kt} \sum_{n=0}^{\infty} \frac{(Kt)^n}{(2n+1)\, n!} \tag{184}$$

Ficks' first law for diffusion has been given as

$$J_{x=0} = - D\, A_s \nabla C_{x=0} \tag{185}$$

The area of a cylinderical capillary is $A_s = \pi a^2$, so

$$J_{x=0} = 2\, K\, A_s\, (C_s - C_o) \sqrt{\frac{Dt}{\pi}} \quad e^{-Kt} \sum_{n=0}^{\infty} \frac{(Kt)^n}{(2n+1)\, n!} \tag{186}$$

APPENDIX H

NUMERICAL SOLUTION OF DIFFUSION EQUATION

Consider diffusion in a semi-infinite cylinderical path, the bounded end of which is hemispherical in shape. All diffusing material enters this path through the hemispherical surface.

Cylinderical corrdinates are used for the numerical solution. Ficks' second law is

$$\frac{\partial C}{\partial t} = D\left(\frac{\partial^2 C}{\partial r^2} + \frac{1}{r}\frac{\partial C}{\partial r} + \frac{\partial^2 C}{\partial z^2}\right) \tag{187}$$

Figure H-1 illustrates the geometry of the path. The radius of the cylinder is R_o. The distance Z_o is equal to R_o.

The initial and boundary conditions for this problem are,

$$C(r,z,0) = C_o \tag{188}$$

$$\lim_{z \to \infty} (r,z,t) = C_o \tag{189}$$

$$\frac{\partial C\ (R_o,\ z>Z_o,\ t)}{\partial r} = 0 \tag{190}$$

$$\frac{\partial C\ (0,z,t)}{\partial r} = 0 \tag{191}$$

In addition, for $t > 0$ the concentration on the curved boundary is raised to and maintained at a constant value C_s.

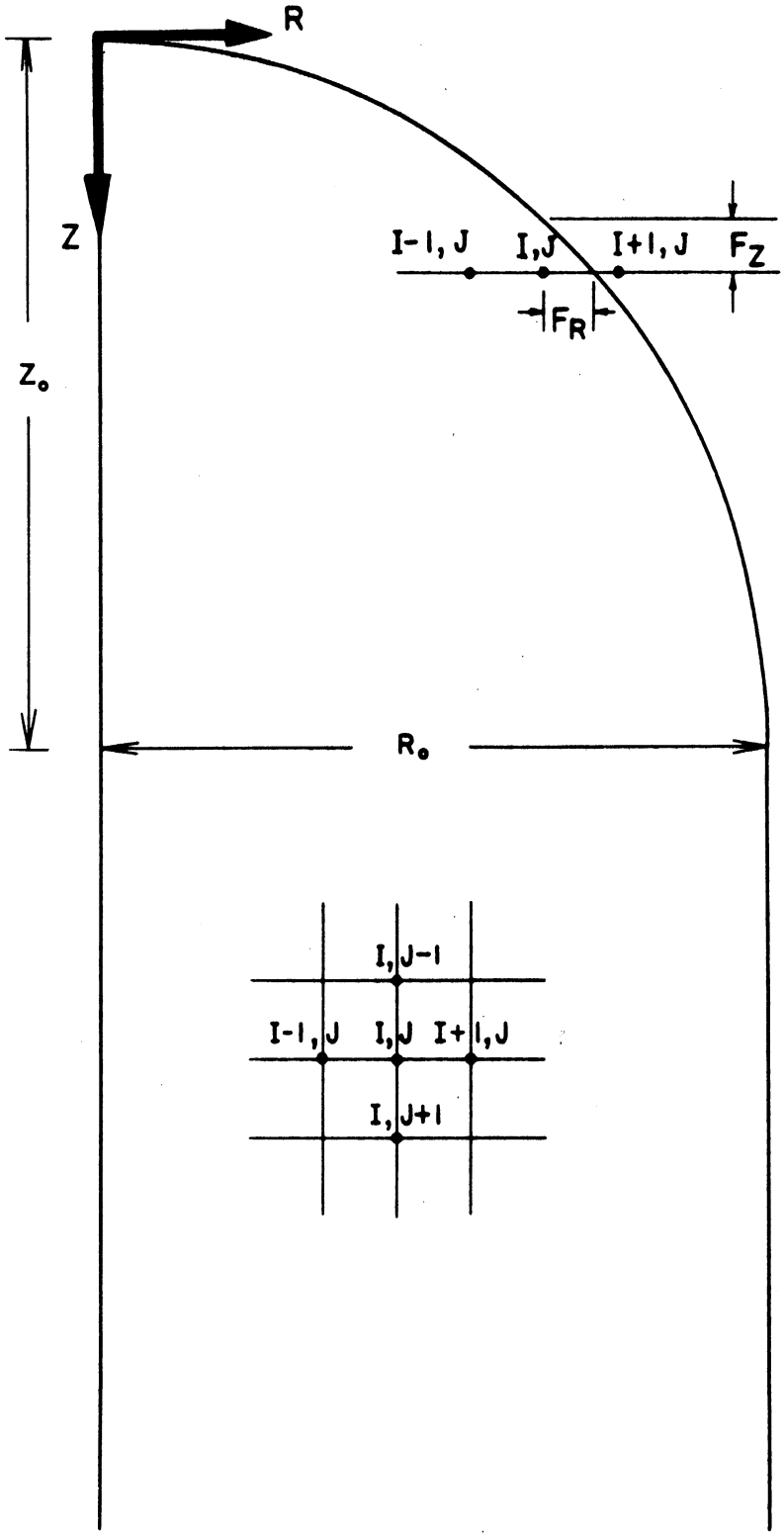

Figure H-1. Grid Arrangement for Numerical Approximation

Equation (187) is transformed according to the following equations.

$$r = RR_o \tag{192}$$

$$z = ZZ_o \tag{193}$$

$$t = t_o\tau \tag{194}$$

$$C = \frac{c-c_o}{c_s-c_o} \tag{195}$$

This gives

$$\frac{1}{t_o}\frac{\partial C}{\partial \tau} = D\left[\frac{1}{R_o^2}\frac{\partial^2 C}{\partial R^2} + \frac{1}{R_o^2 R}\frac{\partial C}{\partial R} + \frac{1}{Z_o}\frac{\partial^2 C}{\partial Z^2}\right] \tag{196}$$

If $t_o = DR^2$, then the dimensionless form of equation (187) is obtained.

$$\frac{\partial C}{\partial \tau} = \frac{\partial^2 C}{\partial R^2} + \frac{1}{R}\frac{\partial C}{\partial R} + \left(\frac{R_o}{Z_o}\right)^2 \frac{\partial^2 C}{\partial Z^2} \tag{197}$$

The derivatives in equation (197) may be approximated by Taylor expansions. In the following equations X may represent either the Z or the R directions

$$C_{-1} = C_o - \Delta x\frac{\partial C}{\partial x} + \frac{(\Delta x)^2}{2}\frac{\partial^2 C}{\partial x^2} + \ldots \tag{198}$$

$$C_{+1} = C_o + \Delta x\frac{\partial C}{\partial x} + \frac{(\Delta x)^2}{2}\frac{\partial^2 C}{\partial x^2} + \ldots \tag{199}$$

The grid points closest to the boundary will be dealt with separately later. For interior points $\partial^2 C/\partial x^2$ is obtained by addition of (198) and (199)

$$\frac{\partial^2 C}{\partial x^2} = \left[\frac{C_{-1} + C_{+1} - 2C_o}{(\Delta x)^2}\right] \tag{200}$$

$\partial C/\partial x$ is obtained by subtraction of (198) from (199)

$$\frac{\partial C}{\partial x} = \frac{C_{+1} - C_{-1}}{2\Delta x} \tag{201}$$

I is the index for incrimenting in the R direction and J that for the Z direction as shown in Figure H-1. For the R direction equations (200) and (201) become

$$\left(\frac{\partial^2 C}{\partial R^2}\right)_{I,J} = \frac{C_{I+1,J} + C_{I-1,J} - 2C_{I,J}}{(\Delta R)^2} \tag{202}$$

$$\frac{1}{R}\left(\frac{\partial C}{\partial R}\right)_{I,J} = \frac{C_{I+1,J} - C_{I-1,J}}{2R(\Delta R)^2} \tag{203}$$

It is apparent from Figure H-1 that $R=I\Delta R$, therefore

$$\frac{1}{R}\left(\frac{\partial C}{\partial R}\right)_{I,J} = \frac{C_{I+1,J} - C_{I-1,J}}{2I(\Delta R)^2} \tag{204}$$

Equation (200) for the Z direction is

$$\left(\frac{R_o}{Z_o}\right)^2\left(\frac{\partial^2 C}{\partial Z^2}\right)_{I,J} = \left(\frac{R_o}{Z_o}\right)^2 \frac{C_{I,J+1} + C_{I,J-1} - 2C_{I,J}}{(\Delta Z)^2} \tag{205}$$

The implicit alternating direction method is used. The procedure is to consider two half time steps, each of duration $\Delta\tau/2$. Over the first of these time steps the derivatives in the Z direction are approximated assuming no mass flow in the R direction. Then, for the second half step the derivatives in the R direction are calculated assuming no diffusion in the Z direction. The method is discussed by Wilkes et. al. (24)

$$\frac{\partial C}{\partial \tau} = \frac{C^*_{I,J} - C_{I,J}}{\Delta\tau/2} \qquad (206)$$

$C^*_{I,J}$ are the new values of $C_{I,J}$ obtained from the first half time step. These values are used for computation of concentrations at the end of the second half time step.

The derivative approximations, equations (202), (204), (205) and (206), are substituted into equation (197). For each half step a set of simultaneous equations arise. There are at most three unknowns in these equations, $C^*_{I-1,J}$, $C^*_{I,J}$ and $C^*_{I+1,J}$. A tri-diagonal matrix results for the coefficients of these equations. A simple algorithm is available to invert the matrix. This algorithm is discussed by Peaceman et. al. (105) and by Carnahan et. al. (24). The external function TRIDA in the program which follows is used to invert the matrix.

Grid points closest to a boundary must be dealt with separately because the distance from the point to the boundary may not equal ΔR

or ΔZ. In Figure H-1 the distance for one case is denoted as F_i (i = R or Z). Equations (198) and (199) become

$$C_{-1} = C_o - \Delta x\left(\frac{\partial C}{\partial x}\right) + \frac{(\Delta x)^2}{2}\frac{\partial^2 C}{\partial x^2} + \cdots \qquad (207)$$

$$C_{+1} = C_o + F_i \Delta x \frac{\partial C}{\partial x} + \frac{F_i^2 \Delta x}{2}\frac{\partial^2 C}{\partial x^2} \qquad (208)$$

To obtain $\partial^2 C/\partial x^2$ multiply (207) by F_i and add the result to (208)

$$\frac{\partial^2 C}{\partial x^2} = 2\left[\frac{C_{+1} + F_i C_{-1} - (1 + F_i)\, C_o}{(\Delta x)^2\, F\, (1 + F_i)}\right] \qquad (209)$$

$\partial C/\partial x$ is obtained by multiplying (207) by F_i^2 and subtracting (208)

$$\frac{\partial C}{\partial x} = \frac{C_{+1} - F_i^2 C_{-1} - (1 - F_i^2)\, C_o}{F_i (F_i + 1)\, \Delta x} \qquad (210)$$

The values of $\partial^2 C/\partial R^2$, $(1/R)\,(\partial C/\partial R)$, $(R_o/Z_o)^2\, \partial^2 C/\partial Z^2$ are evaluated from equations (209) and (210) as was done for the previous case. Coefficients for the points closest to the boundary are calculated by the external function BONDY and stored for later use.

Concentrations at the end of each time incriment are summed and weighted according to the area swept out as the plane shown in Figure H-1 is rotated about the axis R = 0. The concentration change during the incriment is divided by the time to obtain the flux.

The program has three sections, the main section noted as MAIN which is the basic program used to compute the derivatives, and two

external functions TRIDA and BONDY which were discussed above. The program is written in MAD (Michigan Algorithmic Decoder) language (177).

The program follows, output is presented in tabular form. The convergence of the program was checked by varying the time step. The diameter of the capillary used in this program was 1.0 mm and the diffusion coefficient was 1.0×10^{-5} cm^2/sec.

```
                                MAINB001
                  FTRAP.
                  PROGRAM COMMON AR,BR,CR,DDR,T,TSTAR,AC,BC,CC,DDC,P,FZ,S,FR,X
                 1 ,IF,N,M,L
                  DIMENSION AR(80),BR(80),CR(80),DDR(80),T(891),TSTAR(891),AC(8
                 1 0),BC(80),CC(80),DDC(80),P(80),FZ(80),S(80),FR(80),X(80)
                 2 ,IF(80)
                  DIMENSION FLUX(1000),SUM(1000)
                  INTEGER N,M,L,P,S,X
                  INTEGER I,J,K,SJ,PI,TAU,INCR,INCRMX,TAUFIN,TAUBIN
                  INTEGER JXL,JX,MAX,TAUSP
                  DIMENSION         KF(80),JF(80),AFR(80),AFZ(80),BFR(80),BFZ(80
                 1 ),CFR(80),CFZ(80)
                  VECTOR VALUES INGPNT=$1HC,S6,I3,S6,I3,S6,F10.8*$
                  VECTOR VALUES TPRT=$1H ,11E10.4*$
                  VECTOR VALUES HEADG=$10H1AT TIME= F10.6,32H+SEC THE POTENTIAL
                 1  FLOW FIELD IS*$
                  VECTOR VALUES FPRT=$1H ,10E10.4/(S4,10E10.4)*$
                  VECTOR VALUES HEAD=$1H1*$
                  INCR=0
                  TAU=0
                  TAUSP=-10
                  TIME=0.
                  READ AND PRINT DATA
                  DR=1./L
                  DZ=1./N
                  MAX=M-1
                  VOL=3.1416*DR*DR*DZ*RR.P.3
                  TIMEZ=RR*RR/DIF
                  DT=PRTIME/TIMEZ/((TAUFIN-TAUBIN)*1.)
                  ALF=DT/2./DR/DR
                  ROZ2=DR*DR/DZ/DZ
                  ALFZ=ALF*ROZ2
                  PRINT RESULTS TIMEZ,DT,ALF,ALFZ
                  IF(0)=0.
                  THROUGH FIX,FOR K=1,1,K.G.M
                  IF(K)=IF(K-1)+1.
                  JF(K)=1.+.5/IF(K)
FIX               KF(K)=1.-.5/IF(K)
                  THROUGH FIX1,FOR J=0,1,J.G.80
FIX1              X(J)=(L+1)*J
                 INITIALIZING COEFFICIENTS
                  SPRAY.(BOT,T(0)...T(891),TSTAR(0)...TSTAR(891))
                  ZERO.(P(0)...P(L))
                  SPRAY.(1.,FR(0)...FR(M),FZ(0)...FZ(L))
                  SPRAY.(L,S(0)...S(M))
                  ZERO.(AR(0)...AR(M),BR(0)...BR(M),CR(0)...CR(M),AC(0)...AC(M)
                 1 ,BC(0)...BC(M),CC(0)...CC(M),DDR(0)...DDR(M),DDC(0)...DDC(M))
                  ZERO.(FLUX(0)...FLUX(1000))
                  SUM=0
                  SUML=0
                  RADIUS.(DR,DZ)
                  PRINT RESULTS P(0)...P(L),FZ(0)...FZ(L),S(0)...S(M),FR(0)...FR(M)
                  SPRAY.(TOP,T(0)...T(L),TSTAR(0)...TSTAR(L))
                  THROUGH FIVE,FOR J=0,1,J.G.M
                  THROUGH FIVE,FOR I=S(J)+1,1,I.G.L
                  T(X(J)+I)=TOP
FIVE              TSTAR(X(J)+I)=TOP
                  THROUGH SET,FOR J=1,1,J.E.N
                  FRJ=FR(J)
                  K=S(J)
                  IFS=IF(S(J))
                  AFR(J)=ALF*2./(1.+FRJ)*(1.-FRJ/2./IFS)*-1.
                  BFR(J)=+ALF*2./FRJ*JF(K)-ALF/IFS
SET               CFR(J)=ALF*2./FRJ/(1.+FRJ)*JF(K)*-1.
                  THROUGH SET4, FOR J=N,1,J.G.M
                  AFR(J)=ALF*2.*-1.
                  BFR(J)=ALF*2.
SET4              CFR(J)=0.
                  AR=0.
                  BR=+4.*ALF
```

```
            CR=-4.*ALF
            THROUGH SET 2, FOR I=0,1,I.G.L
            FZI=FZ(I)
            CFZ(I)=ALFZ*2./(1.+FZI)*-1.
            BFZ(I)=ALFZ*2./FZI
SET2        AFZ(I)=ALFZ*2./FZI/(1.+FZI)*-1.
            THROUGH SET3,FOR I=1,1,I.G.L
            CR(I)=JF(I)*ALF*-1.
            BR(I)=2.*ALF
SET3        AR(I)=KF(I)*ALF*-1.
            CC=ALFZ*-1.
            BC=+2.*ALFZ
            AC=ALFZ*-1.
            PRINT RESULTS   AFZ(0)...AFZ(M),BFZ(0)...BFZ(M),CFZ(0)...CFZ(M),
           1  AFR(0)...AFR(L),BFR(0)...BFR(L),CFR(0)...CFR(L),
           2  AR(0)...AR(L), BR(0)...BR(L),CR(0)...CR(L),AC,BC,CC
 CYCLE      TIME=TIME+DT*TIMEZ
            TAU=TAU+1
            INCR=INCR+1
            WHENEVER TAU.E.TAUSP
            READ AND PRINT DATA
            OTHERWISE
            CONTINUE
            END OF CONDITIONAL
            THROUGH ONE,FOR J=1,1,J.E.M
            SJ=S(J)
            AR(SJ)=AFR(J)
            BR(SJ)=BFR(J)
            CR(SJ)=CFR(J)
            THROUGH TWO, FOR I=0,1,I.G.SJ
            PI=P(I)
            WHENEVER PI.L.J
            DDR(I)=-AC*T(X(J-1)+I)+(1.-BC)*T(X(J)+I)-CC*T(X(J+1)+I)
            OTHERWISE
            DDR(I)=-AFZ(I)*T(X(J-1)+I)+(1.-BFZ(I))*T(X(J)+I)-CFZ(I)*T(X(J
           1 +1)+I)
 TWO        END OF CONDITIONAL
            DDR(SJ)=DDR(SJ)-CR(SJ)*T(X(J)+SJ+1)
            ROWS.(0,SJ,J)
            AR(SJ)=JF(SJ)*ALF*-1.
            BR(SJ)=2.*ALF
ONE         CR(SJ)=KF(SJ)*ALF*-1.
            THROUGH THREE,FOR I=0,1,I.G.L
            PI=P(I)
            AC(1)=AFZ(I)
            BC(1)=BFZ(I)
            CC(1)=CFZ(I)
            THROUGH FOUR,FOR J=PI,1,J.E.MAX+1
            SJ=S(J)
            WHENEVER SJ.G.I
            DDC(J)=-AR(I)*TSTAR(X(J)+I-1)+(1.-BR(I))*TSTAR(X(J)+I)-CR(I)
           1 *TSTAR(X(J)+I+1)
            OTHERWISE
            DDC(J)=-AFR(J)*TSTAR(X(J)+I-1)+(1.-BFR(J))*TSTAR(X(J)+I)-CFR(
           1 J)*TSTAR(X(J)+I+1)
 FOUR       END OF CONDITIONAL
            DDC(PI)=DDC(PI)-AC(1)*TSTAR(X(PI-1)+I)
            DDC(MAX)=DDC(MAX)-CC*TSTAR(X(M)+I)
THREE       COLS.(PI,MAX,I)
            SAM=0
            THROUGH BETA,FOR I=0,1,I.G.L
            WHENEVER I.G.0
            WHENEVER I.L.L
            VOLUME=2.*IF(I)*VOL
            OTHERWISE
            VOLUME=(IF(L)-.25)*VOL
            END OF CONDITIONAL
            OTHERWISE
            VOLUME =VOL/4.
            END OF CONDITIONAL
            THROUGH GAMMA,FORJ=P(I)+1,1,J.G.M
  GAMMA     SAM=SAM+T(X(J)+I)*VOLUME
```

```
          VOLUMT=VOLUME*FZ(I)
BETA      SAM=SAM+T(X(P(I))+I)*VOLUMT
          SUM(TAU)=SAM
          FLUX(TAU)=(SUM(TAU)-SUM(TAU-1))/DT/TIMEZ
          WHENEVER INCR.GE.INCRMX
          PRINT FORMAT HEADG,TIME
          THROUGH PRT, FOR J=0,1,J.G.M
          PRINT FORMAT INGPNT,J,S(J),FR(J)
 PRT      PRINT FORMAT TPRT,T(X(J))...T(X(J+1)-1)
          INCR=0
          OTHERWISE
          CONTINUE
          END OF CONDITIONAL
          WHENEVER TAU.L.TAUFIN
          TRANSFER TO CYCLE
          OTHERWISE
          TRANSFER TO FIN
          END OF CONDITIONAL
FIN       CONTINUE
          PRINT FORMAT HEAD
          PRINT COMMENT $ VALUES OF FLUX AT EACH TIME STEP $
          PRINT FORMAT FPRT, FLUX(1)...FLUX(TAUFIN)
          PRINT FORMAT HEAD
          PRINT COMMENT $ TOTAL DIFFUSATE AT EACH TIME STEP $
          PRINT FORMAT FPRT, SUM(1)...SUM(TAUFIN)
          END OF PROGRAM

                              TRIDAGG1
          EXTERNAL FUNCTION (FF,EE,H)
          PROGRAM COMMON AR,BR,CR,DDR,T,TSTAR,AC,BC,CC,DDC,P,FZ,S,FR,X
         1 ,IF,N,M,L
          DIMENSION AR(80),BR(80),CR(80),DDR(80),T(891),TSTAR(891),AC(8
         1 0),BC(80),CC(80),DDC(80),P(80),FZ(80),S(80),FR(80),X(80)
         2 ,IF(80)
          INTEGER N,M,L,P,S,X
          DIMENSION A(80),B(80),C(80),D(80),U(80),DELT(80),BTA(80)
          INTEGER K,F,FF,E,EE,H
          BOOLEAN DEC
          ENTRY TO ROWS.
          DEC=1B
          F=FF
          E=EE
          THROUGH ONET,FOR K=F,1,K.G.E
          A(K)=AR(K)
          B(K)=BR(K)+1.
          C(K)=CR(K)
ONET      D(K)=DDR(K)
          TRANSFER TO START
          ENTRY TO COLS.
          DEC=0B
          F=FF
          E=EE
          THROUGH ONEF,FOR K=F+1,1,K.G.E
          A(K)=AC
          B(K)=BC+1.
          C(K)=CC
ONEF      D(K)=DDC(K)
          A(F)=AC(1)
          B(F)=BC(1)+1.
          D(F)=DDC(F)
          C(F)=CC(1)
 START    DELT(F)=D(F)/B(F)
          BTA(F)=B(F)
          THROUGH ONE,FOR K=F+1,1,K.G.E
          BTA(K)=B(K)-C(K-1)/BTA(K-1)*A(K)
 ONE      DELT(K)=(D(K)-DELT(K-1)*A(K))/BTA(K)
          U(E)=DELT(E)
          THROUGH TWO,FOR K=E-1,-1,K.L.F
TWO       U(K)=DELT(K)-U(K+1)*C(K)/BTA(K)
          WHENEVER DEC
          THROUGH TWOT,FOR K=F,1,K.G.E
TWOT      TSTAR(X(H)+K)=U(K)
```

```
            OTHERWISE
            THROUGH TWOF, FOR K=F,1,K.G.E
TWOF        T(X(K)+H)=U(K)
            END OF CONDITIONAL
            FUNCTION RETURN
            END OF FUNCTION

                                BONDY001
            EXTERNAL FUNCTION (DRR,DZZ)
            PROGRAM COMMON AR,BR,CR,DDR,T,TSTAR,AC,BC,CC,DDC,P,FZ,S,FR,X
           1 ,IF,N,M,L
            DIMENSION AR(80),BR(80),CR(80),DDR(80),T(891),TSTAR(891),AC(8
           1 0),BC(80),CC(80),DDC(80),P(80),FZ(80),S(80),FR(80),X(80)
           2 ,IF(80)
            INTEGER N,M,L,P,S,X
            INTEGER I,J,K
            ENTRY TO RADIUS.
            DR=DRR
            DZ=DZZ
            THROUGH ALPHA,FOR I=0,1,I.G.L
            SIDE=SQRT.(1.-(DR*IF(I)).P.2)
BETA        THROUGH BETA,FOR K=0,1,DZ*IF(K).G.SIDE
            P(I)=N-K+1
            FZ(I)=(SIDE-DZ*IF(K-1))/DZ
            WHENEVER (FZ(I)-.05).L.0.
            P(I)=P(I)+1
            FZ(I)=FZ(I)+1.
            OTHERWISE
            CONTINUE
ALPHA       END OF CONDITIONAL
            THROUGH GAMMA, FOR J=1,1,J.G.N
            SIDE=SQRT.(1.-(DZ*IF(N-J)).P.2)
DELTA       THROUGH DELTA,FOR K=0,1,DR*IF(K).G.SIDE
            S(J)=K-1
            FR(J)=(SIDE-DR*IF(K-1))/DR
            WHENEVER (FR(J)-.05).L.0
            S(J)=K-2
            FR(J)=FR(J)+1.
            OTHERWISE
            CONTINUE
 GAMMA      END OF CONDITIONAL
            FUNCTION RETURN
            END OF FUNCTION
```

AT TIME= 1.000000+SEC THE POTENTIAL FLOW FIELD IS

0 10 1.00000000
.1000E 01 .1000E 01 .1000E 01 .1000E 01 .1000E 01 .1000E 01 .1000E 01 .1000E 01 .1000E 01 .1000E 01 .1000E 01

1 4 .35889920
.2974E 00 .3194E 00 .3999E 00 .5858E 00 .8902E 00 .1000E 01 .1000E 01 .1000E 01 .1000E 01 .1000E 01 .1000E 01

2 5 1.00000015
.5321E-01 .5810E-01 .7749E-01 .1312E 00 .2527E 00 .5466E 00 .1000E 01 .1000E 01 .1000E 01 .1000E 01 .1000E 01

3 7 .14142856
.6717E-02 .7428E-02 .1044E-01 .2001E-01 .4734E-01 .1417E 00 .4175E 00 .9276E 00 .1000E 01 .1000E 01 .1000E 01

4 7 1.00000000
.6549E-03 .7322E-03 .1081E-02 .2347E-02 .6876E-02 .2883E-01 .1268E 00 .4164E 00 .1000E 01 .1000E 01 .1000E 01

5 8 .66025406
.5225E-04 .5907E-04 .9200E-04 .2306E-03 .8654E-03 .5104E-02 .3139E-01 .1414E 00 .5462E 00 .1000E 01 .1000E 01

6 9 .16515143
.3553E-05 .4068E-05 .6800E-05 .2084E-04 .1075E-03 .9074E-03 .7639E-02 .4639E-01 .2505E 00 .8898E 00 .1000E 01

7 9 .53939208
.2124E-06 .2485E-06 .4754E-06 .2086E-05 .1650E-04 .1990E-03 .2206E-02 .1720E-01 .1209E 00 .5843E 00 .1000E 01

8 9 .79795904
.1158E-07 .1475E-07 .4468E-07 .3868E-06 .4695E-05 .7270E-04 .9575E-03 .8653E-02 .7035E-01 .3987E 00 .1000E 01

9 9 .94987445
.6844E-09 .1448E-08 .1214E-07 .1681E-06 .2381E-05 .3987E-04 .5567E-03 .5322E-02 .4620E-01 .2880E 00 .1000E 01

10 9 1.00000007
.6018E-10 .2417E-09 .2944E-08 .4321E-07 .6146E-06 .1018E-04 .1386E-03 .1261E-02 .9834E-02 .4566E-01 .1000E 01

11 10 1.00000000
.9337E-11 .5208E-10 .7129E-09 .1096E-07 .1635E-06 .2886E-05 .4302E-04 .4500E-03 .4475E-02 .3484E-01 .2104E 00

12 10 1.00000000
.1604E-11 .9770E-11 .1384E-09 .2177E-08 .3327E-07 .6030E-06 .9239E-05 .9899E-04 .9900E-03 .7263E-02 .3223E-01

13 10 1.00000000
.2216E-12 .1379E-11 .1972E-10 .3121E-09 .4799E-08 .8733E-07 .1339E-05 .1424E-04 .1392E-03 .9652E-03 .3743E-02

```
        14        10       1.00000000
 .2383E-13 .1490E-12 .2135E-11 .3382E-10 .5195E-09 .9427E-08 .1436E-06 .1510E-05 .1444E-04 .9618E-04 .3468E-03

        15        10       1.00000000
 .2067E-14 .1293E-13 .1852E-12 .2927E-11 .4484E-10 .8101E-09 .1225E-07 .1274E-06 .1197E-05 .7752E-05 .2673E-04

        16        10       1.00000000
 .1502E-15 .9390E-15 .1343E-13 .2118E-12 .3234E-11 .5815E-10 .8738E-09 .8997E-08 .8337E-07 .5292E-06 .1772E-05

        17        10       1.00000000
 .9443E-17 .5898E-16 .8417E-15 .1325E-13 .2017E-12 .3611E-11 .5396E-10 .5513E-09 .5053E-08 .3159E-07 .1036E-06

        18        10       1.00000000
 .5268E-18 .3286E-17 .4682E-16 .7353E-15 .1116E-13 .1992E-12 .2962E-11 .3007E-10 .2733E-09 .1689E-08 .5454E-08

        19        10       1.00000000

 .2654E-19 .1654E-18 .2353E-17 .3688E-16 .5584E-15 .9933E-14 .1471E-12 .1486E-11 .1341E-10 .8212E-10 .2622E-09

        20        10       1.00000000
 .0000E 00 .0000E 00 .0000E 00 .0000E 00 .0000E 00 .0000E 00 .0000E 00 .0000E 00 .0000E 00 .0000E 00 .0000E 00

AT TIME=   9.999996+SEC THE POTENTIAL FLOW FIELD IS

         0        10       1.00000000
 .1000E 01 .1000E 01 .1000E 01 .1000E 01 .1000E 01 .1000E 01 .1000E 01 .1000E 01 .1000E 01 .1000E 01 .1000E 01

         1         4        .35889920
 .7984E 00 .8095E 00 .8421E 00 .8952E 00 .9681E 00 .1000E 01 .1000E 01 .1000E 01 .1000E 01 .1000E 01 .1000E 01

         2         5       1.00000015
 .5875E 00 .5984E 00 .6307E 00 .6828E 00 .7516E 00 .8708E 00 .1000E 01 .1000E 01 .1000E 01 .1000E 01 .1000E 01

         3         7        .14142856
 .3975E 00 .4072E 00 .4361E 00 .4834E 00 .5471E 00 .6628E 00 .8237E 00 .9787E 00 .1000E 01 .1000E 01 .1000E 01

         4         7       1.00000000
 .2476E 00 .2556E 00 .2795E 00 .3198E 00 .3765E 00 .4860E 00 .6531E 00 .8227E 00 .1000E 01 .1000E 01 .1000E 01

         5         8        .66025406
 .1429E 00 .1489E 00 .1674E 00 .1996E 00 .2473E 00 .3441E 00 .4993E 00 .6597E 00 .8652E 00 .1000E 01 .1000E 01
```

```
       6         9        .16515143
.7701E-01 .8133E-01 .9482E-01 .1193E 00 .1573E 00 .2384E 00 .3745E 00 .5226E 00 .7246E 00 .9633E 00 .1000E 01

       7         9        .53939208
.3933E-01 .4228E-01 .5170E-01 .6947E-01 .9860E-01 .1637E 00 .2787E 00 .4122E 00 .6090E 00 .8663E 00 .1000E 01

       8         9        .79795904
.1939E-01 .2134E-01 .2770E-01 .4018E-01 .6169E-01 .1120E 00 .2052E 00 .3203E 00 .5032E 00 .7681E 00 .1000E 01

       9         9        .94987445
.9432E-02 .1068E-01 .1484E-01 .2331E-01 .3851E-01 .7535E-01 .1460E 00 .2368E 00 .3880E 00 .6312E 00 .1000E 01

      10         9       1.00000007
.4608E-02 .5385E-02 .8009E-02 .1351E-01 .2367E-01 .4879E-01 .9744E-01 .1585E 00 .2491E 00 .3369E 00 .1000E 01

      11        10       1.00000000
.2277E-02 .2741E-02 .4327E-02 .7720E-02 .1412E-01 .3021E-01 .6176E-01 .1021E 00 .1657E 00 .2564E 00 .4210E 00

      12        10       1.00000000
.1131E-02 .1395E-02 .2306E-02 .4285E-02 .8077E-02 .1771E-01 .3677E-01 .6127E-01 .9962E-01 .1494E 00 .1968E 00

      13        10       1.00000000
.5557E-03 .6977E-03 .1191E-02 .2274E-02 .4370E-02 .9727E-02 .2034E-01 .3386E-01 .5430E-01 .7807E-01 .9383E-01

      14        10       1.00000000
.2649E-03 .3366E-03 .5869E-03 .1140E-02 .2216E-02 .4972E-02 .1041E-01 .1722E-01 .2714E-01 .3777E-01 .4355E-01

      15        10       1.00000000
.1206E-03 .1545E-03 .2729E-03 .5355E-03 .1047E-02 .2356E-02 .4920E-02 .8076E-02 .1253E-01 .1704E-01 .1924E-01

      16        10       1.00000000
.5185E-04 .6674E-04 .1188E-03 .2345E-03 .4599E-03 .1034E-02 .2150E-02 .3501E-02 .5358E-02 .7170E-02 .8007E-02

      17        10       1.00000000
.2091E-04 .2699E-04 .4826E-04 .9549E-04 .1873E-03 .4203E-03 .8697E-03 .1406E-02 .2128E-02 .2815E-02 .3122E-02

      18        10       1.00000000
.7824E-05 .1011E-04 .1812E-04 .3589E-04 .7033E-04 .1573E-03 .3240E-03 .5204E-03 .7809E-03 .1024E-02 .1131E-02

      19        10       1.00000000
.2507E-05 .3242E-05 .5815E-05 .1151E-04 .2253E-04 .5027E-04 .1031E-03 .1648E-03 .2458E-03 .3205E-03 .3530E-03

      20        10       1.00000000
.0000E 00 .0000E 00 .0000E 00 .0000E 00 .0000E 00 .0000E 00 .0000E 00 .0000E 00 .0000E 00 .0000E 00 .0000E 00
```

AT TIME= 99.999946+SEC THE POTENTIAL FLOW FIELD IS

0 10 1.00000000
.1000E 01 .1000E 01 .1000E 01 .1000E 01 .1000E 01 .1000E 01 .1000E 01 .1000E 01 .1000E 01 .1000E 01 .1000E 01

1 4 .35889920
.9691E 00 .9707E 00 .9753E 00 .9832E 00 .9947E 00 .1000E 01 .1000E 01 .1000E 01 .1000E 01 .1000E 01 .1000E 01

2 5 1.00000015
.9327E 00 .9343E 00 .9351E 00 .9470E 00 .9577E 00 .9772E 00 .1000E 01 .1000E 01 .1000E 01 .1000E 01 .1000E 01

3 7 .14142856
.8912E 00 .8929E 00 .8978E 00 .9058E 00 .9167E 00 .9369E 00 .9659E 00 .9957E 00 .1000E 01 .1000E 01 .1000E 01

4 7 1.00000000
.8453E 00 .8470E 00 .8521E 00 .8604E 00 .8719E 00 .8937E 00 .9270E 00 .9615E 00 .1000E 01 .1000E 01 .1000E 01

5 8 .66025406
.7956E 00 .7973E 00 .8025E 00 .8112E 00 .8233E 00 .8465E 00 .8824E 00 .9188E 00 .9667E 00 .1000E 01 .1000E 01

6 8 .16515143
.7425E 00 .7443E 00 .7496E 00 .7585E 00 .7710E 00 .7953E 00 .8332E 00 .8722E 00 .9247E 00 .9895E 00 .1000E 01

7 9 .53939208
.6869E 00 .6887E 00 .6940E 00 .7029E 00 .7155E 00 .7402E 00 .7793E 00 .8206E 00 .8790E 00 .9571E 00 .1000E 01

8 9 .79795904
.6294E 00 .6311E 00 .6363E 00 .6449E 00 .6572E 00 .6814E 00 .7200E 00 .7618E 00 .8238E 00 .9149E 00 .1000E 01

9 9 .94987445
.5708E 00 .5724E 00 .5773E 00 .5854E 00 .5968E 00 .6193E 00 .6550E 00 .6936E 00 .7517E 00 .8455E 00 .1000E 01

10 9 1.00000007
.5122E 00 .5137E 00 .5180E 00 .5252E 00 .5354E 00 .5552E 00 .5858E 00 .6169E 00 .6567E 00 .6929E 00 .1000E 01

11 10 1.00000000
.4545E 00 .4558E 00 .4596E 00 .4658E 00 .4745E 00 .4911E 00 .5164E 00 .5415E 00 .5743E 00 .6167E 00 .6925E 00

12 10 1.00000000
.3988E 00 .3999E 00 .4030E 00 .4082E 00 .4153E 00 .4288E 00 .4489E 00 .4681E 00 .4918E 00 .5180E 00 .5407E 00

13 10 1.00000000
.3459E 00 .3468E 00 .3494E 00 .3535E 00 .3592E 00 .3698E 00 .3851E 00 .3992E 00 .4153E 00 .4305E 00 .4392E 00

14 10 1.00000000
.2967E 00 .2973E 00 .2994E 00 .3027E 00 .3071E 00 .3151E 00 .3266E 00 .3366E 00 .3473E 00 .3565E 00 .3607E 00

```
        15        10       1.00000000
 .2515E 00 .2521E 00 .2536E 00 .2562E 00 .2595E 00 .2655E 00 .2739E 00 .2810E 00 .2882E 00 .2939E 00 .2963E 00

        16        10       1.00000000
 .2109E 00 .2113E 00 .2125E 00 .2144E 00 .2169E 00 .2213E 00 .2274E 00 .2324E 00 .2373E 00 .2410E 00 .2425E 00

        17        10       1.00000000
 .1749E 00 .1752E 00 .1761E 00 .1775E 00 .1793E 00 .1825E 00 .1869E 00 .1904E 00 .1938E 00 .1963E 00 .1973E 00

        18        10       1.00000000
 .1434E 00 .1437E 00 .1443E 00 .1454E 00 .1467E 00 .1490E 00 .1522E 00 .1547E 00 .1570E 00 .1587E 00 .1594E 00

        19        10       1.00000000
 .1164E 00 .1166E 00 .1171E 00 .1178E 00 .1188E 00 .1205E 00 .1227E 00 .1245E 00 .1261E 00 .1273E 00 .1277E 00

        20        10       1.00000000
 .9347E-01 .9359E-01 .9394E-01 .9448E-01 .9518E-01 .9638E-01 .9797E-01 .9922E-01 .1004E 00 .1012E 00 .1015E 00

        21        10       1.00000000
 .7427E-01 .7435E-01 .7460E-01 .7500E-01 .7550E-01 .7635E-01 .7748E-01 .7837E-01 .7918E-01 .7976E-01 .7997E-01

        22        10       1.00000000
 .5840E-01 .5846E-01 .5864E-01 .5892E-01 .5928E-01 .5989E-01 .6069E-01 .6132E-01 .6189E-01 .6229E-01 .6245E-01

        23        10       1.00000000
 .4545E-01 .4549E-01 .4562E-01 .4582E-01 .4607E-01 .4651E-01 .4708E-01 .4752E-01 .4792E-01 .4821E-01 .4831E-01

        24        10       1.00000000
 .3501E-01 .3504E-01 .3513E-01 .3527E-01 .3545E-01 .3576E-01 .3616E-01 .3647E-01 .3676E-01 .3696E-01 .3703E-01

        25        10       1.00000000
 .2669E-01 .2671E-01 .2678E-01 .2688E-01 .2700E-01 .2722E-01 .2750E-01 .2772E-01 .2792E-01 .2806E-01 .2812E-01

        26        10       1.00000000
 .2014E-01 .2016E-01 .2020E-01 .2027E-01 .2036E-01 .2052E-01 .2072E-01 .2087E-01 .2101E-01 .2111E-01 .2115E-01

        27        10       1.00000000
 .1505E-01 .1506E-01 .1509E-01 .1514E-01 .1520E-01 .1531E-01 .1545E-01 .1556E-01 .1565E-01 .1572E-01 .1575E-01

        28        10       1.00000000
 .1113E-01 .1113E-01 .1116E-01 .1119E-01 .1124E-01 .1131E-01 .1141E-01 .1148E-01 .1155E-01 .1160E-01 .1162E-01

        29        10       1.00000000
 .8145E-02 .8150E-02 .8166E-02 .8190E-02 .8220E-02 .8271E-02 .8339E-02 .8391E-02 .8438E-02 .8472E-02 .8484E-02
```

```
        30        10       1.00000000
 .5901E-02 .5905E-02 .5916E-02 .5932E-02 .5953E-02 .5989E-02 .6035E-02 .6072E-02 .6104E-02 .6127E-02 .6136E-02

        31        10       1.00000000
 .4232E-02 .4235E-02 .4242E-02 .4253E-02 .4268E-02 .4292E-02 .4324E-02 .4349E-02 .4371E-02 .4387E-02 .4393E-02

        32        10       1.00000000
 .3003E-02 .3005E-02 .3010E-02 .3018E-02 .3028E-02 .3044E-02 .3066E-02 .3083E-02 .3098E-02 .3109E-02 .3113E-02

        33        10       1.00000000
 .2108E-02 .2109E-02 .2113E-02 .2118E-02 .2125E-02 .2136E-02 .2151E-02 .2162E-02 .2173E-02 .2180E-02 .2183E-02

        34        10       1.00000000
 .1462E-02 .1463E-02 .1465E-02 .1469E-02 .1473E-02 .1481E-02 .1491E-02 .1498E-02 .1505E-02 .1510E-02 .1512E-02

        35        10       1.00000000
 .9992E-03 .9997E-03 .1001E-02 .1004E-02 .1007E-02 .1012E-02 .1018E-02 .1023E-02 .1028E-02 .1031E-02 .1032E-02

        36        10       1.00000000
 .6685E-03 .6688E-03 .6698E-03 .6714E-03 .6733E-03 .6766E-03 .6809E-03 .6842E-03 .6872E-03 .6893E-03 .6901E-03

        37        10       1.00000000
 .4308E-03 .4310E-03 .4316E-03 .4326E-03 .4338E-03 .4359E-03 .4386E-03 .4407E-03 .4426E-03 .4439E-03 .4444E-03

        38        10       1.00000000
 .2555E-03 .2557E-03 .2560E-03 .2566E-03 .2573E-03 .2585E-03 .2601E-03 .2613E-03 .2624E-03 .2632E-03 .2635E-03

        39        10       1.00000000
 .1187E-03 .1187E-03 .1189E-03 .1192E-03 .1195E-03 .1200E-03 .1208E-03 .1213E-03 .1218E-03 .1222E-03 .1223E-03

        40        10       1.00000000
 .0000E 00 .0000E 00 .0000E 00 .0000E 00 .0000E 00 .0000E 00 .0000E 00 .0000E 00 .0000E 00 .0000E 00 .0000E 00
```

AT TIME= 399.999783+SEC THE POTENTIAL FLOW FIELD IS

```
         0        10       1.00000000
 .1000E 01 .1000E 01 .1000E 01 .1000E 01 .1000E 01 .1000E 01 .1000E 01 .1000E 01 .1000E 01 .1000E 01 .1000E 01

         1         4        .35889920
 .9877E 00 .9883E 00 .9901E 00 .9932E 00 .9979E 00 .1000E 01 .1000E 01 .1000E 01 .1000E 01 .1000E 01 .1000E 01

         2         5       1.00000015
 .9730E 00 .9736E 00 .9755E 00 .9786E 00 .9829E 00 .9907E 00 .1000E 01 .1000E 01 .1000E 01 .1000E 01 .1000E 01
```

```
        3         7        .14142856
 .9560E 00 .9566E 00 .9585E 00 .9617E 00 .9660E 00 .9741E 00 .9859E 00 .9982E 00 .1000E 01 .1000E 01 .1000E 01

        4         7       1.00000000
 .9365E 00 .9371E 00 .9391E 00 .9424E 00 .9470E 00 .9557E 00 .9693E 00 .9837E 00 .1000E 01 .1000E 01 .1000E 01

        5         8        .66025406
 .9146E 00 .9153E 00 .9173E 00 .9208E 00 .9256E 00 .9350E 00 .9497E 00 .9650E 00 .9855E 00 .1000E 01 .1000E 01

        6         9        .16515143
 .8903E 00 .8910E 00 .8931E 00 .8966E 00 .9017E 00 .9116E 00 .9273E 00 .9438E 00 .9666E 00 .9953E 00 .1000E 01

        7         9        .53939208
 .8635E 00 .8642E 00 .8664E 00 .8699E 00 .8751E 00 .8853E 00 .9017E 00 .9194E 00 .9451E 00 .9804E 00 .1000E 01

        8         9        .79795904
 .8344E 00 .8351E 00 .8372E 00 .8407E 00 .8457E 00 .8558E 00 .8721E 00 .8903E 00 .9181E 00 .9600E 00 .1000E 01

        9         9        .94987445
 .8032E 00 .8038E 00 .8058E 00 .8090E 00 .8137E 00 .8231E 00 .8384E 00 .8553E 00 .8816E 00 .9256E 00 .1000E 01

       10         9       1.00000007
 .7700E 00 .7706E 00 .7723E 00 .7753E 00 .7794E 00 .7877E 00 .8008E 00 .8144E 00 .8323E 00 .8491E 00 .1000E 01

       11        10       1.00000000
 .7352E 00 .7357E 00 .7373E 00 .7398E 00 .7433E 00 .7503E 00 .7610E 00 .7720E 00 .7868E 00 .8067E 00 .8436E 00

       12        10       1.00000000
 .6993E 00 .6997E 00 .7010E 00 .7031E 00 .7060E 00 .7116E 00 .7201E 00 .7284E 00 .7389E 00 .7510E 00 .7619E 00

       13        10       1.00000000
 .6627E 00 .6630E 00 .6640E 00 .6657E 00 .6680E 00 .6723E 00 .6788E 00 .6848E 00 .6918E 00 .6986E 00 .7027E 00

       14        10       1.00000000
 .6257E 00 .6259E 00 .6267E 00 .6281E 00 .6298E 00 .6331E 00 .6378E 00 .6420E 00 .6466E 00 .6506E 00 .6525E 00

       15        10       1.00000000
 .5888E 00 .5890E 00 .5896E 00 .5906E 00 .5919E 00 .5943E 00 .5977E 00 .6006E 00 .6036E 00 .6060E 00 .6071E 00

       16        10       1.00000000
 .5522E 00 .5524E 00 .5528E 00 .5536E 00 .5545E 00 .5563E 00 .5587E 00 .5607E 00 .5627E 00 .5642E 00 .5648E 00

       17        10       1.00000000
 .5164E 00 .5165E 00 .5168E 00 .5174E 00 .5181E 00 .5193E 00 .5210E 00 .5224E 00 .5237E 00 .5247E 00 .5251E 00

       18        10       1.00000000
 .4814E 00 .4815E 00 .4818E 00 .4822E 00 .4827E 00 .4835E 00 .4847E 00 .4857E 00 .4866E 00 .4872E 00 .4875E 00
```

19 10 1.00000000
.4476E 00 .4476E 00 .4478E 00 .4481E 00 .4485E 00 .4491E 00 .4499E 00 .4506E 00 .4512E 00 .4516E 00 .4518E 00

20 10 1.00000000
.4150E 00 .4150E 00 .4151E 00 .4153E 00 .4156E 00 .4160E 00 .4166E 00 .4170E 00 .4175E 00 .4178E 00 .4179E 00

21 10 1.00000000
.3837E 00 .3837E 00 .3838E 00 .3839E 00 .3841E 00 .3844E 00 .3848E 00 .3851E 00 .3854E 00 .3856E 00 .3857E 00

22 10 1.00000000
.3538E 00 .3538E 00 .3539E 00 .3540E 00 .3541E 00 .3543E 00 .3546E 00 .3548E 00 .3550E 00 .3552E 00 .3552E 00

23 10 1.00000000
.3254E 00 .3254E 00 .3254E 00 .3255E 00 .3256E 00 .3258E 00 .3259E 00 .3261E 00 .3262E 00 .3263E 00 .3264E 00

24 10 1.00000000
.2985E 00 .2985E 00 .2985E 00 .2986E 00 .2986E 00 .2987E 00 .2989E 00 .2990E 00 .2991E 00 .2991E 00 .2992E 00

25 10 1.00000000
.2731E 00 .2731E 00 .2731E 00 .2731E 00 .2732E 00 .2733E 00 .2733E 00 .2734E 00 .2735E 00 .2735E 00 .2736E 00

26 10 1.00000000
.2492E 00 .2492E 00 .2492E 00 .2492E 00 .2493E 00 .2493E 00 .2494E 00 .2494E 00 .2495E 00 .2495E 00 .2495E 00

27 10 1.00000000
.2268E 00 .2268E 00 .2268E 00 .2268E 00 .2268E 00 .2269E 00 .2269E 00 .2270E 00 .2270E 00 .2270E 00 .2270E 00

28 10 1.00000000
.2059E 00 .2059E 00 .2059E 00 .2059E 00 .2059E 00 .2059E 00 .2060E 00 .2060E 00 .2060E 00 .2060E 00 .2060E 00

29 10 1.00000000
.1864E 00 .1864E 00 .1864E 00 .1864E 00 .1864E 00 .1864E 00 .1865E 00 .1865E 00 .1865E 00 .1865E 00 .1865E 00

30 10 1.00000000
.1683E 00 .1683E 00 .1683E 00 .1683E 00 .1683E 00 .1683E 00 .1683E 00 .1684E 00 .1684E 00 .1684E 00 .1684E 00

31 10 1.00000000
.1516E 00 .1516E 00 .1516E 00 .1516E 00 .1516E 00 .1516E 00 .1516E 00 .1516E 00 .1516E 00 .1516E 00 .1516E 00

32 10 1.00000000
.1361E 00 .1361E 00 .1362E 00 .1362E 00 .1362E 00 .1362E 00 .1362E 00 .1362E 00 .1362E 00 .1362E 00 .1362E 00

33 10 1.00000000
.1220E 00 .1220E 00 .1220E 00 .1220E 00 .1220E 00 .1220E 00 .1220E 00 .1220E 00 .1220E 00 .1220E 00 .1220E 00

34 10 1.00000000
.1090E 00 .1090E 00 .1090E 00 .1090E 00 .1090E 00 .1090E 00 .1090E 00 .1090E 00 .1090E 00 .1090E 00 .1090E 00

35 10 1.00000000
.9710E-01 .9710E-01 .9710E-01 .9710E-01 .9710E-01 .9710E-01 .9711E-01 .9711E-01 .9711E-01 .9711E-01 .9711E-01

36 10 1.00000000
.8629E-01 .8629E-01 .8629E-01 .8629E-01 .8629E-01 .8629E-01 .8629E-01 .8629E-01 .8630E-01 .8630E-01 .8630E-01

37 10 1.00000000
.7647E-01 .7647E-01 .7647E-01 .7648E-01 .7648E-01 .7648E-01 .7648E-01 .7648E-01 .7648E-01 .7648E-01 .7648E-01

38 10 1.00000000
.6759E-01 .6759E-01 .6759E-01 .6759E-01 .6759E-01 .6760E-01 .6760E-01 .6760E-01 .6760E-01 .6760E-01 .6760E-01

39 10 1.00000000
.5958E-01 .5958E-01 .5958E-01 .5958E-01 .5958E-01 .5958E-01 .5958E-01 .5958E-01 .5959E-01 .5959E-01 .5959E-01

40 10 1.00000000
.5238E-01 .5238E-01 .5238E-01 .5238E-01 .5238E-01 .5238E-01 .5238E-01 .5238E-01 .5238E-01 .5238E-01 .5238E-01

41 10 1.00000000
.4592E-01 .4592E-01 .4592E-01 .4592E-01 .4592E-01 .4592E-01 .4592E-01 .4592E-01 .4592E-01 .4592E-01 .4592E-01

42 10 1.00000000
.4015E-01 .4015E-01 .4015E-01 .4015E-01 .4015E-01 .4015E-01 .4015E-01 .4015E-01 .4015E-01 .4015E-01 .4015E-01

43 10 1.00000000
.3500E-01 .3500E-01 .3500E-01 .3500E-01 .3500E-01 .3500E-01 .3500E-01 .3500E-01 .3500E-01 .3500E-01 .3500E-01

44 10 1.00000000
.3043E-01 .3043E-01 .3043E-01 .3043E-01 .3043E-01 .3044E-01 .3044E-01 .3044E-01 .3044E-01 .3044E-01 .3044E-01

45 10 1.00000000
.2639E-01 .2639E-01 .2639E-01 .2639E-01 .2639E-01 .2639E-01 .2639E-01 .2639E-01 .2639E-01 .2639E-01 .2639E-01

46 10 1.00000000
.2282E-01 .2282E-01 .2282E-01 .2282E-01 .2282E-01 .2282E-01 .2282E-01 .2282E-01 .2282E-01 .2282E-01 .2282E-01

47 10 1.00000000
.1968E-01 .1968E-01 .1968E-01 .1968E-01 .1968E-01 .1968E-01 .1968E-01 .1968E-01 .1968E-01 .1968E-01 .1968E-01

48 10 1.00000000
.1692E-01 .1692E-01 .1692E-01 .1692E-01 .1692E-01 .1692E-01 .1692E-01 .1692E-01 .1692E-01 .1692E-01 .1692E-01

49 10 1.00000000
.1451E-01 .1451E-01 .1451E-01 .1451E-01 .1451E-01 .1451E-01 .1451E-01 .1451E-01 .1451E-01 .1451E-01 .1451E-01

50 10 1.00000000
.1241E-01 .1241E-01 .1241E-01 .1241E-01 .1241E-01 .1241E-01 .1241E-01 .1241E-01 .1241E-01 .1241E-01 .1241E-01

APPENDIX I

CURRENT EFFICIENCY OF A LIQUID METAL CELL

Consider the following concentration cell

anode	electrolyte	cathode
A	A^+	A(B)

The electrolyte is impregnated in a porous matrix and the cathode has capillary dimensions. Upon discharge of sodium at the cathode electrolyte interface, some fraction of the sodium dissolves in the electrolyte while the remainder enters the cathode alloy. Mass transport both in the electrolyte and the cathode is purely diffusive. If equilibrium is assumed with respect to the concentrations of sodium at the anode-electrolyte and cathode-electrolyte interfaces, the concentration profile of sodium at small times will be similar to that shown in Figure I-a . At larger times there will be interference of the concentration profiles advancing toward each other within the fused salt region. This latter case will result in a lowering of the sodium flux into the salt due to the diminished concentration gradient. This is shown in Figure I-b . Only the first case, where there is no interference, will be considered since it represents the extreme conditions which can be expected.

The diffusion can be considered to be one-dimensional and semi-infinite. The origin of the system is taken to be at the cathode-

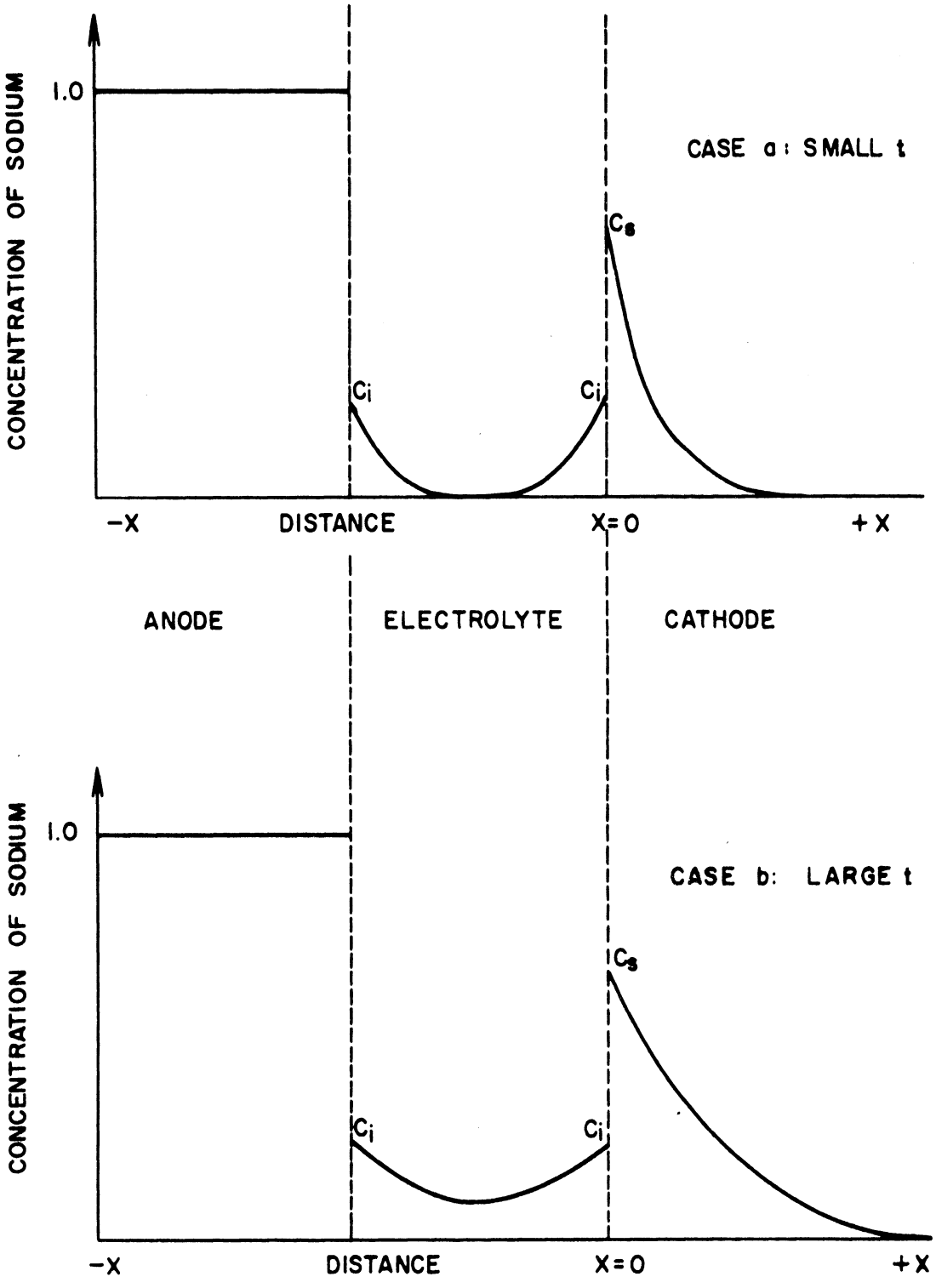

Figure I-1. Concentration Profile for Atomic Sodium in a Liquid Metal Concentration Cell

electrolyte interface. For small times, diffusion of sodium into the salt at the anode-electrolyte interface can be neglected. Diffusion of sodium into the cathode where the initial concentration, $C_o = 0$, and the surface concentration is C_s is described by the following solution to Ficks' laws of diffusion

$$C = C_s \ \text{erfc} \left(\frac{x}{2\sqrt{Dt}} \right) \tag{211}$$

The flux has also been shown to be

$$J_{x=0} = C_s A_s \left(\frac{D}{\pi t} \right)^{1/2} \tag{212}$$

Diffusion of the salt also originates at X=0 but it proceeds in the -X direction. The error function is an even function so the replacement of X in its argument by -X will not change the value of C. The concentration gradient and flux of sodium dissolving in the salt can be expressed by

$$C = C_i \ \text{erfc} \left(\frac{x}{2\sqrt{Dt}} \right) \tag{213}$$

$$J_{x=0} = C_i A_s \left(\frac{D_2}{\pi t} \right)^{1/2} \tag{214}$$

Where J is not taken to be a vector, and C_i is the solubility of sodium in the fused salt.

The fraction of sodium entering the fused salt phase is

$$\frac{C_i A_s \left(\frac{D_1}{\pi t}\right)^{1/2}}{C_i A_s \left(\frac{D_1}{\pi t}\right)^{1/2} + C_s A_s \left(\frac{D_2}{\pi t}\right)^{1/2}} \qquad (215)$$

If (a) the areas for diffusion are taken as equal in the salt and in the cathode, and

(b) the diffusion coefficients for sodium in the salt phase and in the cathode alloy are taken as equal, $D_1 = D_2$

then (215) reduces to

$$\frac{C_i}{C_s + C_i} \qquad (216)$$

Heyman and Weber (72) have investigated the distribution equilibrium for sodium between sodium iodide and molten lead. They report that at 690°C when the concentration of the alloy, C_s, is 40 mole % sodium, the corresponding equilibrium value for sodium in sodium iodide, C_i, is 0.8 mole %. Therefore, the fraction of sodium which will enter the salt phase for the above concentration cell is

$$\frac{0.008}{0.008 + 0.40} = 0.0196 \qquad (217)$$

Or, less than 2% of the sodium atoms discharged at the cathode-electrolyte interface will remain in the salt phase.

APPENDIX J

SAMPLE CALCULATION

The expression for the flux into a semi-infinite one-dimensional plane has been derived in Appendix G.

$$J = A_s(C_s - C_o)\left(\frac{D}{\pi t}\right)^{1/2} \qquad (218)$$

Consider data from experiment DC-55.

Capillary diameter	0.040"
Discharge Potential, φ_d	0.146 volts
Mole Fraction Na in Cathode Alloy	0.3387
Cell Resistance	15
Operating Temperature	550°K
Duration of Experiment	3000 seconds

The current time discharge curve is given in Figure 16, and the raw data tabulated in Appendix B.

I. Calculation of diffusion path area.

Accurate measurements of the capillary diameter are made with a Bausch and Lomb binocular microscope at several points along the diffusion path. The average thermal coefficient of expansion for the fused quartz capillaries is given by the manufacturer (162) and is 0.55×10^{-6} in/in.°C over a range of 20 to 320°C. The diameter can be corrected to allow for thermal expansion as follows

$$d_{277°C} = 0.040\left[1 + 0.55 \times 10^{-6}\,(277-30)\right] \qquad (219)$$
$$= 0.040\left[1 + 0.136 \times 10^{-3}\right]$$

This represents an increase in diameter of only 0.34% which is not significant when compared to the accuracy with which the diameter can be measured.

$$A_s = \frac{\pi d^2}{4} = \frac{\pi(0.040136)^2}{4}\,(2.54)^2\ \text{cm}^2 \qquad (220)$$
$$= 0.00809\ \text{cm}^2$$

II. Calculation of concentration at the cathode-electrolyte interface.

The discharge potential, φ_d is 0.146 volts. The concentration at the interface does not correspond to this potential but to one between this and φ_o.

$$\varphi_o - \varphi_s = \varphi_o - (\varphi_d - iR) \qquad (221)$$
$$= \varphi_o - (0.146 - iR)$$

For large times the iR drop will be small compared to $(\varphi_o - \varphi_s)$ and the average value can be used in the above equation.

$$iR_t = 300 = 0.238 \times 10^{-3} \times 15 = 0.00357 \text{ volts}$$
$$iR_t = 2000 = 0.092 \times 10^{-3} \times 15 \quad 0.00138 \text{ volts}$$
$$iR_{average} = 0.00247 \text{ volts}$$

Therefore,

$$\varphi_o - \varphi_s = 0.205 - 0.14847 = 0.05653$$

$0.05653 \gg 0.00247$ so the use of an average iR drop for $t > 300$ seconds is justified.

The mole fraction of potassium at the interface corresponds to $\varphi_s = 0.14847$ at 500°K.

$$N_s = 0.38$$

The assumption has been made in the above calculations that activation polarization is negligible. From Figure D-3, in Appendix D, the surface concentration is found to be

$$C_s = 0.01762 \ \frac{\text{gram atoms K}}{\text{cm}^3}$$

The initial concentration is determined from the same figure

$$C_o = 0.01633 \ \frac{\text{gram atoms K}}{\text{cm}^3}$$

Therefore,

$$C_s - C_o = 0.01762 - 0.01633$$
$$= 0.00129 \ \frac{\text{gram atoms}}{\text{cm}^3}$$

III. Calculation of the Diffusion Coefficient.

From Figure 16 the smoothed value of the current is 1.30×10^{-4} amps. If equation (218) is solved for D

$$D\left(\frac{cm^2}{sec}\right) = \left[\frac{i \text{ amps}}{A_s cm^2 (C_s - C_o) \frac{\text{gr atoms K}}{cm^3} \; 96{,}500 \frac{\text{amp sec}}{\text{gr atom K}}}\right]^2 \pi \; t \text{ (sec)} \qquad (222)$$

Consistant units are shown. Only a single value of current need be used because the dotted line in Figure 16 is the best straight line that can be put through the data with slope of -1/2. Only values for $t > 300$ are considered when establishing this line.

$$D = \left[\frac{1.30 \times 10^{-4}}{8.09 \times 10^{-3} \times 1.29 \times 10^{-3} \times 9.65 \times 10^{4}}\right]^2 3.1416 \times 10^{3}$$

$$D = 5.32 \times 10^{-5} \quad cm^2/sec$$

Implicit in these calculations is the assumption that current efficiency for discharge of the cell is 100%. This has been shown to be a reasonably good assumption in Appendix I.

IV. Calculation of Concentration Changes at the Bottom of the Capillary

The concentration profile has been shown to be

$$C = C_o + (C_s - C_o) \left[\text{erfc}\left(\frac{x}{2\sqrt{Dt}}\right)\right] \qquad (223)$$

in terms of dimensionless concentration this becomes

$$\frac{C - C_o}{C_s - C_o} = \text{erfc}\left(\frac{x}{2\sqrt{Dt}}\right) \qquad (224)$$

The length of the capillary between the cathode-electrolyte interface and the bend was approximately 2.5 cm.

$$\frac{C - C_o}{C_s - C_o} = \text{erfc}\left[\frac{2.5}{(5.32 \times 10^{-5} \times 3 \times 10^3)^{1/2}\ 2}\right]$$

$$= 0.0000^+$$

This shows there will be no convection at the bottom of the capillary arising from density inversions due to the bend.

V. Calculation of the Total Quantity of Potassium Transferred from the Anode to the Cathode during the Experiment.

The quantity Q, transferred during time t is given by

$$Q = \frac{2}{\sqrt{\pi}} \sqrt{Dt}\ \ A_s(C_s - C_o) \qquad (225)$$

This expression was derived in Appendix G. For an experiment of 3000 seconds duration

$$Q = \frac{2}{\sqrt{\pi}} \sqrt{5.32 \times 10^{-5} \times 3 \times 10^3}\ (8.09 \times 10^{-3})(0.00129)$$

$$= 4.70 \times 10^{-6} \text{ gr atoms K}$$

or,

$$\text{Grams K transferred} = 1.83 \times 10^{-4}$$

This calculation assumes the diffusion process is represented by equation (218) for all time. Figure 16 shows, however, the current is larger than this equation predicts for times less than about 300 seconds. The additional potassium transferred during this time can be obtained by graphical integration of the current time curve. This additional potassium is equal in magnitude to the area between the actual curve obtained experimentally and the dotted straight line with a slope of -1/2 shown in Figure 16. The lower limit for the integration was taken a 1 second. For times shorter than this the cell resistence can safely assumed to be rate limiting. This area is equivalent to 0.068×10^{-4} grams of potassium. Therefore, the total amount of potassium transferred from the anode to the cathode is 3.7% grater than equation (225) predicts.

APPENDIX K

ESTIMATION OF ERRORS

Diffusion coefficients are calculated with the following equation

$$D = \left[\frac{J}{(C_s - C_o) A_s}\right]^2 \pi t \qquad (226)$$

The quantities J, C_s, C_o, A_s and t are all obtained experimentally and subject to errors. The experimental cells used in this investigation take considerable time to prepare. It is not practical to make several runs at each set of experimental conditions from which the error could be determined by statistical analysis. Livingston (85) describes the estimation of probable error for a single measurement. Let ϵ_D be the probable error in D where

$$D = f(V_1, V_2, V_3, \ldots, V_n) \qquad (227)$$

The probable error in D is related to the probable errors ϵ_1, ϵ_2, ϵ_3, ..., ϵ_n of the several independently measured quantities V_1, V_2, V_3, ..., V_n by the following equation

$$\epsilon_D = \sqrt{\sum_j \left(\frac{\partial D}{\partial V_j}\right)^2 \epsilon_j^2} \qquad (228)$$

The partial derivatives of D with respect to J, C_s, C_o, A_s, and t are

$$\frac{\partial D}{\partial J} = \frac{2 J \pi t}{(C_s - C_o)^2 A_s} \tag{229}$$

$$\frac{\partial D}{\partial C_s} = \frac{2 J^2 \pi t}{(C_s - C_o)^3 A_s^2} \tag{230}$$

$$\frac{\partial D}{\partial C_o} = \frac{2 J^2 \pi t}{(C_s - C_o)^3 A_s^2} \tag{231}$$

$$\frac{\partial D}{\partial A_s} = \frac{2 J^2 \pi t}{(C_s - C_o)^2 A_s^3} \tag{232}$$

$$\frac{\partial D}{\partial t} = \frac{J^2 \pi}{(C_s - C_o)^2 A_s^2} \tag{233}$$

If ϵ_J, ϵ_{C_s}, ϵ_{C_o}, ϵ_{A_s} and ϵ_t are the probable errors for each of the independently measured quantities, the probable error in D is

$$\epsilon_D = 2D\left[\frac{\epsilon_{C_s}^2 + \epsilon_{C_o}^2}{(C_s - C_o)^2} + \frac{\epsilon_J^2}{J^2} + \frac{\epsilon_{A_s}^2}{A_s^2} + \frac{\epsilon_t^2}{4t^2}\right]^{1/2} \tag{234}$$

Equation (234) is obtained by substituion of equations (229) through (233) in equation (228), factoring the result and comparing with equation (226).

The error in measurement of time is no more than a second. At t=1000 seconds the value of $\epsilon_t^2/4t^2$ is small, 2.5×10^{-7}. The area A_s

is obtained from measurement of the capillary diameter. Error in this measurement or variations in the diameter are no greater than 0.0005". The value of $\epsilon_{A_s}^2 / A_s^2$ corresponding to this error in the diameter is 1×10^{-4}. The electrical current can be measured to an accuracy of 2%. Then ϵ_J^2/J^2 is 4×10^{-4}. The largest contribution to the error in D is likely to come from the term $(\epsilon_{C_s}^2 + \epsilon_{C_o}^2)/(C_s - C_o)^2$. C_s and C_o are similar in magnitude, for small concentration intervals the denominator will be small. Even small errors in these quantities will give appreciable errors. The error in C_o will be small since the alloys are prepared by accurately weighing the components of the cathode alloy. It is of the order of 1×10^{-5} gr. atoms K/cm^3. C_s is determined not from direct measurement but rather from the cell potential. The cell potential-composition relationship is dependent on the accuracy of the thermodynamic data used in its calculations, also on the accuracy of density data for the alloy.

For the system potassium-mercury, Table C-1 of Appendix C shows an uncertainty of $\pm$ 200 cal/gr atom K. This corresponds to an error of $\pm$ 0.09 v at $N_K = 0.20$. From Figure C-2 of Appendix C an error of 0.09 v means there will be an error in N_K of 0.004. The error in the potassium concentration at C_s will be $\epsilon_{C_s} = 0.00015$ gr atoms K/cm^3 alloy. The probable error may be calculated from equation (234).

$$\epsilon_D = 2D \left[\frac{(1.5 \times 10^{-4})^2 + (10^{-5})^2}{(1.29 \times 10^{-3})^2} + 4 \times 10^{-4} + 1 \times 10^{-4} + 2.5 \times 10^{-7} \right]^{1/2}$$

$$\epsilon_D = 0.2368\ D$$

It is seen from the magnitudes of the various contributions that the uncertainty is largely due to the uncertainty in cell potential.

Therefore, a probable error of approximately 25% exists in the diffusion coefficients based on single measurements. Similar values are obtained for the sodium-lead and the sodium-tin systems. The reproducibility of experimental points where duplicate points were obtained is considerably better than this. For potassium-mercury it was $\pm$ 6%, for sodium-lead $\pm$ 9.5% and for sodium-tin $\pm$ 4.6%.

APPENDIX L

PRELIMINARY DESIGNS OF DIFFUSION CELLS

The design of the diffusion cells used in this investigation and described in the earlier section entitled, "Experimental Equipment" was arrived at after a series of failures with other designs. The 57 diffusion cell runs noted in Appendix A were all made with the refined cell design described earlier. Approximately as many runs were made with the cells described in this appendix before the final design was evolved. Results are not tabulated for these earlier investigations, most of them failed due to problems originating in the cell design.

I. Two Electrode Alumina Cell Body with Interface Probe.

Figure L-1 shows the design of this cell. The body was cast to specification by Coors Porcelain Co. It is fabricated from high density impervious alumina. The tolerance on the diffusion capillary is $\pm$ 0.0002" and its uniformity was checked from an X-ray photograph of the cell. Alumina has high electrical resistance at cell operating temperatures and is a suitable material for construction of the cell body as a single unit. The taper on the upper section of the cell body was provided to allow a matching alumina sleeve to be placed over the upper end of the cell. The offset at the upper face of

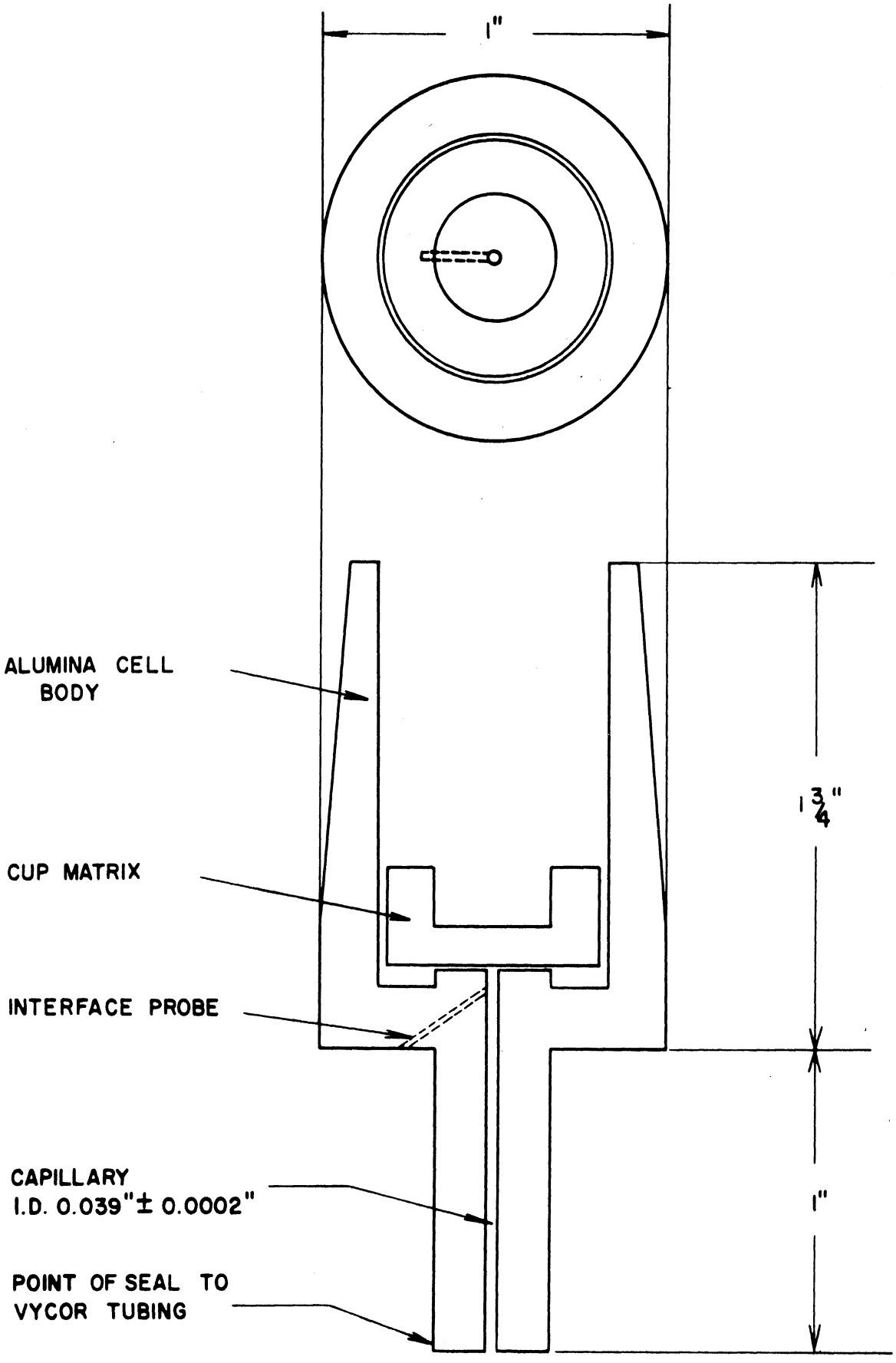

Figure L-1. Two Electrode Cell with Interface Probe

the capillary is provided so that any metal which spills out of the capillary will drop away from the electrolyte. The bottom of the capillary was sealed to Vycor tubing with a graded glass seal. The vycor tubing could be bent to provide a "U" shaped cathode.

The interface probe enters, as shown, just below the cathode-electrolyte interface. Its purpose is to measure the diffusion potential. The diffusion potential is one of the "cross-effects" described by the formalism of the theory of irreversible thermodynamics. The corresponding cross-effect for the diffusion potential is electrodiffusion. Electrodiffusion is the flow of mass caused by a voltage gradient whereas diffusion potential is the generation of an electrical potential by a concentration gradient. Little data is available for diffusion potentials in liquid metals. Angus (3) discusses the interrelation between electrodiffusion and the diffusion potential. The cell shown in Figure L-1, should allow the measurement of diffusion potential since the wall of the capillary which contains the metal is a non-conductor. An electrometer circuit is necessary to measure this potential since a low impedence instrument would disturb the potential.

Attempts to use this cell to measure diffusion potentials and diffusion coefficients for the system potassium-mercury failed. The reasons for these failures include:

(a) The Vycor to alumina graded glass seal proved fragile, in addition the alumina cell cracked in some cases while the seal was being made.

(b) The alumina bodies cost approximately $100.00 each so they must be cleaned for re-use after a diffusion run. It proved difficult to remove the solidified metal from the diffusion path.

(c) The alumina body is not transparent and the formation of bubbles in the diffusion path cannot be detected.

(d) Proper positioning of the tungsten interface probe near the top of the diffusion path is difficult. The probe must neither protrude into the capillary nor be recessed from the capillary wall. If either of these occurs the shape of the diffusion path will be distorted. Sealing of this probe in the capillary proved difficult and the loss of alloy, which may have wet the tungsten better than it wet the alumina, was noticed. The tips of the probes were shaped by the electrolytic method described by Pfann (108).

(e) The cathode metal was pure mercury and wetting problems were encoucntered.

II. Two Electrode Boron Nitride Cell with Interface Probe.

The design of this cell is shown in Figure L-2. The cell bodies were machined from boron nitride stock by Carborundum Co. at a cost of

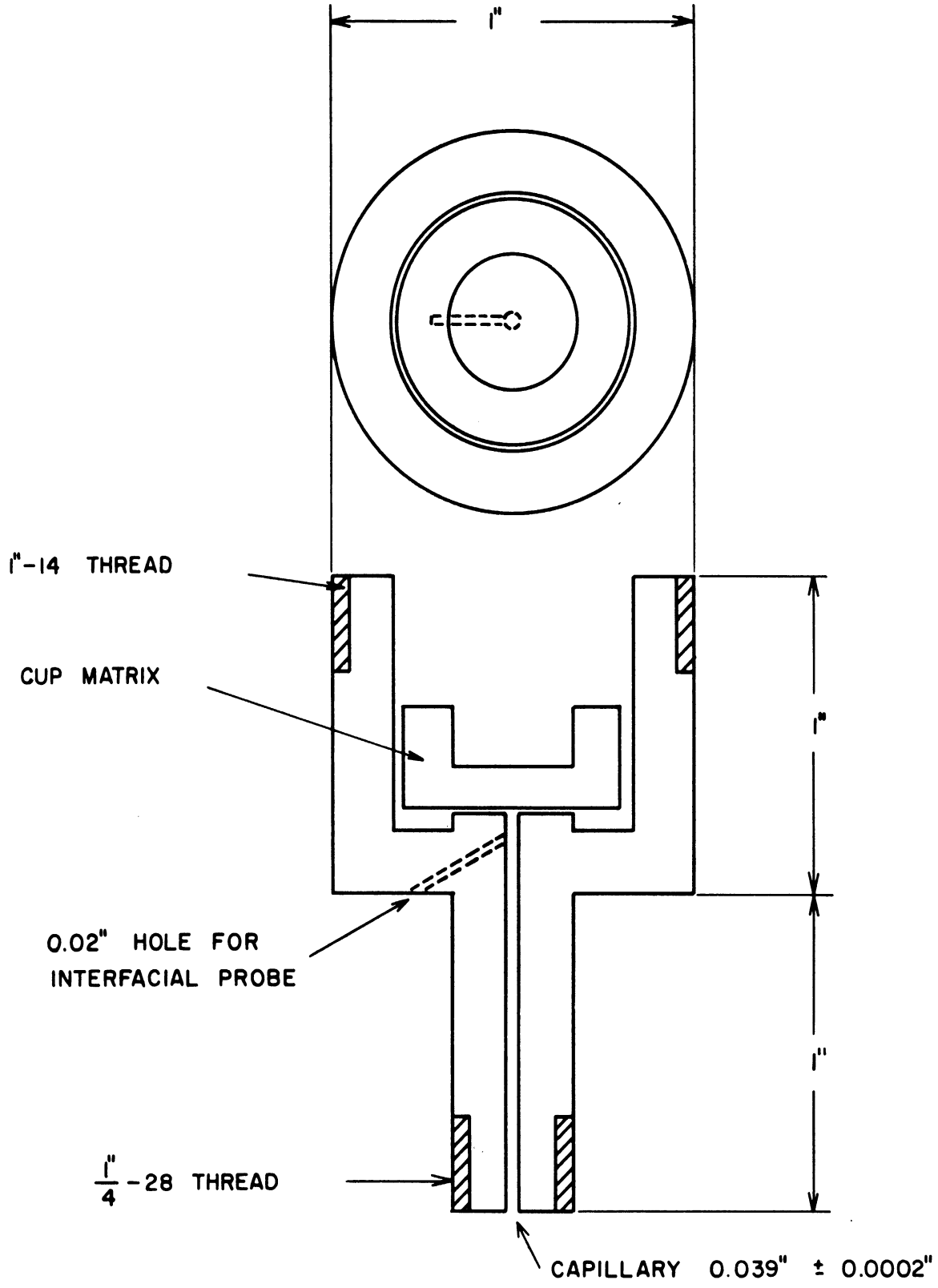

Figure L-2. Two Electrode Cell with Interface Probe and Boron Nitride Cell Body

$150.00 per unit. Threads provide for connection of a stainless steel "U" leg to the bottom of the capillary.

Similar problems arose as in the previous cell. The cost of the cell required re-use while cleaning proved even more difficult than in the previous case because boron nitride hydrolyzes slowly in the presence of water. Difficulty was experienced in the proper positioning of the interface probe though leakage around this probe was less of a problem because a tighter fit could be obtained between the boron nitride and the tungsten.

III. Two Electrode Boron Nitride Cell with a Positive Head of Metal in the Cathode.

A cell similar to that shown in Figure L-2 was employed. The major differences are, no hole was provided in the body for the interface probe, and the supply of cathode metal was contained in a micrometer syringe external to the furnace and fed to the cell through a hypodermic tubing with an i.d. of 0.010". The syringe was located at the same height and the metal was fed through the inverted "U" tube of hypodermic tubing which passed through the head of the furnace. This arrangement allowed fine control over the level of mercury in the cell at room temperature but failed at high temperatures due to cavitation of the column of mercury in the hypodermic tubing within the furnace.

IV. Two Electrode Cell with Tungsten-26% Rhenium Anode and Cathode Compartment.

The design of this cell is shown in Figure L-3. The upper end of the anode compartment is sealed to prevent vaporization of the alkali metal in the anode. The interface in this electrode recedes slightly during the discharge of the cell. The electrolyte was found towet the tungsten alloy sufficiently well that it would flow into the anode compartment and maintain contact with the alkali metal.

Prior to filling, the anode and cathode compartment surfaces which would come in direct contact with the electrolyte were oxidized by heating to red heat in air.

Experimental results for the diffusion of sodium in tin with this diffusion cell, while more successful than the alumina and boron nitride cells described earlier, were still not reproducable.

In addition to not being able to observe any bubbles which have formed in the cathode of this cell the following problems arose.

(a) Unstable operation occurred, perhaps to breakdown of the oxide films on the anode and cathode compartment walls.

(b) Removal of solidified metal from the cathode compartment after a diffusion run is desirable since the tubing costs $8.00 per inch. It proved difficult to clean the metal from the capillary without heating. Heating in turn produced additional oxides on the capillary walls and changed the diameter of the diffusion path.

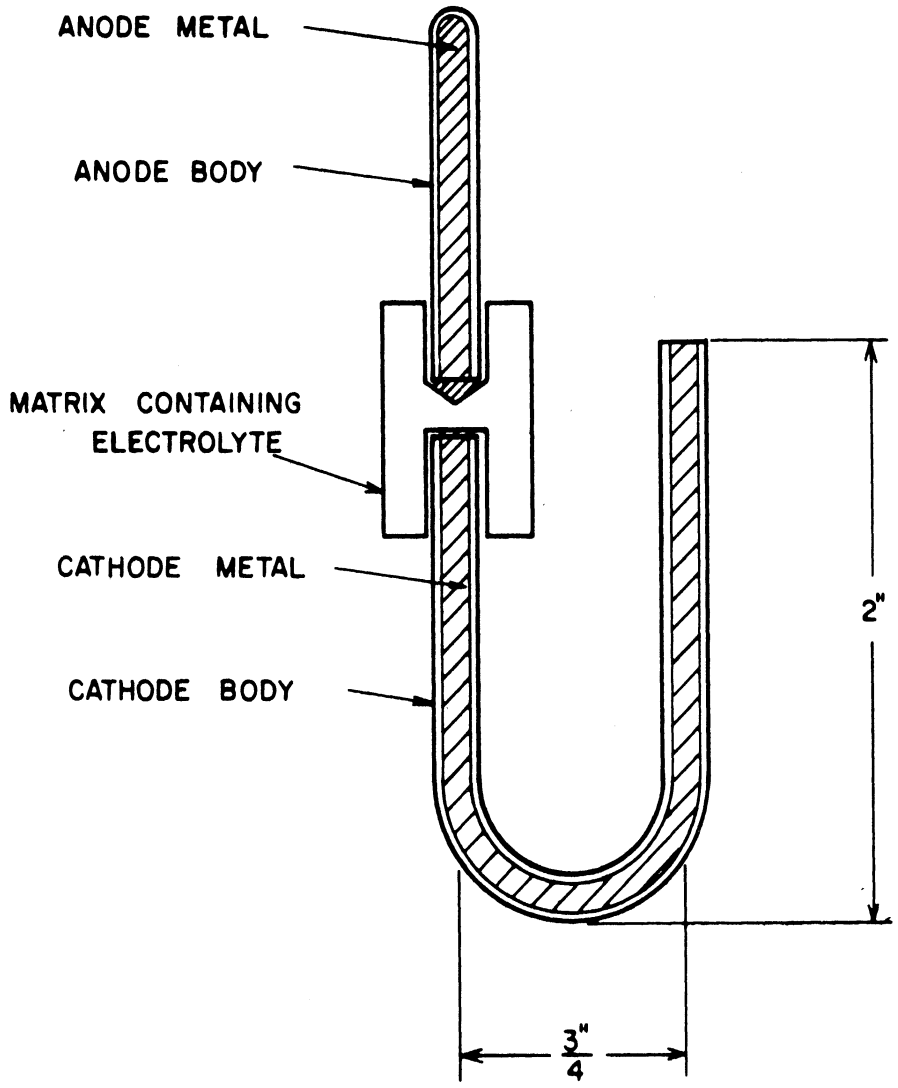

Figure L-3. Two Electrode Cell, Tungsten-26% Rhenium Anode and Cathode Compartment

(c) Tungsten-26% Rhenium tubing while less brittle than pure tungsten tubing is still quite brittle and to make a "U" bend requires heating it to red heat. Oxidation of the tubing during this heating may distort the diffusion path.

V. Three Electrode Cell, Tungsten-26% Rhenium Anode and Cathode Compartments.

This cell was identical to the one shown in Figure L-3, with the exception that a 0.020" tungsten probe was inserted into the matrix midway between the anode and cathode-electrolyte interfaces. Runs were made with bare tungsten probes and with tungsten probes on which AgCl had been deposited electrolytically. These probes yielded no information concerning the nature of the instability in this type cell.

VI. Two Electrode Cell, Alumina Anode and Quartz Cathode Compartments.

The design of this cell is shown in Figure L-4. The cathode compartment is separate from the rest of the cell and can be raised or lowered in the furnace. The experimental procedure for this cell involved heating the anode and electrolyte to operating temperature while the cathode was lowered to a point in the furnace where the temperature was below the melting point of the cathode alloy. After a stable thermal gradient was attained in the furnace the cathode was quickly raised to make contact with the lower surface of the matrix

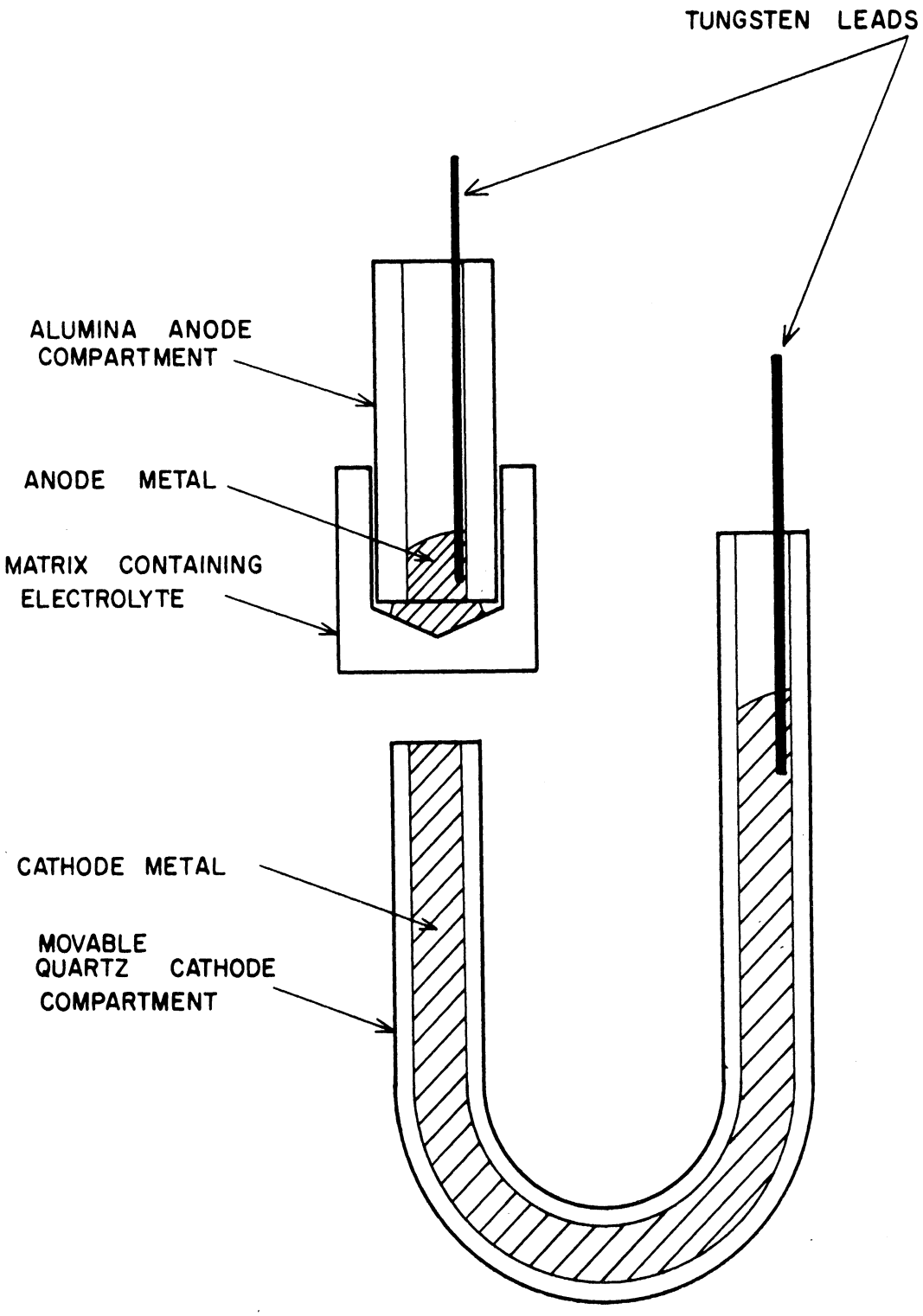

Figure L-4. Two Electrode Cell, Alumina Anode Compartment and Quartz Cathode Compartment

containing the electrolyte. This cell had several advantages. It was possible to observe the shape of the electrolyte-cathode interface during cell operation. Also careful temperature control was possible because the cell cannot be discharged while the cathode was kept separate from the anode and electrolyte. Some discharge is unavoidable in a non-equilibrium cell of this type due to soluability of the alkali metal in the electrolyte, etc. The major disadvantage with this cell was that it is difficult to obtain good positioning of the cathode and matrix relative to each other when the cathode is raised by remote control from outside the furnace. Leakage from the cathode compartment and distortion of the diffusion path was common.

These cell designs lead to the final one described in detail earlier which was used for the experimental investigations reported here. Due to the great difficulties encountered in these preliminary investigations with the interface probe to measure diffusion potential no further attempt was made to incorporate a probe of this nature in the refined cell design.

THE UNIVERSITY OF MICHIGAN

DATE DUE

[illegible] 7:22 pm	
5/20 11.19 PM	
5/21 9A.M.	